

OPTIMIZATION OF DYNAMIC BEHAVIOUR OF PRINTING ROLLER SYSTEMS

Teză destinată obținerii
titlului științific de doctor inginer
la
Universitatea Politehnica Timișoara
în domeniul INGINERIE MECANICĂ
de către

Ing. Mariana-Claudia Voicu

Conducător științific: prof.dr.ing. Inocențiu Maniu
Referenți științifici: prof.dr.ing. Reinhard Schmidt
prof.dr.ing. Benno Lammen
conf.dr.ing. Erwin-Christian Lovasz

Ziua susținerii tezei: 4 noiembrie 2014

Seriile Teze de doctorat ale UPT sunt:

- | | |
|---|--|
| 1. Automatică | 9. Inginerie Mecanică |
| 2. Chimie | 10. Știința Calculatoarelor |
| 3. Energetică | 11. Știința și Ingineria Materialelor |
| 4. Ingineria Chimică | 12. Ingineria sistemelor |
| 5. Inginerie Civilă | 13. Inginerie energetică |
| 6. Inginerie Electrică | 14. Calculatoare și tehnologia informației |
| 7. Inginerie Electronică și Telecomunicații | 15. Ingineria materialelor |
| 8. Inginerie Industrială | 16. Inginerie și Management |

Universitatea Politehnica Timișoara a inițiat seriile de mai sus în scopul diseminării expertizei, cunoștințelor și rezultatelor cercetărilor întreprinse în cadrul Școlii doctorale a universității. Seriile conțin, potrivit H.B.Ex.S Nr. 14 / 14.07.2006, tezele de doctorat susținute în universitate începând cu 1 octombrie 2006.

Copyright © Editura Politehnica – Timișoara, 2014

Această publicație este supusă prevederilor legii dreptului de autor. Multiplicarea acestei publicații, în mod integral sau în parte, traducerea, tipărirea, reutilizarea ilustrațiilor, expunerea, radiodifuzarea, reproducerea pe microfilme sau în orice altă formă este permisă numai cu respectarea prevederilor Legii române a dreptului de autor în vigoare și permisiunea pentru utilizare obținută în scris din partea Universității Politehnica Timișoara. Toate încălcările acestor drepturi vor fi penalizate potrivit Legii române a drepturilor de autor.

România, 300159 Timișoara, Bd. Republicii 9,
Tel./fax 0256 403823
e-mail: editura@edipol.upt.ro

Acknowledgments

This PhD thesis was developed during my work at the University of Applied Sciences Osnabrück, Germany in an international cooperation with Politehnica University of Timișoara, Romania. In this work are included the results of two research projects: "Active roller systems" and "Design of profile rings for vibration damping of rotating shafts", and of a feasibility study "Test exemplary applications of piezoelectric pressure and force sensors based on acrylic paint" granted from ERDF (European Regional Development Fund), the Ministry for Science and Culture of the land Lower Saxony and the Federal Ministry for Economics and Technology.

At first, I would like to express my sincere gratitude to my supervisors from the University of Applied Sciences Osnabrück, Professors Reinhard Schmidt and Benno Lammen for guiding me during all these years with patience and for their wise advices, brilliant ideas, suggestions and professional support and for believing in me, sometimes more than I did.

I thank my PhD supervisor from the Politehnica University of Timișoara, Professor Inocentiu Maniu for his professionalism, support, for having patience and his good advices and for his insistence to achieve better work.

Many thanks go to my colleagues and students who worked in this project, especially: Michael Mersch, Florian Weigt, Fabian Sellmann, Henrik Huffendieck, Michael Schauer, Sören Sanders, for their big efforts and support in this project.

I would like to thank the Doctoral School of the University of Applied Sciences Osnabrück for the 8 months doctoral ship, especially the Professor Peter Seifert.

A special thanks goes to Professor Jack Hale from the University of New Castle upon Tyne, who supported the research and development of the piezoelectric sensors and sent piezoelectric paint and a lot of technical information.

Many thanks go to the professors from the Department of Mechatronics of the Politehnica University of Timișoara for their good suggestions, especially to Cristian Moldovan and associate Professor Erwin-Christian Lowasz for accepting to be referent for my thesis.

The words are too little to describe my thanks to my son Jannis for his patience, love, endless support to withstand the challenges of life and work.

I wish to thank my friends for their human support and for "good vibrations" given by all activities we did together. These vibrations don't need to be damped as roller vibrations are in this thesis.

I am also grateful to the industrial partners in the research project "Active roller systems" who provided the research with helpful ideas and impulses, test setups and technical support.

I am thankful to the people who have patience to correct my thesis, in addition to my supervisors.

Finally, I thank all other people not mentioned here, who contribute to this dissertation.

Timișoara, November 4th 2014

Mariana-Claudia Voicu

Dedication

To my son Iannis

Voicu, Mariana-Claudia

Optimization of Dynamic Behaviour of Printing Roller Systems

Teze de doctorat ale UPT, Seria 9, Nr. 156, Editura Politehnica, 2014, 170 pagini, 140 figuri, 6 tabele.

ISSN: 1842-4937

ISBN: 978-606-554-878-7

Cuvinte cheie: flexography, roller system, active vibration damping, piezoelectric paint, piezoelectric actuators, damping rings, simulation of roller system

Rezumat,

Due to increase roller width and web velocities, the vibration characteristics are significant for the quality and efficiency of the printing processes. Approved methods like balancing of the rollers and maximizing the bending stiffness have come to technical limits. This work deals with finding possibilities for improving the dynamic behaviour of roller systems in flexographic printing machines. Piezoelectric sensors based on piezopaint are developed for measuring dynamic forces in the nip of the printing rollers. A mathematical model of the roller system was derived and implemented in Matlab/Simulink. Active bearings with integrated piezoelectric actuators are designed. An experimental-based control using a feed-forward and a feedback control algorithm shows good results of vibration reduction of the plate cylinder. A semi-active method for reduction of vibration amplitudes of more than 85% using profile rings was designed and verified by the measurements.

CONTENTS

Contents	4
List of Figures	8
List of Tables	12
1. Introduction	13
1.1. Introduction to Printing Processes and Motivation	13
1.1.1. History	13
1.1.2. Process description	17
1.2. Motivation and Goals	19
1.3. Organization of the Thesis	20
1.4. Chapter Summary in Romanian	20
2. State of the Art	23
2.1. Measuring Nip Pressure, Nip Forces and Roller Vibrations	23
2.2. Vibration Reduction of Roller Systems	26
2.2.1. Passive Solutions	26
2.2.2. Active Solutions and Control Algorithms for Active Vibration Damping ..	27
2.2.3. Semi-active Solutions	31
2.3. Piezoelectric Paint	32
2.4. Current State	35
2.4.1. Test Setup Simulating a Coating Machine	36
2.4.2. Test Setup Simulating a Printing Unit from a Flexographic Printing Machine ..	37
2.5. Chapter Summary in Romanian	39
3. Introduction to Piezoelectric Sensors and Actuators	40
3.1. Manufacturing Process	40
3.2. The Piezoelectric Effect	41
3.3. Piezoelectric Sensor	44
3.4. Piezoelectric Actuator	45
3.5. Chapter Summary in Romanian	47
4. Development of Piezoelectric Paint Sensors	49
4.1. Motivation	49
4.2. Fundamentals	52
4.3. Layout of a Piezoelectric Paint Sensor	52

4. 4. Development of Piezoelectric Sensors with Defined Piezo Paint Thickness.....	54
4.5. Experiments	57
4.6. Test Results.....	59
4.7. Chapter Summary in Romanian.....	66
5. Dynamics of Roller System	69
5.1. Mechanical Roller System	69
5.1.1. Mathematical Model for a Beam Element.....	71
5.1.2. Mass matrix and stiffness matrix for an entire roller.....	75
5.1.3. Mathematical Model of the Roller System.....	77
5.2. State-Space.....	80
5.3. Modal Analysis and System Reduction	83
5.4. Implementation of the model in Matlab/Simulink	86
5.4.1. Validation of the mathematical model.....	86
5.4.2. Simulation of the Roller System.....	87
5.4.3. Simulation of the Components of the Closed-loop System.....	89
5.5. Chapter Summary in Romanian.....	93
6. Active Vibration Damping	96
6.1. Concept of Active Vibration Damping	96
6.2. Design of a PD Controller.....	97
6.3. Design of a Feed-Forward Control Using Least Mean Squares Identification Algorithm (LMS)	103
6.4. Test Results of Active Vibration Damping Using Feed-Forward and Feedback Control Algorithm.....	110
6.5. Chapter Summary in Romanian.....	112
7. Development of the Active Bearings	114
7.1. Downscaled Test Setup of the Roller System.....	114
7.2. Industrial test setup simulating a printing unit	116
7.3. Chapter Summary of Romanian.....	123
8. Optimization of Roller Behaviour with Profile Rings.....	125
8.1. Technical Problem and Solution	125
8.2. Test Setup for Semi-Active Damping with Profile Rings.....	130
8.3. Advantages of damping vibration with profile rings	138
8.4. Chapter Summary in Romanian.....	138

9. Contributions, Conclusions and Future Works.....	140
9.1. Conclusions	140
9.2. Contributions to the Fundamental and Experimental Research.....	141
9.3. Dissemination of the Research Results	142
9.4. Future Work.....	144
Bibliography	145
Appendices	154
Appendix A.....	154
Appendix B.....	156

LIST OF FIGURES

Figure 1.1 First Letterpress	13
Figure 1.2 40 years old flexographic printing machine for napkin production	14
Figure 1.3 Flexographic printing machine Olympia 1275	14
Figure 1.4 Comparison between digital and conventional technic for printing plates	15
Figure 1.6 Old flexo print (a) and new flexo print principle (b)	16
Figure 1.7 Flexographic printing machine Astraflex (W&H)	16
Figure 1.8 Flexographic printing machine with central drum	17
Figure 1.9 Flexographic printing unit	18
Figure 1.10 Sleeve with printing plate	18
Figure 2.1 Measuring of static pressure with Prescale Fujifilm	23
Figure 2.2 Measuring nip roller with Tekscan sensors	24
Figure 2.3 Flatness measuring roller with piezoelectric sensors	24
Figure 2.4 Measuring roll gap with laser sensors	25
Figure 2.5 Online measuring of web tension and nip forces with iRoll.....	25
Figure 2.6 Sleeve for passive damping of plate cylinder	26
Figure 2.7 Device for reducing vibrations	28
Figure 2.8 Active bearing unit.....	28
Figure 2.9 Vibration damping of flexible rotors.....	29
Figure 2.10 Printing cylinder with integrated piezoelectric actuators	29
Figure 2.11 Grinding spindle with magnetic bearings	30
Figure 2.12 Principle of magnetic bearing.....	30
Figure 2.13 Portal milling machine	30
Figure 2.14 Actuator-sensor unit for torsion compensation of an x, y, z-Tripod-testing machine	31
Figure 2.15 Roller with passive damper	32
Figure 2.16 PZT particle saw with the microscope	33
Figure 2.17 Structure of the piezoelectric paint sensor.....	33
Figure 2.18 Dynamic range of piezo paint sensors.....	33
Figure 2.19 Sensitivity of sensors versus drying time characteristics after introducing in water for 1 hour (A) and 3 hours (B).....	34
Figure 2.20 Voltage versus drying time characteristics of a sensors first introduced for 3 hours (a) and then for 1 hour in salt solution (b).....	34
Figure 2.21 Sensor array configurations (a) cruciform, (b) circular, (c) spiral	35
Figure 2.22 PVDF sensor.....	35
Figure 2.23 Pressure measurement with PVDF sensor in a shoe sole	35
Figure 2.24 Test setup simulating a coating machine 1-load roller, 2-gap roller, 3-supporting roller, 4- pneumatic cylinder , 5- force sensor	36
Figure 2.25 Printing process	37
Figure 3.1 Flowchart for the production of piezoelectric elements.....	41
Figure 3.2 Piezoelectric structure (left- before and right- after polarization)	41
Figure 3.3 Axes of a piezo element	42
Figure 3.4 Effects of piezoelectric elements	43
Figure 3.5 Large displacements with actuator	45
Figure 3.6 Piezoelectric stack actuator	46
Figure 4.1 Roll with piezoelectric paint sensor, piezoelectric discs and strain gauges	49
Figure 4.2 Different types of sensors for measuring nip forces.....	49

Figure 4.3 Measurement with piezoelectric film sensor.....	50
Figure 4.4 Measurement with strain gauge.....	50
Figure 4.5 Piezoelectric paint – the nip pressure is first increasing and then decreasing	51
Figure 4.6 Layout of a piezoelectric paint sensor.....	53
Figure 4.7 Housing for spraying the PZT-paint	55
Figure 4.8 Slide for raw sensors.....	55
Figure 4.9 Slide in the gripper	56
Figure 4.10 Mask on copper film and support steel plate.....	56
Figure 4.11 Sensor after applying PTZ-paint.....	56
Figure 4.12 Knife coating with the KUKA robot.....	57
Figure 4.13 Geometry of the sensors.....	57
Figure 4.14 Test setup.....	58
Figure 4.15 Entire test setup	58
Figure 4.16 Linearity of the sensor with a piezo paint thickness of 82 μm	60
Figure 4.17 Linearity of the sensor with a piezo paint thickness of 110 μm	60
Figure 4.18 Sensitivity measurement of piezo paint sensor	61
Figure 4.19 Charge displacement for piezo paint sensors with different piezo paint layer thicknesses	62
Figure 4.20 Dependence of the sensitivity on the layer thickness	62
Figure 4.21 Sensor dynamic.....	63
Figure 4.22 Schema of the test setup for dynamic measurement with piezo paint sensors.....	63
Figure 4.23 Comparison of the sensor’s signals for sinus-wave excitation.....	64
Figure 4.24 Comparison of sensor’s signals for saw-tooth wave excitation.....	64
Figure 4.25 Comparison of the piezo paint sensor’s signals with the signals of the calibrated force sensor	65
Figure 4.26 Piezopaint sensors on the plate cylinder a) schema; b) piezopaint sensor glued on the roller; c) sensor underneath the printing plate	66
Figure 4.27 Signals of the piezo paint sensor placed in the middle of the plate cylinder	66
Figure 5.1 Schema of control-loop model of roller system	69
Figure 5.2 Bending beam (a) beam; (b) beam element; (c) infinitesimal beam element.....	70
Figure 5.3 Calculation of the mass matrix and stiffness matrix in Matlab.....	74
Figure 5.4 Adding of two roller elements.....	75
Figure 5.5 Visualization of the adding mode for the total stiffness and mass matrix.....	76
Figure 5.6 Roller system	77
Figure 5.7 Schema of roller system	78
Figure 5.8 Calculation of the stiffness matrix and mass matrix for the roller system	79
Figure 5.9 Calculation of the basic paramters of the 3 rollers.....	79
Table 5.1 Natural frequencies of the printing roller.....	81
Figure 5.10 Calculation of the first eigen frequencies in Hz of the 3 rollers	82
Figure 5.11 First 4 mode shapes of the printing roller on the test rig	82
Figure 5.12 Comparison of bending displacement between measurements and simulation results	87
Figure 5.13 Vibration of the plate cylinder (open loop) for a disturbance force applied in the middle of the roller	88
Figure 5.14 Assymetric disturbance applied on the roller.....	88

Figure 5.15 Vibration of the plate roller after asymmetric disturbance (open loop)	89
Figure 5.16 Simulated curvature	90
Figure 5.17 Characteristic diagram of the amplifier LE200/500	91
Figure 5.18 Characteristic diagram of the amplifier LE1000	91
Figure 5.19 Transfer function for the amplifier RCV1000/7 for the piezo actuator PSt 1000/35/200 VS45	92
Figure 5.20 Transfer function for the amplifier LE200/500	93
Figure 6.1 Downscaled test setup	96
Figure 6.2 Control loop of active vibration damping	97
Figure 6.3 Design of the standard PD-controller	98
Figure 6.4 Simulation model of the roller system in Simulink	98
Figure 6.5 Closed-loop simulation	99
Figure 6.6 Closed loop simulation with modified actuator position	100
Figure 6.7 Periodical disturbance force	100
Figure 6.8 Strain-gauge signal with periodical disturbance	101
Figure 6.9: Disturbance and control signal as a function of the rotational angle	102
Figure 6.10 Control structure	103
Figure 6.11 Schema of the roller system with uneven printing plate and the result disturbance	104
Figure 6.12 Diagram of the control phases	105
Figure 6.13 Control structure	105
Figure 6.14 dSpace interface for measuring and compensation of roller vibrations	106
Figure 6.15 Implemented model in Simulink	108
Figure 6.16 Block for strain gauge signals	108
Figure 6.17 The block "Offsetkorrektur"	109
Figure 6.18 The block "FAnalyse" for identification with LMS Algorithmus	109
Figure 6.19 dSpace interface for feed-forward and feedback control	110
Figure 6.20 Vibration damping for superimposed excitation frequencies of 5 Hz and 15 Hz	111
Figure 6.21 Vibration damping for superimposed excitation frequencies of 10 Hz and 30 Hz	111
Figure 7.1 CAD-Model of the small-scaled test setup	115
Figure 7.2 a) Active bearing; b) Stress analysis of the movable part of the bearing	116
Figure 7.3 Industrial test setup simulating a printing unit of a flexographic printing machine	117
Figure 7.4 Roller system	117
Figure 7.5 CAD-model of the industrial test setup	117
Figure 7.6 Active bearing on the A-side	119
Figure 7.7 CAD-model of the active bearing on the B-side	120
Figure 7.8 Bearing on the B-side	120
Figure 7.9 a) Load forces on the beam in the bearing, b) FEM-Analysis of mechanical stress of the active bearing	121
Figure 7.10 Double cylindrical beams to protect the actuator: a) the element, b) stress analysis	122
Figure 8.1 Periodical force profile of a piezo actuator on the circumference applied at the end of roller	126
Figure 8.2 Control schema	127
Figure 8.3 Simulation results for the roller system in laboratory scale	128
Figure 8.4 Shaft with damping rings outer	128

Figure 8.5 Shaft with two profiles inside the shaft	129
Figure 8.6 Shaft with profile rings outer and fixed pressure rolls	129
Figure 8.7 CAD- Model of the test setup for semi-active vibration damping with profile rings.....	130
Figure 8.8 Test setup with profile rings and applied disturbances	131
Figure 8.9 Simulation parameters of the test setup	132
Figure 8.10 Mathematical model of the test setup	133
Figure 8.11 Adding the 3 masses and the bearing stiffness to the mass and the stiffness matrices.....	133
Figure 8.12 Adding the 3 masses and the bearing stiffness to the mass and the stiffness matrices.....	133
Figure 8.13 Closed-loop model of the roller in Simulink	134
Figure 8.14 State-Space parameters	134
Figure 8.15 a) Parameters for PID controller, b) Parameter for the disturbance ..	135
Figure 8.16 Experimental and simulation results for the displacement of mass 3.	135
Figure 8.17 a) Actuator forces from simulation; b) Profile ring generated from the compensating forces in a)	136
Figure 8.18 Profile ring	137
Figure 8.19 Vibration reducing effect of the profile rings	137
Figure A1. 1 Linearity measurement of the two sensors (a) 82.4K and b) 82.3K) with a thickness of the piezo paint layer of 82 μm	154
Figure A1. 2 Linearity measurement of the two sensors (named a) 120.3K and 120.3K) with a thickness of the piezo paint layer of 120 μm	155

LIST OF TABLES

Table 2.1 Technical data for the printing unit.....	38
Table 3.1 Technical data for piezoelectric actuators.....	47
Table 4.1 Comparison of various types of sensors.....	51
Table 4.2 Material properties of PZT.....	52
Table 8.1 Technical data of the test setup.....	131
Table 8.2 Technical data of the laser distance sensors.....	136

1. INTRODUCTION

This work deals with measuring and damping bending vibrations in a printing unit from a flexographic printing machine. In this chapter, after an introduction in the evolution of the flexography and the description of the printing process, the goal of this thesis is presented.

1.1. Introduction to Printing Processes and Motivation

1.1.1. History

The flexographic printing is a direct high-pressure method using a flexible printing plate, originally called "aniline printing", named from the used aniline dye inks. This plate is usually made of a polymer or rubber. Flexography is a modern form of letterpress printing, which can print with high speed on different materials like paper, flexible, thin and solid films, cardboard or rough-surfaces for packaging materials [52].

Figure 1.1 shows the first letterpress printing machine made of wood invented by Gutenberg in 1445 in Mainz, which contains the basic idea of flexography.

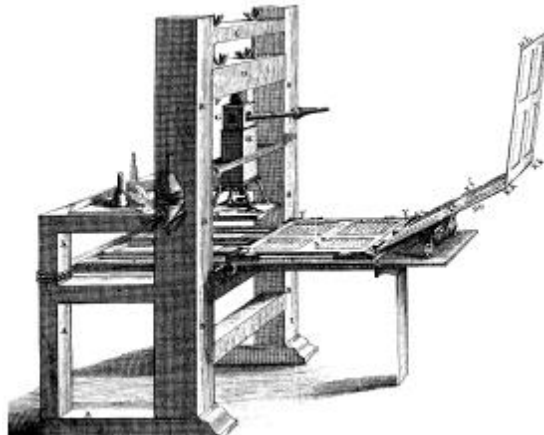


Figure 1.1 First Letterpress

The technological development of flexographic printing started in 1853 in the United State of America, when JA Kingsley had patented the first rubber printing plate, according to [47]. In 1890 the first patented aniline press using a rubber-printing plate and water-based inks was built by Bibby, Baron and Sons in Liverpool England. Other types of presses using rubber printing plates were developed in the wide Europe in the early 20th century, mostly in Germany and carried the name "Gummidruck". In Germany the history of flexography started in 1908, when Carl Holweg patented an aniline printing press. The printing press was a stack type press used in line with a bag making machine.



Figure 1.2 40 years old flexographic printing machine for napkin production

In 1954, Windmüller & Hölscher (W&H) presented their first one-impession cylinder flexographic printing machine, named "Olympia 1275" (Figure 1.3). It was the follower of their first aniline printing press after the bridge principle named Olympia 990.

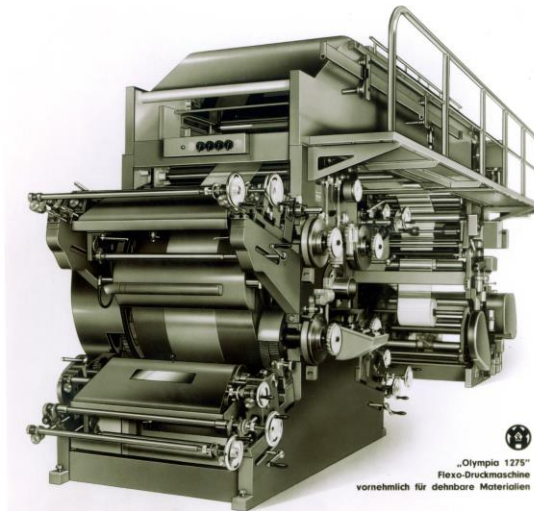


Figure 1.3 Flexographic printing machine Olympia 1275

In the 1970s, flexographic printing entered a new dimension. The quality was significantly increased by the introduction of photopolymer printing plates, which replaced the previously used rubber printing plates. A further step came in the 1980s when automatic feeding systems for high quality printing were invented. In the 1990s the sleeve technique was developed which uses pressure pipes for applying the

printing plates. The automation was also increased by computer-to-plate technology (CtP) [52], which enhances visibly the quality of the printing plates [78] (Figure 1.4).

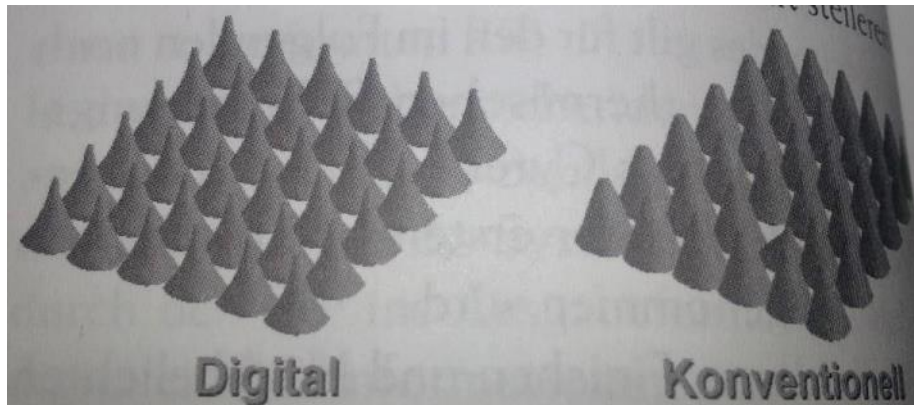


Figure 1.4 Comparison between digital and conventional technique for printing plates

In 1992 W&H developed their first one cylinder sleeve printing machine Soloflex, which is shown in Figure 1.5, increasing visibly their technology.



Figure 1.5 Flexographic printing machine Soloflex

The printing form in flexographic printing is not in continuous contact with the impression cylinder, as opposed to offset or gravure printing where printing process is made with laser engraved plates without reliefs, an anilox roll and thereby edges of the printing reliefs can cause shock due to the pressure cylinder rotation when striking on the respective roll, see Figure 1.9. These impacts can create resonance vibrations in printing and inking unit. Quite often, visible streaks appears on the print outs. These phenomena (named also vibration strips) mainly depend on the printing speed and print motif (which represents the layout of the picture elements on the flexographic printing plate). If the printing image areas are unfavourably distributed the occurrence of oscillation is possible even at a low printing speed according to [24].

A comparison of old and new flexo printing processes with respect to the number and alignment of rollers can be seen in Figure 1.6. The old flexo print principle

(Figure 1.6 a) used a number of four rollers ((1)-impression cylinder, (2)-printing plate, (3)- anilox roll, (4)- fountain roll) and an ink pan (5) in contrast with the new flexoprint principle (Figure 1.6 b) which has only three rollers and one ink chamber (4).

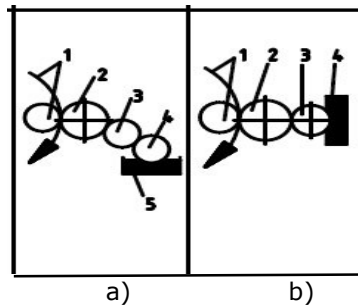


Figure 1.6 Old flexo print (a) and new flexo print principle (b)

In this thesis, a printing unit as a three-roller system from a typical flexographic printing press will be considered, similar to a printing press Astraflex from the company Windmüller & Hölscher presented in Figure 1.7. This machine uses a central impression cylinder and eight printing units, for each colour one. An advantage of such printing machines is the compact form of the printing process, but after each printing cycle, a drying time is required, hence inks with low viscosity are used. A schema of this central drum technology is presented in Figure 1.8, where the blue line shows the path of the printing substrate [17].



Figure 1.7 Flexographic printing machine Astraflex (W&H)

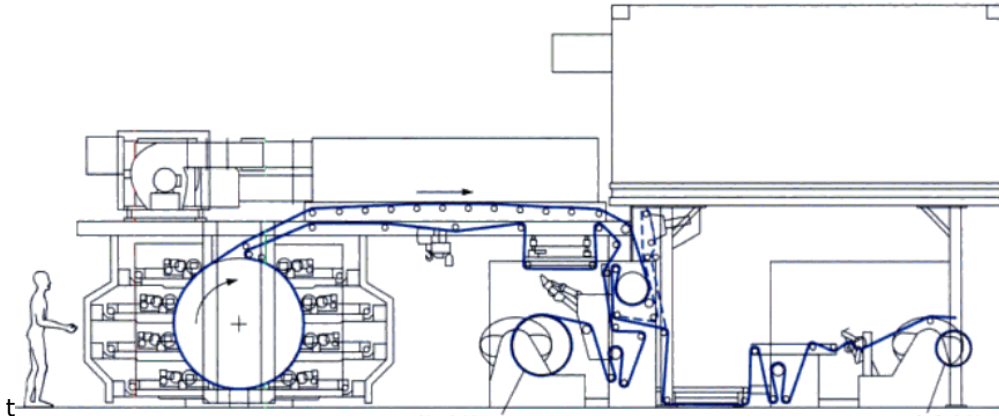


Figure 1.8 Flexographic printing machine with central drum

Modern flexographic printing machines have between 4 and 10 printing units and can be classified in categories as follows:

- stack press, where the print units are stacked one over another in pyramid form and can be easily accessed; this press can print on both sides of the substrate
- central drum, where the print units are placed around a huge central impression cylinder
- in-line press, where the colour stations are aligned horizontally in a line and can print on both sides of the printing substrate

The new development in the flexography can be found in [45, 46, 90].

1.1.2. Process description

The layout of a flexographic printing unit is shown in Figure 1.9 [52]. In the simplest form, the flexo process has the following components: ink supply with doctor blade, anilox roll, a plate cylinder with sleeve and printing plate and an impression cylinder. The anilox roll transfers the ink from the ink supply chamber to the elevated parts of the printing plate. The ink fills tiny cells on the surface of the anilox roll after which the doctor blade cleans its surface of excessive ink before inking the flexible printing plate. In the next step, the ink is transferred to the printing substrate when pressed by the impression cylinder. The pressure between the impression cylinder and the plate cylinder has to be low and constant along the roller; its value is very important for a good printing quality and to avoid stripes on the printed image.

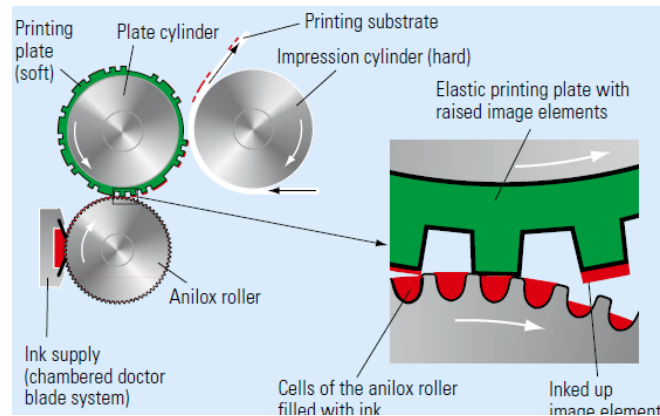


Figure 1.9 Flexographic printing unit

The anilox roll has direct contact to the ink. It is coated with ceramic or chrome material to protect it from corrosion. The number of cells per linear inch on its surface depends on the type of print job and the required quality. The cell's cavity can have different shapes e.g. inverted pyramid, hexagonal, cup shape etc.

For a good printing image, the plate cylinder has to be manufactured very accurately and it has to support the printing plate. The printing plate is made of rubber or photopolymers. The rubber plate is made of mould which is subsequent vulcanized on the plate cylinder and can be used several times to produce new plates [52]. The printing motif is obtained by laser engraving. The second type of printing plate (photopolymers) is mounted on the plate cylinder with a double-sided adhesive tape or is manufactured in cylindrical form named sleeve technology as shown in Figure 1.10 [48].



Figure 1.10 Sleeve with printing plate

The photopolymer printing plate is a flexible film with variable thickness and hardness, depending on the printing substrate. The photopolymer used for printing plates is irradiated with UV light to obtain the desired printing model using special process equipment. Its thickness varies between 0,70 mm (e.g. for plastic bags) to 6,35 mm (e.g. for corrugated cardboard), see [52, 24]. Producers of photopolymer base plates are e.g. BASF (Nyloflex printing plates) and DuPont (Cyrel printing plates) [52].

1.2. Motivation and Goals

Conventional methods for the reduction of roller vibrations reached their limits, as more detailed in chapter 2.2.1. New technologies and methods like active vibration control have to be developed in order to further reduce vibration. The thesis goal is the development of an active vibration control system which could be implemented on a flexographic printing machine. It should increase the production speed and web velocity of printing and coating processes significantly over the current state of the art.

Active vibration control for increasing the performance of printing machines requires:

- sensors for measuring pressure or forces in the nip, where the nip defines the contact between two rollers, here idealized as a line contact. The sensors are necessary for sending in real time the current values from the nip to the control algorithm
- fast-running and heavy-duty actuators for moving the massive roller to minimize its vibrations
- mathematical model for the control design
- controller (controller algorithm, software real-time hardware)

This work deals with each of these topics and contributes to the research project "Active vibration damping of flexible rollers for printing and coating processes", which was granted by ERDF (European Regional Development Funds).

The research project was carried out at the University of Applied Sciences Osnabrück in cooperation with three industrial companies: Windmüller & Hölscher, Weros Technology and Felix Schoeller Technocell with activities in printing and coating processes as follows:

- Windmüller & Hölscher (W&H) is a manufacturer of flexographic printing machines in Lengerich Germany.
- Felix Schoeller Technocell has its main activity in coating of paper webs, e.g. for producing photo paper using coating machines.
- Weros Technology develops rubber coating for rollers e.g. for printing and coating processes.

The motivation of this thesis starts with the needs of the above presented companies: to find new possibilities to improve the efficiency of printing and coating processes by reducing vibrations and for online monitoring of roller vibrations in printing processes, as described in [105].

The production speed of printing and coating machines can be in principle improved by using wider rollers, by increasing the web speed or both. Long and thin rollers are sensitive to vibrations at high web speeds. Deformation of the roller by its own weight, increased sensitivity to vibrations of the rollers and variable contact forces limit the possible width. This can be optimized by means of suitable roll materials with a favourable density/rigidity ratio (e.g.: carbon fibre (CFC)-rollers). While conventional methods reach their limits in efficiency, active components such as piezoelectric actuators open new possibilities for vibration reduction.

This work pursues two aspects in order to reach the main goal - the development of an active vibration control of roller systems. These two aspects are:

- The development of special sensors for measuring forces between rollers in printing and coating processes, without affecting the print image negatively.
- Vibration damping of roller systems in printing processes using:

- active bearings with piezoelectric actuators to reduce vibrations of the plate cylinder and hereby to allow higher web velocities without affecting the quality of the printed image;
- semi-active damping with profile rings applied on the roller.

In conclusion, a mechatronic system has to be developed for active damping of roller vibrations. For this, the piezoelectric actuators integrated in the bearings of the plate cylinder generate high dynamic displacement to counteract the vibration of the roller.

An important aspect is the selection of appropriate sensors and actuators. For the technical problem presented in this work are needed sensors and actuators capable to measure dynamic changes in the system and to compensate the vibrations.

Several contributions show the thorough understanding of the subject and the development of the thesis as follows: [7], [43], [44], [61], [71], [72], [73], [78], [109], [120]-[128], [131], [132]. An idea for semi-active vibration damping with profile rings is presented in Chapter 8 and it was developed during this dissertation and in [16] and published as patent application in [71] (see Appendix B).

1.3. Organization of the Thesis

This thesis consists of 9 chapters. After an introduction, Chapter 2 presents the state of the art for measuring nip forces and pressure, and also for vibration damping solutions. Chapter 3 describes the piezoelectric technology used in sensors and actuators, products developed and used in this thesis. After that, the development of new sensor technologies based on piezoelectric paint for measuring nip pressure in roller systems are presented in Chapter 4. In Chapter 5 is presented the mathematical model of the 3-roller system which was implemented in the software Matlab/Simulink, together with the components for the closed-loop simulation. Chapter 6 describes two concepts of the active vibration control of the roller system: a simulation-based designed control algorithm and a combination of a feed-forward and feedback control tested on the roller system. Chapter 7 handles with constructive design of active bearings for two test setups used in this thesis. Chapter 8 presents the patent ideas about semi-active damping of roller vibrations with damping rings. The idea was developed together with other colleagues during this work. Conclusions, future work and an overview of the original contributions are given in Chapter 9 as follows:

- force/pressure measurements with piezoelectric paint sensors in the nip (see chapters 2.3 and 4),
- active bearings with piezoelectric actuators (see chapter 7),
- profile rings as semi-active solution for damping roller bending vibrations (see chapter 8).

1.4. Chapter Summary in Romanian

In acest capitol "Introducere" se face o trecere in revista a tehnologiei industriei de tiparit cu ajutorul masinilor flexografice si evolutia procesului de tiparire cu aceste masini incepand cu 1445 si pana in zilele noastre, vorbind aici despre tipar inalt.

Sistemul de valturi considerat in aceasta lucrare este o unitate de tiparire din cadrul unei masini flexografice a firmei Windmüller & Hölscher din Lengerich Germania, care este unul dintre cei mai mari producatori de masini flexografice din lume. O astfel de masina are un valt de presiune cu un diametru foarte mare pe care este transportat materialul de imprimat. In jurul acestuia se afla intre 4 si 12 unitari de tiparire, pentru fiecare culoare cate una, in functie de performanta si complexitatea masinii flexografice. In figura 1.8 este prezentata schema de circulare a materialului de tiparit (linia albastra) intr-o masina de tiparit flexografica.

Sistemul de valturi care este considerat in aceasta lucrare include trei valturi prezentate in figura 1.9: valt de apasare, valt de tiparire si valt de presiune. Valtul de apasare preia culoarea de tiparit dintr-un rezervor si o transfera pe matrita de tiparit aflata pe valtul din mijloc, numit valt de tiparire.

De-a lungul timpului, calitatea matritei de tiparire a crescut, incepand de la un caciuc din care se frezau partile ce nu trebuiau tiparite, si pana la prelucrarea acesteia dintr-un material elastic numit fotopolimer, prelucrat computerizat prin expunerea la radiatii ultraviolete. Zonele de imprimat au o inaltime mai mare decat restul materialului. Dupa ce a preluat vopseaua, aceasta este imprimata pe materialul de tiparit, care poate fi: carton, hartie, folie, etc., masinile flexografice fiind foarte populare in special in domeniul tiparirii de ambalaje pentru diferite produse, chiar in cantitati relativ mici.

In figura 1.6 este prezentata alinierea valturilor pe o directie intr-o unitate de tiparire noua si reducerea numarului de valturi, pentru a micșora costurile de productie si automatizarea procesului de schimbare a matritei de tiparire. In masinile moderne, matrita se lipeste pe o teava, construita dintr-un material elastic cu proprietati de amortizare denumit sleeve (prezentat in figura 1.10), care se aplica cu ajutorul unei presiuni mari de aer (se mareste astfel diametrul interior al manusii si se impinge pe valt unde ramane fixat dupa ce aerul cu presiune inalta nu mai este aplicat, fara a mai fi necesara fixarea acestuia prin lipire).

Din cauza discontinuitatilor aflate pe modelul de tiparit care este fixat pe valtul de tiparire apar vibratii in sistemul de valturi. Aceste vibratii cauzeaza distorsiuni ale imaginii de tiparit si influenteaza astfel negativ calitatea produsului de tiparit. De asemenea, vibratiile in sistemele de valturi cresc pe masura ce valturile devin mai lungi, sau viteza de rotatie a valturilor creste pentru a mari productivitatea.

In subcapitolul 1.2 este descris scopul acestei lucrari, acela de a optimiza comportarea dinamica a sistemelor de valturi din masinile flexografice urmarind doua directii:

- dezvoltarea unor senzori piezoelectrice, pe baza de vopsea piezoelectrica, pentru masurarea fortelor, cu aplicatie in masurarea fortelor in suprafata dintre valturi;
- reducerea vibratiilor valtului de tiparire folosind:
 - elemente active in lagare, si anume actuatori piezoelectrice.
 - amortizarea semi-activa cu inele profilate

In aceasta teza de doctorat au fost introduse rezultate intermediare publicate in reviste de specialitate sau prezentate la conferinte nationale si internationale, precum si rezultate obtinute de studenti in cadrul proiectelor de licenta si lucrarilor de disertatie, sub indrumarea mea. In capitolul 8 este prezentata ideea amortizarii semi-activa a vibratiilor cu inele profilate, idee propusa spre brevetare. Propunerea [71] a fost postata pe internet si pe pagina de web a Institutului de Patentare German dpma.de si se afla in curs de verificare.

22 1. Introduction

Aceasta teza este organizata in doua parti, fiecare parte reprezentand unul dintre telurile acestei lucrari si este structurata in noua capitole. Dupa introducerea din acest capitol, se face in capitolul 2 o trecere in revista a solutiilor existente pe piata in domeniul masurarii fortelor si presiunilor dintre valturi, precum si a posibilitatilor de amortizarea a vibratiilor valturilor. Capitolul 3 prezinta informatii generale despre senzori si acuatori piezoelectricsi, elemente folosite in aceasta lucrare. Capitolul 4 descrie procesul de productie si dezvoltare a senzorilor piezoelectricsi pe baza de vopsea piezoelectrica, care urmeaza sa se aplice pe valturi sub matrita de imprimare pentru a masura fortele dintre valturi. In capitolul 5 este descrisa modelarea matematica a sistemului de valturi, precum si a elementelor care iau parte la bucla de reglare (senzori, actuatori, amplificatoare). Simularea sistemului de valturi a fost facuta cu programul Matlab/Simulink. In capitolul 6 sunt prezentate doua modalitati de amortizare a vibratiilor, una folosind un controler proportional-derivativ determinat cu ajutorul modelului matematic si a doua, folosind o combinatie intre un controler in bucla deschisa determinat cu ajutorul unui algoritm de identificare a perturbatiilor periodice si de optimizare a fortelor compensatoare folosind metoda celor mai mici patrate si un controler proportional-derivativ.

2. STATE OF THE ART

In order to develop machines running safe and with a high performance, mechanical problems especially vibrations have to be reduced. Particularly the dynamic behaviour of the rotating components has a great importance for the lifetime and durability of a machine and has to be measured and improved.

This chapter presents some methods for measuring nip pressure/forces, solutions for reducing vibrations of rotating shafts and rollers and also algorithms for damping vibration.

2.1. Measuring Nip Pressure, Nip Forces and Roller Vibrations

In the literature, there are two possibilities to measure nip pressure/forces:

- measuring of static (maximum) pressure
- measuring of dynamic pressure and also dynamic pressure distribution on a roller

The static pressure and the pressure distribution can be measured e.g. with Fuji Prescale film [26] to determine the smoothness and uniformity in wide ranges of industry. This pressure measurement film shows differences of applied pressure as red colour density variations, where colour capsules are broken by applying a pressure to them, as shown in Figure 2.1. This Fujifilm technology uses 200 μm thin films, which can measure variable pressure in range between 0.05-300 MPa. Some applications are: adjustment of nip roll pressure balance, adjustment of uneven pressure distribution and balance for automobile-parts, measuring the foot pressure distribution.

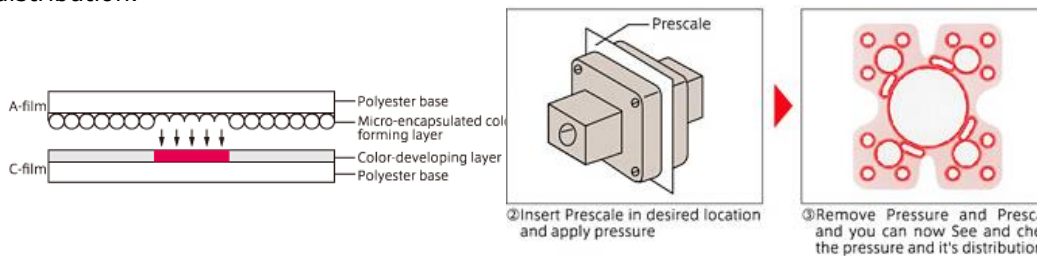


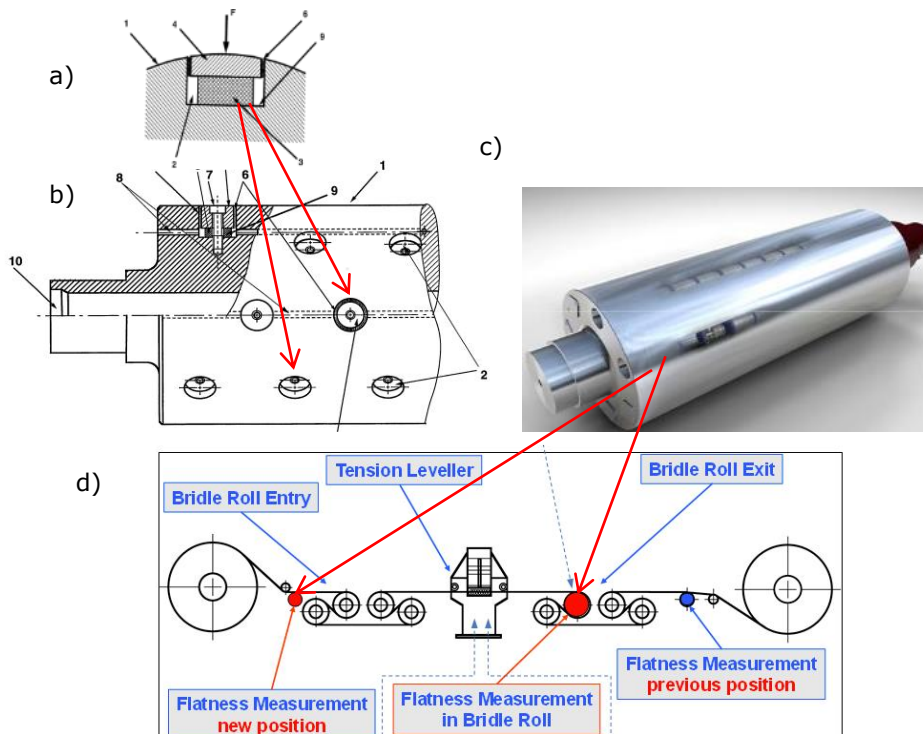
Figure 2.1 Measuring of static pressure with Prescale Fujifilm

To measure the dynamic pressure distribution in the roll gap without affecting the printing process there are a few other options on the market. Company Tekscan has developed films for measurement of the pressure distribution when the rollers come in contact [115], but these measurement systems are very expensive and inadequate for long-term measurements in this case. The sensors are used to determine the roller nip width, nip static pressure distribution, the contact area between rollers (Figure 2.2) and for adjustment of roller pressure.



Figure 2.2 Measuring nip roller with Tekscan sensors

BFI developed deflection pulley as described in [82], [84] and [119] for measuring the flatness of the steel web. This roller has piezoelectric force transducers implemented in radial direction along the roller and is introduced in the roller system as shown in Figure 2.3. It measures stress distribution along the bending rollers, by measuring the difference of the sensor signals. This type of roller is very expensive and cannot be applied in each roller system.



a) sensor mounting in the roller; b) roller – upper view schema; c) entire roller; d) roller mounting in the roller system for flatness measurement

Figure 2.3 Flatness measuring roller with piezoelectric sensors

The company μ Epsilon developed a laser micrometer system for measuring of the roll gap in [79]. The measuring principle is shown in Figure 2.4. Using an emitter and a receiver the displacement between two rollers and their vibrations can be determined.

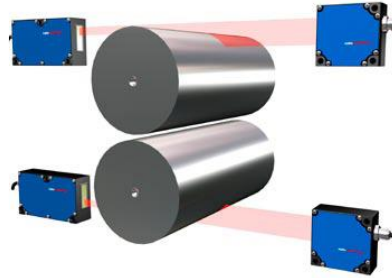


Figure 2.4 Measuring roll gap with laser sensors

In [108] Schmidt and Wöhrmann analysed the vibrations and temperature behaviour of rubber coated steel and carbon fibre (CFRP) rollers for a letter-printing machine. Due to the low heat transfer of the rubber layer and the shock sensitivity of the carbon fibre rollers, they tested the durability of carbon fibre rollers. They measured the mechanical stress of the rollers using strain gauges and compared the experimental measurements of these two types of rollers.

Metso Paper produced a roller named iRoll for online measuring of web tension and nip forces [76, 77]. An electromechanical film sensor is applied on or underneath the surface of the roller in the helical direction as shown in Figure 2.5. It can be used to detected variations in the thickness of the paper web, in the machine direction, alignment errors, oscillation of the coating.

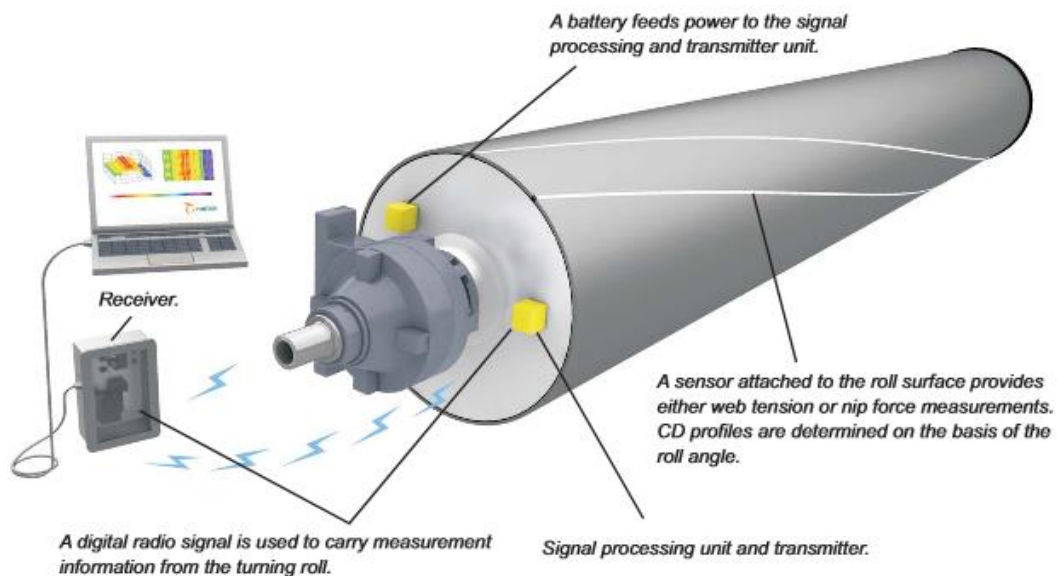


Figure 2.5 Online measuring of web tension and nip forces with iRoll

2.2. Vibration Reduction of Roller Systems

One of the first research works about vibrations in printing machines comes from Holzweißig [41], who has made studies on sheet-fed offset printing presses. He examined the influence of the helical gears on the bending and the torsional vibrations in a printing press. For the calculation of the torsional oscillations, the printing press was reduced to a simplified vibration model with four masses and three springs.

Hoffmann and Liebau carried out in [40] a systematic experimental and theoretical investigation of the cylinder groups of printing units in web offset presses. They investigated bending vibrations and their influence on the roll gap with the help of two computational models.

In [74, 75, 85] are studied vibrations in sheet-fed offset printing machines by excitement in channel strike and Holzweißig and Dresig provide in [18] a model for calculation of torsional vibration of a printing unit in an offset printing press.

As mentioned above, some works studied the roller vibrations. For damping the vibrations of the rollers or shafts in different types of machines, different solutions can also be found in the literature and on the market, which can be selected in three categories: passive, active and semi-active.

2.2.1. Passive Solutions

A classical method to minimize vibrations of roller systems is rollers balancing, which appears because of deformations of the roller shape and are caused by its own weight and irregularities. Roller balancing can be realized statically and dynamically.

The rollers are constructed as stiff and as light as possible, e.g. by using carbon fibre materials, in order to get higher natural frequencies and herewith to reduce roller vibrations. Contact pressure between the rollers must be measured, optimized and should be kept as small as possible.

A solution for minimizing roller vibrations, e.g. in flexography, is to use passive dampers in form of sleeves on the roller [24, 49], applied underneath the printing plate, as shown in Figure 2.6. The sleeves facilitate a flexible change of the printing model in roller system.

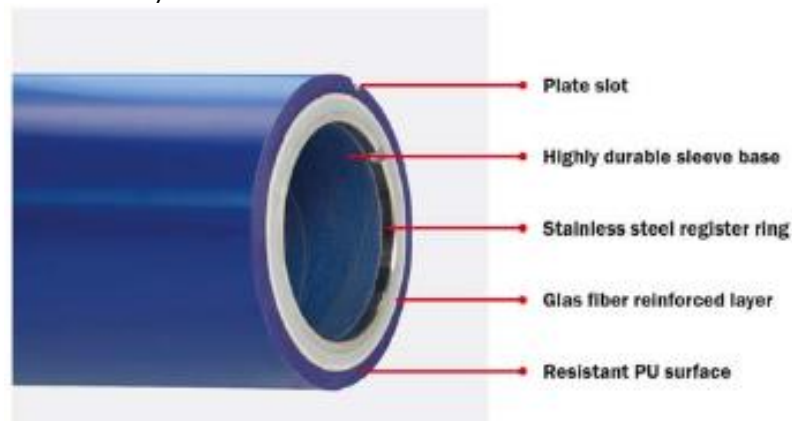


Figure 2.6 Sleeve for passive damping of plate cylinder

Passive magnetic bearings [27] are constructed with a part of the bearing with permanent-magnetic elements and the other bearing part includes a superconductor. The permanent-magnetic elements induce shielding currents in the superconductor as a result of magnetic field changes given from the position changing of these elements. The resulting forces can be repulsive or attractive to counteract the deflection from the nominal position for achieving a stable bearing.

2.2.2. Active Solutions and Control Algorithms for Active Vibration Damping

With increasing roller width and web velocity, traditional passive damping solutions such as balancing or increasing of roller stiffness by reducing its mass as mentioned in 2.2.1 reach their limits. Passive vibration control methods have some advantages like robustness, simplicity and reliability. In contrast, active methods are much more effective with respect to the vibration reduction. That's why several studies have started in recent years, to find active solutions to reduce roller vibrations. Some of these use different control strategies or different actuators, but also different constructions of the active elements. Some of these solutions are presented below.

In [35] is patented the idea of the damping of paper or textile web oscillations, by phase-transposed oscillations in the shaft. The web is in contact with a rolling drum supported by a shaft and the damping forces can be applied on the shafts outside position of the bearings using actuators.

Improved control performance and robustness is obtained for example with feed-forward algorithms [9], least-square optimal controllers [98] or robust control using μ -synthesis-method [42]. Zheng presents a learning control for rotor systems in [142].

Gnad presented in [32] a control algorithm for the voltage on the multilayers-piezoelectric actuators. He developed a switching amplifier for recovering of energy from piezo actuator, which is a capacitive load and uses two coils with different inductivities as temporary storages for energy. The control algorithm is tested in a simulation and the functionality is verified using a FPGA as controller.

Some active solutions have active elements such as piezo actuators placed in bearings, which damp active roller vibrations. Piezoelectric actuators are a good solution for systems with high dynamics, but these are very expensive and their control algorithms must be improved. There are some patents and studies about solutions with piezoelectric actuators, but there are no standard applications.

Patent in [22] describes a method for reducing vibrations on rotating parts, which roll in opposite directions, e.g. printing roller in offset printing machines, generated by the channel impact. As presented in Figure 2.7, vibration is reduced with a protrusion (9) produced by the active element (11). This element is located on a second roller and generates counter oscillations in radial direction by modifying of the height (h09) and eventual of the location on the circumference (a09).

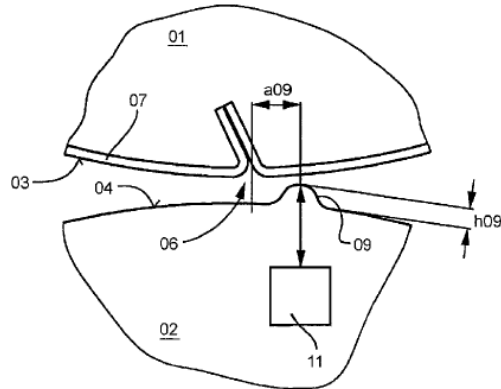


Figure 2.7 Device for reducing vibrations

In [12, 13] and in Figure 2.8 is presented an active bearing unit with two piezoelectric elements to reduce vibration amplitudes of bending shapes of printing rollers. The piezoelectric adjusting elements (26) with integrated force sensors are arranged 90° angle to each other and move the bearing's outer ring (09) in a direction perpendicular to the axis of the active bearing unit. The piezo elements are preloaded with half of their blocking force using the spring package (31) to avoid damages. High dynamic forces are sent to the printing roller for reducing oscillating amplitudes of a bending shape.

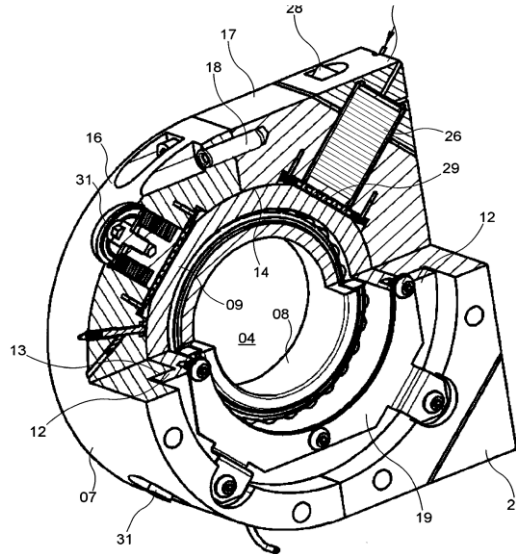


Figure 2.8 Active bearing unit

Another method for reducing damping vibrations due to axial arrangement of actuators in rollers of printing machines describes the patent in [30].

Horst deals in [42] with the active vibration control of flexible rotors by means of piezo-ceramic stack actuators. He simulated flexible rotors with a rotor disk as shown in Figure 2.9 and studied theoretically and experimentally three principles for vibration damping: the active vibration control with an active storage with piezo-ceramic stack actuators, the use of active storage for electromechanical damping and

the active vibration control of rotor-bonded piezo-ceramic elements. For the open-loop case, different control algorithms are compared: linear-quadratic control and μ -synthesis-control.

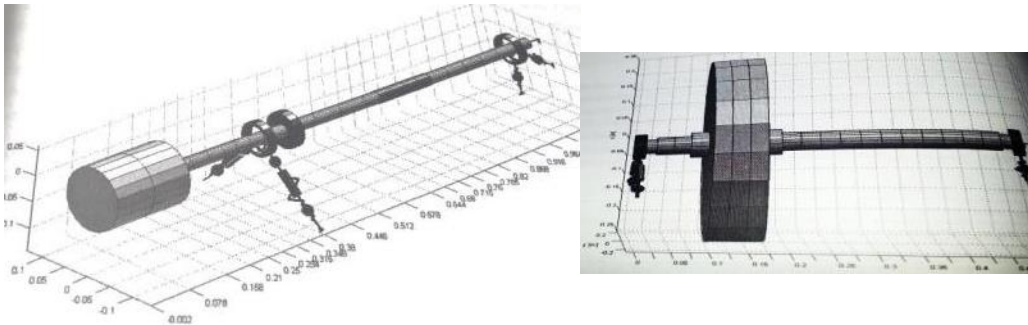


Figure 2.9 Vibration damping of flexible rotors

In [137] Wimmel presents the active vibration control of cylinders of web offset printing machines, using 32 integrated piezoelectric elements in a printing cylinder in order to reduce bending vibrations excited by channel impact (Figure 2.10). The piezoelectric actuators are distributed over the circumference of the roll as described from Glöckner and Keller in the patent [31] and act in the axial cylinder direction. Wimmel developed a controller of a trigger and a displacement signal, phase and amplitude of a pulse- control of the actuators. This process allows the oscillation amplitudes of the pressure cylinder to decrease by 20-50%.

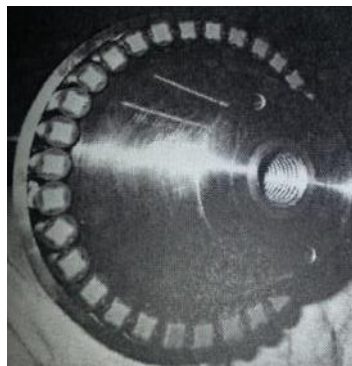


Figure 2.10 Printing cylinder with integrated piezoelectric actuators

In [55] Knopf presents a method of active vibration control in the sheet-fed offset printing machines, which measures the oscillations of the machine, determines the oscillation amplitudes and calculates moments that will be switched to the main drive thereby reducing the vibrations of the printing machine.

Other technical solutions for active vibration damping use e.g.: magnetic, electric, pneumatic or hydraulic actuators, magneto-rheological fluids. Nordmann presented in [86] methods for active vibration damping with magnetic bearings for rotating machinery, e.g. centrifugal pump Figure 2.11. This type of bearings works contactless and generates magnetic forces in the magnetic field to counteract the vibrations. In [1] active magnetic vibration damping is applied in a turbo machinery for identification and diagnosis procedures, based on frequency response functions. This mechatronic

component operates here as actuator and as sensor, and has the advantage to operate contactless as presented in Figure 2.12.

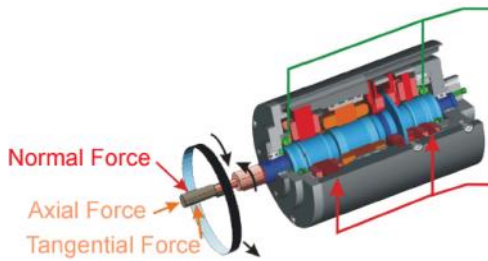


Figure 2.11 Grinding spindle with magnetic bearings

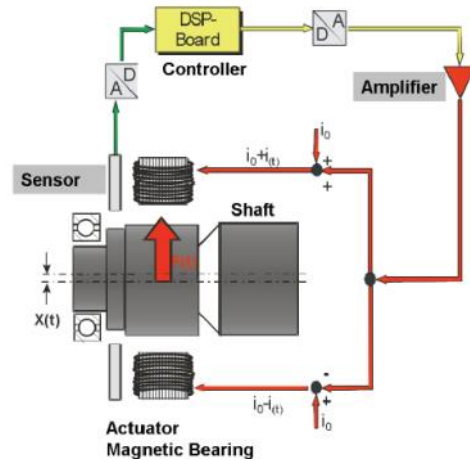


Figure 2.12 Principle of magnetic bearing

Active controllers can be found not only on rotating rollers, but also e.g. in automotive technology [66, 67, 68 and 130] or machining tools where a high degree of precision is required. In [19] is described an active μ -synthesis-control with piezoelectric actuators, used to damp the vibrations at a portal milling machine as shown in Figure 2.13 a). The mathematical model of the milling machine is presented in Figure 2.13 b). In milling process, chatter vibrations affect negatively the quality of the workpiece's surface. With the help of piezo actuators, the milling machine's structural damping is actively increased.

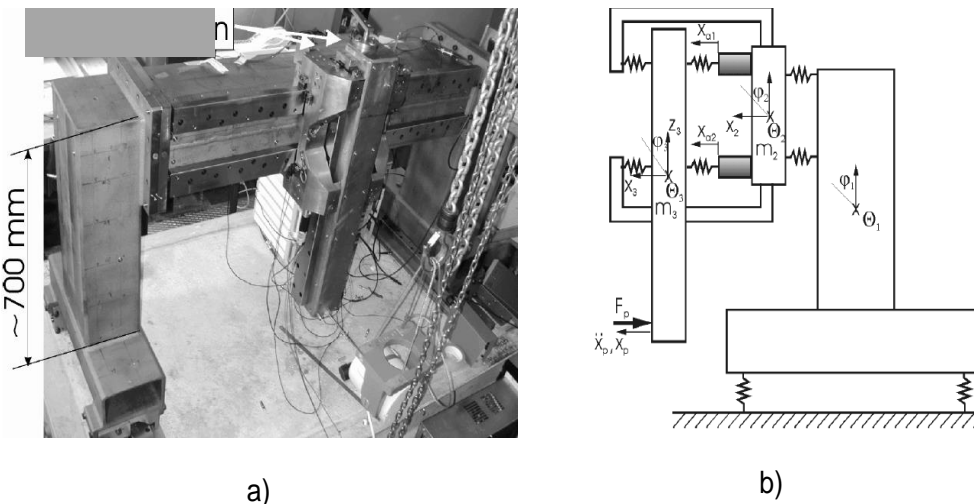


Figure 2.13 Portal milling machine

In [81] is described a feed-forward control algorithm of gear mesh vibration using piezoelectric actuators. Similar to this concept, it is realized in this thesis an active control for damping periodically vibrations of a roller.

A standard control loop is unable to adapt system variations e.g. caused by temperature, in the controlled system. An active controller uses algorithms able to adapt automatically to different conditions of a system. Concretely for the active vibration damping of rollers, this means adapt to variations of stiffness and mass, e.g. caused by different properties of rubber printing plates or of using different sleeves applied of the printing roller.

Such adaptive active systems have some characteristics as follows:

- are able to react autonomously to variable conditions and system requirements;
- can be trained to filter defined disturbances;
- can deal with new situations and adapt the model behaviour, after a short learn phase with a finite number of signals;
- can be described as nonlinear systems with time-varying parameters.

An adaptive system is effective when it is able to improve autonomously and optimally its own performance at variable conditions over time. An adaptive system using a sensor-actuator unit for measuring and damping vibrations of machining tools e.g. milling machine is presented in Figure 2.14 [25].

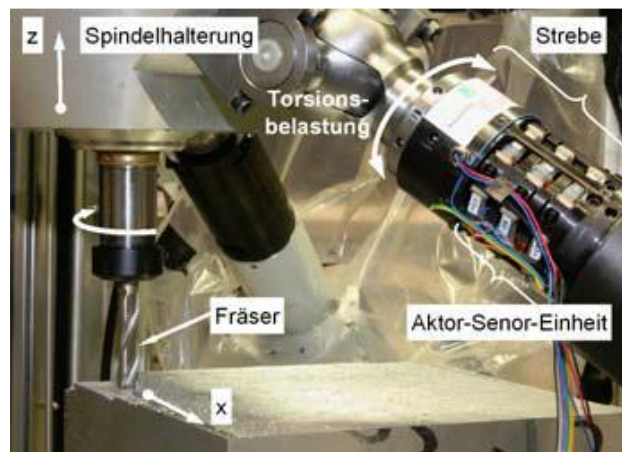


Figure 2.14 Actuator-sensor unit for torsion compensation of an x, y, z-Tripod-testing machine

Other important works for active vibration damping of rotors are presented in [2, 20, 21, 64, 113] and in [114] Tehrani *et al* present a control strategy with active elements on a flexible beam using the method of the partial pole placement.

2.2.3. Semi-active Solutions

In chapter 2.2.1 and 2.2.2 are presented passive and active solutions for damping vibrations in rotating shafts or rollers. In the literature there are presented also semi-active solutions, which use passive elements to produce energy used against vibrations. A semi-active method for damping roller vibration was developed in Chapter 8 and announced for patent application described in [71].

Another semi-active damping solution is presented in [36]. The patent describes the vibration damping of a hollow roller as shown in Figure 2.15. In the roller there is placed a carrier (2) in longitudinal direction with passive damper in form of circular chamber (9, 10). The roller vibration generates friction in the damping elements and herewith forces for minimizing roller vibrations. The patent describes also a semi active vibration damping possibility with this construction. In this case, the circular chambers incorporate a moving mass, a viscoelastic fluid as damper, or shock absorber materials such as granules for converting vibrational energy into friction to damp the vibrations.

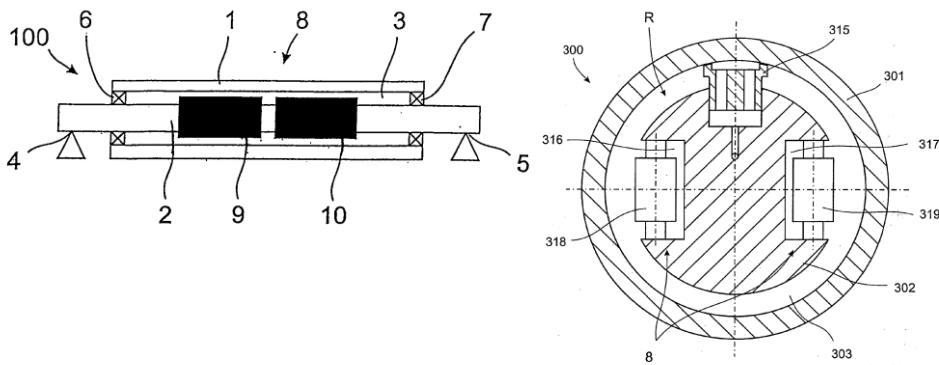


Figure 2.15 Roller with passive damper

2.3. Piezoelectric Paint

There are a few options on the market to measure the pressure distribution in the gap between the rolls without affecting the printing process. Company Tekscan has developed films for measurement of pressure distribution when the roll come in contact [115], but these measurement systems are very expensive and cannot make long-term measurements. BFI has developed measuring rollers as described in [82] which measures the flatness in the steel industry, but this roll is also very expensive. Chapter 4 of this thesis acts with development of piezoelectric sensors for measuring forces between rollers based on piezoelectric paint. The piezoelectric paint is not available on the market but it has potential to be a good solution for this difficult measurement problem. This paint was developed and tested at the University of New Castle upon Tyne, where Professor Hale led the research works. The published results of the research are the start point for the development of the piezoelectric force sensors presented in this work and these are described below.

As described in [136], the piezoelectric paint is composed of water-based acrylic lacquer and a high quantity of piezoelectric particles of lead zirconate titanate (PZT). The PZT particles corresponding to the grade PZT 5A (provided by Morgan Electro Ceramics Ltd.), approximately, were produced by ball milling and were a diameter in micron size spherical as shown in Figure 2.16. The paint is mixed with approx. 70% PZT and has been specifically designed to be sprayed on uneven and rough surface. An airbrush spray-head has been used with a spray valve diameter of 0.8 mm.

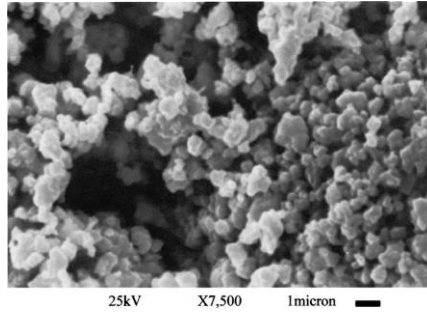


Figure 2.16 PZT particle saw with the microscope

The development of piezoelectric paint and characterization of the sensors, obtained by spraying of PZT-paint on a conductive surface is described in [38]. Figure 2.17 shows the structure of a piezoelectric sensor and has a thin piezo paint film placed between two conductive surfaces as a plate capacitor. After poling the piezoelectric coating by applying a high electric field, the sensors can be used for stress measurements like strain gauges.

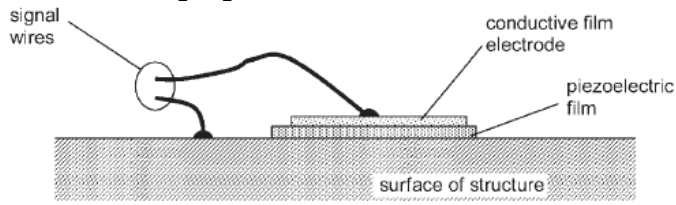


Figure 2.17 Structure of the piezoelectric paint sensor

In [38] is presented a study about the dynamic of piezopaint sensors, exemplified of two samples with the sizes 5x10 mm and 8x10 mm. The measurements of bending strain for tested frequencies between 3-1000 Hz and amplitudes of 10-300 $\mu\epsilon$ (representing typical ranges for vibration applications), shows a sensitivity in the range of ± 3 dB. In Figure 2.18, the dynamic range of these two sensors is 1,5 decades over the full frequency range. The y-axis represents the non-dimensionalized sensitivity, normalized for reference conditions taken as 50 $\mu\epsilon$ and 50 Hz and relative to the signals of a strain gauge, placed in the same position on the bending beam like piezopaint sensors.

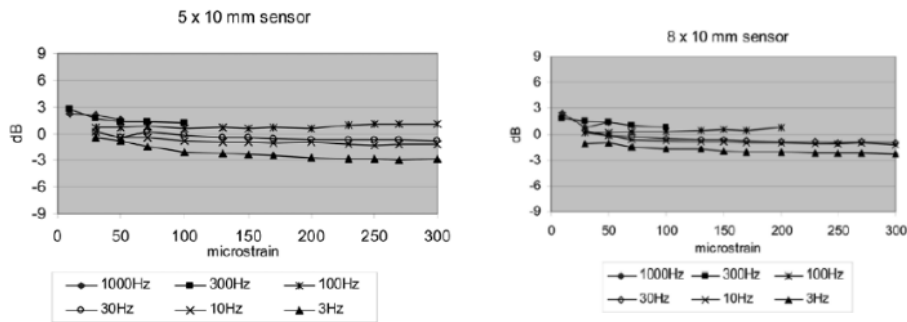


Figure 2.18 Dynamic range of piezo paint sensors

For testing a real application for vibration sensors, a piezopaint sensor has been placed on the Millennium Footbridge over the River Tyne between Gateshead and New Castle in England. The sensor is placed behind an inspection cover, protected from rain to prevent corrosion of the signal wire connections of the electrodes, but exposed to damp and cold. The measurements over more than two years show good functionality of this sensor.

In [99] was studied the functionality of a piezoelectric paint sensors after introducing it in water and salt solution, to test how the behaviour of these sensors to rain or other environmental conditions when used for measurement in different situations. In these experiments, piezoelectric sensors were introduced in water for various periods of time, up to one day, and allowed to dry completely before measuring the stress of a bending beam.

At first, the piezoelectric sensors were poled and their sensitivity was recorded using a charge amplifier as a voltage V_0 . Then, the sensors were immersed in water or salt solution for couple hours, then removed and placed in the test rig and connected to the charge amplifier. The sensitivity of the sensors was recorded after couple of minutes and normalized with the voltage V_0 . Figure 2.19 shows the normalized sensitivity which falls almost linearly with the drying time for two sensors introduced in water for one hour (curve A) and three hours (curve B). Figure 2.20 presents the measurement results obtained with a sensor that was immersed for three hours in water (curve a) and after a drying out time, immersed in a potassium iodide solution (salt solution) (curve b). Test results showed that the piezoelectric paint sensors recovered their functionality after immersing in water or salt solution and after a drying out period.

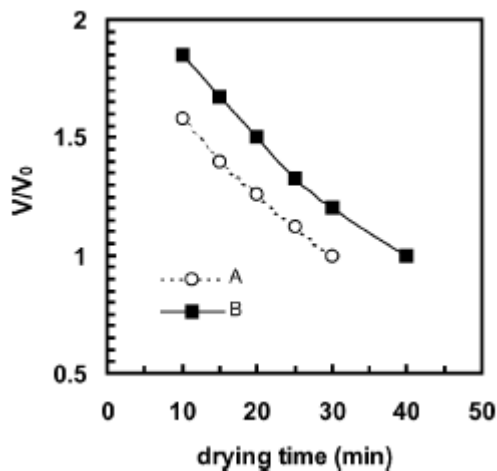


Figure 2.19 Sensitivity of sensors versus drying time characteristics after introducing in water for 1 hour (A) and 3 hours (B)

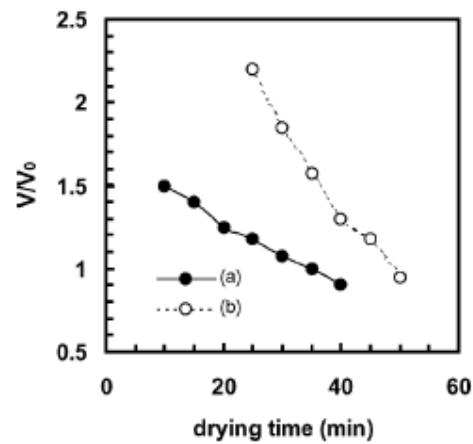


Figure 2.20 Voltage versus drying time characteristics of a sensors first introduced for 3 hours (a) and then for 1 hour in salt solution (b)

Other fundamental works of Professor Hale, which had a contribution to the development of piezoelectric paint sensors for measuring forces and pressures in roller systems are [37] and [89].

In paper [141] there is presented a study on using a two-dimensional phased sensor array based on piezoelectric paint for the detection of damage on thin aluminium panels. The sensors have cruciform, circular and spiral shape as shown in

Figure 2.21. After simulating these three sensors, the spiral sensor was successfully tested in a laboratory environment for detecting various types of damage (hole damages, crack damages).

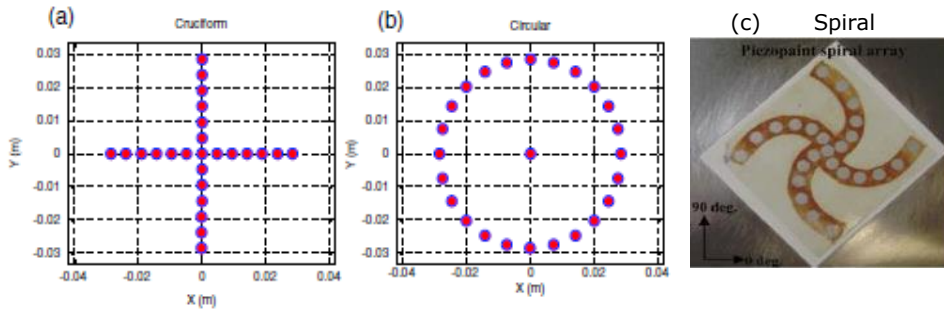


Figure 2.21 Sensor array configurations (a) cruciform, (b) circular, (c) spiral

Other types of thin piezoelectric sensors uses polyvinylidene fluoride films with similar effect as piezopaint when applied between two conductive plates and polarized with an electric field. These sensors have a low sensitivity and can be used e.g. for measuring the pressure in the shoe sole to determine the medicine problems of the foot [139], as shown in Figure 2.23 or for measuring dental occlusion [69]. Kreßmann studied in [56], [57] and [58] the properties of piezoelectric polyvinylidene fluoride (PVDF) and its application as sensors and actuators. Mirow uses polarised PVDF film sensors for measuring pressure [80] (e.g. in dental impression, pull bar bending forces caused by an InterCity train).



Figure 2.22 PVDF sensor



Figure 2.23 Pressure measurement with PVDF sensor in a shoe sole

2.4. Current State

The starting point of this research work is the current development level of coating and printing machines produced in Germany, e.g. a machine for coating photo

paper and a flexographic printing machine for printing models of different materials (paper, plastic etc.). The technical characteristics were given by the industrial partners in the project "Active vibration damping of roller systems", which develops printing machines or works with roller systems. They gave two test setups to be used for research works to develop new force sensors and to find new possibilities to reduce roller vibrations.

2.4.1. Test Setup Simulating a Coating Machine

The first test setup presented here is a roller system simulating a coating machine as shown in Figure 2.24. It is used for testing the sensors. The goal is to find an adequate sensor for measuring vibration of the roller, by applying it on the surface of the roller, without affecting the technological process.

It contains a pneumatic cylinder (4) which presses the load roller (1) against the rubber coated roller (gap roller) (2) by applying a known force to (1). Both move toward the supporting roller (impression cylinder) (3) until desired contact pressure is achieved. The force sensor (5) is the reference for the sensor's calibration used in the tests described in Chapter 4.

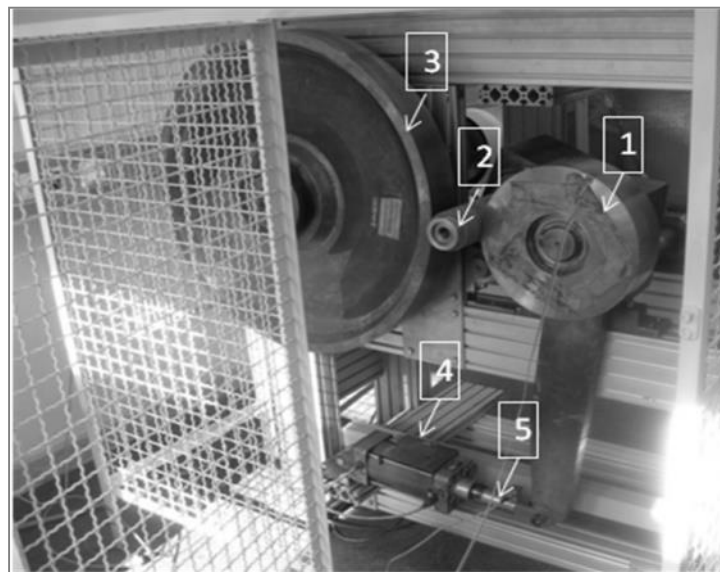


Figure 2.24 Test setup simulating a coating machine 1-load roller, 2-gap roller, 3-supporting roller, 4- pneumatic cylinder , 5- force sensor

Technical data for this roller system simulating a coating machine are:

- Line load: 180 N/mm
- Web velocity: 600 m/min
- Diameter of the pressure roller (NR): 250mm
- Diameter of the gap roller (GR): 90 mm
- Diameter of the supporting roller (SR): 750 mm

2.4.2. Test Setup Simulating a Printing Unit from a Flexographic Printing Machine

The printing unit from a “central drum” flexographic printing machine presented in [138] and Figure 2.25 represents the reference of the second industrial roller system to be considered in this work for testing of active vibration damping as described in Chapter 7. A printing unit has following components: plate cylinder (1) covered with printing plate (4), anilox roll (2), impression cylinder (3), adjusting motor for plate cylinder (9) and precision spindle for plate cylinder (8). The ink chamber (6) is applies the right amount ink (5) to a hollow profile roll which is pressed with a doctor blade and PTFE-rings against the anilox roll. In older machines, the colour is not doctored but applied by a submersible in ink metering roll, which is then pressed against the anilox roller and thus only a certain amount of ink can be transferred. Anilox roll transfers the ink to the printing plate (4) and at least the printing motif defined by printing plate is printed on the printing substrate (7) and transferred with help of impression cylinder to the ink drying station (11) and then to the next printing unit.

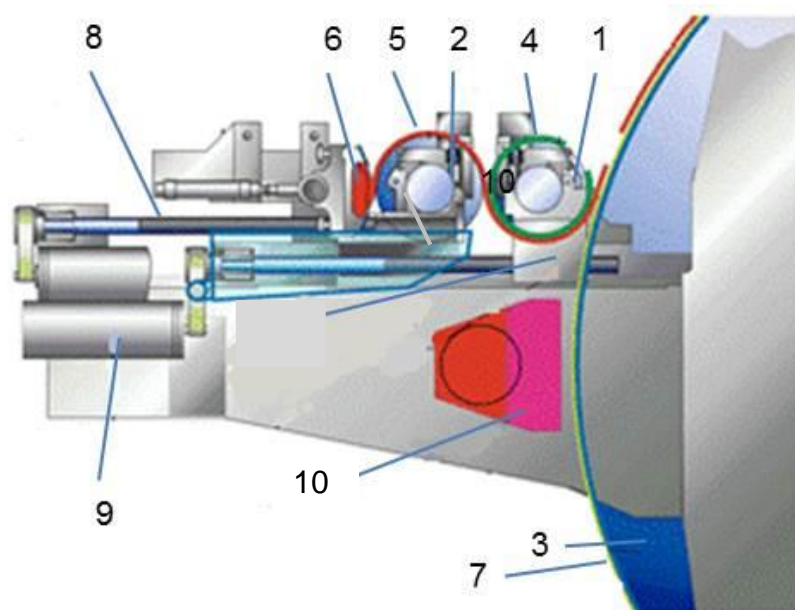


Figure 2.25 Printing process

Due to non-continuous rolling contact between rollers caused by thickness differences in the printing plate as shown in Figure 1.9, vibrational excitation appears with negative consequences in the printing process, like stripes on the printed image.

Active vibration damping is necessary to improve the quality of printing process. This has to be applied to the plate cylinder which supports the flexible printing plate and thus is primarily responsible for printing quality. The plate cylinder is also the roller with the smallest diameter in this system and is the first roller that tends to vibrate because of lowest natural frequency (see Table 2.1).

Technical data for the three-roller system is presented for each roller in Table 2.1, because this test setup was analysed in detail for adapting it to an active vibration damping. The web velocity has a value similar to the coating process, but the line load in flexo print is much less than in a coating process and has a value between 5 and 20 N/mm.




<p>Anilox roll</p> 	$f_0 = 105 \text{ Hz}$ $m = 155 \text{ kg}$ $J_s = 0,756 \text{ kgm}^2$ $D = 178 \text{ mm}$ $l_{\text{complete}} = 2174 \text{ mm}$ $l_{\text{bearing-bearing}} = 1825 \text{ mm}$
<p>Plate cylinder</p> 	$f_0 = 64 \text{ Hz}$ $m = 92 \text{ kg}$ $J_s = 0,120 \text{ kgm}^2$ $D = 102 \text{ mm}$ $l_{\text{complete}} = 2532 \text{ mm}$ $l_{\text{bearing-bearing}} = 1825 \text{ mm}$
<p>Impression cylinder</p> 	$f_0 = 272 \text{ Hz}$ $m = 280 \text{ kg}$ $J_s = 4,841 \text{ kgm}^2$ $D = 318 \text{ mm}$ $l_{\text{complete}} = 1754 \text{ mm}$ $l_{\text{bearing-bearing}} = 1621 \text{ mm}$

Table 2.1 Technical data for the printing unit

f_0 is the first natural frequency, m denotes the mass, J_s denotes the axial momentum of inertia, D is the diameter of the roller, l_{complete} is the complete length of the roller and $l_{\text{bearing-bearing}}$ is the length between the bearings.

2.5. Chapter Summary in Romanian

Acest capitol trece în revistă soluțiile existente pe piață, precum și idei patentate care au legătură cu tema acestei teze, pentru a găsi soluții pentru optimizarea comportamentului dinamic al sistemelor de valțuri.

Subcapitolul 2.1 prezintă posibilități pentru măsurarea forțelor și presiunii în sistemele de valțuri din mașinile de tipărit. Una dintre soluții este măsurarea presiunii statice dintre valțuri, în general dintre două suprafețe, prin folosirea unor folii cu particule de cerneala Prescale Fujifilm, care elimină cerneala proporțional cu presiunea aplicată. Două metode pentru măsurarea dinamică a presiunii dintre valțuri sunt prezentate în figurile 2.2 și 2.3, realizate cu ajutorul unor instalații foarte scumpe. Aceste instalații nu pot fi folosite în proiect, deoarece bugetul disponibil este limitat. De aceea este căutată o altă metodă pentru măsurarea forțelor dintre valțuri la mașinile de tipărit, cercetări care au dus la concluzia necesității folosirii unor senzori foarte subțiri, care să nu influențeze procesul de tipărit. O soluție promițătoare prezintă senzorii piezoelectrice pe baza de lac acrilic în care a fost amestecată o cantitate mare de particule piezoelectrice, prezentate în subcapitolul 2.3. Acest lac piezoelectric a fost cercetat și dezvoltat sub conducerea profesorului Hale la Universitatea din New Castle. Acesta a folosit senzori pe baza de lac piezoelectric (sau vopsea piezoelectrică) pentru măsurarea vibrațiilor ce apar în diferite sisteme, pe principiul asemănător măsurătorilor cu timbre tensometrice. Un exemplu este măsurarea vibrațiilor produse pe un pod foarte îngust din New Castle denumit Millennium Bridge.

Subcapitolul 2.2 prezintă soluții active, semi-active și pasive pentru reducerea vibrațiilor la role aflate în mișcare de rotație. De exemplu, pe lângă măsurile standard care sunt luate pentru a micșora vibrațiile, ca de exemplu balansarea dinamică a valțurilor, se regăsesc aici măsuri dinamice, realizate cu ajutorul unor elemente active sau semi-active. De asemenea, sunt prezentate diferite lucrări care se ocupă cu dezvoltarea algoritmilor de reglare, pentru reducerea activă a vibrațiilor prin intermediul sistemelor de comandă în timp real. Acestea pot fi aplicate folosind elemente active, ca de exemplu actuatori piezoelectrice, magnetici sau hidraulici, în funcție de dinamica necesară și sistemul în care se acționează. Actuatorii piezoelectrice pot crea forțe foarte mari și pot lucra la frecvențe de ordinul kilohertzilor. Ei pot însă crea deplasări foarte mici, ceea ce îngreunează reducerea vibrațiilor cu amplitudini mari.

În ultima parte a capitolului 2, respectiv în paragraful 2.4 sunt prezentate două standuri industriale folosite în acest proiect. Unul dintre ele este prezentat în figura 2.24 și reprezintă modelul unei mașini de acoperire a unui material cu un strat protector (de exemplu: acoperirea hârtiei cu un strat de ulei special pentru obținerea hârtiei fotografice). Al doilea stand de încercare industrial se află în centrul acestei teze și reprezintă o unitate de printare dintr-o mașină de tipărit flexografică. Datele tehnice ale celor două standuri de încercare arată asemănări în ceea ce privește viteza de mișcare a materialului de acoperit/imprimat, rezonanțele valțului din mijloc (care prezintă cel mai mic diametru, fiind astfel primul valț ce începe să vibreze), precum și la alcatuirea sistemului de trei valțuri. Diferențe mari se regăsesc la valorile de linie de încărcare, care este de circa 180 N/mm la mașinile de acoperire și de numai 5-20 N/mm la mașinile de tipărit. O altă diferență constă în natura vibrațiilor ce apar în aceste sisteme. La mașinile de tipărit, o sursă suplimentară de vibrații este contactul variabil dintre valțuri cauzat de matrita de tipărit. Aceste vibrații vor fi simulate în capitolul 5 și compensate în capitolul 6 și 8, cu ajutorul unor lagare cu actuatori piezoelectrice, dezvoltate în capitolul 7.

3. INTRODUCTION TO PIEZOELECTRIC SENSORS AND ACTUATORS

Piezoelectricity was first discovered in 1880 by the Curie brothers during examination of the crystal Tourmaline. It is the characteristic of some crystals to generate electrical charges by applying a mechanical pressure. The name piezoelectricity comes from the Greek word "piezo" meaning "pressing". The so-called direct piezo effect can be found in a wide range of applications. It is used nowadays in sensor applications for measuring dynamic processes, e.g. vibrations, forces, pressures, stress and accelerations, but also for flowmeters, and lighters. The direct piezo effect has an inverse counterpart. Voltage applied across the crystals creates mechanical deformation in the piezoelectric material. This is called the inverse effect and it is found in actuators for generating forces and displacements, e.g. for damping vibrations or as piezo-controlled injection valves in automotive technology, loudspeakers and ultrasonic cleaner. Piezoelectric elements are available in different sizes and shapes on the market.

This chapter presents basic information about piezoelectric sensors and actuators, based on PZT-ceramics (Lead Zirconate Titanate), used for the applications in this work.

3.1. Manufacturing Process

Piezoelectric elements are manufactured from different materials as Pb, Zr, Ti, transition metals, alkalis, quartz etc. by mixing and solid state reactions.

A typical flowchart for the production of piezoelectric elements after [111] is given below and shows the steps for the beginning until the moment when the element has piezoelectric properties and can be used as sensor or actuator.

As presented in Figure 3.1, after sintering PZT-ceramics have no piezoelectric properties. The ceramics shows a random orientation in the structure (Figure 3.2 left) until a strong electric DC field of several kV/mm is applied which causes an alignment to the polarity field (Figure 3.2 right). This process called polarisation needs to be done just once, sometimes at elevated temperature. In the literature are found values between 1-15 kV/mm depending on the material and the application of the sensors. After that, the PZT-material memorizes the direction of polarisation and changes dimensions when applying an electric field.

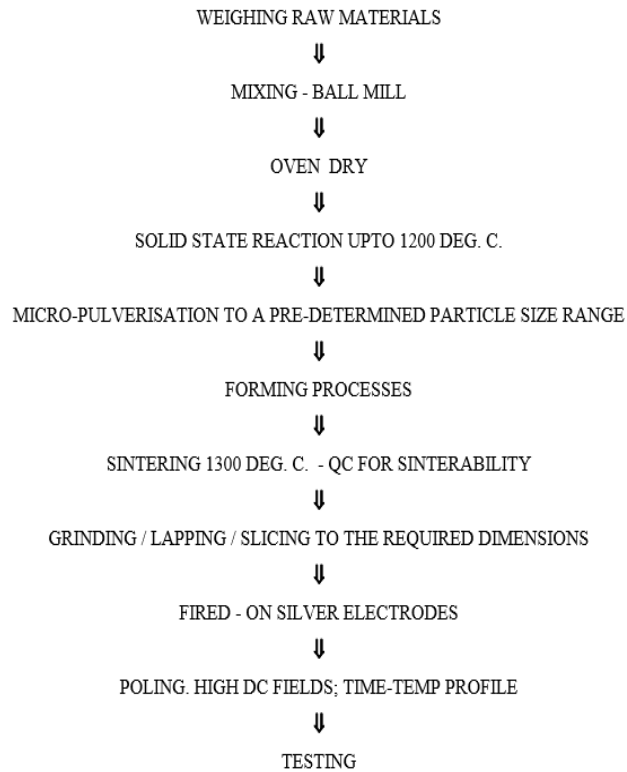


Figure 3.1 Flowchart for the production of piezoelectric elements

3.2. The Piezoelectric Effect

The relationship between the applied stress and the resulting response depends on the piezoelectric properties of the ceramic material, the size and shape of the piezo element, and the direction of the mechanical and electrical direction.

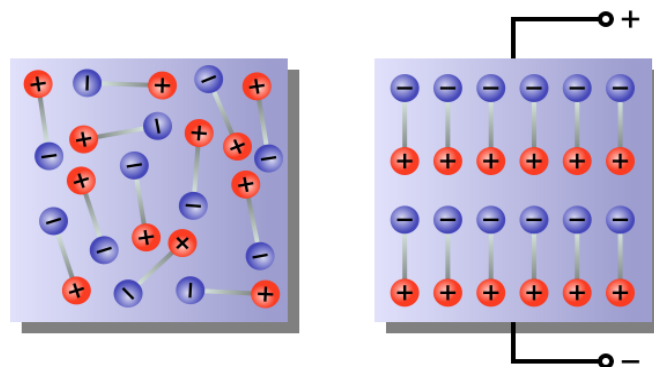


Figure 3.2 Piezoelectric structure (left- before and right- after polarization)

In Figure 3.3 [111] a piezo element is depicted with three orthogonal axes, for identifying the directions and effects which can appear. Material properties in directions 1 and 2 are identical, but different from those in direction 3 which is the poling axis. The arrow P shows the direction of polarisation in the element from the positive to the negative poling electrode (the electrodes are the grey surface and the surface opposite to it).

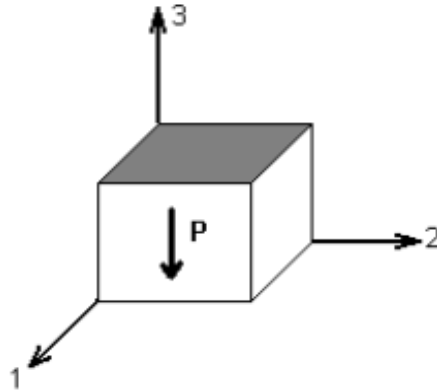
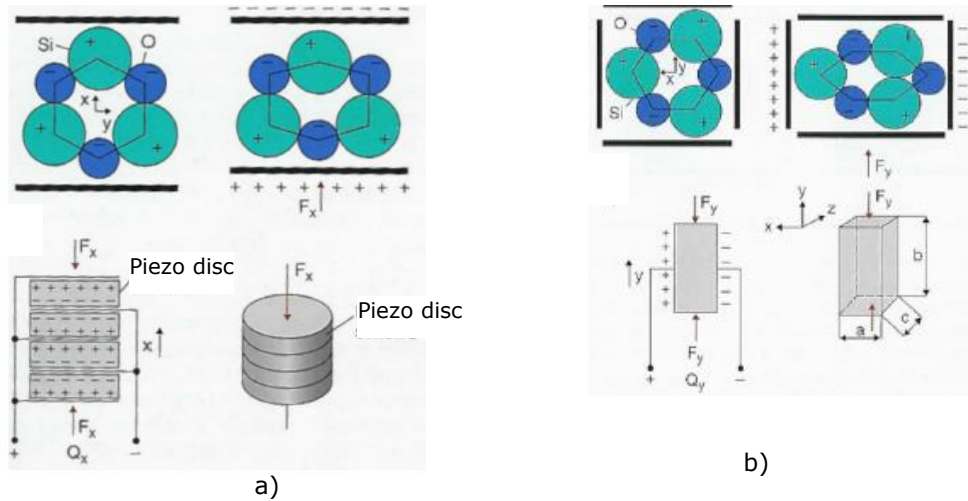


Figure 3.3 Axes of a piezo element

Depending on the alignment of the PZT-crystals, different effects can be achieved as shown on example of a piezo element from the company Kistler [6] in Figure 3.4:

- longitudinal effect: the mechanical stress and the electrical field are both along the polarisation (Figure 3.4 a). It is used e.g. in sensors for measuring forces, pressure, strain, acceleration, but also in piezoelectric stack actuators.
- transversal effect: the mechanical stress is applied perpendicular to the polarisation axis, but the voltage appears in the direction of the polarisation (Figure 3.4 b). This effect is used in some pressure sensors.
- shear effect: the electric field appears on the surface of the piezo element when applying shear forces on it (Figure 3.4 c). It can be found e.g. in acceleration sensors.

undeformed element deformed element undeformed element deformed element



undeformed element deformed element

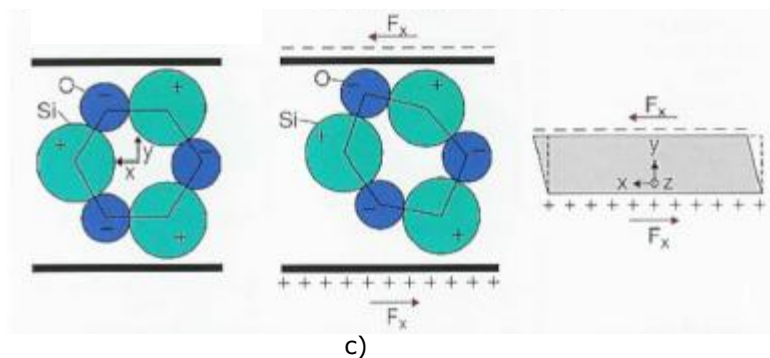


Figure 3.4 Effects of piezoelectric elements

The piezoelectric charge coefficient, known as piezoelectric constant d is an important parameter of a piezo element. It defines the sensitivity of the piezo element as charge density per stress unit and is measured mostly in pC/N.

In this work, piezoelectric sensors are developed, as described in the next chapter. They use the so-called longitudinal effect, where the mechanical force applies parallel to the charge direction. For active vibration damping piezoelectric stack actuators are used.

Due to the brittle nature of ceramics, a stack actuator or sensor using the longitudinal effect should not be exposed to tensile forces. This implies that for dynamic applications a preload force is necessary that compresses the element and can be realized in general by the use of an elastic element like a spring.

Generally, the piezoelectric effect is described mathematically with two coupled equations as combined effect of Hook's Law and the electrical behaviour of the material as follows [50]:

$$\begin{aligned} S &= s^E \cdot T + d^T \cdot E \\ D &= d \cdot T + \varepsilon^T \cdot E \end{aligned} \quad (3.1)$$

The strain tensor S and the electric charge displacement vector D of the piezoelectric element depend on the mechanical stress tensor T caused by external forces, and the electric field vector. The coefficient s^E is the elastic compliance matrix when subjected to a constant electric field. d is the piezoelectric constant matrix and ε^T is the permittivity measured at constant mechanical stress. d^T is the transposed matrix of d . The piezoelectric effect decreases with increasing temperature and vanishes above the so-called Curie temperature. This limits the use of piezoelectric ceramics to temperatures below around 120 °C.

3.3. Piezoelectric Sensor

The direct effect signifies that when loaded with a force, the sensor produces an electric charge proportional to the force and is measured in pC (Picocoulomb, $1\text{pC}=10^{-12}\text{ C}$).

Compared with other types of sensors piezoelectric sensors have some advantages:

- high sensitivity
- high natural frequency
- large measuring range
- high dynamic
- long life
- displacement-free measurement

By applying a force F to the piezoelectric crystal with a capacity C and a piezoelectric constant d results an electrical charge Q . The electric charge generated by sensors using the three effects presented in Figure 3.4 can be calculated as follows [6]:

$$\begin{aligned} Q_x &= F_x \cdot d \cdot n \text{ for longitudinal effect} \\ Q_y &= -F_y \cdot d \cdot \frac{b}{a} \text{ for transversal effect} \\ Q_x &= 2 \cdot F_x \cdot d \cdot n \text{ for shear effect} \end{aligned} \quad (3.2)$$

with:

- n : the number of piezoelectric elements,
- a, b : the geometric dimension,
- F_x, F_y : the applied load forces in direction x , respectively y

If electrodes are connected to opposite surfaces of an element, the charge generates a voltage:

$$U = \frac{Q}{C} = \frac{F \cdot d}{C} \quad (3.3)$$

with

$$C = \varepsilon_0 \cdot \varepsilon_r \cdot \frac{A}{\Delta} \quad (3.4)$$

for a sensor using the longitudinal effect like a plate capacitor, where ε_0 is the dielectric constant of the vacuum and ε_r is the relative permittivity of the dielectric with a thickness Δ and A the surface of the sensor.

For the evaluation of measurements with piezoelectric sensors, the small generated electric charge must be converted to a voltage or a current with an amplifier.

3.4. Piezoelectric Actuator

For actuation, electrical energy is converted into a mechanical reaction. The energy content W of any actuator depends only on the active piezoceramic volume with the capacity C and the applied electrical voltage U and can be expressed as $W = \frac{1}{2}CU^2$. Piezoelectric actuators can move high masses, but the displacements are small, at most, in the μm - range. A solution to obtain larger displacement range is presented in Figure 3.5 [10]. Two piezoelectric actuators are placed in horizontal direction. They are polarized in opposite directions and by applying an electric voltage, they can move the elastic construction along their axis and in the same generate large displacement in the perpendicular direction.

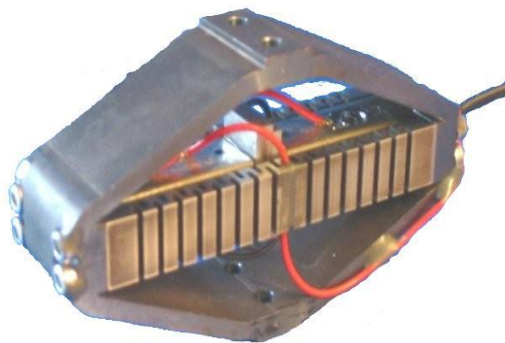


Figure 3.5 Large displacements with actuator

A stack actuator is composed of lots of thin piezoelectric discs, applied between metallic electrodes as shown in Figure 3.6 [91]. It may generate forces of several kN and produce displacements in the μm range. The coupling of the actuator to the driven mechanical assembly therefore must be rigid and backlash-free. Ideally, the actuator's end face is in direct contact with a metal surface. The preload force should be equal to at least one-half of the blocking force.

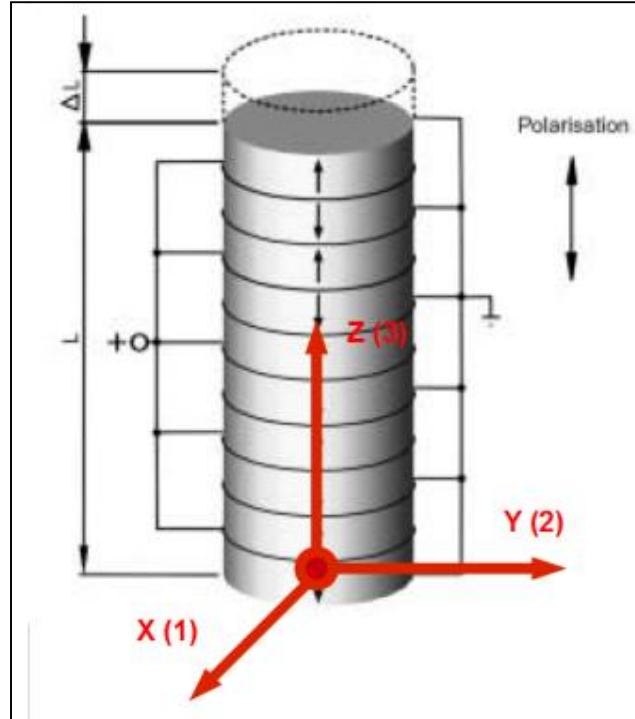


Figure 3.6 Piezoelectric stack actuator

For a stack actuator with linear material properties, the equations (3.1) can be simplified from matrix in scalar equations as follows:

$$S_3 = \frac{\Delta l}{l_0} = s_{33}^E \cdot T_3 + d_{33} \cdot E_3 \quad (3.5)$$

$$D_3 = d_{33} \cdot T_3 + \varepsilon_{33}^T \cdot E_3$$

using scalar values for the coefficient of elasticity for longitudinal effect s_{33}^E , dielectric constant d_{33} and permittivity ε_{33}^T . For the piezoelectric actuator PSt 1000/35/200 VS45 from manufacturer Piezomechanik, the constants are known from the manufacturer as follows: $s_{33}^E = 22 \cdot 10^{-12} \text{ m}^2/\text{N}$, $d_{33} = 680 \cdot 10^{-12} \text{ C}/\text{N}$, $\varepsilon_{33}/\varepsilon_0 = 3800$. Piezoelectric actuators can be modelled as a mechanical spring with constant stiffness, which can be calculated taking into account the stiffness (or force constant) of the ceramic plates and is proportional to the cross section A of the actuator. The stiffness decreases with increasing actuator length:

$$k_T^E = \frac{A}{s_{33}^E \cdot l_0} \quad (3.6)$$

In reality, the number of functional parameters is higher. It is important to keep the high of the piezoelectric actuator as small as possible for having high stiffness.

The actuator specifications are provided by the manufacturer in [92] and [93] and presented in Table 3.1:

	Actuator name		PSt-HD 200/10/90 VS15 (small test setup)	PSt 1000/35/200 VS45 (industrial test setup)
	Manufacturer		Piezomechanik GmbH	Piezomechanik GmbH
Name	Symbol	Unit		
Voltage	U_A	V	Range: 0 → 200	Range: 0 → 1000
Blocking force	F_{Al}	N	2000	70000
Pre-load force	F_{Av}	N	800	6000
Maximum generating force	F_{Ag}	N	1800	30000
Blocking force	F_{Al}	N	2000	70000
Maximum displacement	Δl_A	μm	90	200
Length of the actuator (active part)	l_A	mm	83 (65)	202 (165)
Diameter	D_A	mm	15	45
Capacity	C_A	nF	9000	6500
Stiffness	k	N/ μm	30	150
Resonance frequency	f_{A0}	kHz	6	4

Table 3.1 Technical data for piezoelectric actuators

Some works deal with studies about applications with piezoelectric actuators and their mathematical modelling e.g. [3, 5, 14, 33, 51, 103 and 140].

3.5. Chapter Summary in Romanian

Capitolul 3 prezinta o introducere in lumea senzorilor si actuatorilor piezoelectrice, elemente care constituie focusul acestei lucrari. In figura 3.1 este prezentat ciclul prelucrarii elementelor pana la obtinerea efectului piezoelectric. Acest efect se obtine cu ajutorul unor materiale (de exemplu PZT -Plumb-Zirconiu-Titan) care constituie dielectricul intre doua placi conductoare, realizand astfel un condensator plan. Pentru a obtine un element piezoelectric, este necesar ca acesta sa fie polarizat, ceea ce inseamna ca se aplica o singura data un camp electric continuu cu valori ridicate (intre 1-15 kV/mm) pentru o anumita perioada de timp si la o temperatura care de obicei este inalta, pentru a da posibilitatea cristalelor sa se orienteze in directia dipolilor (figura 3.2).

Efectul piezoelectric inseamna ca la aplicarea unei sarcini mecanice (de exemplu o forta), are loc o deplasare de sarcina electrica si se genereaza in acest fel o tensiune electrica. Acest efect este folosit la senzori, pentru a percepe marimi dinamice ale unui sistem. Senzorii piezoelectrice realizati cu ajutorul cristalelor ceramice PZT pot prezenta trei efecte: efect longitudinal, transversal si de forfecare, care pot fi folosite in diverse aplicatii, in functie de necesitatea masurarii sau compensarii unei marimi. Aceste fenomene sunt exemplificate in figura 3.4 pe senzori piezoelectrice de la firma Kistler. Un element piezoelectric poate fi folosit ca senzor, cand in momentul aplicarii unei sarcini mecanice genereaza o sarcina electrica si prin acest lucru, o tensiune electrica. Daca la dipolii elementului piezoelectric se aplica o tensiune electrica

alternativa, atunci aceste elemente, genereaza sarcini mecanice (de exemplu forte) proportionale cu tensiunea aplicata si se numesc actuatoare. Acest efect este folosit pentru reducerea vibratiilor in diferite aplicatii, datorita frecventelor inalte la care pot lucra si in acelasi timp a dinamicii bune a elementelor.

In general descrierea matematica a elementelor piezoelectrice se poate face prin doua ecuatii prezentate in forma matriceala in (3.1), una pentru descrierea elongatiei si una pentru calcularea deplasarii dielectrice. Aceste ecuatii sunt cuplate intre ele si sunt dependente de caracteristicile materialului, precum si de sarcina mecanica si campul electric.

In cadrul celor doua standuri de incercare descrise in capitolul 7 din aceasta lucrare (model si unitate de tiparire dintr-o masina flexografica), au fost folositi actuatoare piezoelectrice de la Firma Piezomechanik din Germania pentru amortizarea vibratiilor in sistemele de valturi. Acestea folosesc efectul longitudinal (figura 3.6) si pot genera forte pana la 1.800 N (stand de incercare mic), respectiv 30.000 N (stand de incercare industrial) si deplasari pana la 90 μm , respectiv 200 μm .

4. DEVELOPMENT OF PIEZOELECTRIC PAINT SENSORS

This chapter presents tests and results with the new developed piezoelectric paint sensors. These results are obtained during the research work on this thesis and published in [121], [125] and [126].

4.1. Motivation

In Section 2.1 different technologies for measuring roller vibrations were presented. To develop a sensor to measure forces along the nip during the printing or coating operation, some requirements are needed:

- the sensor must be thin and applicable to curved surfaces without affecting the quality of printing image in the flexography;
- the sensor should be able to measure the rapid change of the pressure in the nip;
- the sensor's characteristics must be stable and repeatable with low hysteresis;
- the sensor should be able to detect the contact forces in the nip, by applying it underneath the printing plate made of rubber, plastic, or some other flexible materials;
- the sensor should be relatively easy to produce, inexpensive and robust.

Taking into account this requirements, piezoelectric and piezo resistive sensors were tested for measuring nip pressure on the roller without obtaining promising results for long-time measurements as follows (Figure 4.1, Figure 4.2):

- piezoelectric discs (1) [11]
- piezoelectric films (3) [110]
- strain gauges (2) (piezo resistive sensors)

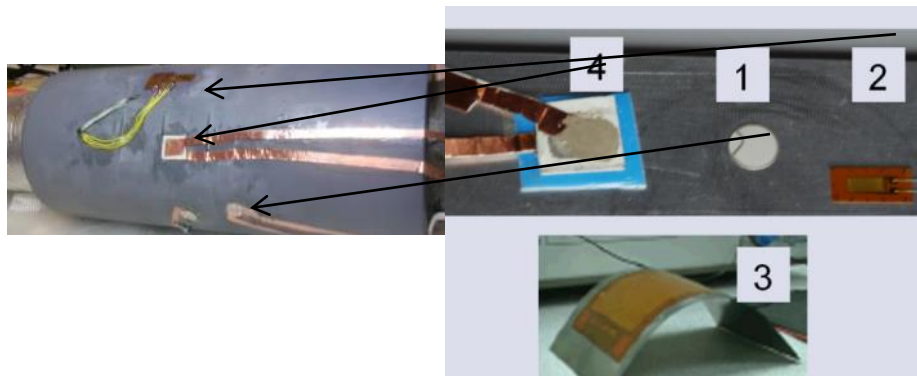


Figure 4.1 Roll with piezoelectric paint sensor, piezoelectric discs and strain gauges

Figure 4.2 Different types of sensors for measuring nip forces

First measurement results with three different types of sensors presented in Figure 4.2 are shown in Figure 4.3 and Figure 4.4.

50 4. Development of Piezoelectric Paint Sensors

The piezoelectric film sensor (3) was applied on the load roller (1) (see the test setup presented in Figure 2.24). It shows good repeatable results. Figure 4.3 presents measured results of the sensors in Volt when rotating the load roller to the left (negative signal, e.g. second 372 to second 375) and when rotating to the right (symmetrical amplitude, e.g. second 377 to second 379). These sensors were destroyed after a short time by the high pressure between rollers and cannot be applied on surfaces with small curvature radius.

Another measurement of the nip pressure was made using strain gauges. In Figure 4.4, the results of the pressure measurement with strain gauge used in a new way (applied on the load roller and pressed directly on it) is presented. The strain gauge also was destroyed after short time.

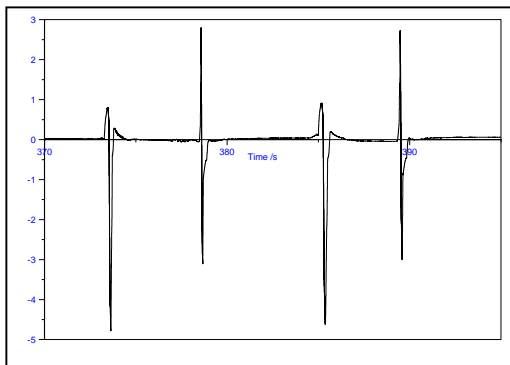


Figure 4.3 Measurement with piezoelectric film sensor

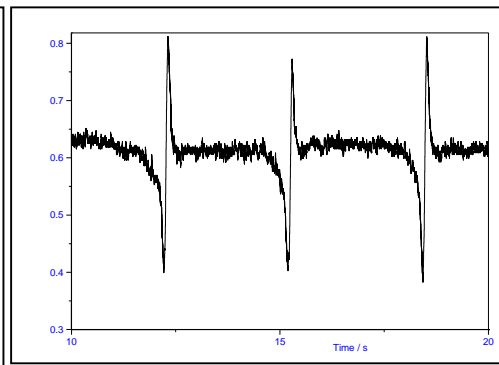


Figure 4.4 Measurement with strain gauge

The signal of the piezoelectric discs was not repeatable although nip pressure was kept constant. The reason may be that the discs are brittle and cannot be fitted exactly to the roller surface so that there is no defined contact between the rubber coating and the discs. Therefore, the results are not presented.

In [125] different sensors for measuring nip pressure are tested and compared, but it was not found an optimal solution for this purpose using a limited budget. Only the piezoelectric paint developed by Prof. Hale from University New Castle upon Tyne seemed to have potential to be a good solution for this difficult measurement problem. Sensors based on piezoelectric paint are new and not available on the market. Also in the literature limited information on this topic is to be found. Because of the novelty and wide application area of these low-cost sensors, which can be easily integrated into force flow, it is important to investigate the advantages of such sensors and to demonstrate their potential applications.

The new developed piezoelectric sensors are compared with the standard sensors mentioned above. The advantages and disadvantages are given in Table 4.1:

Nr.	Sensor	Advantages	Disadvantages
1	piezoelectric disc	<ul style="list-style-type: none"> • inexpensive • available on the market 	<ul style="list-style-type: none"> • nonlinearity • high voltage signals • piezoceramics are brittle
2	strain gauge	<ul style="list-style-type: none"> • flexible • available on the market • well known technology 	<ul style="list-style-type: none"> • pressing directly on the sensor is no standard application

3	piezoelectric film	<ul style="list-style-type: none"> flexible and very thin available on the market 	<ul style="list-style-type: none"> ceramics can be deteriorated by pressing directly on the sensor
4	piezoelectric paint	<ul style="list-style-type: none"> flexible, can be sprayed on any conductive surface, will not affect the quality of printing image 	<ul style="list-style-type: none"> complicate procedure to make a sensor each sensor sensitivity have to be measured is not available on the market no datasheet

Table 4.1 Comparison of various types of sensors

The most important feature of the sensors for our application is that they have to give a reproducible signal, depending on the pressure in the nip of the rollers. We tested all sensors with different pressure levels.

Figure 4.5 shows that piezoelectric paint fulfils these requirements in a good way. In Figure 4.5 is depicted the measurement of the nip pressure between rollers (measurement of one small area) with the help of a new developed piezoelectric paint applied on the gap roller (2) underneath the rubber coating in the test setup from Figure 2.24. On the y-axis are represented the sensor's signals in Volt, amplified with a charge amplifier from Kistler Company. The pneumatic cylinder (4) presses the load roller with two different pressures when the rollers rotate. In the first and the fourth zone, the nip pressure increases slowly when the rollers are coming in contact and after that, a constant value is measured with every rotation (zone ② and ⑤). Zone ③ shows a smaller nip force when the contact between rollers decreases until it disappears. In the case of the second measurement, the rollers rotate just for a short time because of the low angular velocity and the high moment of inertia. The angular velocity is smaller in zone ⑥ and appears a similar phenomena like in ③.

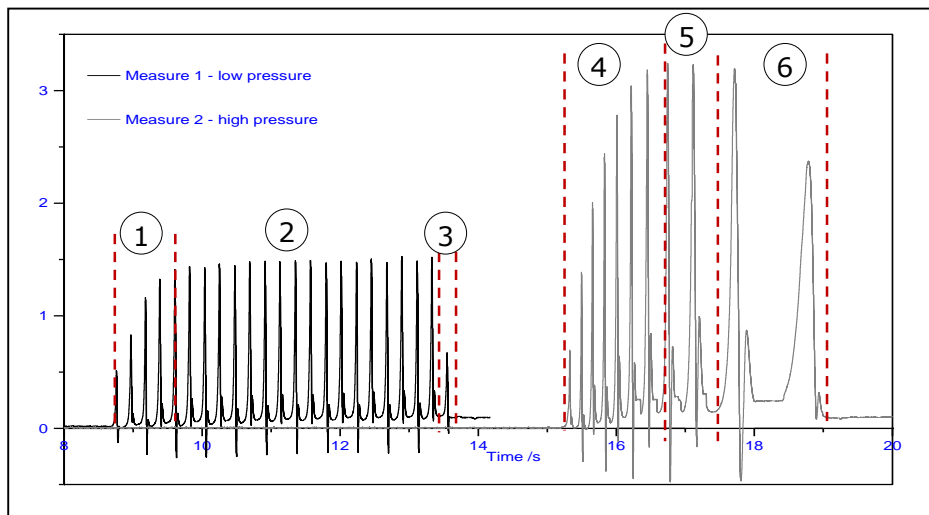


Figure 4.5 Piezoelectric paint – the nip pressure is first increasing and then decreasing

The piezopaint sensor used for these measurements had a thickness of 90 μm , polarized with an electric voltage of 300 V at room temperature of 25°C.

4.2. Fundamentals

Water-based acrylic lacquer with a high concentration of PZT particles was developed and the composition was improved during more years from Professor Hale. Fundamental works of him presented in Section 2.3 give the start for developing the sensors for the application in the roller systems. Various applications e.g. measuring of the vibrations on the Millennium Bridge in New Castle upon Tyne were successful tested. The key component of the sensor is the PZT powder which gives at the end the piezoelectric properties of the sensor.

According to [29], piezoelectric materials are usually crystals such as quartz and tourmaline or polycrystalline piezoceramics. PZT films can usually be generated by sputtering or sol-gel technology. However, these methods are relatively expensive because special equipment is needed. Piezopaint tried to simplify the film formation, so that the production of piezoelectric layers is cheaper. Moreover, the paint can be applied on a non-planar surfaces with 3-dimensional bending or on rough surface.

The storage life of the paint is limited because the PZT particles tend to settle and because there are some chemical reactions between PZT particles and the paint too. According to [136], it is necessary to mix the colour for half an hour with high shear agitation, but not stirred too fast, otherwise the temperature in the solution raises and the water evaporates, causing the paint dry.

Important works for the development of piezoelectric paint are also [14, 16, 28, 37, 39, 53, 60, 65, 89, 116, 118], not only for the developing method, but also for measuring with piezoelectric sensors.

Before the piezoelectric paint can be used as a sensor, the PZT particles must be oriented by polarization with a voltage of 5-10kV per millimetre of thickness [136]. Only after this step, the sensor can measure pressure or forces by generating an electrical charge proportional to the load. Examples of the piezoelectric properties of PZT are shown in Table 4.2 after [129]:

Piezoelectric properties of PZT		
material	piezoelectric coefficient d_{ij} in 10^{-12} m/V	relative dielectrical constant ϵ_{ij}^r
PZT	$d_{31} = -94 \dots -275$ $d_{33} = 80 \dots 593$	$\epsilon_{11} = 1730$ $\epsilon_{33} = 1700$ (425...1900)

Table 4.2 Material properties of PZT

4.3. Layout of a Piezoelectric Paint Sensor

A piezoelectric force sensor based on piezoelectric paint has a layout as shown in Figure 4.6.

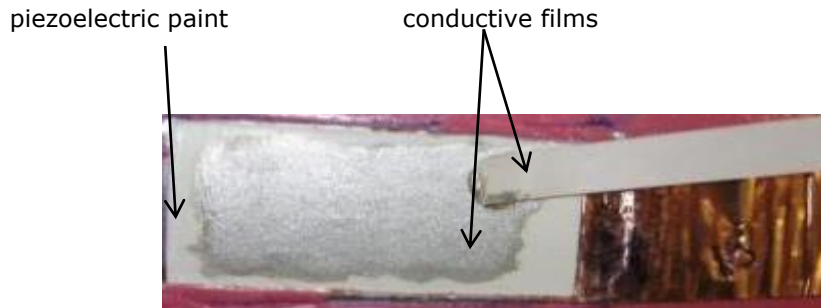


Figure 4.6 Layout of a piezoelectric paint sensor

The main part of a sensor is the piezoelectric paint. This is applied as a thick film on a conductive layer (e.g. steel roller). If the object that is to be measured is not conductive, a conductive electrode has to be applied before the piezoelectric paint is applied. Another electrode must be applied on the other side of the piezoelectric paint layer. This layer defines the size of the sensor which means that the output signal is proportional to the average pressure on the surface of this electrode.

With that setting the piezoelectric paint sensor is a plate capacitor, where the piezoelectric paint is the dielectric. So the capacity of the sensor C can be calculated with the formulas (3.3) and (3.4) mentioned in Chapter 3 and is greatest in devices made from materials with a high permittivity ε , large plate area A and small distance between electrodes Δ .

Solving this equation reveals that capacitance increases with area and decreases with the thickness of the dielectric field. Because the capacity is constant, the voltage U is defined as a line integral of the electric field E between the plates rises with increasing electric charge displacement:

$$U = \int_0^{\Delta} E dz = \int_0^t \frac{\rho}{\varepsilon} dz = \frac{\rho \cdot \Delta}{\varepsilon} = \frac{Q \cdot \Delta}{\varepsilon \cdot A} \quad (4.1)$$

where:

$E = \frac{Q}{\varepsilon A} = \frac{\rho}{\varepsilon}$ is electric magnitude

$\rho = \frac{Q}{A}$ charge density

ε permittivity

As carrier material for sensor's manufacturing is used steel sheet and self-adhesive copper film, so that the sensors can be tested in both ways presented in Figure 4.6 and also on non-metallic or non-stainless materials.

For the manufacture of a piezoelectric paint sensor, the following steps are necessary:

1. After a very good cleaning of conducting surface, a defined color layer is applied to the copper film with appropriate and automated technology.
2. After 24 hours, in the next step, a conductive layer with silver paint is applied to the piezo paint. After that, the second electrode is contacted with silver paint by using conductive 2-component epoxy.
3. In the last step, the sensors are connected for a defined period to a high DC voltage to be polarized, that's means that the PZT-crystals are oriented in the measure position.

The automated process of coating is necessary because the piezoelectric layer has to be uniform and the layer thickness has to be manufactured in a repeatable way. An uneven coating leads to location-dependent measuring signals and increases the probability that a short-circuit occurs in the sensor during polarization, which will disturb the sensor.

4.4. Development of Piezoelectric Sensors with Defined Piezo Paint Thickness

For manufacturing the piezoelectric layers with constant thickness, several options were examined as follows:

- colour distribution using vibration plate
- spin coating
- screen printing
- coating with a doctor blade

Good results have been achieved by spraying and coating with a doctor blade, first by hand and then with help of a KUKA KR3 robot in the laboratory.

Spraying with the paint gun has a very high paint consumption when spraying only small surfaces like sensors. The prepared piezoelectric paint is usable just for short time and only a limited amount of trial paint was available for the experiments. Some alternatives have been examined to optimize the spraying process.

A flow cup gun SATA minijet 3000 B HVLP with a nozzle aperture of 0.8 mm was used for spraying. The flow cup is screwed onto the gun body. The paint flows by gravity toward the exit and then is swept up by the airflow and atomized, so that it is realized a complete emptying of the flow cup.

The gun check rail and their settings are important factors to achieve a uniform thickness of the piezo paint on a surface. When painting, it is especially important to pay attention to the support of the spray gun and its relative position to the surface to be sprayed. The distance of the spray gun to the workpiece and the angle between the spray cone and workpiece are two important factors, as well is a smooth movement of the hand and a defined distance of 10-15 cm between spray gun and workpiece to get a uniform paint.

The sensors are manufactured in the laboratory, where the robot moves the workpieces and the spray gun relative to each other. The painting with PZT-paint is done in a special housing as shown in Figure 4.7, which has to fulfil following functions:

- protecting the surrounding air from spray and dirt mist by encapsulation of the painting process and extraction of excess colour
- maintaining the correct position and orientation of the spray gun in the housing

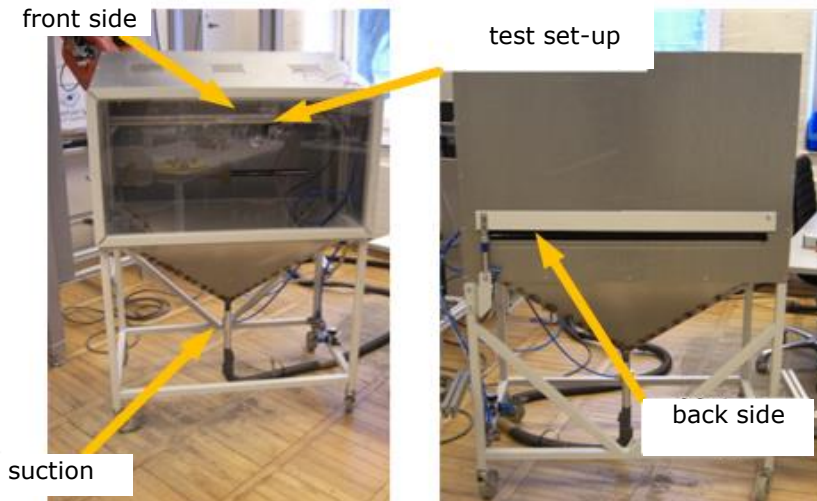


Figure 4.7 Housing for spraying the PZT-paint

After analysis of advantages and disadvantages, the housing has been designed and presented in [43] so that the workpiece is moved by the robot, which leads the raw sensors on a slide into the housing, under the spray gun and back out of the housing.

The base plate for the sensors is shown in Figure 4.8. The gripper remains outside the housing to protect the robot from paint. The slide consists of a wooden surface, in which a carrier plate for sensors and a masking plate is inserted. Figure 4.9 shows the slide in the gripper just before it is introduced into the body. Every movement of the robot was taught at the start of experiments.

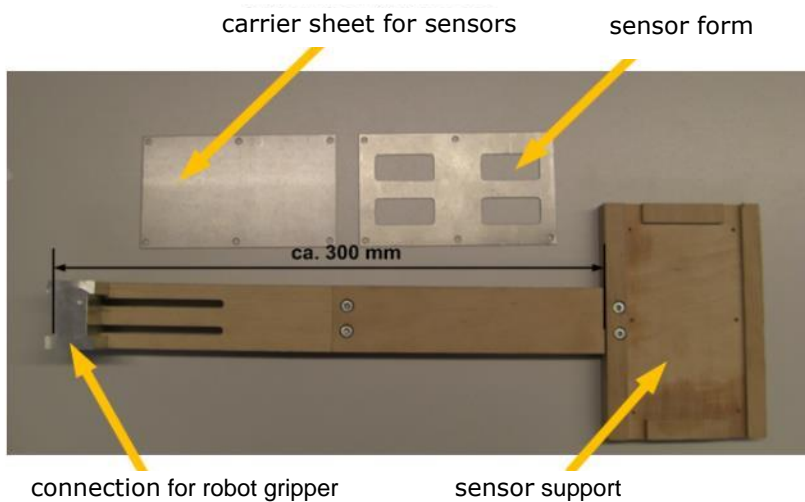


Figure 4.8 Slide for raw sensors

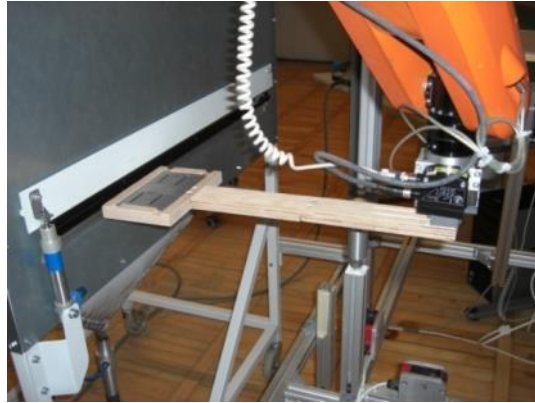


Figure 4.9 Slide in the gripper

Spraying is a good solution to obtain large-area sensors with a uniform PZT film, but when spraying of small surfaces, too much PZT-paint get lost. For small sizes manufacturing the sensors using a doctor blade turned out to be a better solution.

The sensor's geometry is cut out of a laminating film and laminated on a substrate to create a mask with a defined thickness (a negative). The benefits are that no paint can run under the negative. Furthermore, laminating films are offered in different thicknesses in μm -range. The defined thickness permits the realization of a reproducible sensors mask as presented in Figure 4.10.



Figure 4.10 Mask on copper film and support steel plate



Figure 4.11 Sensor after applying PZT-paint

The mask is painted on a side with a thick film of PZT-paint, which is distributed by a doctor blade through the entire mask (Figure 4.11). The doctor blade here is a spring steel of 0,5 mm thickness and it is guided by gripper with smooth movement to obtain a uniform paint thickness. The doctor blade is placed at an angle of 90° to the surface of the sensor as shown in Figure 4.12.

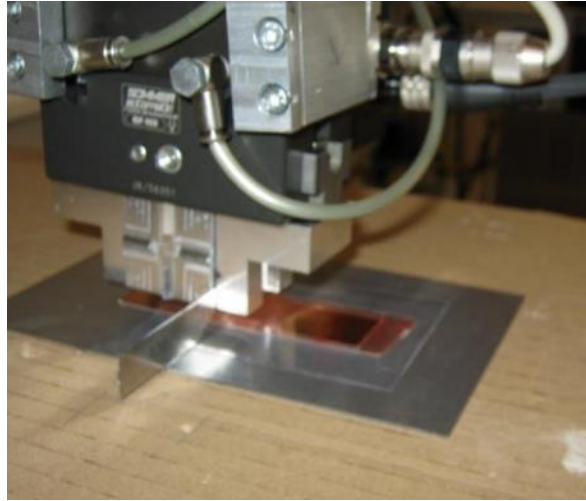


Figure 4.12 Knife coating with the KUKA robot

4.5. Experiments

After polarization, some sensors were destroyed by short-circuit. The poled sensors were tested with a test setup presented in Figure 4.14. After first experiments, only 21% of the sensors can be used for further measurements.

Goal of measurements is to determine the influence of the thickness of piezo paint layer on the range and sensitivity of the sensors. All sensors have the same geometry. As shown in Figure 4.13, the piezo paint film (2) with a defined surface of 15 x 40 mm is applied directly to metal or copper foil (1). After drying, a silver paint film (3) (13x38 mm) is applied as a second conductive layer and defines the surface of the sensor. The sensors are developed with different thicknesses of the piezoelectric paint layer, to investigate the influence of it to the sensitivity of the sensors.

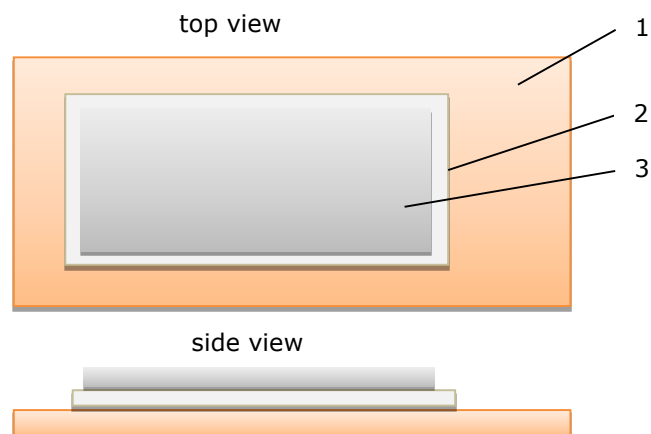


Figure 4.13 Geometry of the sensors

58 4. Development of Piezoelectric Paint Sensors

The sensor is mounted between a piezoelectric actuator and a plate prestressed with a clamping torque of 5 Nm. The piezoelectric actuator is controlled by a frequency generator and excites the sensor with a sinus-wave signal with variable amplitude and frequency. A calibrated force transducer working as described in [59] with dedicated amplifier is placed between the piezoelectric actuator and prestressed plate and is used to validate the developed sensors. The piezopaint sensor is connected to the charge amplifier. Both amplifiers are connected via analog-digital converter to a computer. For recording and evaluating the results has been used DIAdem V.8.1. The entire experimental setup is illustrated in Figure 4.15.

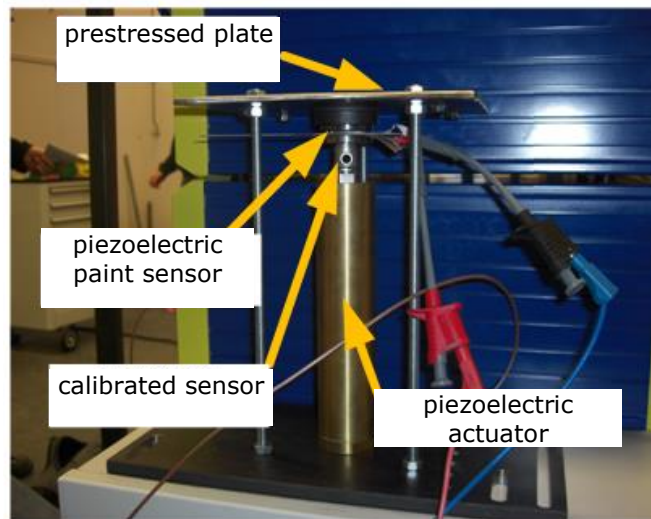


Figure 4.14 Test setup

Employed measurement equipment:

- calibrated force transducer IEPE (Integrated Electronics Piezo Electric) type 8230-002 from Bruel & Kjaer.
- Kistler Charge Amplifier type 5011
- amplifier Kistler Power Supply / Coupler type 5134B

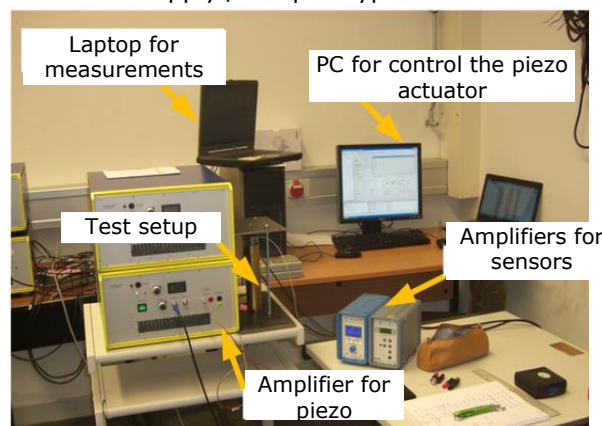


Figure 4.15 Entire test setup

All sensors are tested with sinus-wave signals when applying a voltage to a frequency generator with amplitudes of 0.2 V, 0.5 V and 0.7 V (corresponding to the forces of 158 N, 395 N and 553 N, measured with the calibrated sensor) and then amplified from the voltage amplifier for piezoelectric actuator. The frequencies 2 Hz, 25 Hz, 100 Hz, and 200 Hz are excited. The test results of the measurements with piezoelectric paint sensors are presented in 4.6.

At first, each sensor must be calibrated by comparing the measured signals with the calibrated force sensor from Brüel & Kjær. Because piezoelectric sensors cannot measure static loads, it is used here a quasi-static calibration by applying a low frequency sinus-wave excitation with the piezo actuator.

When calibrating the sensitivity of each piezo paint sensor will be determined. This is an important characteristic of the piezoelectric sensor and describes the ratio between the applied force and transfer load.

In order to determine the sensitivity, the gain to the charge amplifier has been modified, that peak-to-peak amplitude values of piezo paint sensor and of force sensor coincided. With the amplification factor and the sensitivity of the calibrated sensor the sensitivity of the piezoelectric paint sensor was calculated and applied for further measurements.

Next, the name of the tested sensors is noted as follows: *thickness of the piezo paint layer. number of the sensor*, where K represents the sensors, which were prepared on copper foil. It is important to notice, that just a few sensors could be used after polarisation, the rest were destroyed by short circuit caused by air bubbles in the dielectric.

4.6. Test Results

Looking at the theory of the piezoelectric effect described in Chapter 3, a linear dependence between the load force F on the piezoelectric sensor and charge transfer Q can be expected, depending of the dielectric constant d , which defines also the sensitivity of the sensor:

$$Q = d \cdot F \quad (4.2)$$

In the next two figures, the linearity of the piezoelectric paint sensors is examined. On the x-axis is represented the excited voltage signal applied to the frequency generator as described above. On the y-axis are represented the increased amplitudes of the signal, compared to the amplitude of the first measurement (which represents 100%). The measurements are done for two different excitation frequencies 2Hz and 25 Hz by keeping a constant frequency and increasing the load signal. The results are depicted for the calibrated sensor from the company Bruel & Kjaer (named B+K) and for the developed sensors (named as mentioned above after the thickness of the piezo paint thickness).

It will be appreciated that the sensors with a piezo paint layer of 84 μm and 110 μm are linear, comparing with the ideal linearity shown in every figure. The sensors with a layer thickness of 120 μm (120.2 K and 120.3 K) have visible deviations from linearity. More results can be found in Appendix A.

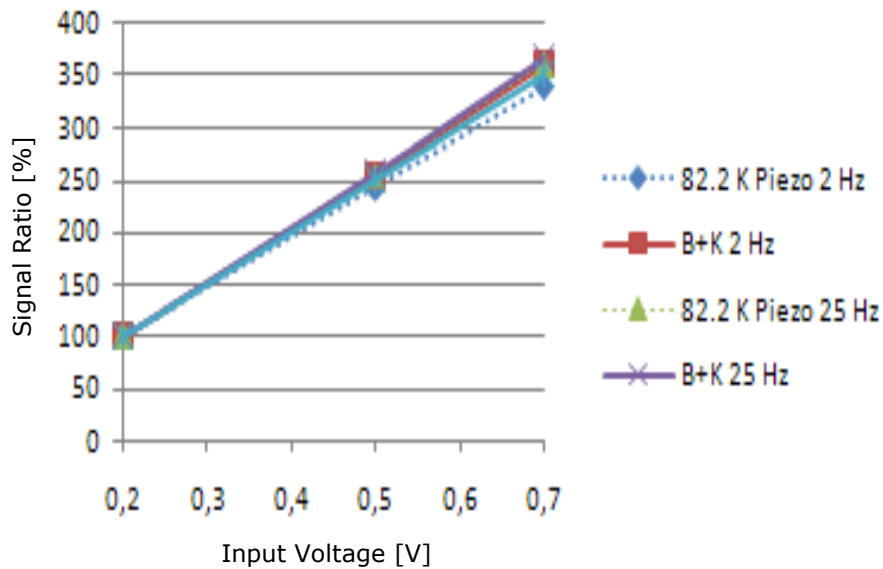


Figure 4.16 Linearity of the sensor with a piezo paint thickness of 82 μm

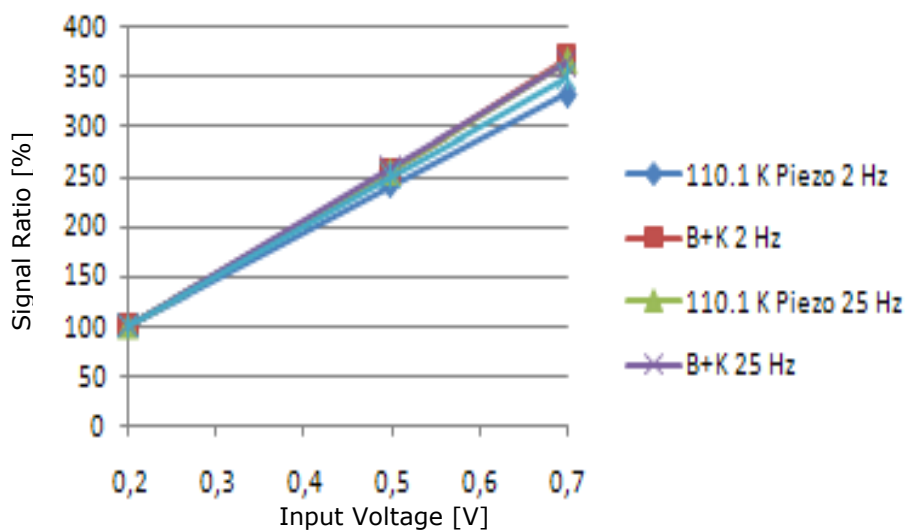


Figure 4.17 Linearity of the sensor with a piezo paint thickness of 110 μm

For another measurement, the actuator is excited with a sinus-wave signal with a frequency of 1 Hz. The amplitude of the sine-wave is increased during the measurement from 0V to 1.5 V in 0.25 V steps, which defines the load force to measure. The force measured with the commercial sensor and the charge displacement of the piezo paint sensor are measured. In order to minimize the

measuring error, five measurements are done for each step. To ensure that all results of these experiments are valid also for higher frequencies, the entire series of measurements are repeated for 100 Hz excitation and the results are compared with those gained with the quasi-stationary measurements.

Figure 4.18 shows the linear dependency of the measured force F from the electric charge for a sensor with piezo paint layer of $82\ \mu\text{m}$ applied on a copper layer. The force was measured with the calibrated force sensor (see Figure 4.14), for a defined applied load. The sensitivity of the sensor of approx. $0,57\ \text{pC/N}$ was adjusted in the piezoelectric amplifier, until it was reach the calibrated force.

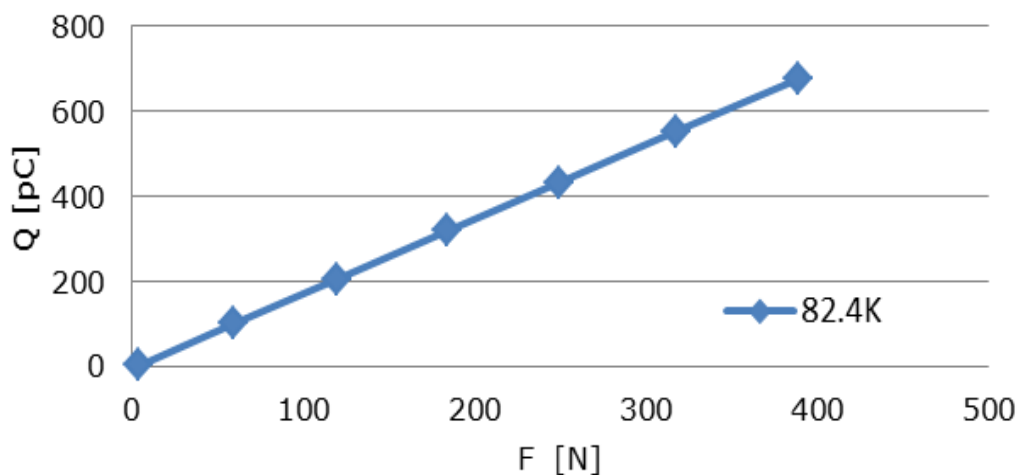


Figure 4.18 Sensitivity measurement of piezo paint sensor

To determine the sensitivity of the sensor it is applied a linear regression. The gradient of this line corresponds to the sensitivity of the sensor. Each sensor has a small offset, which can be explained. The reason is that resistance of the sensor is not infinite. As shown in Figure 4.19, all sensors have similar behaviour. All of them have a linear characteristic and only the gradient and thus sensitivity varies. In Figure 4.20 is illustrated the charge displacement of 5 sensors with different thicknesses of the piezoelectric paint. All sensors are polarised with a DC voltage of 175 V for 20 minutes to a temperature of 21°C . It can be seen that the sensitivity of the sensors decreases with increasing the dielectric thickness for the same poling voltage.

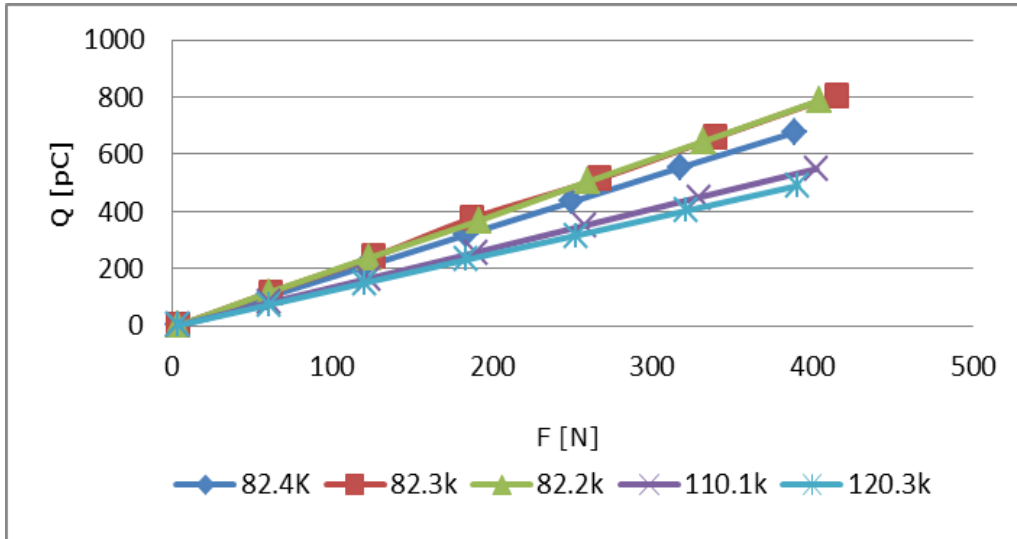


Figure 4.19 Charge displacement for piezo paint sensors with different piezo paint layer thicknesses

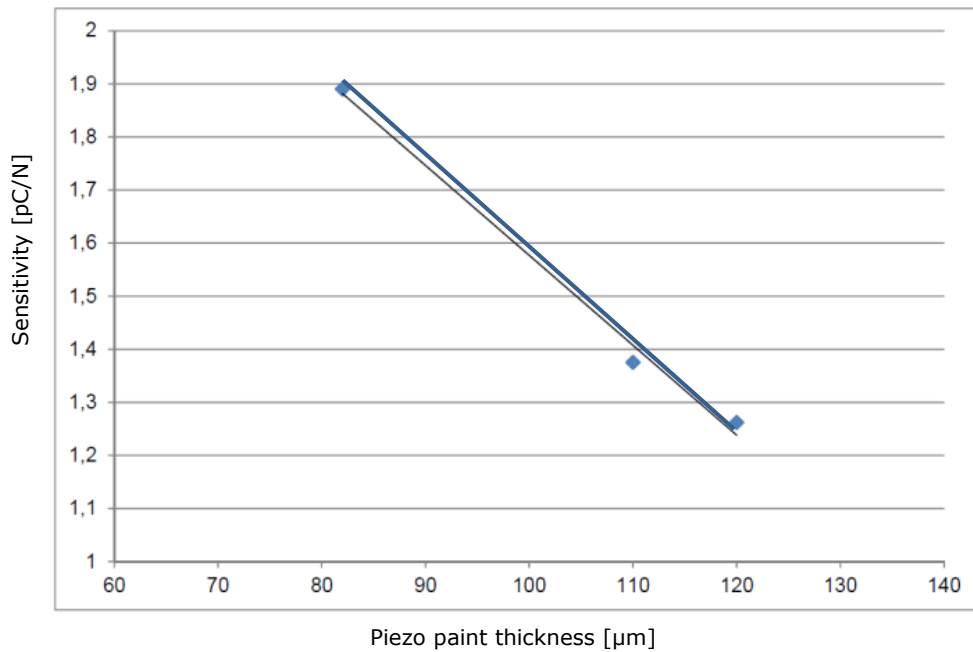


Figure 4.20 Dependence of the sensitivity on the layer thickness

In conclusion, the sensors with a greater layer thickness are less sensitive. This is normal because all sensors are polarized with the same voltage 175 V for 20 minutes and sensitivity is higher when the electrostatic field during

polarization is higher. A small distance between electrodes results in a higher electrostatic field.

The sensors show very good dynamic behaviour, an important property to measure rapid changes in the printing process. Further on the sensors show linear characteristic for different mechanical loads and an approximately constant proportion between the output voltages of the piezo paint sensor (F_{paint_s}) and the output voltage of the calibrated sensor (F_{cal_s}). Considering the dynamic characteristic of the calibrated sensor [8] and the characteristic of the developed sensor, the proportion of the forces for these two sensors was calculated throughout the analysed frequencies (see Figure 4.21). The ratio remains relatively constant, which demonstrates the quality of the sensor.

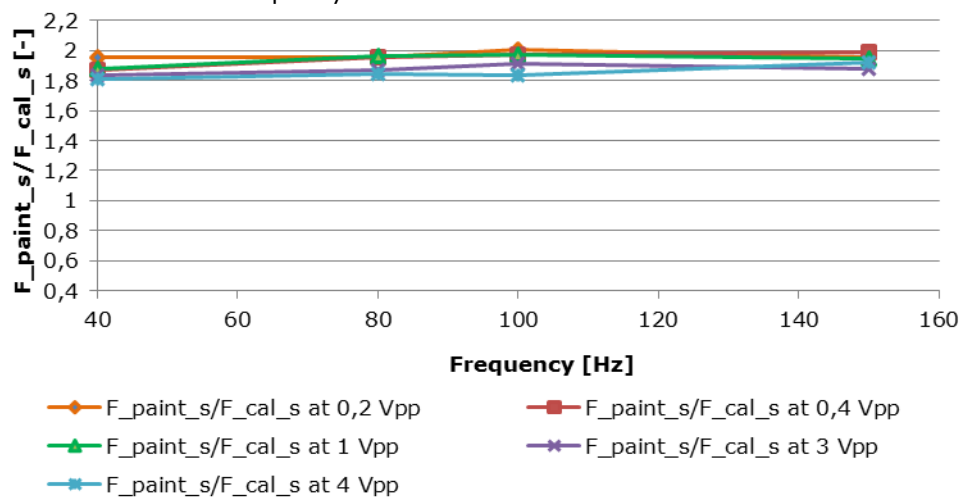


Figure 4.21 Sensor dynamic

In Figure 4.21, V_{pp} means Voltage peak-to-peak amplitude of the sinus-wave signal.

Considering the dynamic characteristic of the calibrated sensor [8] and the characteristic of the developed sensor, the proportion of the forces for these two sensors was calculated throughout the analysed frequencies (see Figure 4.21). The ratio remains relatively constant, which demonstrates the quality of the sensor.

With the help of another test setup presented in Figure 4.22, the dynamic measurements presented in Figure 4.23-Figure 4.25 are made for comparison of the new developed sensor with a calibrated force sensor (Bruel & Kjaer type 8230-002). Here an electrodynamic shaker loads the piezoelectric sensors (developed and calibrated) with dynamic forces in vertical direction.

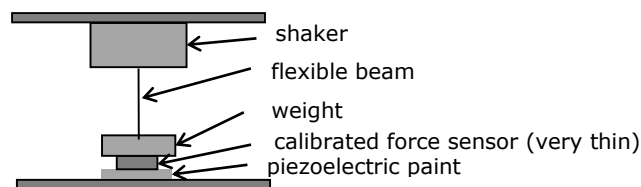


Figure 4.22 Schema of the test setup for dynamic measurement with piezo paint sensors

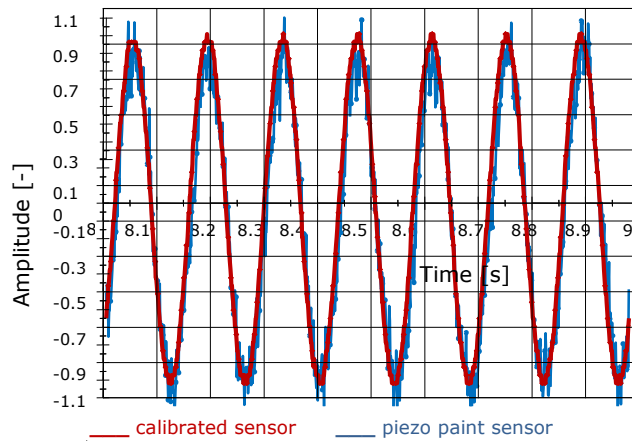


Figure 4.23 Comparison of the sensor's signals for sinus-wave excitation

In Figure 4.24 the correlation of the sensor's signals measured in Volt, for a saw-tooth wave excitation of 20 Hz with the shaker is depicted. The signals were filtered, but it can be seen that the piezo paint sensor shows a small phase shift referenced to the calibrated sensor's signals and high frequency disturbances. The piezo paint signal has to be improved by connecting it to electrical grounding and by using highly-isolated wires.

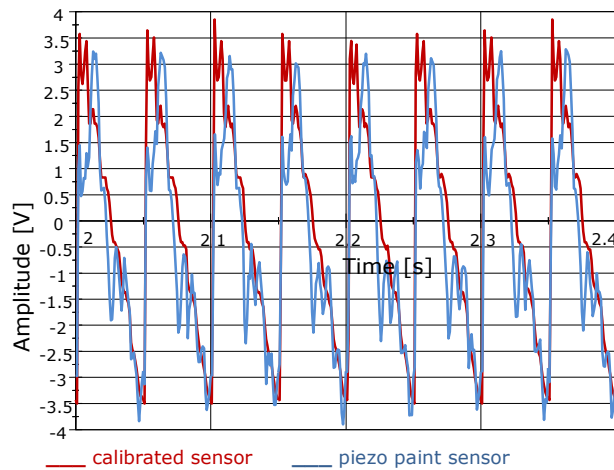


Figure 4.24 Comparison of sensor's signals for saw-tooth wave excitation

Tests have been carried out with different frequencies, up to 500 Hz, and different amplitudes. The measurements show a good correlation between the calibrated force sensor and the new piezoelectric paint sensor. In Figure 4.25 are presented the signals of the calibrated and piezo paint sensor with different amplitudes of the exciting forces normalized with the smallest amplitude.

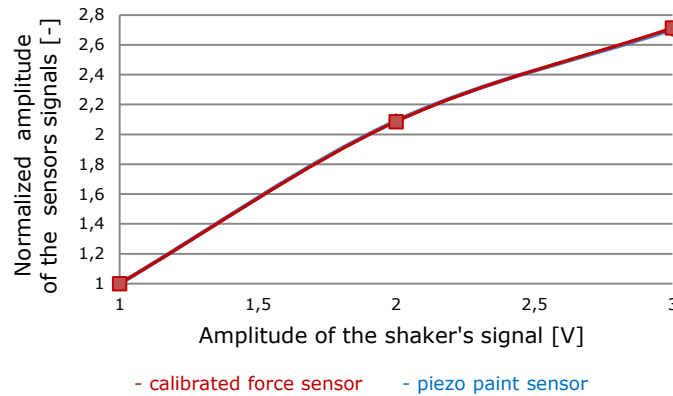


Figure 4.25 Comparison of the piezo paint sensor's signals with the signals of the calibrated force sensor

After testing the piezo paint signals, it could be seen, that they have the dynamic properties that are necessary to measure the dynamic forces in the nip. Three sensors polarized with an electrical charge of 300 V at 40°C were applied onto the plate cylinder from the industrial printing unit as presented in Figure 7.3, underneath the printing plate. The sensors are glued directly on the roller, the double-sided adhesive tape used to fix the printing plate was removed where the sensors are applied to obtain a constant thickness as shown in Figure 4.26. The signals are transferred to the charge amplifier placed in an adapter at the end of the roller. After that, the amplified signals are sent with the help of a slip ring to the dSpace card to be recorded. The analysis of the signals is made with Matlab. One sensor measures two contacts at one rotation, because of the contact of the plate cylinder with the anilox roll and impression cylinder.

The transfer of the signals, from the sensor to the computer is very difficult to be realized when the roller is rotating and without changing the quality of the roller (e.g. drill-hole) and the printing process. In the test rig, the sensor signals are sent via thin copper foils glued on the roller. They are applied in the part of the surface without printing plate. A charge amplifier with a reduced mass and which can rotate with the roller had to be found. The employed solution is to use a 4 channels charge amplifier Kistler ICAM 5073. The disadvantage of this amplifier is that it allows to measure just using a long time constant, which can cause an uncompleted discharge of the sensor's signals.

The measurements with the sensor placed in the middle of the plate cylinder for a basic rotating frequency of 0,2 Hz are presented in Figure 4.27. It can be seen that the sensor has an offset by measuring the pressure forces and the discharge is not complete. But the sensor shows also a relative constant absolute amplitude during the measuring time. Other measurements showed the same characteristic, a sign that the signals of the piezoelectric paint sensors on the roller are very promising. The concept with the piezoelectric paint sensors measuring nip force on the roller, seems to work, but the signal processing has to be improved. As a result of time limitation of the project and the complexity of the task, these problems couldn't be fixed in time, but there are planes to resolve this problems through student projects and master thesis.

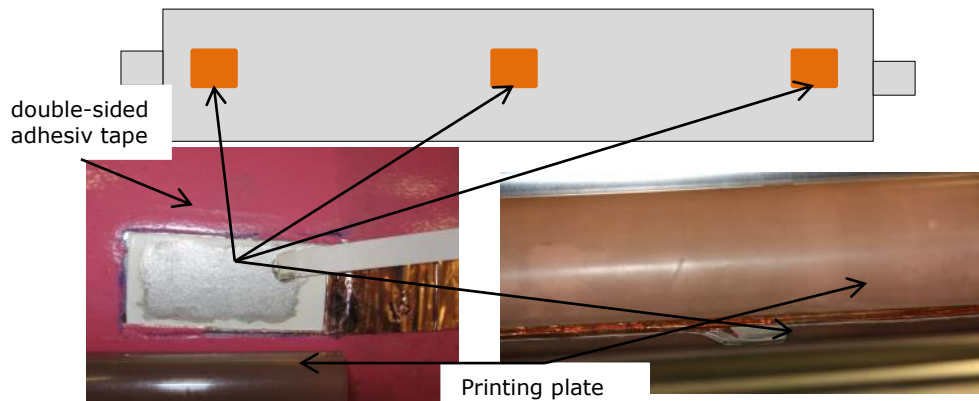


Figure 4.26 Piezopaint sensors on the plate cylinder a) schema; b) piezopaint sensor glued on the roller; c) sensor underneath the printing plate

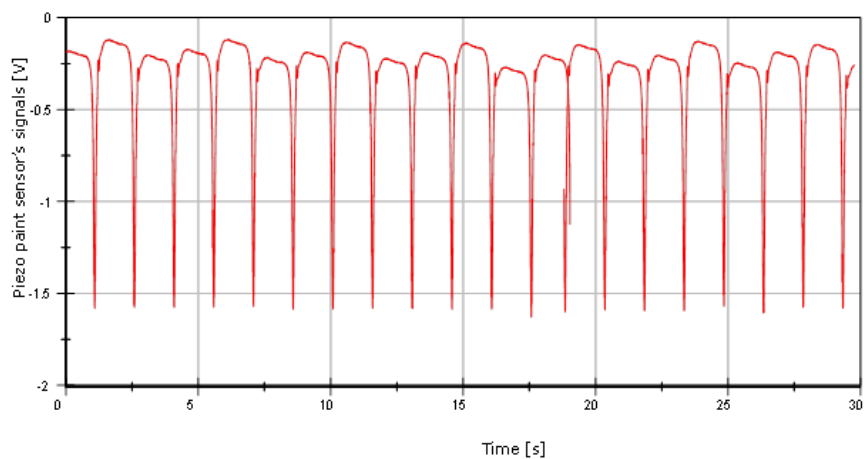


Figure 4.27 Signals of the piezo paint sensor placed in the middle of the plate cylinder

4.7. Chapter Summary in Romanian

Acest capitol prezinta cercetarile pentru a realiza prima parte a scopului propus in aceasta teza de doctorat, acela de a dezvolta si realiza senzori pe baza de vopsea piezoelectrica care sa poata masura fortele dintre valturi in sistemele de imprimare. Aceasta este un lac acrylic pe baza de apa, in care sunt amestecate particule piezoelectrice (PZT), descoperit si patentat de profesorul Hale, dupa cum s-a specificat in capitolul 2.

In subcapitolul 2.3. au fost prezentate aplicatii realizate cu acesti senzori, care pana acum au fost folositi in mare parte pentru masurarea vibratiilor intr-un mod asemanator cu timbrele tensometrice. Realizarea acestor senzori cu ajutorul unui proces semi-automatizat, precum si folosirea lor ca si senzori pentru masurarea presiunii si a fortelor in general este noua, mai ales aplicarea acestora pe un valt.

Inainte de a incepe dezvoltarea senzorilor pe baza de lac piezoelectric, au fost cercetate diferite posibilitati de masurare a presiunii dintre valturi cu senzori aflati pe piata, dar care nu au avut pana in prezent o asemenea utilizare. Pentru acest lucru au fost aplicate pe un valt discuri ceramice piezoelectrice (figura 4.2 (1)), timbre tensometrice (figura 4.2 (2)) si filme piezoelectrice (figura 4.2 (3)). La masurarile efectuate cu acesti senzori a reiesit ca nu au calitatile corespunzatoare pentru aplicatia propusa. De aceea s-a procedat la cercetarea senzorilor pe baza de lac piezoelectric.

Avantajul lacului piezoelectric este ca poate fi aplicat in strat foarte subtire (de cativa micrometri) pe diferite suprafete conductoare de tensiune electrica, chiar si pe suprafete care nu sunt plane.

Procesul de fabricatie al senzorilor pe baza de lac piezoelectric este realizat cu ajutorul unui robot KUKA, aflat in dotatia laboratorului. Au fost incercate mai multe metode de aplicare a lacului PZT pe o suprafata metalica constand din tabla de otel si folie de cupru flexibila, dar numai doua metode au putut fi urmarite in continuare: spreierea si raclarea vopselei (subcapitolul 4.4.). In cele din urma raclarea s-a dovedit a fi cea mai eficienta, deoarece lacul piezoelectric era pus la dispozitie numai in cantitati mici de Prof. Hale de la Universitatea din Anglia, iar prin aceasta metoda se risipeste foarte multa materie prima.

Senzorii obtinuti prin raclare sunt lasati la uscat timp de cel putin 24 de ore, dupa care se aplica un strat de vopsea cu argint care constituie a doua suprafata metalica. In urmatorul pas se polarizeaza senzorii prin conectarea dipolilor timp de cel putin 20 de minute la o sursa de tensiune continua inalta.

Semiautomatizarea procesului de fabricatie a senzorilor este importanta, deoarece grosimea substratului de lac piezoelectric obtinut trebuie sa fie relativ constanta pentru un senzor. Daca grosimea variaza foarte mult, la polarizare, campul electric variaza in diferite puncte ale senzorului si se obtine un scurt circuit, fapt care duce la distrugerea senzorului.

Fiind un proces foarte nou de productie precisa a senzorilor pe baza de lac piezoelectric, dupa prima sarja semi-automatizata, numai 21% din senzori au putut fi folositi pentru incercari, iar din a doua sarja, peste 60%.

In subcapitolul 4.5. sunt descrise metodele de masurare si standul de incercare pentru a caracteriza senzorul. Ca si comparatie pentru masuratori, a fost ales un senzor piezoelectric (IEPE) de la firma Bruel&Kjaer. In figurile 4.16 si 4.17 este prezentata cresterea liniara a semnalului de senzor raportat la prima masuratoare, in functie de cresterea fortei perturbatoare proportional cu cresterea amplitudinii tensiunii generate si transmise la amplificatorul pentru actuatorul piezoelectric.

Avand in vedere caracteristica dinamica a senzorului calibrat si caracteristica senzorului dezvoltat pe parcursul experimentelor, a fost realizat raportul fortelor intr-un numar de 4 puncte (figurile 4.22, 4.26). Pe tot domeniul analizat de frecvente, raportul ramane aproximativ constant, ceea ce scoate in evidenta calitatea senzorului.

In figura 4.20 este reprezentata scaderea liniara a sensibilitatii senzorului cu cresterea grosimii stratului de lac piezoelectric, senzorii fiind polarizati cu aceeasi tensiune electrica de 175 V. Acest efect corespunde asteptarilor, deoarece sensibilitatea senzorilor ar trebui sa creasca odata cu cresterea campului electric aplicat dipolilor sai. In figurile 4.24 si 4.25 este reprezentata buna corelare a

semnalului sensorului dezvoltat cu cel al sensorului calibru.

Din testele precedente a reiesit ca senzorii pe baza de lac piezoelectric indeplinesc calitatile necesare pentru a masura fortele ce apar intre valturi. S-au aplicat trei senzori pe valtul de tiparit din unitatea de printat si s-au facut masuratori cu acestia. Masurarea s-a dovedit a fi foarte complicata, deoarece nu a putut fi folosit decat un amplificator de sarcina electrica cu o constanta de timp mare, ceea ce poate cauza descarcarea inceata a senzorilor. In figura 4.27 sunt prezentate masuratorile cu sensorul aplicat in centrul valtului care prezinta o amplitudine absoluta aproape constanta. Semnalul insa prezinta un offset, ceea ce arata ca transportul acestuia prin intermediul foilor de cupru, fara izolare foarte mare (cum se intampla in cazul unui sistem industrial) trebuie imbunatatit, la fel ca si calitatea semnalului de pe valt.

Din cauza timpului limitat in proiect, aceste imbunatatiri precum si testarea avansata a senzorilor, se desfasoara in prezent in proiectele de licenta ale studentilor si propuneri de teme pentru lucrarile de disertatie la masterat.

5. DYNAMICS OF ROLLER SYSTEM

Calculation of eigenvalues, simulation of vibration behaviour of the roller system and design of control algorithms is performed with the software Matlab/Simulink from the company Mathworks.

This chapter presents the model of a three-roller-system simulating a printing device of a flexographic printing machine. The contact between the rollers is carried out over a printing plate, which causes a variable contact, depending on printed image. This variable contact produces vibrations in the printing process with negative effects of the quality of the print (stripes in the printing image). The design of the mechatronic overall system is based on a mathematical model of the roller system and on simulation of the closed loop behaviour as shown in Figure 5.1:

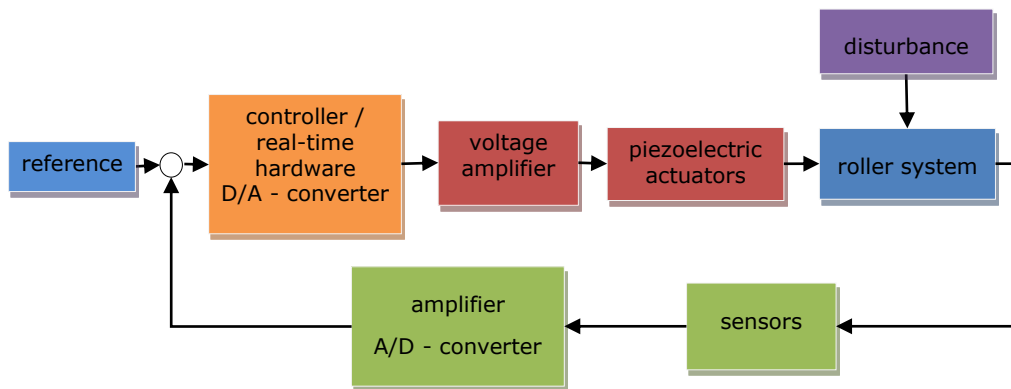


Figure 5.1 Schema of control-loop model of roller system

Vibration of the plate cylinder (printing roller) is detected by means of strain gauges. The sensor signals are amplified on the roller and then transferred using a slip ring placed on the end of the roller. The signals are received by the real-time hardware system dSpace and sent to the control algorithm. Then the control signals are sent to the high-voltage amplifiers as voltages and the actuators generate forces proportional to this voltage needed for vibration damping. The contact between the rollers in a flexographic printing unit is realized radial by the printing plate, in a similar way as described in [133].

In the following sections of this chapter, the mathematical model of the components of the roller system will be described.

5.1. Mechanical Roller System

The first problem of the theoretical analysis of roller bending vibrations is to choose a good mathematical model, which describes dynamic behaviour of a real

system. The local and time discretization of the model have to be both fine enough to provide significant simulation results and rough enough to limit the simulation time.

First, the mathematical equations are derived for a roller, where each roller is considered as a continuum bending beam with two bearings as shown in Figure 5.2. It is discretized in a number of n beam elements with the purpose to define a less complicated equation for each single part.

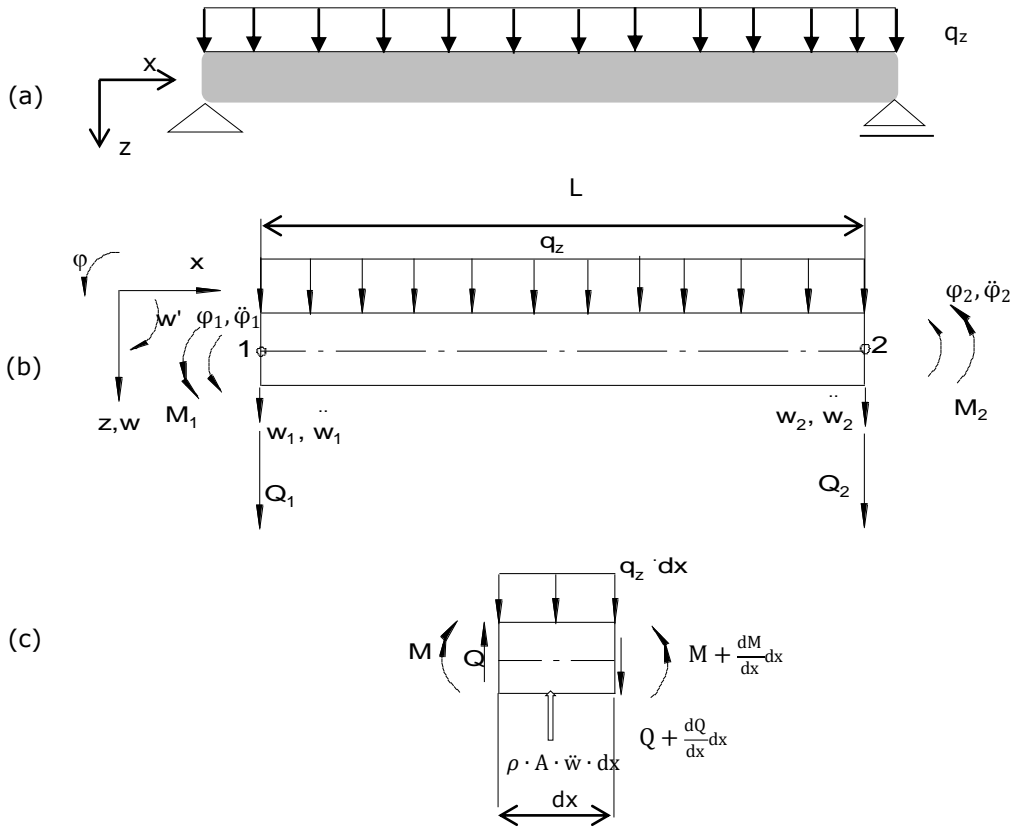


Figure 5.2 Bending beam (a) beam; (b) beam element; (c) infinitesimal beam element

In this figure, M is the bending moment, Q is the shear force in z -axis, q_z is the load, ρ density of the steel material, A : cross-section area section and w is the linear displacement of the beam in z -direction, $\rho \cdot A \cdot \ddot{w} \cdot dx$ is the inertia force, with $\rho \cdot A \cdot dx$ is the mass of the infinitesimal beam element.

In general, in this work are made following notations:

- \ddot{w}, \ddot{x} : second-order differential term with respect to time, e.g. acceleration $\ddot{w} = \frac{d^2w}{dt^2}$
- Q', M', w', ϕ' : first-order differential term with respect to the length, e.g. $Q' = \frac{dQ}{dx}$
- M'', w'' : second-order differential term with respect to the length, e.g. $M'' = \frac{d^2M}{dx^2}$
- w'''' : 4th-order differential term with respect to the length.

5.1.1. Mathematical Model for a Beam Element

In dynamic equilibrium state of a beam element as shown in Figure 5.2 (c) the equations $\sum F_z = 0$ and $\sum M = 0$ have to be satisfied. This yields equations (5.1) and (5.3):

$$-Q - \rho \cdot A \cdot \ddot{w} \cdot dx + Q + \frac{dQ}{dx} \cdot dx + q_z \cdot dx = 0 \quad (5.1)$$

Reducing Q and simplifying this equation with $-dx$, it gets:

$$\rho \cdot A \cdot \ddot{w} - \frac{dQ}{dx} - q_z = 0 \quad (5.2)$$

$$-M - Q \cdot dx - \rho \cdot A \cdot \ddot{w} \cdot dx \cdot \frac{dx}{2} + M + \frac{dM}{dx} \cdot dx + q_z \cdot dx \cdot \frac{dx}{2} = 0 \quad (5.3)$$

The equation (5.3) can be simplified by neglecting the second order terms for small changes. After reducing M and simplifying the rest with dx , it gets finally:

$$Q = M', \quad Q' = M'' \quad (5.4)$$

From the bending moment equation, named also Hook's Law

$$M = -EIw'' = EI\varphi' \quad (5.5)$$

and (5.4) follows the next equation:

$$Q' = -EIw'''' \quad (5.6)$$

where:

E : Young's modulus

I : area moment of inertia

With respect to the differential equation for a roller with a constant cross-section without distributed load, $w'''' = 0$ (normally $w'''' = -q_z(x)$, but the term $-q_z(x)$ will be considered as forces and moments in the nodes of each beam element). The bending displacement w is obtained after four times integration of this equation as follows:

$$\begin{aligned} w'''' &= c_3 \\ w''' &= c_2 + c_3x \\ w'' &= c_1 + c_2x + c_3 \frac{x^2}{2} \\ w &= c_0 + c_1x + c_2 \frac{x^2}{2} + c_3 \frac{x^3}{6} \end{aligned} \quad (5.7)$$

The constants c_0 , c_1 , c_2 and c_3 are determined by deriving from the boundary conditions of the roller, considering the relation between the rotation of a node and the derivation of the bending displacement $\varphi \approx \tan \varphi = w'$ for small displacements:

$$\begin{aligned} w(x=0) &= c_0 = w_1 \\ w'(x=0) &= c_1 = \varphi_1 \\ w(x=L) &= w_1 + \varphi_1 L + c_2 \frac{L^2}{2} + c_3 \frac{L^3}{6} = w_2 \\ w'(x=L) &= \varphi_1 + c_2 L + c_3 \frac{L^2}{2} = \varphi_2 \\ M(0) &= -EIw''(0) = -M_1 \end{aligned} \quad (5.8)$$

$$M(L) = -EIw''(L) = M_2$$

From the last two equations in (5.9) can be calculated the constants c_2 and c_3 :

$$\begin{aligned} c_2 &= \frac{2}{L^2}(-3w_1 + 3w_2 - 2\varphi_1L - 2\varphi_2L) \\ c_3 &= \frac{12}{L^3}(w_1 - w_2 + \frac{\varphi_1L}{2} + \frac{\varphi_2L}{2}) \end{aligned} \quad (5.9)$$

It results the bending equation:

$$\begin{aligned} w(x) &= \left(1 - \frac{3x^2}{L^2} + \frac{2x^3}{L^3}\right)w_1 + \left(\frac{x}{L} - \frac{2x^2}{L^2} + \frac{x^3}{L^3}\right)L\varphi_1 + \left(\frac{3x^2}{L^2} - \frac{2x^3}{L^3}\right)w_2 \\ &+ \left(-\frac{x^2}{L^2} + \frac{2x^3}{L^3}\right)L\varphi_2 \end{aligned} \quad (5.10)$$

Now, the coefficients of the 4 DOF from the bending equation are orthogonal and are named basic functions $G_i(x)$, where $i=1...4$.

Position 1:

Position 2:

$$\begin{aligned} G_1 &= 1 - \frac{3x^2}{L^2} + \frac{2x^3}{L^3} & G_3 &= \frac{3x^2}{L^2} - \frac{2x^3}{L^3} \\ G_2 &= \left(\frac{x}{L} - \frac{2x^2}{L^2} + \frac{x^3}{L^3}\right)L & G_4 &= \left(-\frac{x^2}{L^2} + \frac{2x^3}{L^3}\right)L \end{aligned} \quad (5.11)$$

Now the first and second derivatives of this function are calculated and will be used later for determination of the stiffness matrix.

$$\begin{aligned} G_1' &= -\frac{6x}{L^2} + \frac{6x^2}{L^3} & G_1'' &= -\frac{6}{L^2} + \frac{12x}{L^3} \\ G_2' &= \left(\frac{1}{L} - \frac{4x}{L^2} + \frac{3x^2}{L^3}\right)L & G_2'' &= \left(-\frac{4}{L^2} + \frac{6x}{L^3}\right)L \\ G_3' &= \frac{6x}{L^2} - \frac{6x^2}{L^3} & G_3'' &= \frac{6}{L^2} - \frac{12x}{L^3} \\ G_4' &= \left(-\frac{2x}{L^2} + \frac{3x^2}{L^3}\right)L & G_4'' &= \left(-\frac{2}{L^2} + \frac{6x}{L^3}\right)L \end{aligned} \quad (5.12)$$

Integrating the equation (5.6) for the variation of the shear force with x in (5.2), dynamic behaviour of a roller is described by a differential equation for a bending beam using Bernoulli's hypothesis for a roller with big proportion length/diameter [54, 107]:

$$\rho A \ddot{w} + EI w'''' - q_z = 0 \quad (5.13)$$

For converting the differential equation (5.13) with a continuous operator problem to a discrete equation, it will be used the Galerkin method of mean weighted residuals [143], which is a well-known method in finite element method for calculating the stiffness matrix and the mass matrix. This method uses the orthogonal functions $G_i(x)$ determined with (5.11) and the following equation for the beam with the length L is obtained:

$$\int_0^L [G_i(x) \cdot (\rho A \ddot{w} + EI w'''' - q_z)] dx = 0 \quad (5.14)$$

where $i=1,...,4$ for 4 DOF for each beam element: 2 bending translations w and 2 rotations φ .

The order of the term $(G_i(x) \cdot EI w'''')$ can be reduced using the rules of partial

differential equation with $EI = \text{constant}$ as follows:

$$\frac{\partial}{\partial x}(EI \cdot G_i(x) \cdot w''') = EI((G_i(x) \cdot w'''' + G_i'(x) \cdot w''')) \quad (5.15)$$

$$EI \cdot G_i(x) \cdot w'''' = EI(G_i(x) \cdot w''''') - G_i'(x) \cdot w'''' \quad (5.16)$$

This operation is repeated until obtaining a second order of the bending translation:

$$EI \cdot (G_i'(x) \cdot w''') = EI((G_i'(x) \cdot w''')' - G_i''(x) \cdot w'') \quad (5.17)$$

Now the term $(G_i(x) \cdot EIw''''')$ can be written as follows:

$$G_i(x) \cdot EIw''''' = (G_i(x) \cdot EIw''''')' - (G_i'(x) \cdot EIw''''') + G_i''(x) \cdot EIw'''' \quad (5.18)$$

and will be introduces in (5.14):

$$\int_0^L (G_i(x) \cdot \rho A \ddot{w} + G_i''(x) \cdot EIw'' - G_i(x) \cdot q_z) dx + (G_i(x) \cdot EIw''')|_0^L - (G_i'(x) \cdot EIw'')|_0^L = 0 \quad (5.19)$$

After transformation, we obtain the dynamic equation of a continuum roller with an infinite number of DOF:

$$\int_0^L (G_i(x) \cdot \rho A \ddot{w}) dx = \quad (5.20)$$

$$= -[(G_i(x) \cdot EIw''')|_0^L + (G_i'(x) \cdot EIw'')|_0^L] + \int_0^L (G_i(x) \cdot q_z) dx$$

The rand terms are neglected for simplify the equations.

The bending translation w depends on the regarded position x on the roller and the time t . To simplify the complexity of the mechanical model, it is necessary to separate the local solution from the time solution using Bernoulli approach and then to discretize the roller in more elements of the same length:

$$w(x, t) = \sum_{j=1}^4 G_j(x) \cdot z_j(t), \quad (5.21)$$

where z_j is a vector which contains the DOF of a roller element:

$$z_j = \begin{pmatrix} w_1 \\ \varphi_1 \\ w_2 \\ \varphi_2 \end{pmatrix} \text{ and } \dot{z}_j = \begin{pmatrix} \dot{w}_1 \\ \dot{\varphi}_1 \\ \dot{w}_2 \\ \dot{\varphi}_2 \end{pmatrix} \quad (5.22)$$

Introducing the following substitutions for the 2nd-order and 4th-order derivations of the bending translation:

$$\ddot{w} = \sum_{j=1}^4 G_j(x) \cdot \ddot{z}_j(t), \quad (5.23)$$

$$w'' = \sum_{j=1}^4 G_j''(x) \cdot z_j(t) \text{ and } w'''' = \sum_{j=1}^4 G_j''''(x) \cdot z_j(t)$$

into equation (5.19) gives:

$$\sum_{j=1}^4 \int_0^L (G_i(x) \cdot G_j(x) \cdot \rho \cdot A) dx \cdot \ddot{z}_j(t) + \sum_{j=1}^4 \int_0^L (G_i''(x) \cdot G_j''(x) \cdot E \cdot I) dx \cdot z_j(t) = \quad (5.24)$$

$$= \int_0^L (G_i(x) \cdot q_z) dx + E \cdot I \cdot \sum_{j=1}^4 (G_i'(x) \cdot G_j''(x) - G_i(x) \cdot G_j'''(x))|_0^L \cdot z_j(t),$$

with $i=1, \dots, 4$.

The general equation of a mass-spring-system is:

$$m \cdot \ddot{z} + c \cdot \dot{z} = f, \tag{5.25}$$

where m is the mass matrix, k is the stiffness matrix, and f is the excitation matrix with forces and moments applied on the system. Comparing this equation with the equation for a beam element obtained in (5.24), the following correlations result:

- for the elements of the mass matrix:

$$m_{ij} = \int_0^L (G_i \cdot G_j \cdot \rho \cdot A) dx, \text{ with } i, j=1, \dots, 4 \tag{5.26}$$

- for the elements of the stiffness matrix:

$$k_{ij} = \int_0^L (G_i'' \cdot G_j'' \cdot \rho \cdot A) dx, \text{ with } i, j=1, \dots, 4 \tag{5.27}$$

The mass and stiffness matrices for a roller element with the length l are calculated with (5.26) and (5.27), with respect to the boundary conditions (5.8) (the bending moments and the shear forces at the both ends of the beam (b) have now the same orientation for good defining of the DOF – M_1 and Q_1 have an opposit orientation as for the beam element (c) and have the next form [107, 54, 70]:

$$m = \frac{\rho A l}{420} \begin{bmatrix} 156 & -22l & 54 & 13l \\ -22l & 4l^2 & -13l & -3l^2 \\ 54 & -13l & 156 & 22l \\ 13l & -3l^2 & 22l & 4l^2 \end{bmatrix}, \quad k = \frac{EI}{l^3} \begin{bmatrix} 12 & -6l & -12 & -6l \\ -6l & 4l^2 & 6l & 2l^2 \\ -12 & 6l & 12 & 6l \\ -6l & 2l^2 & 6l & 4l^2 \end{bmatrix} \tag{5.28}$$

The calculation in Matlab of these matrices is depicted in Figure 5.3, without the factors $\frac{\rho A l}{420}$ and $\frac{EI}{l^3}$ which are introduced later in the matrices for the entire roller system.

```

% Mass and stiffness matrices for an element
M_e1_k=[156    -22*d1    54    13*d1
        -22*d1    4*d1^2   -13*d1   -3*d1^2
         54     -13*d1    156    22*d1
        13*d1   -3*d1^2    22*d1    4*d1^2];

C_e1_k=[12    -6*d1    -12    -6*d1
        -6*d1    4*d1^2    6*d1    2*d1^2
        -12    6*d1     12     6*d1
        -6*d1    2*d1^2    6*d1    4*d1^2];
    
```

Figure 5.3 Calculation of the mass matrix and stiffness matrix in Matlab

The equations (5.4) and (5.5), the next equation for an infinitesimal beam element dx is obtained:

$$\frac{d}{dx} \begin{bmatrix} w \\ \varphi \\ M \\ Q \end{bmatrix} = \begin{bmatrix} 0 & -1 & 0 & 0 \\ 0 & 0 & \frac{1}{EI} & 0 \\ 0 & 0 & 0 & 1 \\ 0 & 0 & 0 & 0 \end{bmatrix} \cdot \begin{bmatrix} w \\ \varphi \\ M \\ Q \end{bmatrix} \tag{5.29}$$

Equation (5.30) represents the transfer matrix from the left side to the right side of the beam element presented in Figure 5.2 (b), as specified in [107]. In the case of a beam element, the direction of the bending moments, as well as of the shear

forces are chosen to be the same, for simplification of calculation the stiffness matrix for entire beam.

$$\begin{bmatrix} w \\ \varphi \\ M \\ Q \end{bmatrix}_1 = \begin{bmatrix} 1 & -l & -\frac{l^2}{2EI} & -\frac{l^3}{6EI} \\ 0 & 1 & \frac{l}{EI} & \frac{l^2}{2EI} \\ 0 & 0 & 1 & l \\ 0 & 0 & 0 & 1 \end{bmatrix} \cdot \begin{bmatrix} w \\ \varphi \\ M \\ Q \end{bmatrix}_2 \quad (5.30)$$

5.1.2. Mass matrix and stiffness matrix for an entire roller

The stiffness and mass matrix calculated in section 5.1.1 belong to each discretized element. To define the dynamical behavior of the roller the total stiffness and mass matrix of the roller is needed. The total mass and stiffness matrix are calculated by combining the stiffness and mass matrix of each discretized element and taking into account of the common DOF.

Taking into account the continuity of the bending curve and the boundaries of the discrete elements, the total stiffness and mass matrix for a beam discretized in 2 elements are calculated as described next. In Figure 5.4 it is visible that, when the 2 elements are added the last 2 DOF of the first element are identical with the first DOF of the second element.

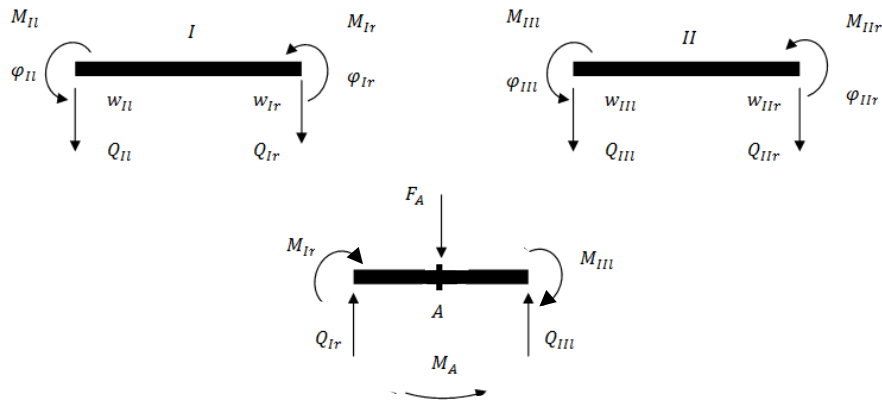


Figure 5.4 Adding of two roller elements

For this example, following equations for a node A can be written:

$$F_A = Q_{Ir} + Q_{III} \quad (5.31)$$

$$M_A = M_{Ir} + M_{III}$$

where F_A and M_A are the force and the moment applied in the node A. The two elements are added in matrices as depicted in Figure 5.5, with respect to the equations (5.31).

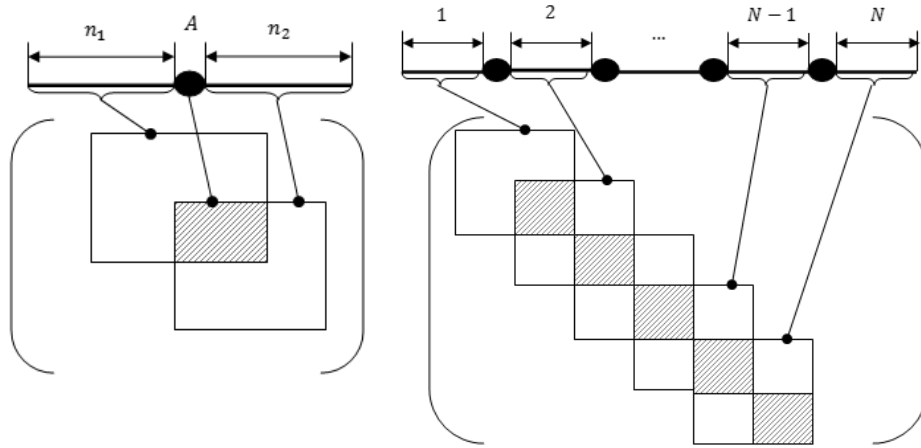


Figure 5.5 Visualization of the adding mode for the total stiffness and mass matrix

The total stiffness and mass matrices have the dimensions $(2n+2) \times (2n+2)$, where n denotes the number of discretized elements of a roller. The length of an element l is calculated when dividing the length of the roller L with n . A roller with constant cross section and mass distribution, discretized in two elements has 6 DOF and the mentioned matrices are:

$$M = A\rho * \begin{bmatrix} \frac{13l}{35} & \frac{11l^2}{210} & \frac{9l}{70} & \frac{13l^2}{420} & 0 & 0 \\ & \frac{1l^3}{105} & \frac{13l^2}{420} & \frac{1l^3}{140} & 0 & 0 \\ & & \frac{26l}{35} & 0 & \frac{9l}{70} & \frac{13l^2}{420} \\ & \text{sym.} & & \frac{2l^3}{105} & \frac{13l^2}{420} & \frac{l^3}{140} \\ & & & & \frac{13l}{35} & \frac{11l^2}{210} \\ & & & & & \frac{l^3}{105} \end{bmatrix} \quad (5.32)$$

$$C = EI \begin{bmatrix} \frac{12}{l} & -\frac{6}{l^2} & \frac{12}{l^3} & -\frac{6}{l^2} & 0 & 0 \\ & \frac{4}{l} & \frac{6}{l^2} & \frac{2}{l} & 0 & 0 \\ & & \frac{24}{l^3} & 0 & \frac{12}{l^3} & -\frac{6}{l^2} \\ & \text{sym.} & & \frac{8}{l} & \frac{6}{l^2} & \frac{2}{l} \\ & & & & \frac{12}{l^3} & \frac{6}{l^2} \\ & & & & & \frac{4}{l} \end{bmatrix} \quad (5.33)$$

Taking into account that the roller also has damping properties, it is the easiest way to assume that the damping matrix is proportional to the stiffness and the mass matrix and is calculated with the help of Rayleigh theorem as a linear combination of these two matrices:

$$D = \alpha \cdot M + \beta \cdot C \quad (5.34)$$

This damping matrix is just a mathematical approach in order to consider losses of mechanical energy e.g. caused by friction. The parameters α and β are

empirical adjusted to become a realistic approximation of the damping in the simulation.

Now the description of the equation of motion for a roller can be expressed in matrix form as:

$$M\ddot{x} + D\dot{x} + Cx = f(t) \quad (5.35)$$

where: $f(t)$ is the excitation vector containing the dynamic forces and moments applied to the roller.

In the discussed case in this work, just forces are applied on the roller, every second position in this excitation vector representing a moment is zero.

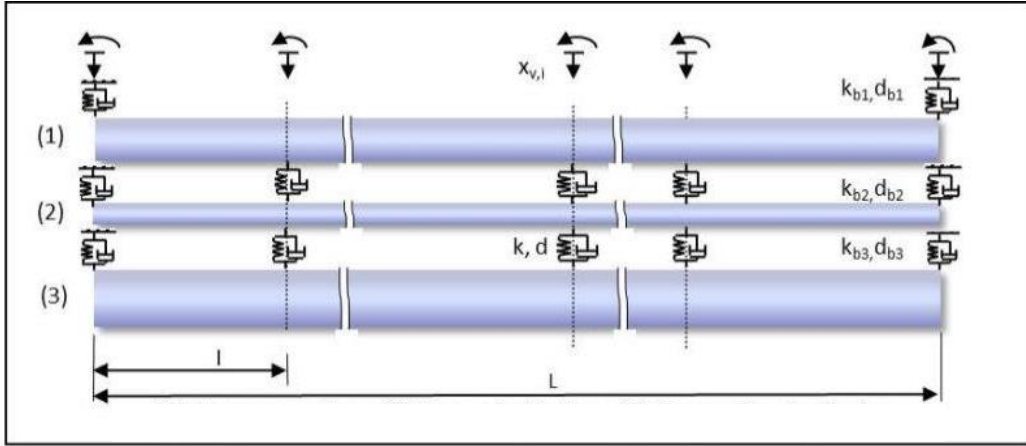
5.1.3. Mathematical Model of the Roller System

The roller system described in this work is an approximation of a printing unit of a flexographic printing machine. The test setup is described in detail in Chapter 7 and has 3 roller placed in a line. The three rollers - anilox roll, plate cylinder and impression cylinder have different diameters and properties and have to be modelled individually. The contact between rollers is realized with the printing plate (red in the next picture).



Figure 5.6 Roller system

The design of the mechatronic overall system is based on a mathematical model of the roller system and on simulation of the closed loop behaviour. The mathematical model of the roller system is depicted in Figure 5.7 (upper view). In this work it is important to have a mathematical model to analyze the nip vibration direction.



(1) Anilox roll, (2) plate cylinder, (3) impression cylinder

Figure 5.7 Schema of roller system

The contact between rollers realized by the elastic printing plate is described as stiffness-damping element.

For the decoupled three-roller system, the mass and the stiffness matrices are as follows:

$$C_{ng} = \frac{E}{l^3} \begin{bmatrix} C_1 \cdot I_1 & 0_{(Ng,Ng)} & 0_{(Ng,Ng)} \\ 0_{(Ng,Ng)} & C_{g2} \cdot I_2 & 0_{(Ng,Ng)} \\ 0_{(Ng,Ng)} & 0_{(Ng,Ng)} & C_{g3} \cdot I_3 \end{bmatrix} \quad (5.36)$$

$$M_{ges} = \frac{\rho \cdot l}{420} \begin{bmatrix} M_{g1} \cdot A_1 & 0_{(Ng,Ng)} & 0_{(Ng,Ng)} \\ 0_{(Ng,Ng)} & M_{g2} \cdot A_2 & 0_{(Ng,Ng)} \\ 0_{(Ng,Ng)} & 0_{(Ng,Ng)} & M_{g3} \cdot A_3 \end{bmatrix}, \quad (5.37)$$

where:

I_i : aria moment of inertia of the roller i

A_i : cross section of the roller i

M_{gi} : part of the mass matrix of the roller i, without the common factor $\frac{\rho \cdot l \cdot A}{420}$

C_{gi} : part of the stiffness matrix of the roller i, without the common factor $\frac{EI}{l^3}$

1,2,3: number of roller

Figure 5.8 shows the calculation in Matlab of the stiffness matrix C_{ges} and the mass matrix M_{ges} for entire system containing three rollers without contact.

```

Cges=E/dl^3*[Cg*I (1)      zeros (Ng,Ng) zeros (Ng,Ng) ;
             zeros (Ng,Ng) Cg*I (2)      zeros (Ng,Ng) ;
             zeros (Ng,Ng) zeros (Ng,Ng) Cg*I (3) ] ;

Mges=rho*dl/420*[Mg*A (1)      zeros (Ng,Ng) zeros (Ng,Ng) ;
                 zeros (Ng,Ng) Mg*A (2)      zeros (Ng,Ng) ;
                 zeros (Ng,Ng) zeros (Ng,Ng) Mg*A (3) ] ;

```

Figure 5.8 Calculation of the stiffness matrix and mass matrix for the roller system

The parameter depending on the geometry of the rollers and on the material as follows: aria momentum of inertia I , cross- sectional aria A , the entire mass of each roller and the radius are calculated as shown in Figure 5.9.

```

for i=1:walzennr
    r(i)=d(i)/2;ri(i)=di(i)/2;
    I(i)=pi/4*(r(i)^4-ri(i)^4);
    A(i)=pi*(r(i)^2-ri(i)^2);
    m(i)=rho*L*A(i);
end

```

Figure 5.9 Calculation of the basic paramters of the 3 rollers

The entire simulated system includes three rollers: an anilox roll (pressure roller), a plate cylinder (rubber roller) and an impression cylinder (support cylinder). The rollers are simulated with elastic bearings with the stiffness k_{bi} and the damping d_{bi} , with $i = 1,2,3$ for each roller.

The printing plate is an elastic rubber glued to a support and placed onto plate cylinder. It is intended to make contact between rollers and is named coupling element of the roller system.

In order to simplify the model, the printing plate is modeled as a linear spring and a viscous damper. In reality, its behavior has some temperature and frequency dependencies. For calculating the influence of the printing plate of each element, it is discretized in the same way as the roller. The stiffness of the printing plate for each element k_g is calculated as $k_g = \frac{k_{ges}}{n}$ and the damping as $d_g = \frac{d_{ges}}{n}$:

The following approximation is made: between rollers are transferred just forces, no moments occur in bearings and coupling the rollers. That means that only the differential equations for linear displacements of each discretized part have to be considered. It results from the equilibrium conditions of forces $\sum \vec{F}_i = 0$, here e.g. the positions 1 (in the bearing) and 3 (with contact) for the three rollers, with $k_{b1} = k_{b2} = k_{b3} = k_b$ and $d_{b1} = d_{b2} = d_{b3} = d_b$:

Position 1 – in the bearing:

$$\begin{aligned}
 m_{11}\ddot{x}_{11} + d_b\dot{x}_{11} + k_b x_{11} &= f_{11} \\
 m_{21}\ddot{x}_{21} + d_b\dot{x}_{21} + k_b x_{21} &= f_{21} \\
 m_{31}\ddot{x}_{31} + d_b\dot{x}_{31} + k_b x_{31} &= f_{31}
 \end{aligned}
 \tag{5.38}$$

Position 3 – with contact:

$$\begin{aligned}
 m_{13}\ddot{x}_{13} - k_g(x_{23} - x_{13}) - d_g(\dot{x}_{23} - \dot{x}_{13}) &= f_{13} \\
 m_{23}\ddot{x}_{23} + k_g(x_{23} - x_{13}) - k_g(x_{33} - x_{23}) + d_g(\dot{x}_{23} - \dot{x}_{13}) - d_g(\dot{x}_{33} - \dot{x}_{23}) &= f_{23} \\
 m_{33}\ddot{x}_{33} + k_g(x_{33} - x_{23}) + d_g(\dot{x}_{33} - \dot{x}_{23}) &= f_{33}
 \end{aligned} \tag{5.39}$$

where:

(*ij*): *i* – Number of the roller (1, 2 or 3)

j – Number of the DOF for linear displacement on the roller

f_{ij} – load applied on the position (*i,j*)

k_{ges} – total stiffness of the coupling element

Now the coupling matrix *K_{ges}* of the rollers is calculated with respect to the equations (5.38) and (5.39) for small displacements of the three rollers and a linear coupling force between the rollers by the printing plate.

In the first and the (*N_g-1*) DOF of each roller is added the stiffness of the bearings *k_b*.

The entire stiffness matrix and damping matrix of the roller system are:

$$C_{ges} = C_{Ng} + K_{ges} \tag{5.40}$$

$$D_{ges} = \alpha \cdot M_{ges} + \beta \cdot C_{ges}$$

This approach was proven adequate to reproduce the damping behavior of the printing plate.

Now that the total stiffness, mass and damping matrices are defined, the dynamic behavior of roller system is described with the following equation:

$$M_{ges}\ddot{x} + D_{ges}\dot{x} + C_{ges}x = f_{ges} \tag{5.41}$$

The exterior stimulation signal *f_{ges}* is defined as a vector with 3*(2*n*+2) elements, which contains the forces and moments applied on each discretized element of the roller:

$$f_{ges} = [F_1 \ M_2 \ F_3 \ M_4 \ \dots \ F_{3(2n+2)-1} \ M_{3(2n+2)}]^T \tag{5.42}$$

Vector "x" represents the solution of the differential equation and is defined as a vector with (2*n*+2) elements at every time step, containing the linear and angular displacements of each discretized element:

$$x = [w_1 \ \varphi_2 \ w_3 \ \varphi_4 \ \dots \ w_{3(2n+2)-1} \ \varphi_{3(2n+2)}]^T \tag{5.43}$$

5.2. State-Space

For simulation and control purposes the second order differential equation (5.41) can be transferred into a set of first order differential equations. For this purpose a state vector *z* is introduced. It contains the DOF *w* and φ and the velocities \dot{w} and $\dot{\varphi}$ and is:

$$z = \begin{bmatrix} x \\ v \end{bmatrix}, \tag{5.44}$$

where *v* is the first-order derivative of the vector *x* with respect to time. This column vector has 2**N_{ges}* elements, where *N_{ges}* is the total number of DOF of the roller system and has a value of 3(2*n*+2).

Equation (5.41) can be expressed in a state-space representation, which contains the smallest set of numbers that must be known in order that its future response to any given input can be calculated from the dynamic equation. The state equations are arranged as a set of first-order differential equations, and have the

following form for a linear time-invariant system:

$$\dot{z} = Az + Bu \quad (5.45)$$

where

$A = \begin{bmatrix} 0 & E \\ -M_{ges}^{-1} \cdot C_{ges} & -M_{ges}^{-1} \cdot D_{ges} \end{bmatrix}$ is the state matrix and contains the dynamic properties of the system,

$B = \begin{bmatrix} 0 \\ M_{ges}^{-1} \cdot f_{ges} \end{bmatrix}$ is the control matrix,

u is the input matrix

E is the unit matrix

The output of the system is given by

$$y = C \cdot z \quad (5.46)$$

where C is a constant matrix with 0 and 1 elements, which defines the outputs. u is also a matrix with elements 0 and 1. The element 1 is defined for the position where a disturbance appears.

The eigenvalue problem is solved in two different ways:

- considering the damping matrix zero – the system is not damped
- considering the damped system.

In the first case, the linear and homogeneous equation (5.41) with $D_{ges} = 0$ has a nontrivial solution only if $\det(M_{ges} \cdot \Lambda + C_{ges}) = 0$, where $\Lambda = \text{diag}(\lambda_i)$ represents the diagonal matrix containing the eigenvalues of the system $\lambda_i = \omega_i^2$. In this way, it can be proved that the FEM model is correct. For this, 20 discretization parts of the roller are needed for finding similar solution for natural frequencies of the uncoupled system $f_i = \frac{\omega_i}{2\pi}$ as the natural frequencies calculated using the analytic method for a hinged-hinged beam with uniform sections and uniform load as described in [18]:

$$f_i = \frac{i^2 \cdot \pi}{2} \sqrt{\frac{EI}{\rho AL^4}}, \quad \text{with } i=1,2,\dots \quad (5.47)$$

Table 5.1 shows the natural frequencies of the plate cylinder from the downscaled test setup, calculated analytical and with FEM method and demonstrate that the FEM model is correct and 20 discretizations are enough for good results.

Natural frequency	1 st	2 nd	3 rd	4 th
Analytical	84.258	337.206	758.074	1348.825
FEM undamped	84.255	337.024	758.324	1348.230

Table 5.1 Natural frequencies of the printing roller

In the second case, for the damped system, the matrix D_{ges} is calculated from (5.40), similar as the stiffness matrix, considering $\alpha=0$ and $\beta>0$. In this case, the eigenvalues and eigenvectors are determined with the help of the state matrix A :

$$A \cdot \Phi = \Phi \cdot \Lambda, \quad (5.48)$$

with

Φ : matrix with eigenvectors ordered on the columns

Λ : matrix containing eigenvalues on the diagonal

The solution of equation (5.41) is again, a matrix that has on its diagonal the eigenvalues λ of the system. This time, the eigenvalues are conjugate complex pairs of the form:

$$\lambda_k = \delta_k \pm j \cdot \omega_k \quad (5.49)$$

where δ_k is the damping factor and ω_k is the angular frequency of the k^{th} -DOF .

It follows the eigenvalues matrix:

$$\Lambda = \begin{bmatrix} \delta_1 + j \cdot \omega_1 & & & & 0 \\ & \delta_2 - j \cdot \omega_2 & & & \\ & & \ddots & & \\ & & & \delta_{2n} + j \cdot \omega_{2n} & \\ 0 & & & & \delta_{2n} - j \cdot \omega_{2n} \end{bmatrix} \quad (5.50)$$

In Matlab the eigen values of the roller system are saved in a vector EW. The natural frequencies in Herz are calculated from the imaginary part of the eigen values by division with 2π , as depicted in Figure 5.10.

```
40 %with FEM calculated natural frequencies in Hertz
41 - f1_FEM=imag(EW(2*N-1))/(2*pi)
42 - f2_FEM=imag(EW(2*N-3))/(2*pi)
43 - f3_FEM=imag(EW(2*N-5))/(2*pi)
44 - f4_FEM=imag(EW(2*N-7))/(2*pi)
```

Figure 5.10 Calculation of the first eigen frequencies in Hz of the 3 rollers

In Figure 5.11 are depicted the first 4 mode shapes of the plate cylinder on the small test bed, described in Section 7.1.

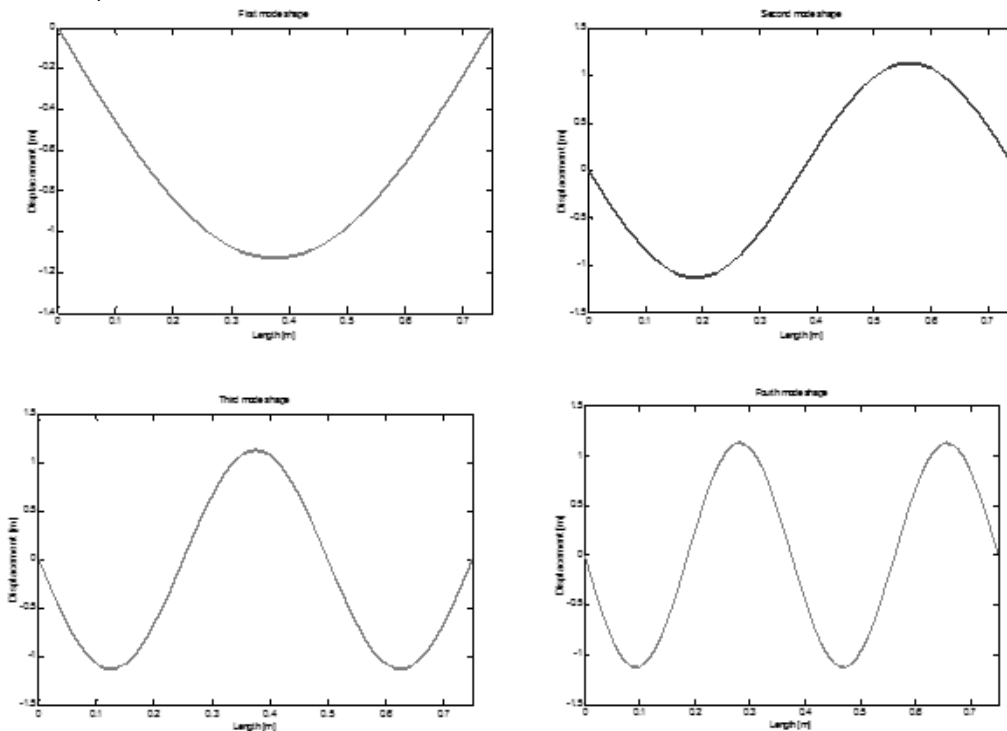


Figure 5.11 First 4 mode shapes of the printing roller on the test rig

5.3. Modal Analysis and System Reduction

For good results with the help of finite elements method, the number of discretizations of a roller has to be large, which generate a large number of degrees of freedom. The computational resources needed for the simulation can be costly. Modal analysis of the system makes possible to cut down the size of the computation, by reducing the system and in the same time by uncoupling the equations of motion (5.41). With the help of modal analysis, only the important states are taken into consideration.

Modal analysis is realized with the help of the eigenvalues and the eigenvectors of the system, where the eigenvectors describe the normal or natural modes of the system. A disadvantage of this method is that the entire calculation is complex, because of the complex eigenvalues and complex eigenvectors. This leads to an increase of the computation time during the computer-aided simulation. Therefore, it is appropriate to work with the so-called modified modal form, where calculation with complex values is avoided and the model size is drastically reduced.

In reality, the roller system can reach maximum the 6th natural frequency, the higher modes are not excited. Thus, the simulation interested only of the behavior of the roller until the 6th natural frequency. Therefore the modal matrix Φ and contains only the first six eigenvectors.

Modified modal form

In the next pages is presented the transformation of the complex numbers in real numbers, by separation of the real and the imaginary part a. It calls modified modal form [106].

The eigenvalue problem

$$A \cdot V = \lambda \cdot V \quad (5.51)$$

gives eigenvectors V_i . For each eigenvector V_i , a factor c_i can be chosen and $\phi_i = c_i \cdot z_i$ is still a solution of the eigenvalue problem. c_i is now chosen according to following equation

$$\phi_i = c_i \cdot z_i \text{ with } c_i = \frac{1}{\sqrt{V_i^T \cdot V_i}} \quad (5.52)$$

With that (5.51) it follows:

$$A\phi_i = \lambda_i \phi_i, \quad (5.53)$$

and when multiplying the equation with ϕ_i^T it gets:

$$\begin{aligned} \phi_i^T A \phi_i &= \lambda_i \underbrace{\phi_i^T \phi_i}_{=1} \Rightarrow \phi_i^T A \phi_i = \lambda_i \\ &= 1 \end{aligned} \quad (5.54)$$

With $\phi_i = \phi_{i_{real}} + j \phi_{i_{imag}}$ and $\lambda_i = \delta_i + j \omega_i$ the equation (5.5) can be transformed and the real and imaginary parts are separated:

$$\begin{aligned} \phi_{i_{real}}^T A \phi_{i_{real}} - \phi_{i_{imag}}^T A \phi_{i_{imag}} &= \delta_k \\ \phi_{i_{real}}^T A \phi_{i_{imag}} + \phi_{i_{imag}}^T A \phi_{i_{real}} &= \omega_k \end{aligned} \quad (5.55)$$

The eigenvalue problem of a real matrix A gives conjugate complex pairs of eigenvectors. If $\phi_i = \phi_{i_{real}} + j \phi_{i_{imag}}$ then, its conjugate complex vector $\tilde{\phi}_i = \phi_{i_{real}} - j \phi_{i_{imag}}$ is also an eigenvector. The orthogonality of eigenvectors gives:

$$\begin{aligned}
& \tilde{\phi}_i^T A \phi_i = 0 \\
& (\phi_{i_{real}} - j\phi_{i_{imag}})^T A (\phi_{i_{real}} + j\phi_{i_{imag}}) = \\
& = \phi_{i_{real}}^T A \phi_{i_{real}} + \phi_{i_{imag}}^T A \phi_{i_{imag}} + j\phi_{i_{real}}^T A \phi_{i_{imag}} - j\phi_{i_{imag}}^T A \phi_{i_{real}} = 0
\end{aligned} \tag{5.56}$$

Separation real and imaginary part gives:

$$\begin{aligned}
& \phi_{i_{real}}^T A \phi_{i_{real}} + \phi_{i_{imag}}^T A \phi_{i_{imag}} = 0 \Rightarrow \phi_{i_{real}}^T A \phi_{i_{real}} = -\phi_{i_{imag}}^T A \phi_{i_{imag}} \\
& \phi_{i_{real}}^T A \phi_{i_{imag}} - \phi_{i_{imag}}^T A \phi_{i_{real}} = 0 \Rightarrow \phi_{i_{real}}^T A \phi_{i_{imag}} = \phi_{i_{imag}}^T A \phi_{i_{real}}
\end{aligned} \tag{5.57}$$

Using a modified modal form with a real two columns vector $\phi_{i_{mod}} = [\phi_{i_{real}}, \phi_{i_{imag}}]$ for each conjugate complex eigenvector:

$$\begin{pmatrix} \phi_{i_{real}}^T \\ \phi_{i_{imag}}^T \end{pmatrix} A \begin{pmatrix} \phi_{i_{real}} \\ \phi_{i_{imag}} \end{pmatrix} = \begin{vmatrix} \phi_{i_{real}}^T A \phi_{i_{real}} & \phi_{i_{real}}^T A \phi_{i_{imag}} \\ \phi_{i_{imag}}^T A \phi_{i_{real}} & \phi_{i_{imag}}^T A \phi_{i_{imag}} \end{vmatrix} = \begin{pmatrix} a & b \\ c & d \end{pmatrix} \tag{5.58}$$

where:

$$\begin{aligned}
a &= \phi_{i_{real}}^T A \phi_{i_{real}} \\
d &= \phi_{i_{imag}}^T A \phi_{i_{imag}} \\
b &= \phi_{i_{real}}^T A \phi_{i_{imag}} \\
c &= \phi_{i_{imag}}^T A \phi_{i_{real}}
\end{aligned} \tag{5.59}$$

With (5.55) and (5.57) it follows:

$$\begin{aligned}
a - d &= \delta_i \\
b + c &= \omega_i \\
a + d &= 0 \\
b - c &= 0
\end{aligned} \tag{5.60}$$

It results $a = \frac{\delta_i}{2}$, $d = -\frac{\delta_i}{2}$, $b = \frac{\omega_i}{2}$, $c = -\frac{\omega_i}{2}$ and the equation (5.58) can be written:

$$\begin{pmatrix} \phi_{i_{real}}^T \\ \phi_{i_{imag}}^T \end{pmatrix} A \begin{pmatrix} \phi_{i_{real}} \\ \phi_{i_{imag}} \end{pmatrix} = \begin{vmatrix} \phi_{i_{imag}}^T A \phi_{i_{real}} & \phi_{i_{imag}}^T A \phi_{i_{imag}} \\ \phi_{i_{real}}^T A \phi_{i_{real}} & \phi_{i_{real}}^T A \phi_{i_{imag}} \end{vmatrix} = \frac{1}{2} \begin{pmatrix} \delta_i & \omega_i \\ \omega_i & -\delta_i \end{pmatrix} \tag{5.61}$$

With the modified form of the eigenvector matrix it follows:

$$\Phi_{mod} = [\phi_{1_{real}}, \phi_{1_{imag}}, \dots, \phi_{i_{real}}, \phi_{i_{imag}}, \dots, \phi_{N_{real}}, \phi_{N_{imag}}] \tag{5.62}$$

Now the term $\Phi_{mod}^T A \Phi_{mod}$ can be written with the following block diagonal structure:

Now following transformation for the state-space model can be carried out:

$$z = \Phi_{mod} \cdot q \quad (5.71)$$

with q : modal state vector

The state space model gets the form:

$$\Phi_{mod} \dot{q} = A \Phi_{mod} q + Bu \quad (5.72)$$

$$y = C \Phi_{mod} \dot{q}$$

Premultiplication with Φ_{mod}^T gives

$$\Phi_{mod}^T \Phi_{mod} \dot{q} = \Phi_{mod}^T A \Phi_{mod} q + \Phi_{mod}^T B u \quad (5.73)$$

$$y = C \Phi_{mod} \dot{q}$$

with $Z = \text{diag}(Z_i)$ (diagonal matrix) and (5.74)

$$\Lambda_{mod} = \Phi_{mod}^{-1} \cdot A \cdot \Phi_{mod}$$

it can be written:

$$Z \dot{q} = \Lambda_{mod} q + \Phi_{mod}^T B u \quad (5.75)$$

$$y = C \Phi_{mod} \dot{q}$$

With (5.75) it gets a set of decoupled pairs of differential equations, where each pair describes one natural vibration [15]:

$$\dot{q} = Z^{-1} \Lambda_{mod} q + Z^{-1} \Phi_{mod}^T B u \quad (5.76)$$

$$y = C \Phi_{mod} \dot{q}$$

with $Z^{-1} = \text{diag}(2, -2, 2, -2 \dots)$.

All natural vibrations that are not excited, can be neglected. In the case of the roller system only the first 6 eigenvalues and eigenvectors have to be considered, the rest can be cut, so that the simulation model becomes very small and has only 12 DOF (6 displacements and 6 velocities).

5.4. Implementation of the model in Matlab/Simulink

When implementing the mathematical model of the roller system in the simulation software Matlab/Simulink [4, 97, 134], the deformation of the plate cylinder is shown first. In the second step, the measurements of the oscillations with the help of sensors like strain gauges, is included in the simulation. These signals have to be regulated with the control algorithm as described in Chapter 6.

5.4.1. Validation of the mathematical model

The first step to validate the model was already described Section 5.2 where the analytical calculations of the natural frequencies of the rollers were identical with the natural frequencies calculated with FEM, which are similar with the measured natural frequencies.

The second step is to validate the mathematical model by comparing static measurements with the simulated measurements. The bending displacements of the

plate cylinder from the industrial test setup are measured from the middle of the roller with strain gauges for different loads between 0-5 kN in the middle of the roller. The bending displacements were measured four times and the arithmetical averaged value is compared with the simulation results. Figure 5.12 shows a good correlation between measurements and roller system. The small differences appear because of approximation of the bearing stiffness, and in the same time, the roller cannot be perfectly modelled due to the complexity of its inner structure.

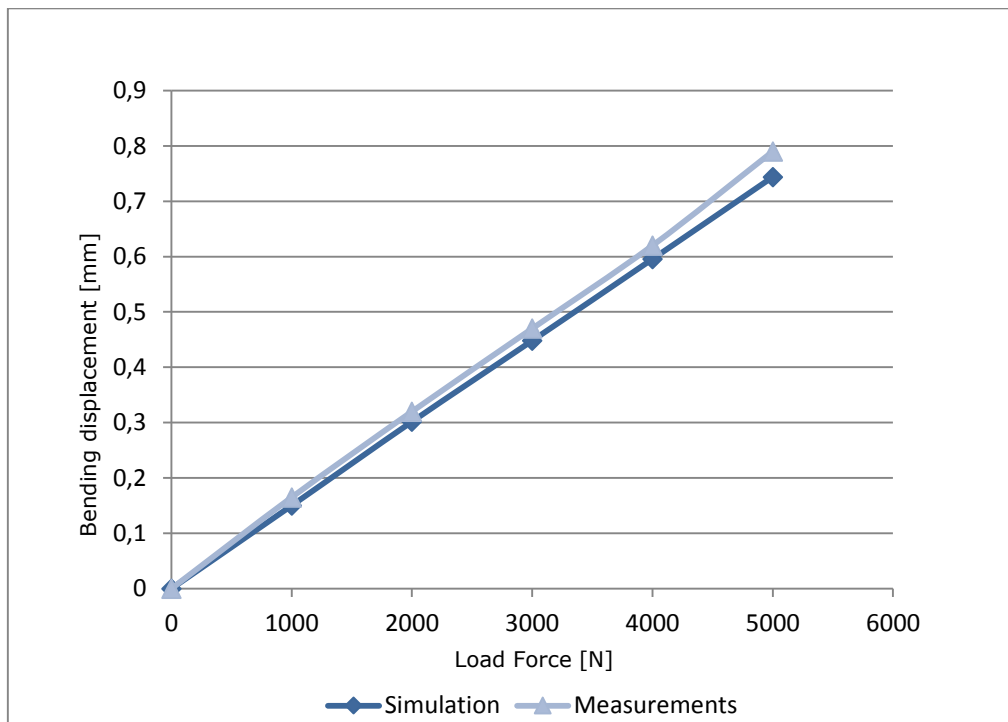


Figure 5.12 Comparison of bending displacement between measurements and simulation results

5.4.2. Simulation of the Roller System

The open-loop simulation of the vibrations of this roller as response to an excitation with a sinuswave force of 1000 N in the middle of the plate cylinder is presented in Figure 5.13. This figure shows the bending of the plate cylinder in 10 different step times of the simulation, and the deformation is shown along the roller. The roller is discretized in 20 elements and the simulation is made with 42 DOF.

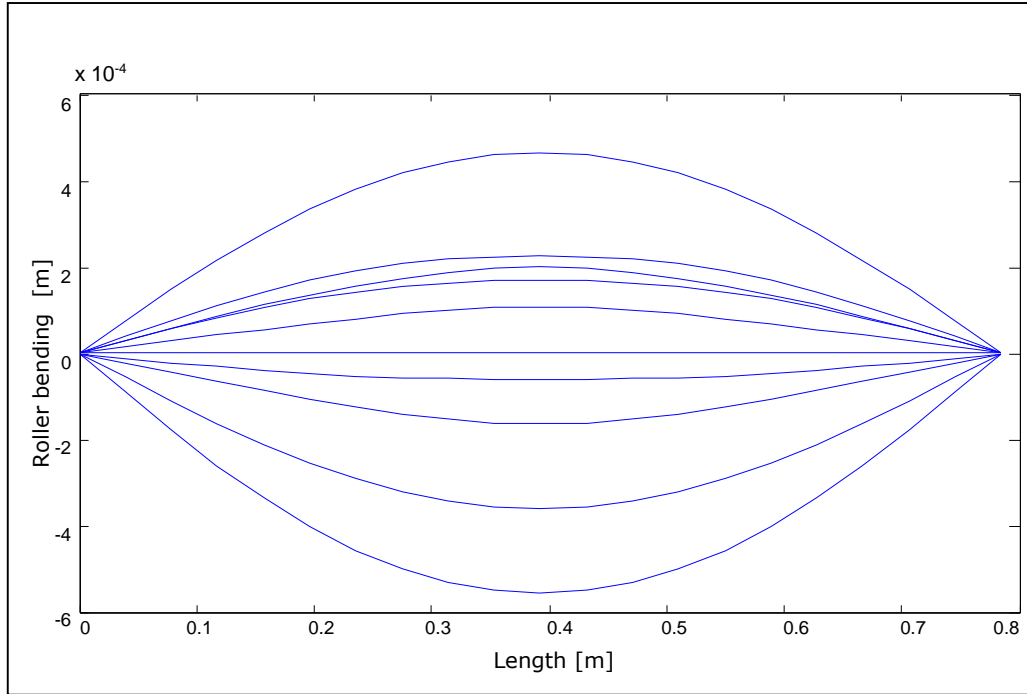


Figure 5.13 Vibration of the plate cylinder (open loop) for a disturbance force applied in the middle of the roller

The simulation of the plate cylinder using FEM method needs high computer resources. Using modal analysis, the simulated system was reduced to the first 6 mode shapes and frequencies because higher frequencies cannot be achieved during operating state. Modal analysis uses eigen values and eigenvectors to simplify the FEM model.

In Figure 5.15 is depicted the bending curve at a sequence of time steps of 1 ms after exciting with an impulse force with 1000 N in a distance of 0.15 m from the left bearing as shown in Figure 5.14. The bending curve consists of superimposed mode shapes of different orders. It is no longer symmetric to the center. The figure illustrates that two independent control loops for the actuators in the bearings are required.

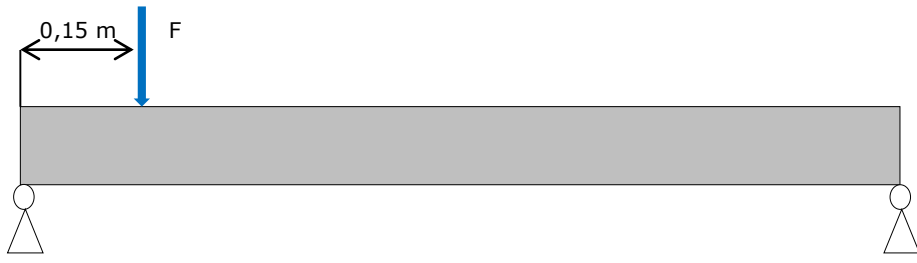


Figure 5.14 Assymmetric disturbance applied on the roller

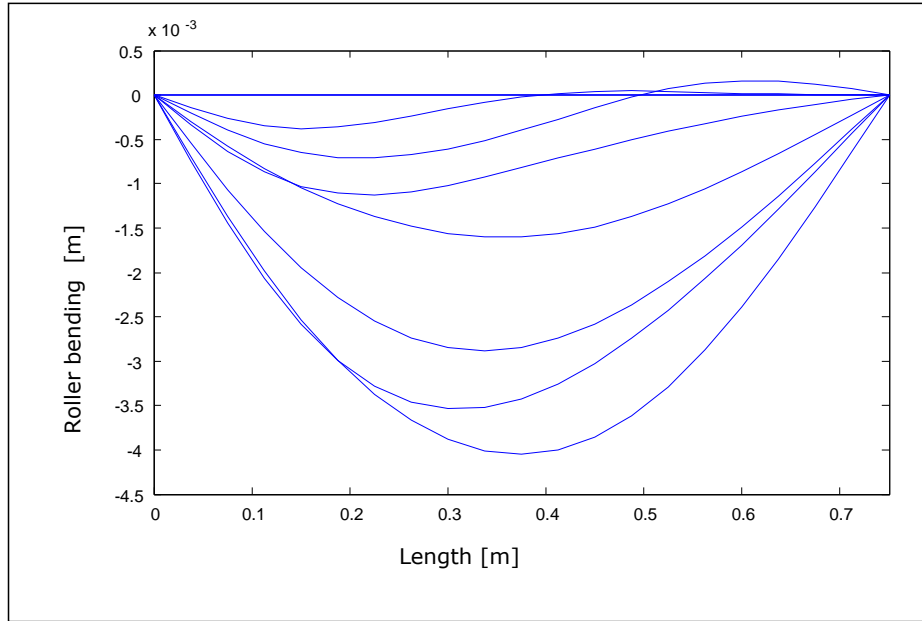


Figure 5.15 Vibration of the plate roller after asymmetric disturbance (open loop)

5.4.3. Simulation of the Components of the Closed-loop System

5.4.3.1. Simulation of the Strain Gauges

For determining the vibration of the plate cylinder, strain gauges are applied. Strain gauge is a thin sensor with maze-like wiring patterns applied on a rectangular plastic layer. Changing the width of a metal wire, changes its electrical resistance. This change is proportional to the stress applied, which can be then calculated using Hook's law. The strain is a ratio and has no unit. Strain gauge transducer transforms mechanical elongation and compression into measurable value.

Onto the plate cylinder are applied 8 linear strain gauges connected in half-bridges to measure the vibrations. These are applied at 2 cross-area sections on the roller. In simulation, the signals of the strain gauges are derived from the curvature of the bending line and are modelled using a mathematical approximation.

From [34] the curvature κ is the reciprocal value of the vibration radius and is given from:

$$\kappa = -\frac{w''}{(1 + w'^2)^{3/2}} \quad (5.77)$$

For small bending displacements and small pitches, $w'^2 \ll 1$ and the curvature can be calculated as the negative value of the second derivative of the displacement w :

$$\kappa = -w'' \quad (5.78)$$

In this form, the curvature can be approximated by differential quotient between two angular DOFs of a discretization on the roller and the length of the discretization as follows:

$$\kappa = -\frac{\Delta\varphi}{\Delta x} = -\frac{\varphi_{i+1} - \varphi_i}{x_{i+1} - x_i} \quad (5.79)$$

Figure 5.16 shows the curvature signals of the simulation model of the plate cylinder in laboratory scale, at the corresponding positions of the strain gauges.

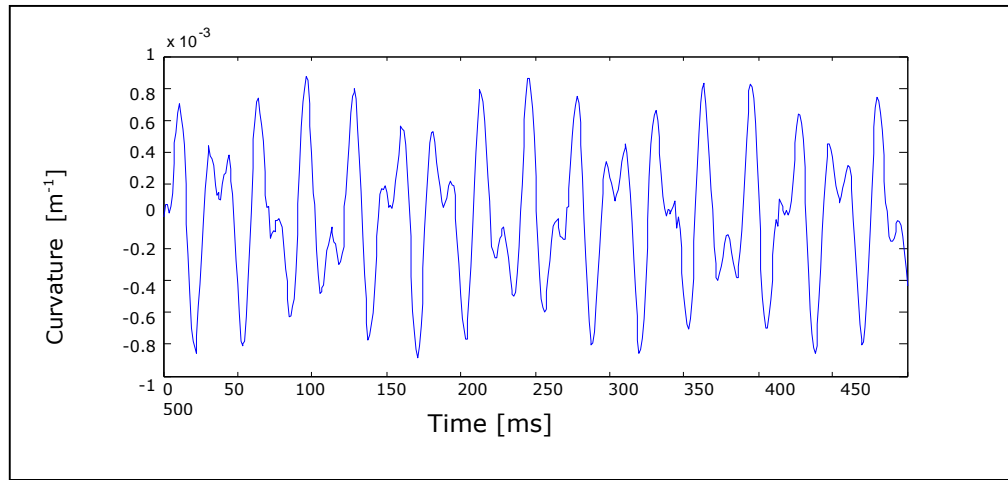


Figure 5.16 Simulated curvature

5.4.3.2. Simulation of the Piezoelectric Amplifier

Two types of piezoelectric actuators are used for testing active vibration damping for the two test setups: low-voltage actuators for the test setup in laboratory scale, and high-voltage actuators for the industrial test setup depending of the needed different types of masses and forces. The mathematical model for a piezoelectric actuator was already described in Chapter 3. First, the model of the piezoelectric amplifier is not considered in the simulation. The signal for piezoelectric actuator is given from the controller.

Two amplifiers are allocated for the two types of actuators: LE200/500 for the small test setup and RCV 1000/7 for the industrial test setup. Both are from the Company Piezomechanik. The amplifier has its own dynamic which can influence the dynamic behavior of the entire closed-loop control of the roller system. The behavior of the amplifier is approximate with a second-order lag element (PT2-element) in frequency domain. The transfer function is calculated, starting from the dynamic equation as a function of time:

$$T_{amp}^2 \cdot \ddot{u}_A + 2d_{amp}T_{amp}\dot{u}_A + u_A = K_{amp}u_E \quad (5.80)$$

where:

- u_E : input signal
- u_A : output voltage
- K_{amp} : proportional gain

T_{amp} : time constant

d_{amp} : damping constant

The transfer function for the amplifier is:

$$G_{amp}(s) = \frac{K_{amp}}{T_{amp}^2 \cdot s^2 + 2d_{amp}T_{amp}s + 1} \quad (5.81)$$

The technical data for these two amplifiers are obtained from the manufacturer [94], as presented in Figure 5.17 and Figure 5.18. Every actuator is individual manufactured and its characteristic has to be approximated similar to the depicted actuators.

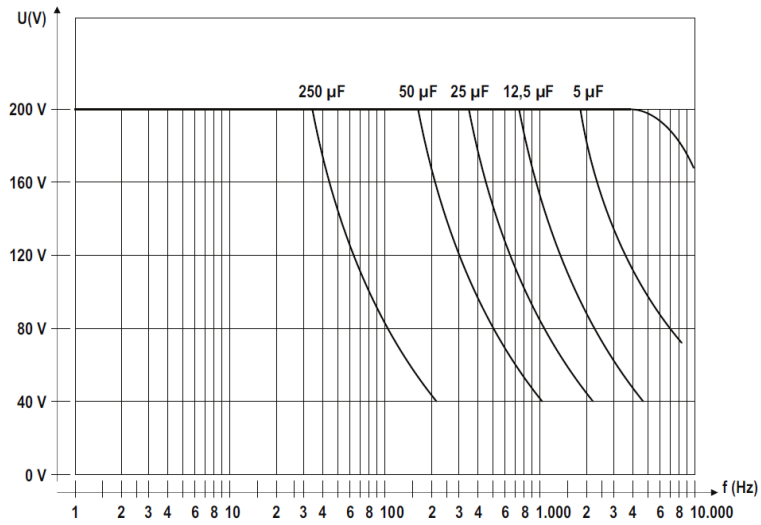


Figure 5.17 Characteristic diagram of the amplifier LE200/500

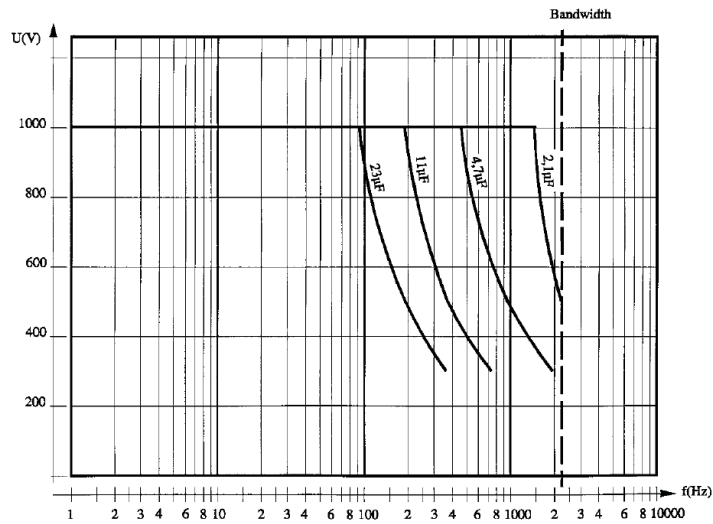


Figure 5.18 Characteristic diagram of the amplifier LE1000

Using the technical data for the amplifier RCV1000/7, which gives the characteristics for difference sensors, the characteristic of the sensor PSt 1000/35/200 VS45 with a capacity $C=6,5\ \mu\text{F}$ can be approximated as shown in Figure 5.19. The parameters of the transfer function are determined as: $K_{amp}=1000\ \text{V}$, time constant $T_{amp}=0,000321\ \text{s}$ and damping constant $d_{amp}=0.7015$. The amplifier has an output to the actuator in a range between 0 and 1000 V and amplifies the input voltage.

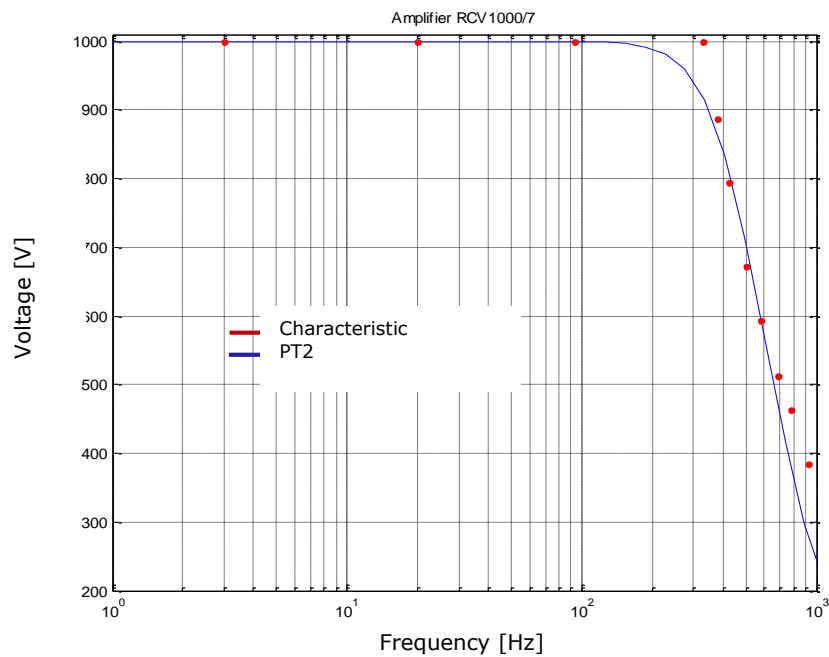


Figure 5.19 Transfer function for the amplifier RCV1000/7 for the piezo actuator PSt 1000/35/200 VS45

The characteristic of the amplifier LE200/500 for the piezoelectric actuator PSt-HD 200/10/90 VS15 with a capacity $C=9\ \mu\text{F}$ is approximated as shown in Figure 5.20. Red presents the characteristic of the amplifier and blue is the approximated transfer function. The calculated parameters are: $K_{amp}=200\ \text{V}$, time constant $T_{amp}=0,000075\ \text{s}$ and damping constant $d_{amp}=0.8201$. The damping vibration is lower than 1000 V, therefore the deviations over this frequency can be neglected.

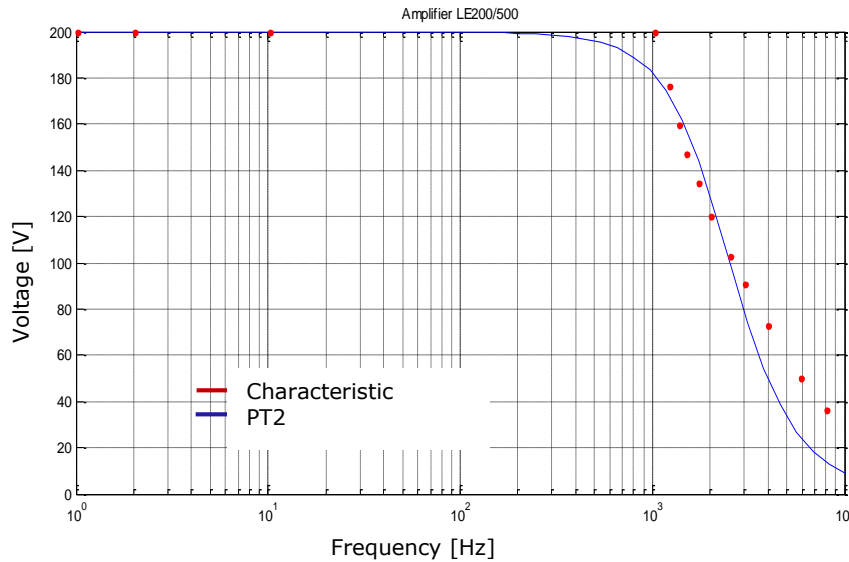


Figure 5.20 Transfer function for the amplifier LE200/500

Piezoelectric actuators may generate forces of several kN and produce displacements in the μm range. The coupling of the actuator to the driven mechanical assembly therefore must be rigid and backlash-free. Ideally, the actuator's end face is in direct contact with a metal surface. The pre-stressing force should be equal to at least one-half of the blocking force.

The mathematical equations for the description of a piezoelectric actuator are presented in Chapter 3. However, piezoelectric actuators can be simply modeled as a mechanical spring with constant stiffness. The extended model description of the roller system with incorporated piezoelectric actuators means that the equation (5.34) contains the actuator force f_A as follows:

$$M\ddot{x} + D\dot{x} + Cx = f + f_A \quad (5.82)$$

In the state equation (5.45) the actuator forces are included in the matrix control matrix B:

$$B = \begin{bmatrix} 0 & 0 \\ M_{ges}^{-1} \cdot f_{ges} & M_{ges}^{-1} \cdot f_A \end{bmatrix} \quad (5.83)$$

5.5. Chapter Summary in Romanian

In acest capitol este descrisa modelarea matematica a unui sistem de trei valuri care simuleaza o unitate de tiparire a unei prese flexografice, precum si a modelului construit in laborator dupa dimensiunile standului de incercare industrial. Fiecare valt este considerat la inceput ca element elastic continuu care trebuie discretizat pentru a putea obtine un model ce urmeaza a fi implementat intr-un software de simulare. Gradele de libertate ale unui valt sunt considerate sageata si

deplasarea unghiulara la incovoiere. Cu ajutorul metodei elementelor finite, au fost discretizate cele trei valturi si au fost calculate pentru acestea matricea de masa si de elasticitate. Folosind ecuatia de echilibru dinamic a lui Newton, este descris comportamentul dinamic al sistemului. Contactul dintre valturi este asigurat prin matrita de printat, care este modelat ca un element elastic cu o anumita amortizare. Elasticitatea matritei de printat se imparte la numarul de elemente in care se asigura contact intre valturi, ca si cum ar fi construita din mai multe elemente elastice legate in paralel.

In ecuatia dinamica a sistemului de valturi (5.35), vectorul-coloana f contine fortele si momentele dinamice care sunt aplicate in fiecare grad de libertate al valturilor. Fiecare pozitie para in vectorul f este zero, reprezentand momentul la incovoiere dinamic ce nu apare in acest sistem.

Deoarece valturile sunt sprijinite pe lagare care prezinta o elasticitate proprie, valorile elasticitatii lor s-au adaugat in primul si penultimul element din matricea de elasticitate pentru fiecare valt, respectiv $C(1,1)$ si $C(2n-1,2n-1)$, n reprezentand numarul de discretizari.

Matricea de amortizare a intregului system a fost calculata proportional cu matricea de elasticitate, folosind principiul lui Rayleigh.

Ecuatia dinamica a sistemului a fost transformata in ecuatia de stare (5.47), pentru a usura simularea sistemului prin reducerea sistemului de ecuatii diferentiale de ordinul doi la un sistem de ecuatii diferentiale de ordinul unu. Astfel, vectorul de stare z contine gradele de libertate ale valturilor si derivata acestora ca functie de timp, avand astfel un numar dublu de grade de libertate. In aceasta ecuatie, A reprezinta matricea de stare, B este matricea de control, u este matricea continand fortele de perturbare (si de control in cazul simularii sistemului cu bucla inchisa), iar C este matricea de iesire, care defineste valorile vectorului de iesire y .

Deoarece numarul de grade de libertate este foarte mare si vectorii proprii, precum si valorile proprii ale sistemului sunt complexe, este nevoie de reducerea gradelor de libertate, fara a pierde din calitatea rezultatelor. In plus, prin matricile de masa si de elasticitate, sagetile si deplasările unghiulare sunt cuplate in ecuatiile dinamice si este necesara o decuplare a acestora, in asa fel incat fiecare grad de libertate sa fie dependent numai de el insusi.

Decuplarea ecuatiilor dinamice si reducerea gradelor de libertate s-a realizat folosind analiza modala cu forma modificata. Prin aceasta metoda, numerele complexe sunt separate in parte reala si parte imaginara care se pun intr-un vector ca doua elemente reale. In acest fel, se pot face operatii numai cu numere reale, ceea ce reduce timpul de calcul.

Reducerea gradelor de libertate se realizeaza luand in calcul numai primele 6 frecvente proprii care pot aparea in testele de laborator, celelalte frecvente fiind neglijate, Numarul de grade de libertate este redus astfel la 12, reducand si timpul de calcul.

In a doua parte a acestui capitol (subcapitolul 5.4) este descrisa implementarea modelarii matematice a sistemului de valturi in programul de simulare Matlab/Simulink.

Modelul matematic este validat prin regasirea frecventelor proprii calculate analitic, in urma calcului cu metoda elementelor finite prin discretizarea valturilor intr-un numar de 20 de elemente, tinand cont de geometria si proprietatile materialului din valturi (otel). Al doilea pas in validarea modelului matematic, este compararea rezultatelor din simulare cu masuratorile statice realizate la valtul de printat industrial. Pe langa sistemul mecanic de valturi, au fost simulate si componentele

corespunzatoare sistemului cu bucla inchisa: senzorii (timbrele tensometrice), actuatore piezoelectrice si amplificatoarele de tensiune ale acestora.

Timbrele tensometrice sunt approximate folosind ecuatia matematica (5.81). Acestea masoara curbura valtului, aparuta in urma unei forte de apasare perturbatoare. Functiile de transfer ale amplificatoarelor de tensiune pentru actuatore piezoelectrice (unul pentru model si unul pentru unitatea de printare) au fost determinate din ecuatia diferentia de ordinul doi, determinata prin aproximare cu ajutorul caracteristicii amplificatorului pentru anumite actuatore, furnizata de producator (figurile 5.15 si 5.16).

In subcapitolul 5.4.2 sunt prezentate rezultatele simularii valtului de printat din sistemul model de valturi, perturbat de o forta cu amplitudinea de 1.000 N in mijlocul valtului (figura 5.9), precum si de o forta dinamica ce actioneaza la o distanta de 150 mm de unul din lagare (figura 5.11). Acestea sunt situatii care pot aparea in cadrul procesului de tiparire, matrita de tiparit variind in functie de imaginea de printat si de culoarea folosita (pentru fiecare culoare este folosita o unitate de printare).

6. ACTIVE VIBRATION DAMPING

The goal of the active control is to minimize vibration amplitudes of the considered roller systems. This chapter presents two concepts for active vibration damping, using active bearings with piezoelectric actuators described in Chapter 8.

6.1. Concept of Active Vibration Damping

The concept of active vibration damping of roller system, which is being pursued in this work, provided that piezoelectric actuators are integrated into the bearings of the plate cylinder, which is particularly susceptible to vibration. With the help of this piezo actuators counter-vibrations can be introduced in the roller to compensate roller vibrations.

In Figure 6.1 is depicted the downscaled roller system with active bearings including piezoelectric actuators. Onto the middle roller (1) are applied disturbances with the help of a piece of printing plate (3). The vibrations are measured with $350\ \Omega$ strain gauges (2) connected in half-bridges, placed at two cross-sections every 90° to the circumference of the plate cylinder. The active bearing (4) is designed to produce counteracting vibration to damp the roller oscillations.

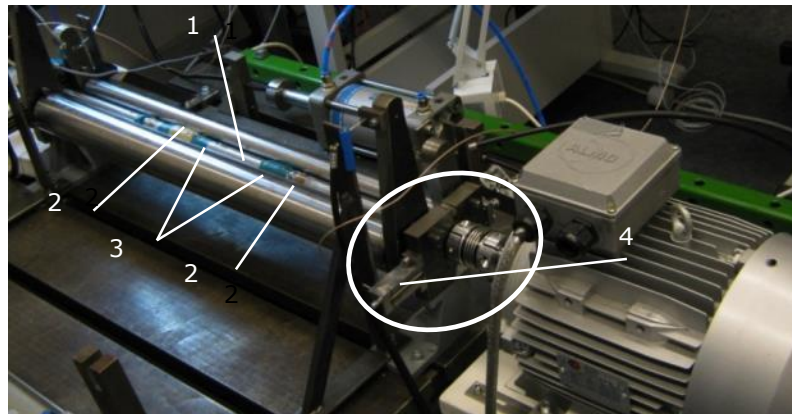


Figure 6.1 Downscaled test setup

The active bearing consists first of an outer stator and the inner rolling bearing, which supports the shaft. The stator is moved by the piezo actuator. Because of the small adjustment paths of the piezo actuators, the bearing slackness has to be as small as possible. The components of the active bearing must be as stiff as possible, that no adjustment paths are lost due to the elastic deformation of the stator or the support of the piezoelectric actuator. In the direction of movement of the piezoelectric actuator, the stator should be moved relative easy, without resistance from elastic components and friction. When using piezoelectric actuators, well-designed flexible components have to be supported, for a good control algorithm to damp vibrations.

For active vibration damping, the following control structure is defined. The signals from the strain gauges are amplified and sent as voltage to the dSpace real-time hardware card. With the help of Matlab/Simulink, the designed controller sends the control signal to the actuators through the piezo amplifiers.

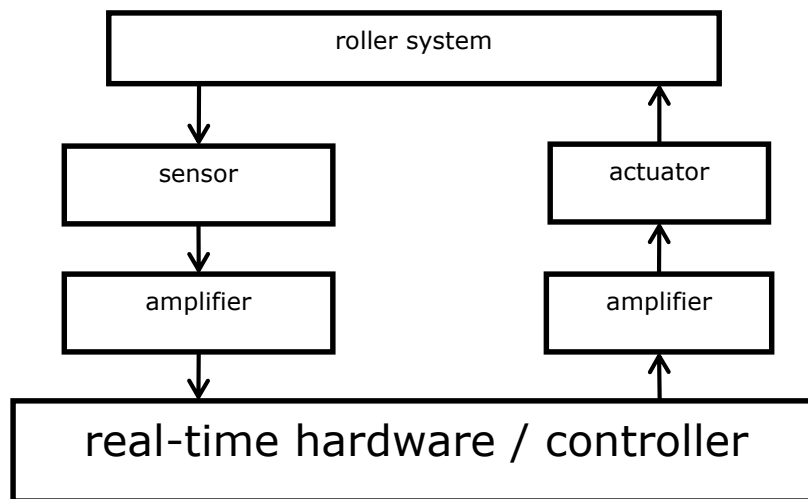


Figure 6.2 Control loop of active vibration damping

High control forces, high dynamic, but small displacements, characterize piezoelectric actuators. The integration of the piezo actuators can be problematic, because the small adjustment paths may get lost in the bearing slackness or by using a too elastic construction.

Technical data for the actuators used for active vibration damping of the roller systems are presented in Table 3.1:

Two types of control are developed in this work:

- using the closed-loop simulation of the roller system with Matlab/Simulink
- experimentally defined feed-forward control using a Least Mean Squares (LMS) identification algorithm for determination of optimal compensation forces for the actuators, combined with a PD-controller

6.2. Design of a PD Controller

In a simulation, different control algorithms can easily be developed. Additionally, it is possible to evaluate the effects in variations of the system design (e.g. bearing stiffness, application points of the actuator forces, dynamics of the actuators and sensors) [109].

An approach is to investigate the effectivity of a PD-control for vibration damping. The radial stiffness of the bearings is modelled through a spring and the actuators are placed in the bearings of plate cylinder (middle roller).

The schema of a PD-controller is presented in Figure 6.3 [62]. " K_p " is the proportional gain of the controller and " $K_D d/dt$ " is the differential term. For the improvement of the control, a first order low-pass filter was used. The first order low-pass filter improves the control by eliminating the high frequency signals.

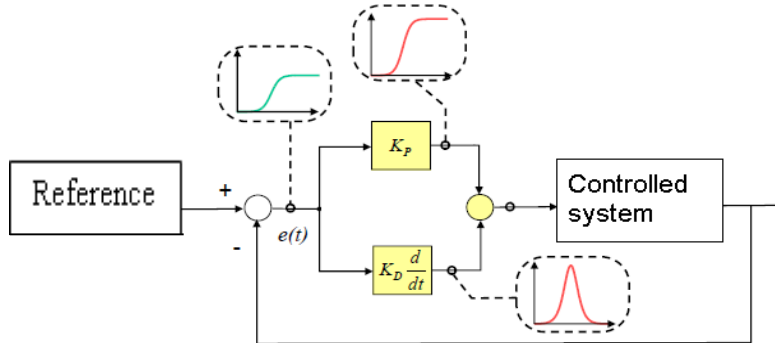


Figure 6.3 Design of the standard PD-controller

At first, the proportional gain is established until the response of the system to a signal becomes closer to the one needed. After that, the derivative gain is determined. The stability of the closed-loop control is examined with the help of the Matlab function *linmod* which linearizes the mathematical model. Thus the poles of the closed-loop system have the form $\lambda_i = \delta_i \pm j\omega_i$. The closed-loop is stable when the real part of the poles (damping) is negative.

The closed-loop simulation is implemented in Simulink as shown in Figure 6.4. The model of the piezoelectric amplifiers is not included here, and the actuators are simulated as a proportional gain. First, the disturbance is given by the addition of two steps, generating a force for 0,2 s. When the roller rotates with a frequency of 5 Hz, this signal simulates a disturbance applied for a complete rotation of the roller. The force is applied in the middle of the roller in one displacement-DOF, simulating the contact between roller in this point, for testing the functionality of the control algorithm.

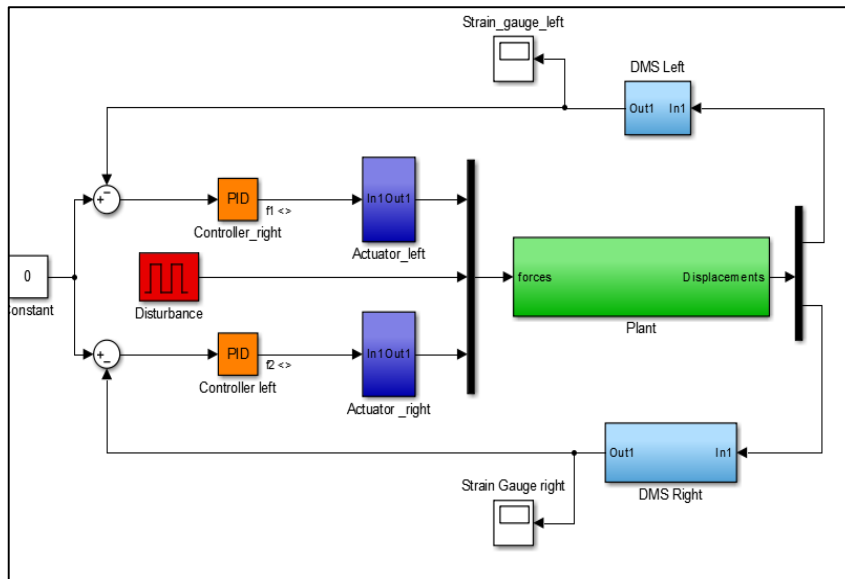


Figure 6.4 Simulation model of the roller system in Simulink

The state-space model of the system is in the block *Plant*. The output of the simulation gives the displacements of the plate cylinder by matrix *C*. The strain gauge signals are calculated in 'DMS_left' and 'DMS_right' as presented in Chapter 5. The signals from the strain gauges are compared to the reference value '0'. The difference is compensated with a PD-controller. The position of the actuators is given in the matrix *B*.

In Figure 6.5 is represented the simulated output signal of the strain gauges, first the open-loop (zone (1) and (2)) and after that the closed-loop simulation. The vibration of the plate cylinder is stimulated by a constant force with amplitude of 1000 N lasting for 0.2 s in the middle of the roller shown in the zone (1). After that, the excitation force is zero. The strain gauge shows a vibration symmetric to a point moved in the negative domain. The control loop is closed after 0.5 s simulation time. The results show the effect of the active vibration damping. After about 0.7 s when the vibration is reduced and the rest of amplitude has accepted tolerances.

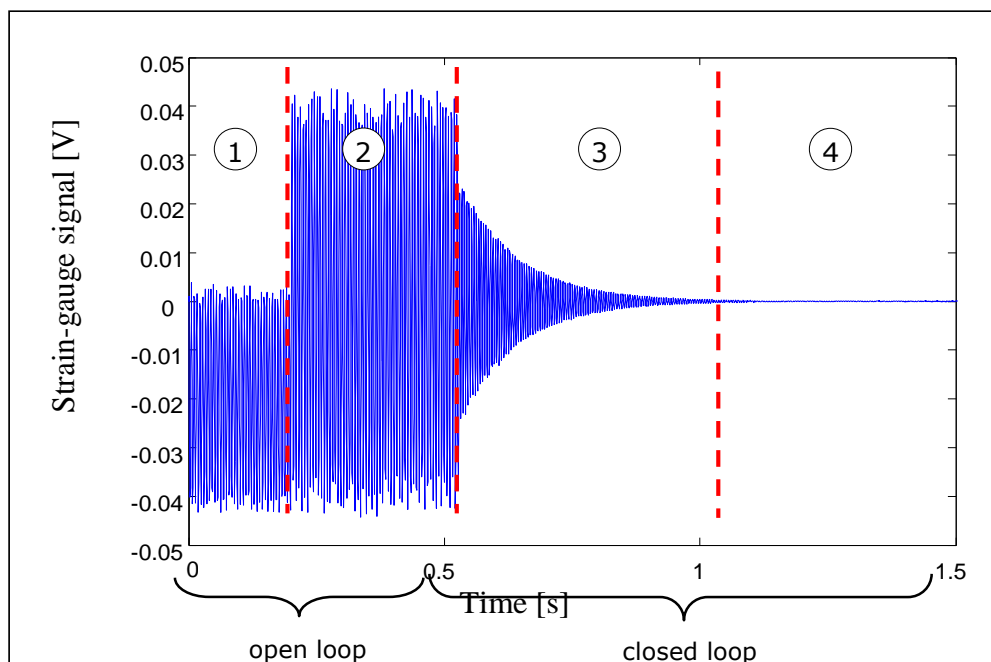


Figure 6.5 Closed-loop simulation

Figure 6.6 shows a similar simulation. With respect to the simulation in Figure 6.5, the application points of the actuators are now shifted 10 mm towards the ends of the roller. These are placed outside the bearings. Thus, the actuators introduce a bending torque with respect to the bearing. The simulation shows an improved attenuation of the vibration that is now compensated after about 0.5 s from the activating time of the controller.

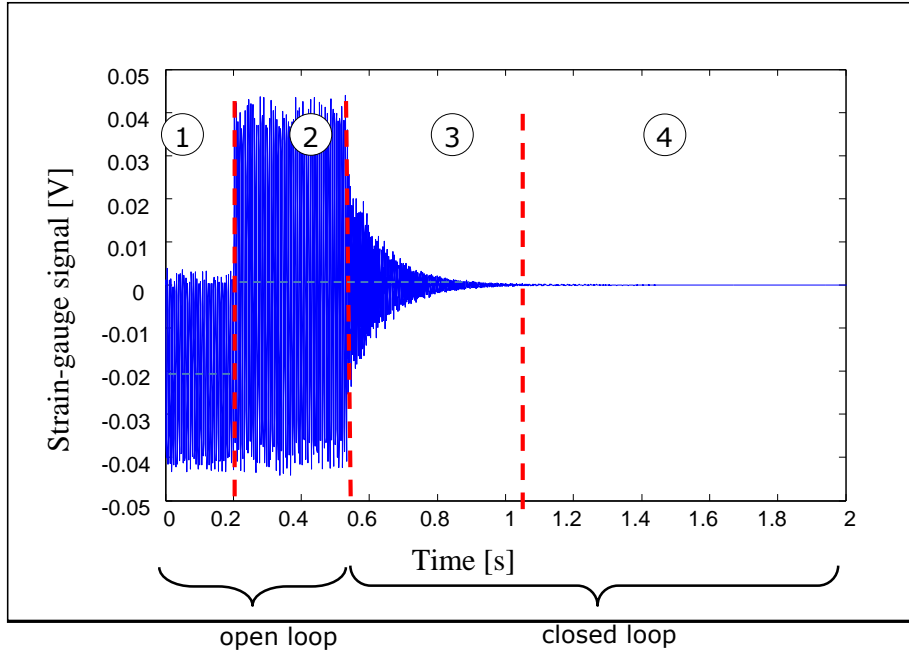


Figure 6.6 Closed loop simulation with modified actuator position

In flexographic printing machines and other applications the relevant disturbances, e.g. due to the channel effect in sheed-fed printing machines and due to printing plate in flexographic printing machines, appear periodically according to the rotation of the roller. This situation has been studied in simulations with a periodical disturbance force as illustrated in Figure 6.7. The excitation force is defined as function of the rotational angle and is applied for every rotation in one DOF radial to the roller. It simulates the excitation in the nip by printing plate applied onto the circumference of the plate cylinder during its rotation for 72° .

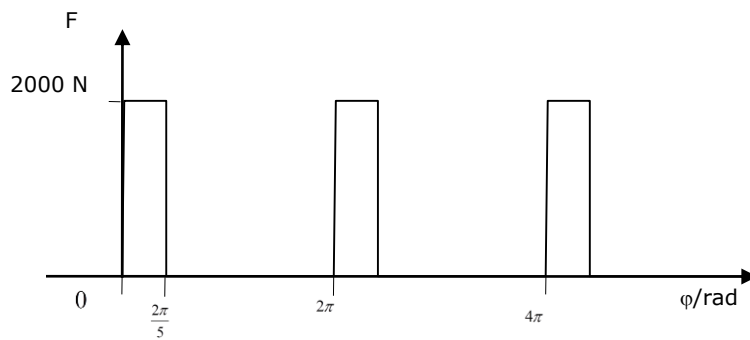


Figure 6.7 Periodical disturbance force

Figure 6.8 depicts the resulting strain-gauge signal as a response to the periodical disturbance. In zones (1)-(4) is presented the open-loop simulation and after that the closed-loop simulation. In zones (1), (3) and (5), the force is applied onto the roller in nip direction. After rotating the roller with 72° , the force disappears. The effects are similar to the presented results in Figure 6.5 (zone (1) and (2)). After a rotation, in zone (3) the force generates a movement of the symmetric line of the roller vibrations, adding the amplitude of the excitation to the value of the vibration in the moment of force application. The control-loop is closed after 0.45 s simulation time (zone 7). The piezoelectric actuators are placed in the bearings, like in the test setup. The control algorithm significantly reduces the vibrations (zone 9). The strain-gauge signal and the actuator forces, respectively, show a periodic shape according to the frequency of the stimulating disturbance. Moreover, the actuator force, required to compensate the periodical disturbance, can obviously be predicted.

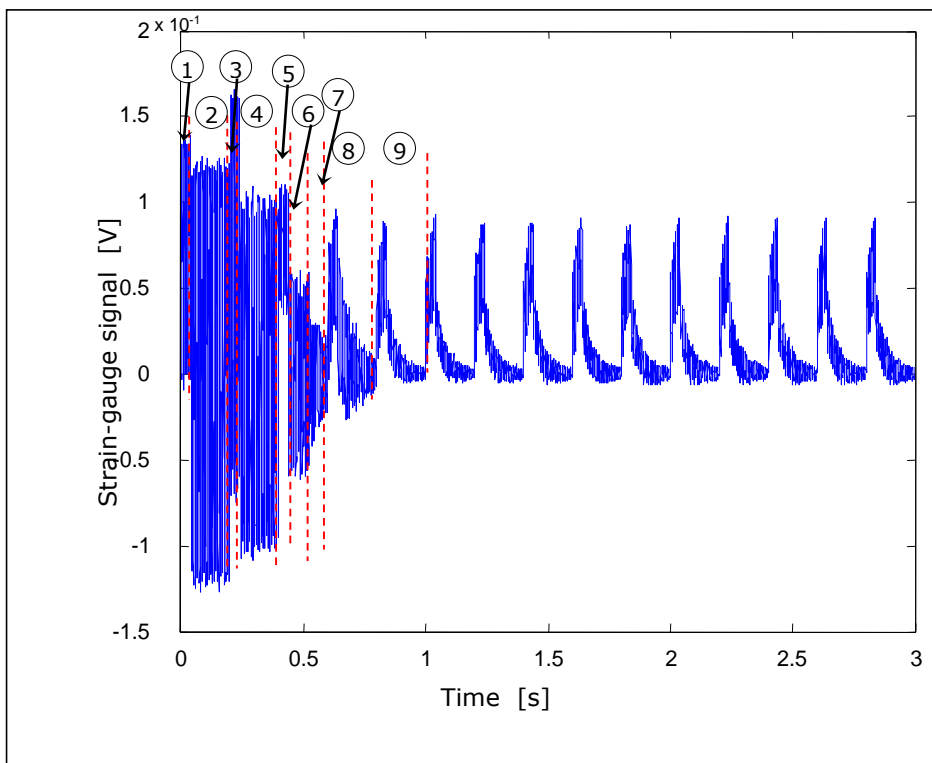


Figure 6.8 Strain-gauge signal with periodical disturbance

Based on this, a control strategy was developed, that consists of a feed-forward control to compensate predictable disturbances and a subsequent feedback control.

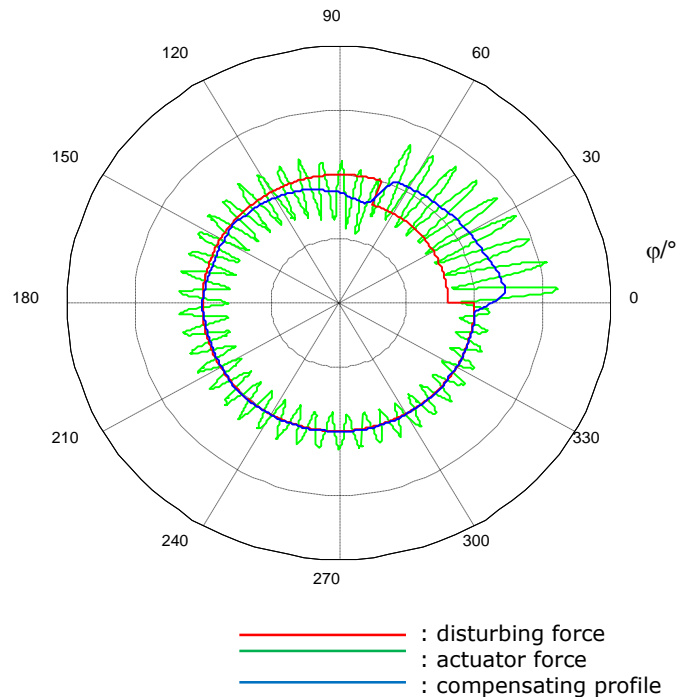


Figure 6.9: Disturbance and control signal as a function of the rotational angle

Figure 6.9 illustrates the disturbing force (as defined in Figure 6.7) and the resulting actuator force as a function of the rotational angle φ . The relative signal amplitudes are disproportionally gained for clarification. The disturbance affects the roller in normal direction towards the center. The correcting counter force of the actuator includes of a portion determined by the shape of the disturbance. It is superimposed with the natural harmonics of the roller.

The frequency of the harmonics with respect to the rotational angle depends on the rotational speed of the roller. Compared to that, the influence of the shape of the disturbance with respect to the rotational angle does not significantly vary with the rotational speed. In Figure 6.9 the influence of the shape is depicted as a compensating profile.

The compensating profile does not necessarily have to be generated actively by the actuators in the closed loop. Given the shape of the disturbance, it can be determined in simulations or experiments and then be copied to special rings. These profile rings can be mounted on the axle of the roller and rotate with it. They passively provide a counter force when rolling against the central impression cylinder or any other counter surface [71]. However, the profile rings have to be adapted if e.g. the printing plate and the disturbances, respectively, change. The design and test of the profile rings is part of ongoing research work.

Another part of the current research work is focused on an improved closed loop control algorithms. The equations of motion of the roller system are given as set of second order differential equations (ODE's) as presented in Chapter 5. These can be rewritten as a state space model of coupled first order ODE's and then be decoupled

using modal transformation. Moreover, it is possible to reduce the system order by neglecting higher frequency modes. The reduced order model can be used for accelerating simulation or for model based controller design.

6.3. Design of a Feed-Forward Control Using Least Mean Squares Identification Algorithm (LMS)

A second investigation of active vibration damping is made using a feed-forward control and determination of optimal actuator forces using Least Mean Squares Algorithm (LMS) [88] [87] [107]. The concept was tested on the downscaled test setup, used for the identification of compensation actuator forces [132]. It contains in a feed-forward and a feedback control as shown in Figure 6.10. As feedback control, was implemented a PD -controller which already was tested in the simulation with good results.

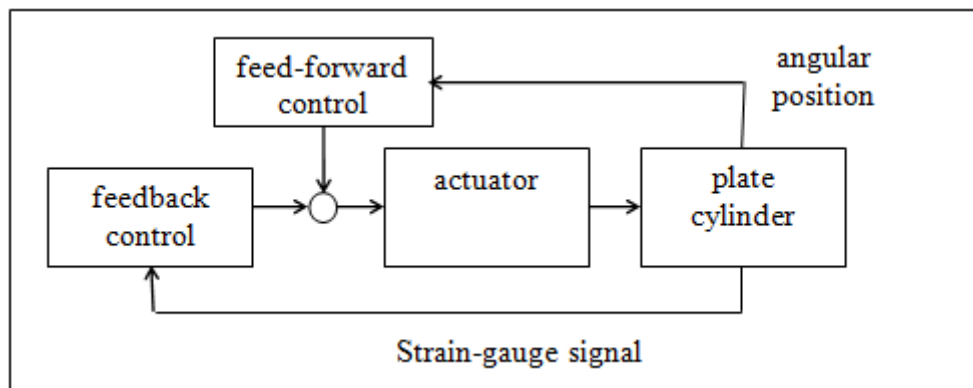


Figure 6.10 Control structure

The roller vibration is measured with strain gauges and the signals are amplified on the roller. After that, these signals are sent with the help of a slip ring to real-time hardware system dSpace, together with the angular position measured with the hall sensor. The signals are visualized on the interface as shown in Figure 6.14.

It is assumed, that disturbances appear periodically with the rotational frequency or one of its multiples (see Figure 6.11). The idea is to replace the feedback control that compensates the difference between a set point and actual value of sensor signals with a combination between feedback and forward control. For this purpose, the disturbance is first recorded without the effect of the actuators. From this data, an appropriate counteract control is calculated, which cancels in the best case all periodical disturbances.

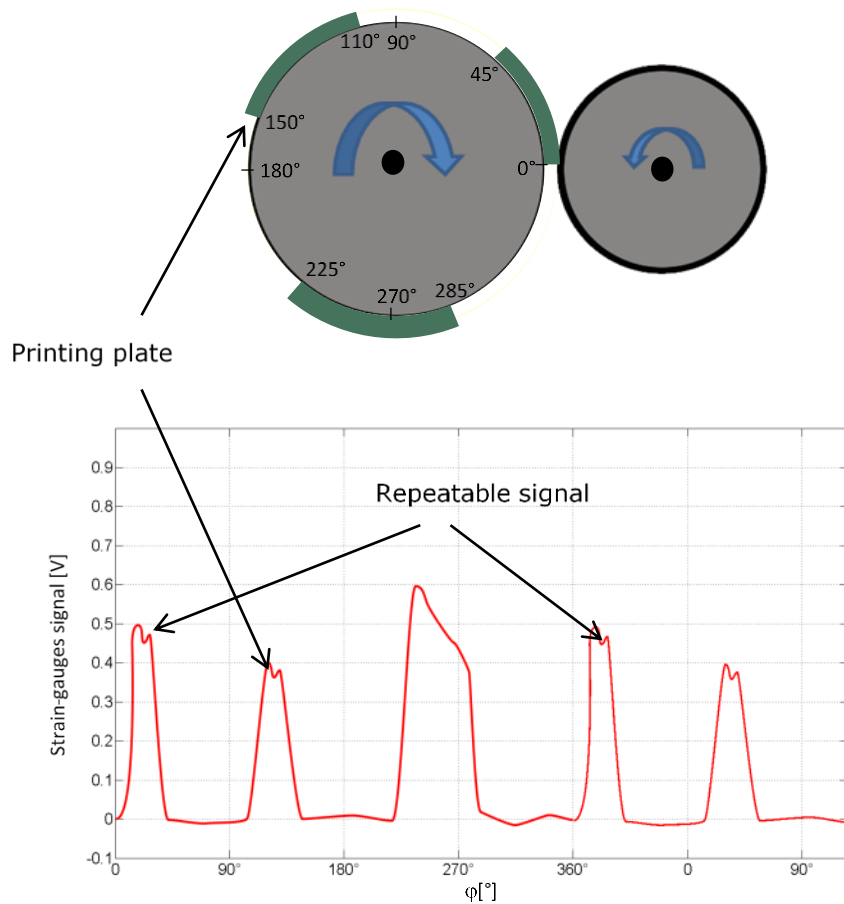


Figure 6.11 Schema of the roller system with uneven printing plate and the result disturbance

The control algorithm for the actuators by means of the mathematical model of the roller system is designed and implemented in Matlab / Simulink. The roller system is controlled as described below with feed-forward control and feedback control. The algorithms and the control are realized with a rapid-control-prototyping system. Bending vibrations are measured with strain gauges placed on the roller, by measuring the curvature of the bending roller. These form the input of the feedback controller which optimizes the control signals $u_1(t)$ and $u_2(t)$ and thus the positioning forces of the piezo actuators, so that the measured vibrations are minimal.

The structure of determination of actuator forces for the feed-forward control using a LMS algorithm is depicted in Figure 6.12, where the signals used for learn and work phases are measured with strain gauges placed on the roller in two directions. The signal must be transformed for a rotating coordinate system fixed on the roller to a special coordinate direction with the angle φ in the rotation mode as follows:

$$\begin{aligned} DMS_x &= DMS_1 \cdot \sin\left(\frac{\pi}{2} - \varphi\right) + DMS_2 \cdot \sin(\varphi) \\ DMS_z &= DMS_1 \cdot \cos\left(\frac{\pi}{2} - \varphi\right) + DMS_2 \cdot \cos(\varphi) \end{aligned} \quad (6.1)$$

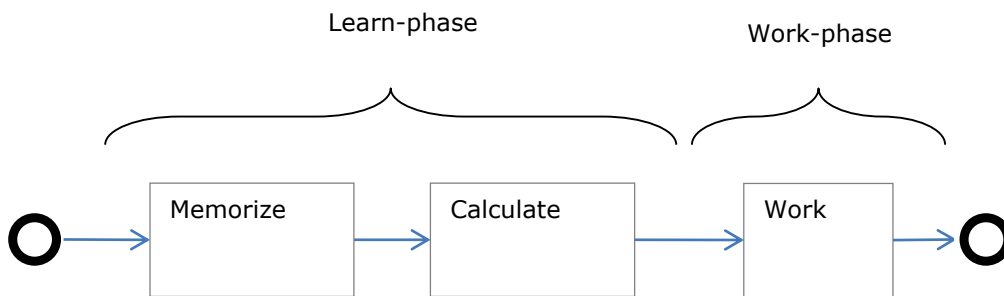


Figure 6.12 Diagram of the control phases

The position angle $\varphi(t)$ is measured with a hall sensor to determine the rotational speed and to synchronize the feed-forward control (see Figure 6.13).

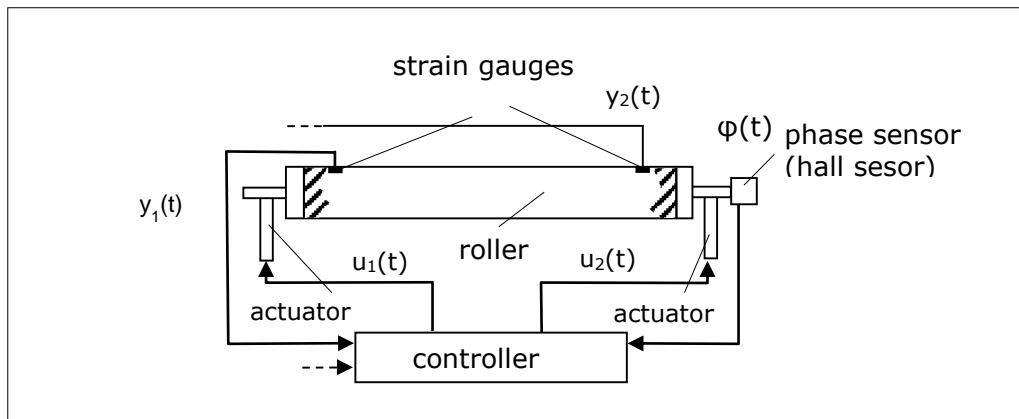


Figure 6.13 Control structure

The calculation of the feed-forward control requires a run-in-phase with the piezoelectric actuators. The pilot control signal is calculated with a Least Mean Squares Algorithm that minimizes the error by modifying coefficients of superimposed harmonic functions. In the current implementation, the feedback control is designed as a PD-controller.

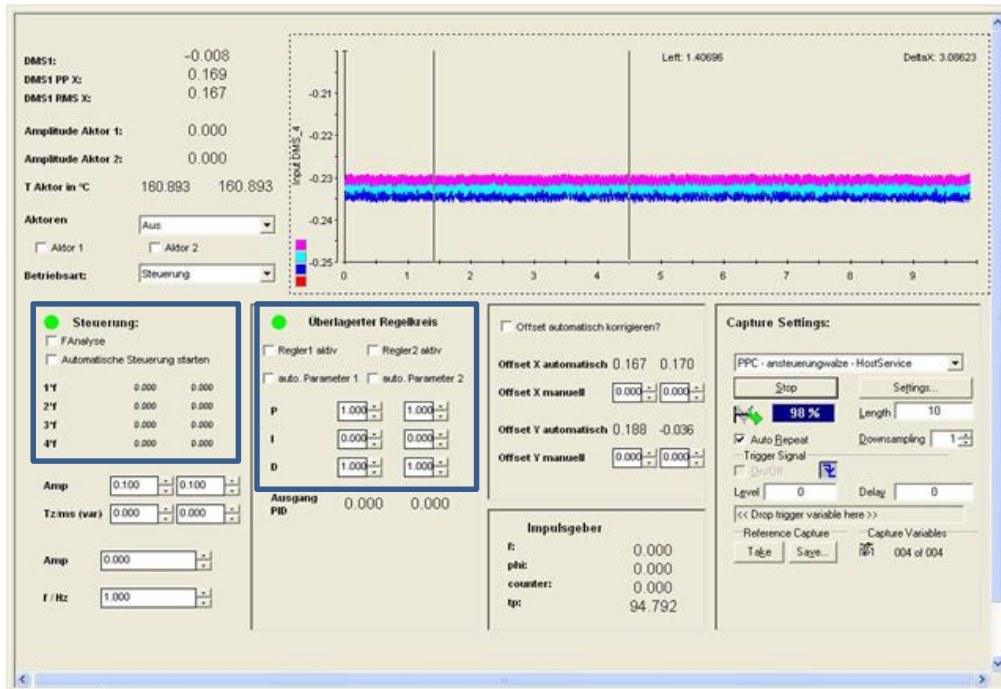


Figure 6.14 dSpace interface for measuring and compensation of roller vibrations

When designing a control algorithm for damping of roller vibrations, excitation forces are considered to be periodic during the rotation of the roller. The controller consists of a feed-forward algorithm that compensates a predominant part of the vibration excitation, and a feedback control.

The feed-forward generates periodical signals adapted to the excitation. Particularly in flexo printing, it must be assumed that different printing plates (and also printing images) generate different excitations. Thus, the time records of feed-forward control must be individually adapted and optimized at each new print. For this, the excitation can be resolved according to a Fourier-series, in a fundamental oscillation and harmonic oscillations, whose amplitudes and phase angle are determined in advance during an identification phase. A very robust and fast identification procedure is presented below. A dSPACE digital data acquisition and real-time control system is used for data collection and implementation of control algorithms.

The measurement of roll vibrations can be carried out using conventional strain gauges or with a novel, based on piezoelectric paint sensor technology [121]. Such sensors can be applied under the coating of rollers, without affecting mechanical properties of elastomer coating or to disturb the quality of printing process. It can be used also for online monitoring of roller vibration and optimal adjustment of contact forces.

For feed-forward control, the periodic excitation forces are first identified. These are first developed in a Fourier series as follows:

$$F(t) = \frac{1}{T} \left(\frac{a_0}{2} + \frac{1}{2} \sum_{i=1}^{\infty} (a_i \cos(i \Omega t) + b_i \sin(i \Omega t)) \right) \quad (6.2)$$

$$\text{with } \Omega = \frac{2\pi}{T} : \text{ angular velocity of the roller} \quad (6.3)$$

and T : period of a roller rotation.

Accordingly, it is also assumed, that forces for vibration damping in the bearings can be described with the following function:

$$\text{Left bearing: } F_L(t) = \sum_{i=1}^m (A_{iL} \cos(i \Omega t) + B_{iL} \sin(i \Omega t)) \quad (6.4)$$

$$\text{Right bearing: } F_R(t) = \sum_{i=1}^m (A_{iR} \cos(i \Omega t) + B_{iR} \sin(i \Omega t)) \quad (6.5)$$

where m : number of harmonics considered. In this application, $m = 4$ for the first four harmonics considered, as shown in Figure 6.14 "Steuerung".

The bending vibrations v_{kL} (left measuring point) and v_{kR} (right measuring point) of the roller are measured at two cross-sections. The parameters A_{iL} , A_{iR} , B_{iL} and B_{iR} are with LMS algorithm determined by minimizing the bending vibration. An error vector has to be defined as follows:

$$v^T = [v_{1L}, v_{1R}, \dots, v_{kL}, v_{kR}, \dots, v_{NL}, v_{NL}] \quad (6.6)$$

with v : error vector and N : number of the considered measured values.

The fact that for the harmonic functions of actuator forces F_L and F_R , not amplitude and phase, but for each frequency an amplitude is identified for the sine and one for the cosine function, so that it has been obtained a linear relationship between identification parameters and error:

$$v_{kL} = c_{1L} F(k * \Delta t) + c_{2L} F_L(k * \Delta t) + c_{3L} F_R(k * \Delta t) \quad (6.7)$$

$$v_{kR} = c_{1R} F(k * \Delta t) + c_{2R} F_L(k * \Delta t) + c_{3R} F_R(k * \Delta t) \quad (6.8)$$

where F are forces (e.g. weight force, other forces in the bearings) that can be influenced by F_L and F_R .

The influence factors c_{2L} , c_{3L} , c_{2R} , c_{3R} has to be identified in advance just ones, by applying test functions. For the LMS algorithm it is defined a square quality criterion J :

$$J = v^T G v, \quad (6.9)$$

depending from the weighted matrix G , which is chosen as unit matrix.

Starting from a linear or linearized relationship between the error vector v and a vector a containing the parameter A_i and B_i :

$$v = v_0 - Dv a, \quad (6.10)$$

with

$$a^T = [A_{1L}, A_{1R}, \dots], \quad (6.11)$$

it follows the matrix Dv :

$$Dv = - \begin{bmatrix} \frac{\partial v_1}{\partial A_{1L}} & \frac{\partial v_1}{\partial B_{1L}} & \frac{\partial v_1}{\partial A_{1R}} & \frac{\partial v_1}{\partial B_{1R}} & \dots & \frac{\partial v_1}{\partial A_{mL}} & \frac{\partial v_1}{\partial B_{mL}} & \frac{\partial v_1}{\partial A_{mR}} & \frac{\partial v_1}{\partial B_{mR}} \\ \vdots & \vdots & \vdots & \vdots & \vdots & \vdots & \vdots & \vdots & \vdots \\ \frac{\partial v_N}{\partial A_{1L}} & \frac{\partial v_N}{\partial B_{1L}} & \frac{\partial v_N}{\partial A_{1R}} & \frac{\partial v_N}{\partial B_{1R}} & \dots & \frac{\partial v_N}{\partial A_{mL}} & \frac{\partial v_N}{\partial B_{mL}} & \frac{\partial v_N}{\partial A_{mR}} & \frac{\partial v_N}{\partial B_{mR}} \end{bmatrix} \quad (6.12)$$

$$\text{with e.g. } \frac{\partial v_k}{\partial A_{iL}} = \cos(i \Omega k \Delta t), \quad (6.13)$$

The Least Squares Algorithm delivers thus after a calculation run of 2 seconds the optimized parameters A_{iL} , A_{iR} , B_{iL} und B_{iR} . The necessary condition for a minimum of the quality criterion J is:

$$\frac{\partial J}{\partial a_i} = \frac{\partial v^T}{\partial a_i} G v + v^T G \frac{\partial v}{\partial a_i} = 2 \frac{\partial v^T}{\partial a_i} G v = 0 \quad (6.14)$$

With the definition of the matrix, it results the necessary condition for a minimum:

$$Dv^T G v = 0 \tag{6.15}$$

When inserting the linear relationship for v and solving the equation for a gives:

$$a = (Dv^T G v)^{-1} Dv^T G v_0 \tag{6.16}$$

With the optimized control functions of the actuators $F_L(t)$ and $F_R(t)$ is the feed-forward algorithm implemented in the control. This measure already has proved in experiments to be extremely effective in reducing the bending vibration of the roller. Residual vibrations, caused i.e. by random excitations or excitation, that do not appear periodically with the roller rotation are corrected with a PD feedback controller. On the output to the actuator is applied a low-pass filter with $T=10$ ms for protection of the actuators, D-part of the controller introducing high dynamic signals in the system.

The algorithm is implemented in Simulink using special blocks for dSpace cards. After compiling the model with a discrete step time of 1 ms, a C-code is generated for communication of the real-time system with the mechanical systems (by means of measurements with sensors and reducing vibration with actuators). The main model is shown in Figure 6.15.

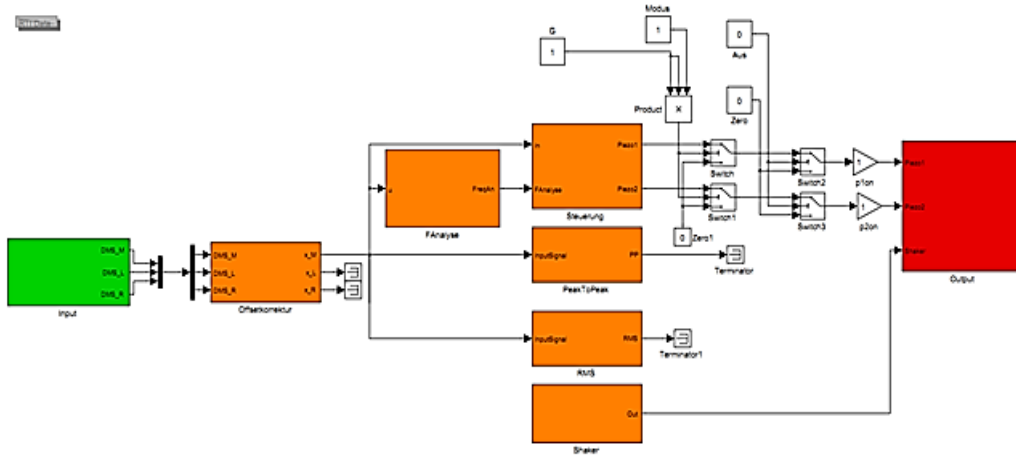


Figure 6.15 Implemented model in Simulink

In the block "Input" are the received the strain gauge signals from the strain gauges placed on the left, on the right side and in the middle of the roller named "DMS" (Figure 6.16). These are filtered with a low pass filter with a time constant $T=0,01$ s.

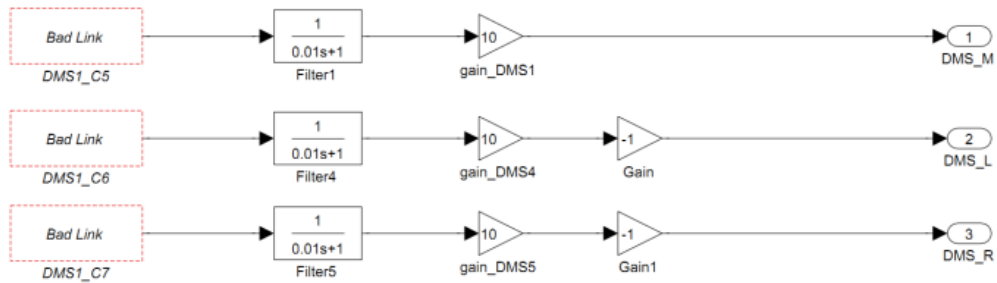


Figure 6.16 Block for strain gauge signals

After that, in the block "Offsetkorrektur", the average of the strain gauges signals is calculated in intervals of 2 seconds and then subtracted from the signal, to remove the sensor's offset, as shown in Figure 6.17.

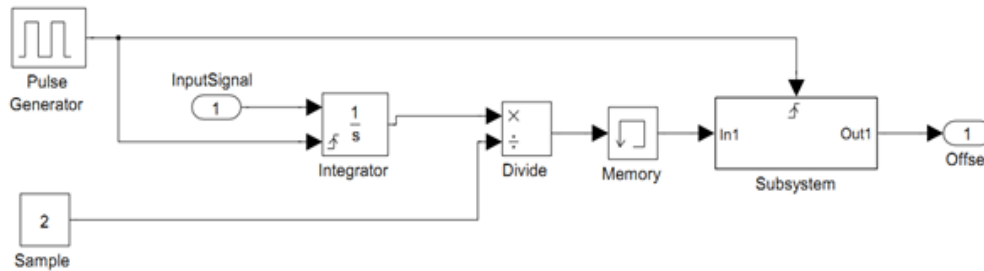


Figure 6.17 The block "Offsetkorrektur"

In the block "FAnalyse" shown in Figure 6.18 is implemented the described LMS algorithm for frequency analysis. For this purpose, "buffer" recorded for two seconds the strain gauges signals and save the values in a vector. The vector is sent to the analysis block. In order to reduce memory consumption from this algorithm, only the fundamental oscillation and the first five harmonics are calculated.

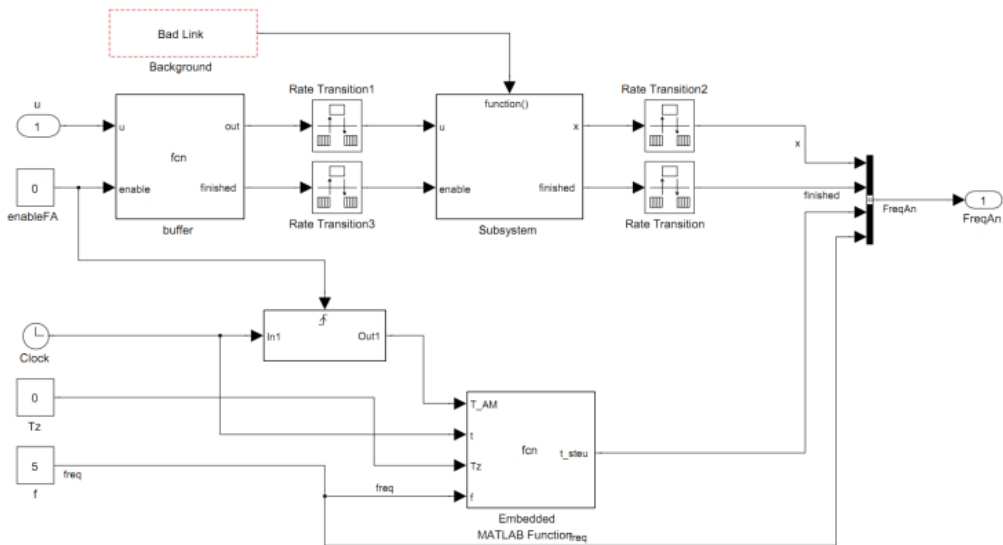


Figure 6.18 The block "FAnalyse" for identification with LMS Algorithmus

6.4. Test Results of Active Vibration Damping Using Feed-Forward and Feedback Control Algorithm

The basic procedure for determination of the optimal force profile is to generate counter-vibrations with piezoelectric actuators. The control is as described above with feed-forward control and feedback control. The algorithms programming and the control are realized with Rapid Control Prototyping system dSpace. On the roller, strain gauge bridges for measuring bending vibrations are located in two cross-sections. They form the inputs of the controller, that the control signals $u_1(t)$ and $u_2(t)$ and thus the actuating forces optimized so that the measured vibrations are minimal. The angle $\varphi(t)$ is measured for determining the rotational speed of the roller and for synchronization of the feed-forward control.

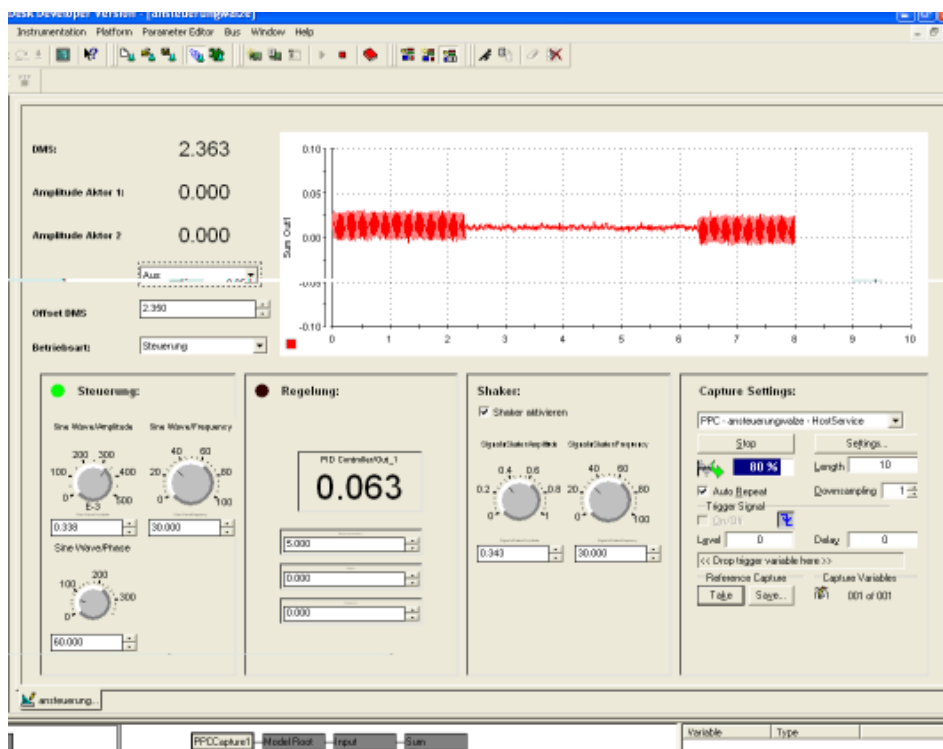


Figure 6.19 dSpace interface for feed-forward and feedback control

The test results in Figure 6.20 show the effect of the proposed control strategy. Different periodic stimuli are evaluated. The results are taken with superimposed sinusoidal stimulation of 5 Hz and 15 Hz. The control is activated after a time of 1.18 s. It significantly reduces the oscillation of the roller.

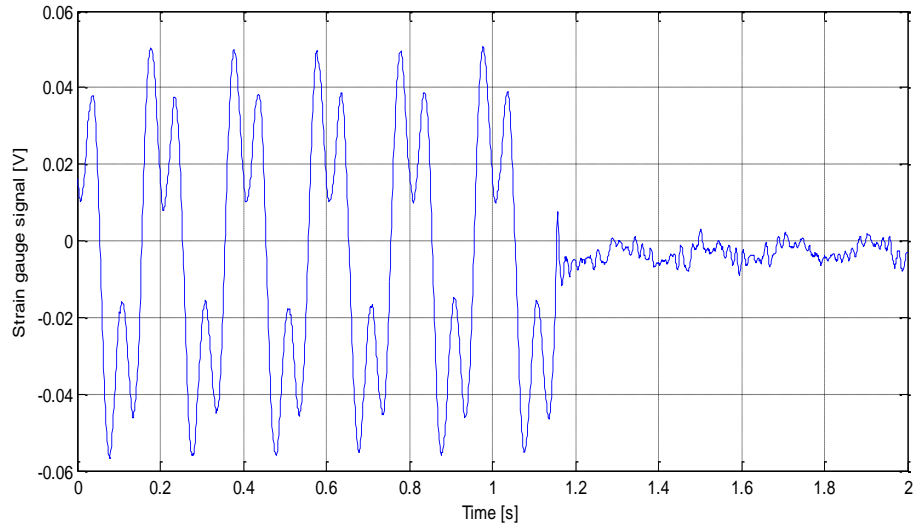


Figure 6.20 Vibration damping for superimposed excitation frequencies of 5 Hz and 15 Hz

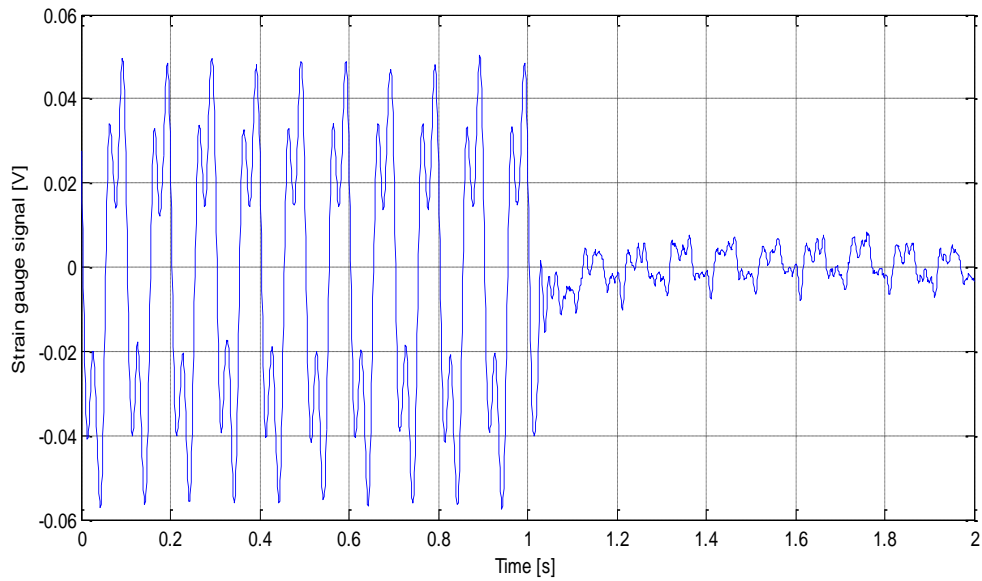


Figure 6.21 Vibration damping for superimposed excitation frequencies of 10 Hz and 30 Hz

These results have been obtained while the roller does not rotate, but is excited by an electrodynamic shaker from the company Bruel & Kjaer. A significant reduction of the vibrations (over 85 %) can be recognized.

6.5. Chapter Summary in Romanian

In acest capitol este prezentat conceptul si realizarea reducerii active a vibratiilor in sistemul de valturi prezentat in figura 6.1. Acest stand de incercare este modelul realizat dupa unitatea de printare dintr-o masina flexografica si este alcatuit din 3 valturi asezate in linie orizontala. Contactul dintre valturi este realizat cu ajutorul unui material elastic (3) (o parte dintr-o matrita de tiparit folosita la masinile flexografice). Valtul de tiparire aflat in mijloc este fixat cu lagare active cu actuatore piezoelectrice pentru a-i amortiza vibratiile produse de matrita de tiparit. Masurarea vibratiilor se face folosind timbre tensometrice (2) ale caror semnale sunt amplificate, digitizate si inregistrate pe sistemul de operare in timp real dSpace. Semnalele senzorilor masurate in Volti constituie valorile de intrare in controler, care aici e determinat ca fiind proportional-derivativ. Acesta compara semnalele timbrilor tensometrice cu o valoare de referinta si transmite semnale optimizate la amplificatorul de tensiune al actuatorelor piezoelectrice. Actuatorele genereaza forte proportionale cu tensiunea electrica primita si micsoreaza vibratiile valtului. Conceptul de reducere a vibratiilor este prezentat schematic in figura 6.2.

In prima parte a acestui capitol este prezentata simularea sistemului de valturi cu bucla inchisa, folosind un controler proportional-derivativ care a fost parametrizat utilizand modelul matematic descris in capitolul 5. Pentru a optimiza comportamentul dinamic al valtului, s-a testat prin software amortizarea vibratiilor prin plasarea actuatorelor in diferite pozitii: in lagare, in partea exterioara a valtului (intre lagare si terminatia valtului) precum si in partea interioara a valtului (intre lagare si centrul valtului). Primele doua metode au adus cele mai bune rezultate in timpul simularii. Rezultatele reducerii vibratiilor cu actuatorele plasati in lagare sunt prezentate in figura 6.4 unde semnalul trimbrului tensometric este redus pana la o valoare minima accesibila. In 0,2 s de la inceputul simularii este aplicata o forta de 1.000 N. Se observa ca valtul vibreaza in acest timp simetric in jurul valorii de -0,02 V. Pana la activarea controlerului la 0,5 s, timp in care forta perturbatoare este inlaturata, valtul vibreaza simetric in jurul valorii 0. Prin activarea controlerului proportional-derivativ, se observa o reducere foarte mare a vibratiilor valtului de printare.

Matrita de tiparit prezinta forte perturbatoare care se repeta periodic cu fiecare rotatie a valtului. De aceea este prezentata in figura 6.7 efectul unei perturbatii periodice de 2.000 N. Asemnator cu graficul descris anterior, pe o rotatie, este aplicata pe circumferinta valtului o forta punctuala pe lungime, ce actioneaza sub un unghi de aproximativ 70°. Pana la activarea controlerului, valtul vibreaza simetric fata de o axa care se modifica cu timpul. Primele doua zone sunt asemanatoare cu exemplul anterior. In zona a treia se observa ca amplitudinea datorata fortei perturbatoare aplicata la a doua rotatie se adauga la amplitudinea din momentul aparitiei acesteia. Acelasi fenomen se repeta, de data aceasta insa este activat controlerul, care incepe sa reduca vibratiile. Reducerea optima nu este realizata de la prima rotatie, deoarece perturbatia a determinat deviatia punctului zero al senzorului. In final, se observa ca la fiecare rotatie, vibratia determinata de forta perturbatoare este redusa, generand astfel ideea compensarii vibratiilor in bucla deschisa. Aceasta se poate realiza folosind forte care sa fie identificate in prealabil si care sa creeze vibratii cu o amplitudine negativa fata de cea creata de fortele perturbatoare. Acest efect este prezentat in figura 6.8, unde sunt reprezentate forta perturbatoare (linia rosie) si valoarea medie a fortelor compensatoare (linia albastra).

Urmarind aceste efecte determinate prin simulare, s-a pornind la realizarea unui concept de reducere a vibratiilor pentru standul model, realizat experimental. Acest concept introduce cele doua idei:

- compensarea vibratiilor ce apar periodic cu unghiul de rotatie datorate matritei de tiparit in bucla deschisa
- compensarea vibratiilor ce pot aparea intamplator, sau in cazul cedarii primului algoritm, prin folosirea unui controller proportional-derivativ, intr-un mod asemanator cu cel prezentat in subcapitolul anterior.

Compensarea vibratiilor periodice in bucla deschisa se realizeaza folosind un algoritm de optimizare a fortelor compensatoare cu metoda celor mai mici patrate.

Fortelor perturbatoare sunt aproximate printr-o serie Fourier, dependenta de viteza unghiulara a valtului (formula (6.2)). Fortele compensatoare care trebuie generate periodic cu actuatorile piezoelectrice sunt considerate a fi functii armonice, folosind frecventa de rotatie a valtului si un numar de 4 frecvente armonice. Parametrii A_i si B_i pentru fiecare actuator sunt determinati prin minimizarea vectorului de eroare v in asa fel incat criteriul de calitate J definit in ecuatie (6.9) sa fie indeplinit. Algoritmul este implementat in Matlab/Simulink. Vibratiile valtului sunt masurate timp de 2 s cu ajutorul timbrelor tensometrice aplicate in pozitiile (2) din figura 6.1, dupa care fortele compensatoare determinate sunt activate pentru a reduce vibratiile. Restul vibratiilor ce apar sunt reduse cu ajutorul unui controller propotional-derivativ. Partea derivativa a controlerului introduce dinamica in sistem, care in anumite situatii poate dauna actuatorilor. De aceea se aplica o filtrare a frecventelor inalte cu ajutorul unui filtru low-pass cu o constanta de timp de 10 ms.

Asupra valtului au fost aplicate o suprapunere de doua vibratii perturbatoare cu frecvente diferite, pentru a testa algoritmul de identificare a fortelor compensatoare. In figura 6.17 este prezentata reducerea amplitudinii vibratiilor aplicate valtului de tiparit in proportie de peste 90%, la o aplicare a unor forte perturbatoare cu frecvente de 5 si 15 Hz. In figura 6.18 sunt aplicate forte perturbatoare cu frecvente de 10 si 30 Hz si se observa de asemenea o reducere semnificativa a vibratiilor.

Lucrarile de modificare a lagarelor valtului de tiparit din cadrul unitatii de printare a masinii flexografice si transformarea acestora in lagare active, s-au dovedit mult mai complicate decat s-a presupus la inceput. De aceea, prin rezultatele obtinute pe standul model s-a deschis ca obiectiv de cercetare in viitorul apropiat, testarea acestui algoritm pe standul de incercare industrial.

7. DEVELOPMENT OF THE ACTIVE BEARINGS

In order to reach the thesis's aim of developing an active vibration control for printing machines different topics had to be treated in parallel. The development of new piezoelectric paint sensors for force measurement is necessary as well as the conception of an active vibration control system. The sensors can measure the vibration of the roller in form of excitation forces in the nip and with the help of active bearings with piezoelectric actuators, the vibration can be damped. Furthermore an important work is the design and construction of an active bearing in order to damp roller vibrations. Piezoelectric actuators are chosen for this purpose because they can develop with high dynamic forces, parameters that play a crucial role in vibration damping.

Section 2.4.2 presents a printing unit as a test setup taken from an industrial flexographic printing machine. The bearings of the plate cylinder are modified to incorporate bearings with piezoelectric actuators in order to damp the roller vibration, as this roller is vibrating with the lowest natural frequencies. The description of the active bearing is presented in Section 7.2.

As a preliminary study before modifying the industrial printing unit, a downscaled test setup is constructed with similar natural frequencies. It is a good solution for troubleshooting with limited financial resources and to protect the expensive piezoelectric actuators of the industrial scale test setup. New knowledge is then applied to the industrial test setup.

7.1. Downscaled Test Setup of the Roller System

A test setup based on a printing unit of the industrial roller system in a flexographic printing machine is presented in Figure 7.3. It is a one color unit of a real printing unit. In order to perform tests up to that of active vibration damping, first a small model of a real roller system is built. The natural frequencies are very similar to those of a real printing unit before modifying it. Piezoelectric actuators are integrated in the bearings of the plate cylinder. The experimental setup has been redesigned and rebuilt for testing active vibration damping.

In addition to the natural frequencies, the proportion between the diameters ($4:2:1 - d_{impression\ cylinder} : d_{anilox\ roll} : d_{plate\ cylinder}$) and length of the three rollers are similar to those of an industrial flexographic printing unit. There are some differences to the industrial test rig, especially when driving and pressing the roller system. The printing unit is equipped with a precision spindle and in this test setup the anilox roll (1) and the impression cylinder (2) are pressed against the plate cylinder (2) by means of two pneumatic cylinders (5) via ropes (6), as shown in Figure 7.1. These lead to an uniform application of force up to 1500 N, in order to ensure a constant line load up to 20 N/mm. The plate cylinder is the only roller driven by a motor (7) and the contact between the rollers is given by printing plate (4) mounted on the plate cylinder.

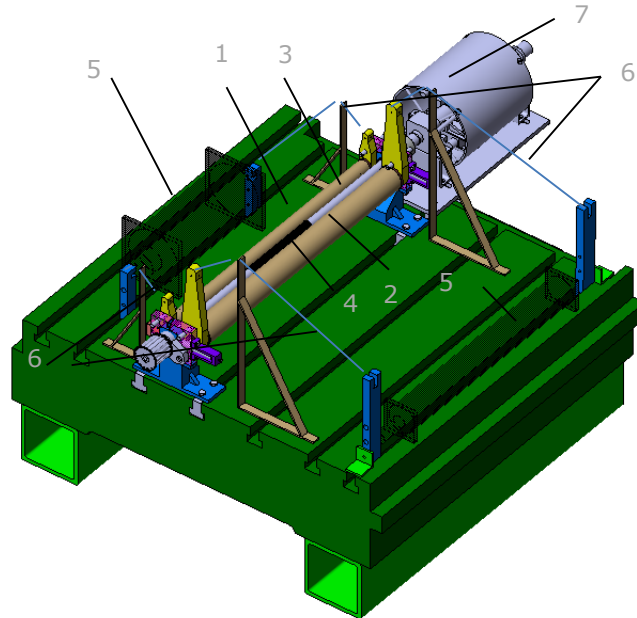


Figure 7.1 CAD-Model of the small-scaled test setup

The most important roller is the plate cylinder. It is downscaled to reach a natural frequency of 83 Hz as follows:

- Length: $L = 750$ mm
- External diameter: $d_a = 21$ mm
- Internal diameter: $d_i = 10$ mm

Piezoelectric actuators were integrated in the bearings of this roller for active vibration damping by generating counter-vibrations. The design of the active bearings is presented in the next section.

Piezoelectric actuators type PST-HD 200/10/90 VS 15 from the company Piezomechanik are considered adequate after interpreting the simulation results. The piezo actuators are internally preloaded with 800 N to avoid tensile forces which can destroy the actuator; they can generate forces up to 1800 N. Because the generated displacements are very small (up to 90 μm), the computation and the design of the active bearing is very important. The Bearing has to be stiff and clearance free, otherwise the displacement of the actuator is used just to compensate the internal clearance, present in each bearing. The plate cylinder is mounted with needle-roller bearings type NK 20/16 from the company SKF in the movable part of the active bearing. They have a longer lifetime as roller bearings because the load is applied on a bigger surface. The second reason is that they have a small internal clearance, about 25 μm . The clearance has to be minimized but not completely eliminated, because the lifetime of the bearings decreases with reducing the bearing clearance.

Minimizing the clearance was made as follows:

- pressing the bearings on the roller with a slight oversize;
- lubrication with oil;
- pre-stressing the actuator with saucer spring packages.

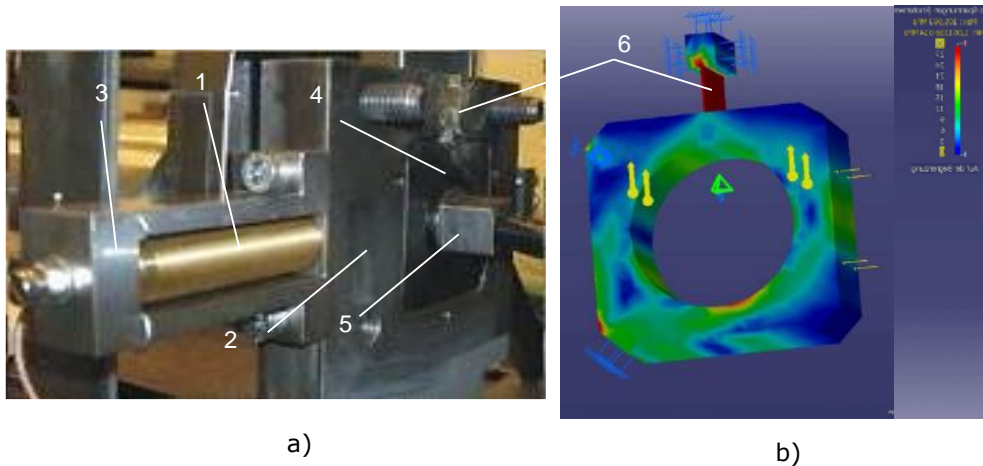


Figure 7.2 a) Active bearing; b) Stress analysis of the movable part of the bearing

As shown in Figure 7.2a, the piezoelectric actuator (1) is orientated in nip direction and is integrated in the bearing with a bracket (3) screwed in the housing (2). In this way, the air cooling avoids destroying of the actuator by heating. Saucer springs packages prestress the actuator to allow a permanent contact between the movable part of the bearing (4), where supported the roller (5). Therefore, the actuator does not have to be screwed-in movable part and tensile forces are prevented. The bearing was designed, so that the roller vibrates just in nip direction.

A beam (6) is welded to the movable part of the bearing to move it in horizontal direction. This was constructed to be flexible in the horizontal direction and resistant to bending and buckling in vertical direction. Figure 7.2b shows the stress analysis of the movable part of the bearing for a load of 2 kN in the bearing, including its own weight. The maximum stress of the bending beam has a value of 35 MPa, which is smaller than the yield strength for the material St37. The maximal displacement of the movable part on the bottom part was calculated as 154 μm , using the maximal displacement of the actuator.

The results of the active vibration control with this active bearing were presented in Chapter 6.

7.2. Industrial test setup simulating a printing unit

The test setup is very similar to a printing unit of a flexographic printing machine, with original components, but with some differences presented below. The test setup depicted in Figure 7.3 was designed from one of the industrial partners for experimental purposes and then delivered to the University of Applied Sciences Osnabrück to be redesigned for incorporation of active bearings with piezoelectric actuators for vibration damping. Technical data for the test setup are presented in Section 2.4.2.

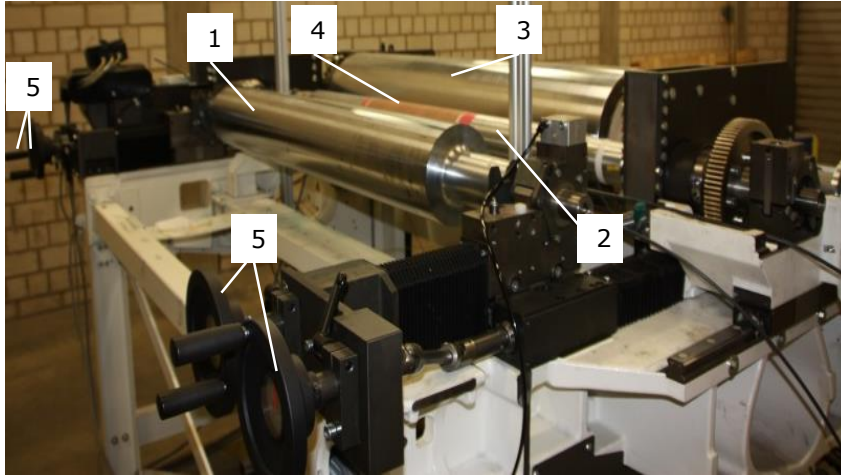


Figure 7.3 Industrial test setup simulating a printing unit of a flexographic printing machine

This printing unit has three rollers: anilox roll (1), plate cylinder (2) and impression cylinder (3). As opposed to the older versions of printing units, where the rollers are driven by a central drive by means of geared wheels (except the impression cylinder), each roller has its own drive. Thus, the printing plate can be changed almost continuously with the help of a sleeve. The contact between the rollers is realized by a photopolymer printing plate (4), applied with double-sided adhesive tape onto the sleeve.

In next pages, the notations "A-side" and "B-side" are used for better association of the type of active bearing to adapt to the test setup. From the view as shown in Figure 7.3, A-side is on the right side (drive side for the plate cylinder), and B-side is on the left side.

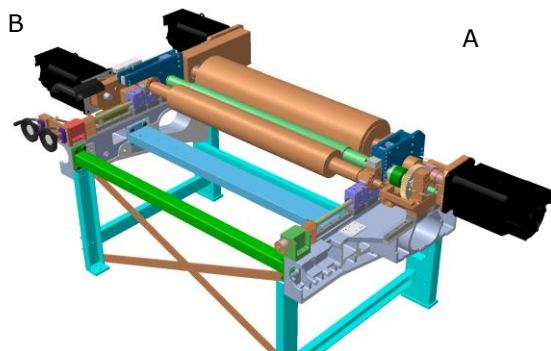


Figure 7.5 CAD-model of the industrial test setup

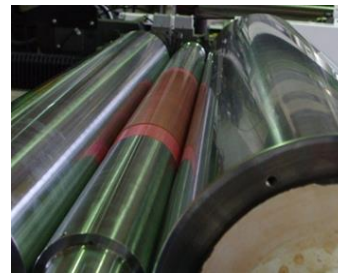


Figure 7.4 Roller system

The plate cylinder is driven by a motor and a gear drive, which allows it to be removed and replaced quickly and easily. The anilox roll is driven on the B-side through a transmission consisting of a toothed belt and a geared wheel. The impression cylinder is driven via another motor and a toothed belt and has a cooling device to dissipate the heat, which may be caused by friction of rollers. It was mounted in a fixed position. Four precision wheels (5) allow to manually adjust the plate cylinder and anilox roll.

Differences between the test setup and a real printing unit

The test setup had the following differences to a real printing unit:

- Dry drive. There is no paint, thus the doctor blade has been eliminated. The resulting changes of friction - solid instead of liquid friction, changes of the friction coefficient due to other surfaces have to be taken into account in the industrial implementation if necessary.
- No printing substrate. The supply of printing material does not exist here. The contact between plate cylinder and impression cylinder is different and may need to be taken into account as well.
- No sleeve. The printing plate is glued without a sleeve directly onto the plate cylinder with double-sided adhesive tape, unlike in industrial application where the printing plate has to be changed often, here this is not necessary.
- Small-scaled impression cylinder. A real impression cylinder is shared by several printing units, thus it is quite large - several meters in diameter (see Figure 1.8). On the test setup, the diameter of the impression cylinder was reduced in order to ensure reasonable construction size, but it is dimensioned to have high natural frequencies too.
- Adjustment of the plate cylinder. Since the printing process does not exist here, an automatic regulation of the printing image is not necessary. Therefore the axial adjustment of the plate cylinder is made manually, as mentioned above.
- Limited web speed. For safety reasons, the web velocity of the test setup is electronically limited at maximum 460 m/min [117] (in a flexographic printing machine, the web velocity is approx. 600 m/min), this means a frequency of approx. 24 Hz of the plate cylinder. To generate the first resonance at 64 Hz, the plate cylinder has to be driven with a frequency of 21,33 Hz and has to be excited three times per rotation.

As already described above, piezoelectric actuators were chosen for damping roller vibrations. They have high dynamics (work also kHz range), compared with e.g. hydraulic actuators and can generate very high forces.

Boundary Conditions for Modification of the Bearings

The integration of actuators in the bearings of the industrial plant was complicated for the following reasons:

- Piezoelectric actuators can only generate small displacements, which means that the bearing must work backlash-free as much as possible
- Piezo actuators can only generate compressive forces and therefore have to be pre-stressed
- Piezo actuators have to be protected against bending moments to avoid

damages

- In the test setup, the construction space in the bearing is limited
- The piezoelectric actuators used for experiments can generate forces up to 30 kN, which are necessary to generate high dynamic counter-oscillations of the 100 kg roller. The displacements of these actuators are up to 200 μ m.
- The roller bearings have to move in nip direction, i.e. in the direction of the contact line of rollers. This movement has to be backlash-free and free of wear with specially designed bending beams integrated in the bearing block. The design and optimization of these beams is complicated and is presented in [72, 73]. On the one hand, the beams have to be bendable, on the other hand, they have to absorb relatively high forces perpendicular to nip direction.

Design of Active Bearings

Two different active bearings for the roller system had to be designed as described in [73]. On the A-side the actuator was pressed directly on the plate cylinder as shown in Figure 7.6.

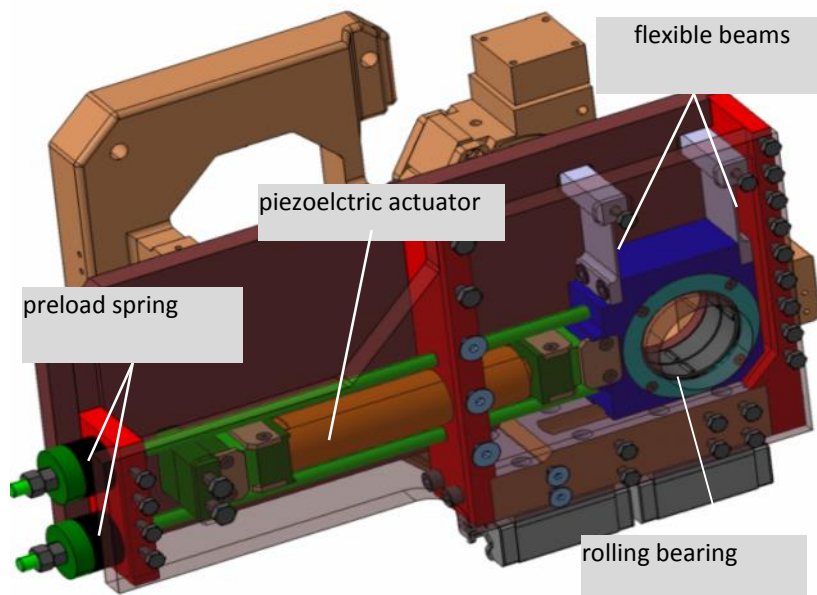


Figure 7.6 Active bearing on the A-side

The bearing on the B-side is complicated and is described below. Here, the actuator has to be positioned above the roller bearing because of the small space between the rollers (Figure 7.7).

Figure 7.6 and Figure 7.7 show the flexible hinge two flexible beams. The beams are integrated into the housing that was manufactured as one single part. There is no other possibility to transmit the high-pressure forces occurring in the beams when operating the actuator.

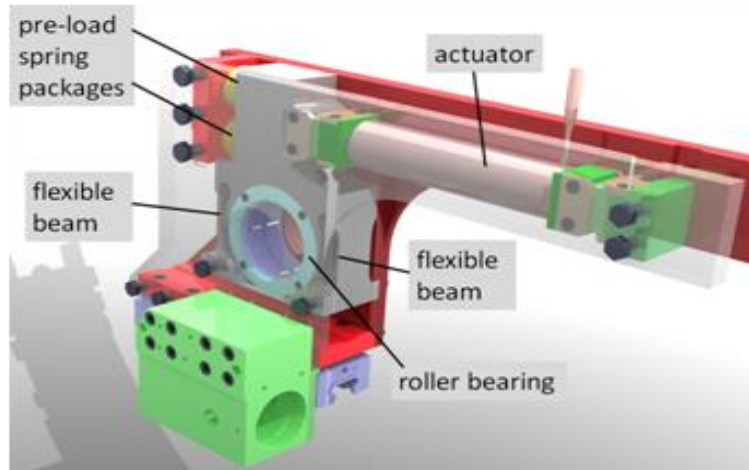


Figure 7.7 CAD-model of the active bearing on the B-side

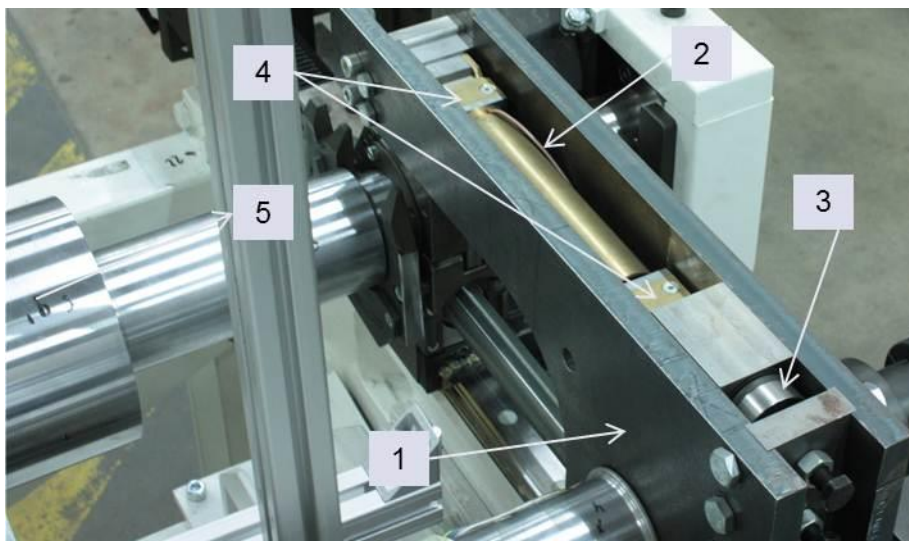


Figure 7.8 Bearing on the B-side

(1- housing of the active bearing, 2- piezoelectric actuator, 3- pre-load spring packages, 4- double cylindrical beams, 5- plate cylinder)

As depicted in Figure 7.6 and Figure 7.7 the active horizontal displacement of the bearing outer ring is realized with two flexible beams (Figure 7.9), which are bent under the influence of high actuator forces. The arrangement of the beams on the left and right side of the bearing shell ensured the movement almost exclusively in

horizontal direction. The bearing is designed to be stiff in the vertical direction and elastic in the horizontal direction.

The bearing on the A-side is relatively simple, because the forces of the piezo actuator can be directly fed into the bearing centre (Figure 7.6).

The bending beams shown in Figure 7.8 have to absorb only vertical bearing forces, i.e. essentially the gravitational force. This is not possible in the bearing on the B-side due to design space limitations and the piezo actuator had to be positioned above the roller bearing. This produced displacement moments and the component had to fulfil conflicting requirements [73, 83]:

On the one hand:

- the operating actuator caused high pressure and tension forces in the beams, which resulted high stress in the junction between the connection of the beams;
- buckling must be avoided.

On the other hand:

- deflection of the movable bearing caused bending stress that gets larger with increasing thickness of the beams;
- the bending stiffness of the beam is too large, it should be smaller than 10% of the actuator stiffness.

The bearing is designed to be elastic in horizontal direction and also endure high tensile and compressive stress. It is milled from high-strength steel. Figure 7.9a demonstrates the load forces of the beams. In horizontal direction operate to the right the external preload forces F_v and a component of the bearing force F_{th} . To the left is oriented the actuator force and the internal preload force of it. In vertical direction shows the bearing force component F_{fv} . Finite element calculation and optimization of the design of the beams – the shape and the edges at the ends of the beams, provided a practicable solution as shown in Figure 7.9b.

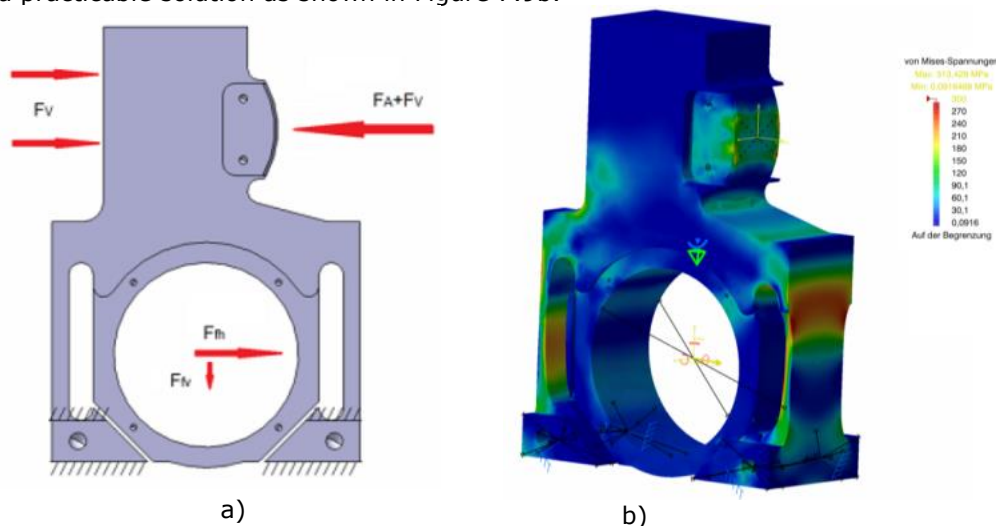


Figure 7.9 a) Load forces on the beam in the bearing, b) FEM-Analysis of mechanical stress of the active bearing

Actuator mounting

During assembly, care must be taken to avoid actuator damages. To generate required deformation (displacement), piezoelectric elements were mechanically connected in series and grouped in stacks. When using such actuators, the following points should be noted:

- The piezoelectric stack actuators can single handedly transmit only significant compressive forces. When tensile forces and compressive forces of the actuator are necessary as described, the stack actuators must be pre-stressed with one half of the blocking force. The stiffness of the pre-stressing device should not exceed 10% of the piezo actuator stiffness, to use the whole actuator deformation.
- Piezoelectric stack actuators will be destroyed by bending moments [95], i.e. the connection has to be constructively realized, so that no bending moments can be initiated. Due to the great forces generated by the actuator, surface pressure in the connecting elements (i.e. ball joint) must not be exceeded, otherwise mechanical failure of the bearing can occur.
- The preload force in this application must be 15 kN and is realized with the help of disc spring packages.

In order to protect the actuator from disturbances caused by bending moments, two perpendicularly arranged cylindrical bearings were positioned at both ends of the actuator as shown in Figure 7.10 and were designed as described in [73]. The first solution with spherical contact has been disregarded because the Herzian stress would be too large or the radius of the spheres has to be so large that a small angular deviation of the actuator will cause an unallowable shift of the force application point causing bending moments.

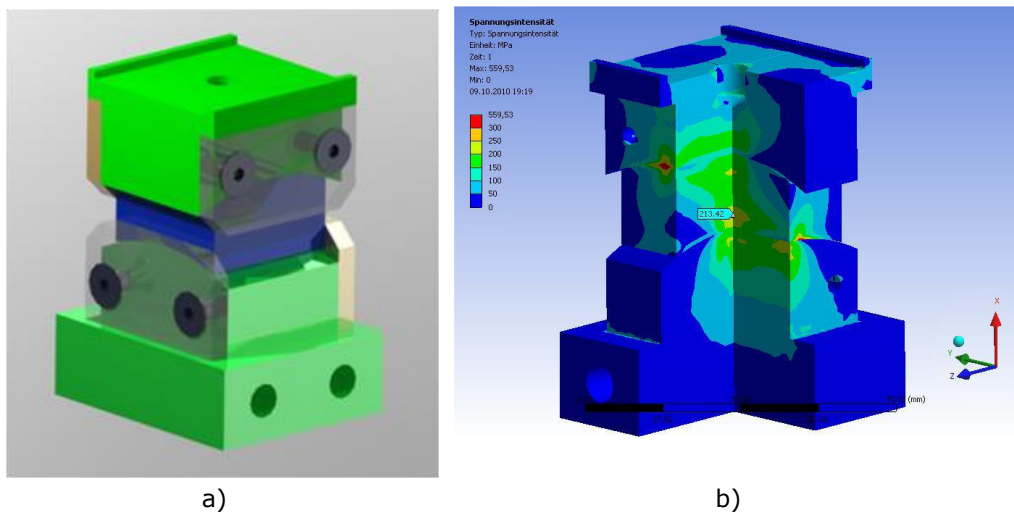


Figure 7.10 Double cylindrical beams to protect the actuator: a) the element, b) stress analysis

Tension on the actuator is not possible in this construction. In order to apply push-pull action to the roller, the actuator will be pre-loaded using saucer spring packages.

7.3. Chapter Summary of Romanian

Acest capitol intitulat "Lagare active" prezinta doua standuri de incercare: unul industrial reprezentand o unitate de printare modificata, celalalt construit in laborator ca model al standului de incercare industrial. Pentru amandoua standurile de incercare au fost construite lagare active cu actuatoare piezoelectrice, pentru a amortiza dinamic vibratiile aparute in sistemul de valturi. Constructia lor este prezentata pe larg in cadrul acestui capitol, scotand in evidenta dificultatile si cerintele unui lagar activ, precum si conditiile impuse pentru protectia actuatorului si folosirea eficienta a deplasarilor mici ale acestora pentru reducerea vibratiilor. Aceste lagare au fost construite pentru valtul de tiparire, aflat in mijloc, deoarece acesta incepe prima data sa vibreze din cauza diametrului mic in comparatie cu celelate valturi, prima rezonanta aparand la aproximativ 83 Hz la standul model si 64 Hz la standul industrial. Diferenta de frecvente proprii se datoreaza modificarii standului de incercare industrial de catre firma colaboratoare in proiect din cauza unor decizii interne, standul initial avand frecventa proprie de 84 Hz.

Dimensionarea si construirea standului de incercare model s-a facut tinand cont de frecventele proprii cunoscute initial despre unitatea de printare, precum si de dimensiunile geometrice ale valturilor (lungimea si raportul diametrelor valturilor) si de incarcarea in linie a valturilor (intre 5-20 N/mm). Modelul este prezentat in figura 7.1.

Constructia lagarelor active care sustin valtul de printare este foarte complicata si trebuie tinut cont de deplasari foarte mici pe care le pot realiza actuatoarele si de conditia ca acestia sa fie supuse numai la forte de apasare. Momentele si fortele de extindere pot determina distrugerea actualelor prin deteriorarea ceramicilor PZT. In figura 7.2 este prezentat lagarul activ, construit din doua parti principale: statorul (2) si partea mobila (4). Partea mobila este dezvoltata si construita pentru a permite numai miscari in directia orizontala (directia liniei de contact dintre valturi), determinate de grinda din otel elastic (6). In figura 7.2 b este prezentata analiza de solicitare mecanica a partii mobile pentru o forta de apasare in lagar de 2 kN, care ajuta la dimensionarea grinzii (6) pentru ca actuatorul sa realizeze numai miscari in limita deplasarilor permise lui, in total de $90 \mu\text{m}$ ($\pm 45 \mu\text{m}$). S-a realizat o pretensionare externa a actuatorului cu ajutorul unor arcuri-placa, asigurand astfel contactul permanent al acestuia cu valtul. In acest fel, vibratiile valtului pot fi reduse generand cu actuatoarele forte in ambele directii (extindere si contractie), amandoua directiile fiind acum posibile. Rezultatele obtinute folosind aceste lagare au fost prezentate in capitolul precedent.

In subcapitolul 7.2 sunt prezentate lagare active dezvoltate si construite pentru reducerea vibratiilor valtului de printare din cadrul standului de incercare industrial. Pentru a putea realiza miscarea valtului, au fost dimensionati actuatoare piezoelectrice care pot genera forte de pana la 30 kN si deplasari de $200 \mu\text{m}$. Din cauza spatiului limitat in care pot fi incorporate lagarele si de dimensiunile actualelor, a fost necesara dezvoltarea a doua lagare diferite, denumite lagar pe partea A si lagar pe partea B, dupa cum se poate vedea in figura 7.5 (cu albastru inchis).

Primul lagar mentionat este mai usor de realizat, deoarece spatiul de constructie permite fixarea actuatorului in asa fel incat sa apese direct pe valt pentru a genera forte compensatoare pentru reducerea vibratiilor (figura 7.6). Grinzile elastice „flexible beams” permit miscarea orizontala a lagarului in directia liniei de contact dintre valturi si impiedica in acelasi timp miscarea verticala a acestuia.

Pe partea B, lagarul nu a putut fi construit in acelasi mod din cauza constructiei standului de incercare. Dezvoltarea acestuia a necesitat alegerea solutiei optime, in

asa fel incat sa poata fi realizat, ca actuatorul sa lucreze eficient, dar si din punct de vedere tehnologic. Dupa cum se poate vedea in figura 7.7, actuatorul este pozitionat deasupra valtului. El nu poate transmite direct forte valtului, dar prin miscarile efectuate, grinzile elastice „flexible beam” permit miscarea valtului in directie orizontala.

Pentru a evita fortele verticale si momentele asupra actuatorelor care ar putea apare in timpul functionarii standului de incercare, s-au folosit constructii cu constructii cu suprafete sferice prezentati in figura 7.10 a, care permit miscarea minimala a lagarului si prin acest fapt, permit rearanjarea fortelor in directia actuatorului.

Functionarea lagarelor active a fost probata in bucla deschisa, urmarind in primul pas miscarea valtului cu ajutorul actuatorelor si asigurarea ca dezvoltarea lagarelor a fost facuta cu succes. Dupa cum s-a precizat si in capitolul precedent, din cauza lucrarilor tehnologice pentru realizarea lagarului de pe partea B, precum si dimensionarea lagarelor care s-a dovedit a fi complicata, conceptul de reglare realizat pe standul model nu a putut fi probat pe standul industrial. Acest scop este insa urmarit in continuare, lucrarile desfasurandu-se in prezent si in viitorul apropiat, iar rezultatele vor fi prezentate la conferinte internationale.

8. Optimization of Roller Behaviour with Profile Rings

During the research project "Active roller systems" and this thesis, the idea described in this chapter of semi-active vibration damping [71] led to a patent application. In this case, vibrations are not damped with additional actuators, but with passive components and can be applied on rolls and shafts. These passive components are called profile rings, damping profiles or ring-shaped profiles.

The idea of vibration damping with profile rings was tested with success [102] at the University of Applied Sciences Osnabruck in Germany.

8.1. Technical Problem and Solution

When passive components are used, the energy for the vibration damping comes from the rolls during the rotatory motion. The basic idea is that ring-shaped profiles are developed, which directly counteract undesirable vibrations. In this way, unwanted vibrations caused by periodic excitations, can be reduced efficiently and cost-effectively. Expensive actuators are not necessary anymore.

With the invention described below, the oscillations of a roll or shaft should be effectively diminished by generating "counter-vibrations" with compensating profiles.

The idea of vibration damping with ring-shaped profiles started with the simulation results presented in Chapter 0. These showed that it is possible to reduce vibrations of long slender shafts by introducing dynamically defined displacements in bearings or nearest bearings. This can be realized with forces or displacement excitations that produce counter-vibrations to damp the vibrations. In contrast to other systems and solutions, this invention is neither a passive damper as e.g. presented in [36], where the damping is realized with a mass (e.g. granulate or sand), nor an expensive active system for generating force and displacement excitations [100,13].

Each profile has to be designed according to a specific disturbance pattern, so that counter-vibrations can be generated in the shaft (see Figure 8.4 –number 2) by non-uniform pressure against another roll (see Figure 8.4 –number 3) in order to damp the vibrations caused by disturbance.

On one hand, it is a passive system, because no additional actuators are used and no external energy is introduced in the system. On the other hand, active forces are generated in the shaft through the designed profile. The required energy is taken from the drive of the roller system.

In Figure 7.1 the test setup used for experiments, where the oscillations of the plate cylinder are damped using active bearings with piezoelectric actuators is depicted. Due to periodic excitation appearing each one rotation e.g. in flexography by printing plate, the actuating forces F are also periodically repeating over the circumference and the position angle φ and can be recorded.

Using a finite element model of a roller system simulating a printing unit from a flexographic printing machine, where the printing plate defines a periodical vibration excitation of the plate cylinder, the profile of the damping rings can be calculated and designed. After that, it is possible to produce the damping rings once with the design of the printing plate, when its elastic properties and thickness fulfil the size of the damping forces. In this case, the distribution of the excitation on the circumference

of the roller depends on profile of a particular printing plate and has to be calculated for each printing plate.

As shown in Figure 8.1, the forces are applied as a function of the position angle φ . After that, forces can be implemented in appropriate arrangement of elevations and depressions of the profile, using the elastic properties of the profile ring (an elastic force F is the product of deformation x and material stiffness c). The profile can be realized e.g. with a tape or an elastic ring mounted on the roller. Now the roller can be mounted on the machine and work with optimized vibration behaviour without active elements.

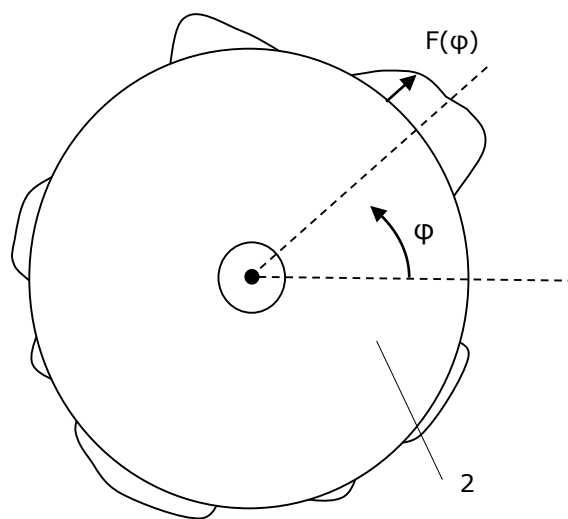


Figure 8.1 Periodical force profile of a piezo actuator on the circumference applied at the end of roller

The shape of the damping profile can be applied on the circumference of a shaft determined experimentally with a test rig as shown in Figure 7.1 or using simulations with e.g. Matlab/Simulink. Determining the optimal shape of the profile rings by the use of simulations is similar to the experimental procedure, excepting that the shaft vibrations do not have to be measured, but simulated as shown in Figure 8.2.

Usually, the actuator generates counter-vibrations. The optimal force profile applied by the actuators (1) on the shaft can be determined with a control circuit presented below. The shaft oscillations are measured with the sensors (5), e.g. strain gauges. Actual vibration values given by the strain gauges are sent to the controller (4) and this optimizes the control signals $u_1(t)$ and $u_2(t)$ for the actuators. Actuator force profile is optimized for one rotation of the shaft using a controller or enhanced with help of optimization strategies that the bending vibrations of the roller are minimal. The forces are applied as a function of the angle φ recorded with the sensor (3).

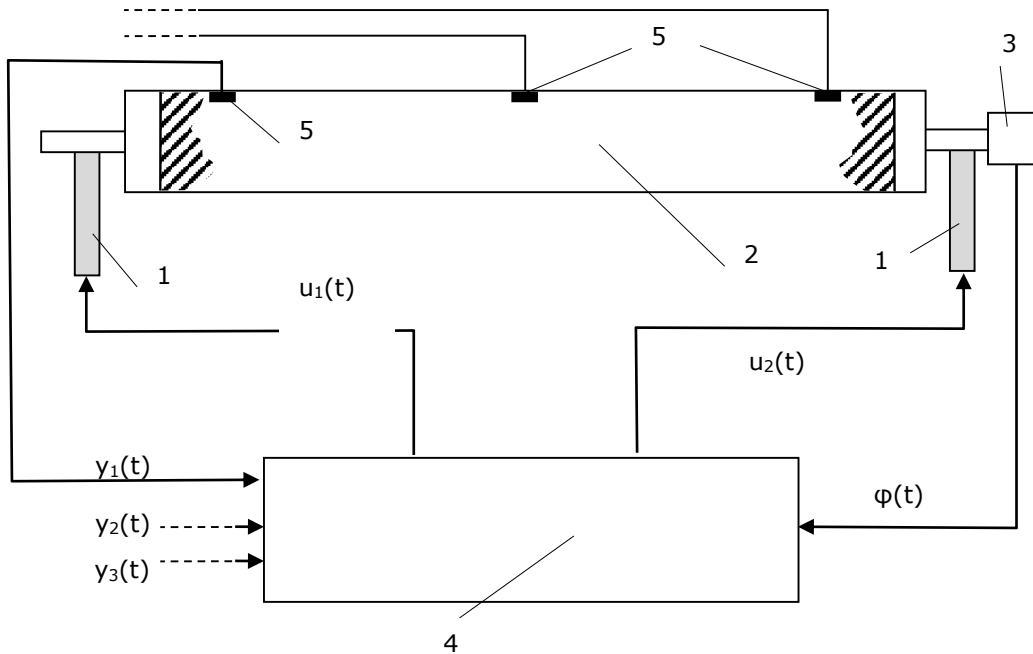


Figure 8.2 Control schema

The compensating profile does not necessarily have to be generated actively by the actuators in the closed loop. Given the shape of the disturbance, it can be determined in simulations or experiments and then be applied to special rings. These profile rings can be mounted on the axle of the roller and rotate with it. They provide a counter force passively when rolling against the central impression cylinder or any other counter surface [71]. However, the profile rings have to be adapted if e.g. the printing plate and the disturbances, respectively, change.

Using a closed-loop simulation as described above, the damping profile is generated from the simulation results presented in Figure 6.9.

Profile ring works similar to a disturbance feed-forward control. In Figure 8.3 is depicted a force (blue line) which compensate the disturbance force (red line) between 0° and 70° on the circumference of the roller. In this example, the compensation force changes its direction starting after disturbance disappears at 70° .

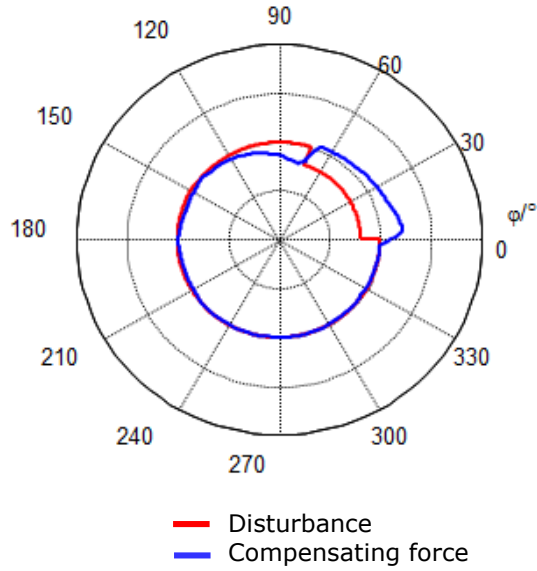


Figure 8.3 Simulation results for the roller system in laboratory scale

Figure 8.4 presents this innovative idea exemplified for a roll with two damping profiles (1) mounted onto the circumference of the shaft (2). These profiles can effectively damp disturbances that appear periodically according to the rotation of the roller. Here, the profile rings are applied on the shaft nearest to the bearings, because generally, there is more free construction space. It is also possible to apply the profile at a different position on the shaft. The position can be chosen with respect to constructive constrains so that it does not disturb the process.

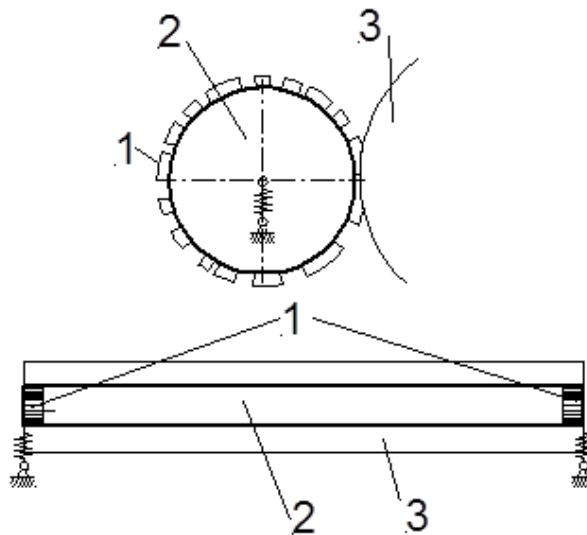


Figure 8.4 Shaft with damping rings outer

Another technical solution is shown in Figure 8.5, where damping profiles are applied inside the adapter rings. In this case, vibration damping forces due to rolling off profile (1) on at least one role (4) mounted inside of the shaft.

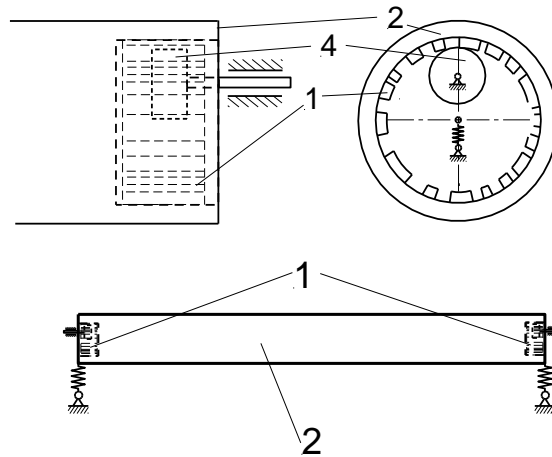


Figure 8.5 Shaft with two profiles inside the shaft

When a profile ring has contact with a shaft, only compressive forces are generated. When forces in the opposite direction (with reverse sign) are required, multiple pressure rolls (4) have to be used, e.g. the solution presented in Figure 8.6.

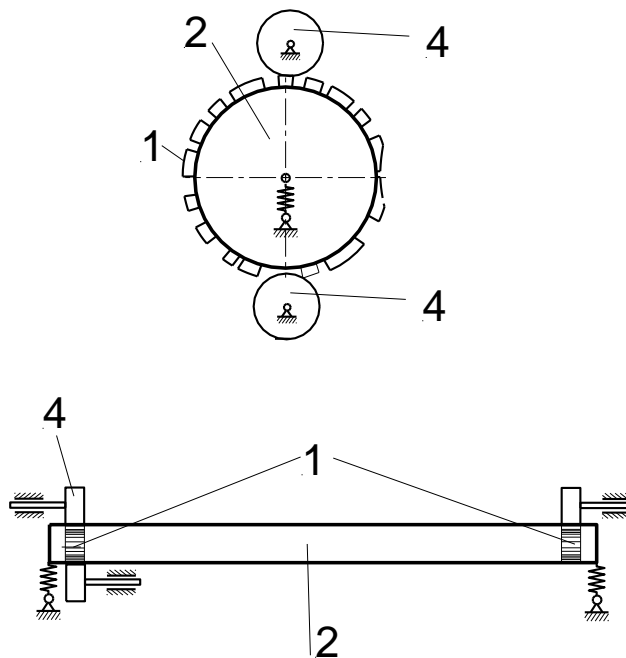


Figure 8.6 Shaft with profile rings outer and fixed pressure rolls

8.2. Test Setup for Semi-Active Damping with Profile Rings

For testing the idea of semi-active vibration damping with profile rings, a test setup following the solution presented in Figure 8.4 was designed and constructed. The test setup was designed to realize large vibration amplitudes. For this purpose, a steel mass (2) with a large diameter was placed in the middle of a roller (1) as depicted in Figure 8.7. The test setup is designed to have a relatively low first natural frequency, to easily excite the first bending resonant vibration.

On the cylindrical surface of the steel mass are applied excitations (in Figure 8.8 – the green strips) in form of pieces from a printing plate using adhesive tape (green strips in Figure 8.8). The other two masses (3) are produced from an engineering plastic named polyoxymethylene (POM), with high stiffness, low friction values and good thermal stability. Furthermore, this material has a lower density as steel ($\rho \approx 1410 \text{ kg/m}^3$) and thus a lower mass as (2) (see Table 4.2). These masses, so-called profile rings are used for damping vibrations. For this purpose, they are mounted 76 mm from the bearings of the roller, for a distance between both bearings of 612 mm. They generate forces by pressing against a carriage (4) with an elastic suspension (spring) preloaded with the help of a screw. The forces are converted into variation of the profile ring. This constructed solution was chosen for avoiding the difficulties of developing of elastic rings (finding the right material) for generating elastic forces for damping roller vibration by pressing against a fixed carriage.

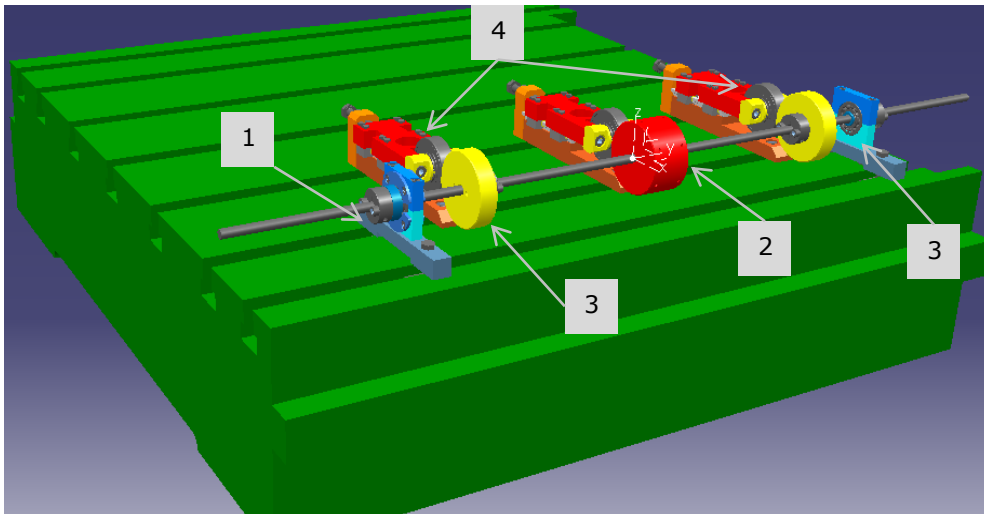


Figure 8.7 CAD- Model of the test setup for semi-active vibration damping with profile rings

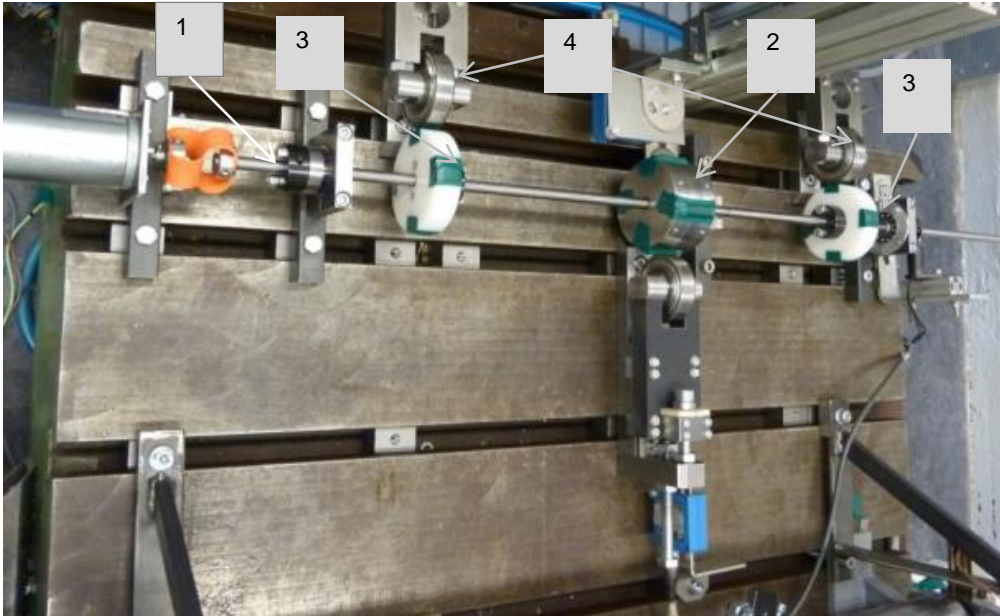


Figure 8.8 Test setup with profile rings and applied disturbances

The first natural frequency of the system was measured as approximately 18 Hz. Four excitations applied on the steel mass allowed to reduce the frequency of rotation of the roller to 4,5 Hz to get resonance.

Name	Material	Mass [kg]	Diameter [mm]	Width [mm]
Roller (1)	115CrV3	0,62	10	1000
Steel mass (2)	S235	1,734	80	45
Profile rings	POM	0,24	80	20

Table 8.1 Technical data of the test setup

Figure 8.9 depicts a part from the simulation program in Matlab with the defined parameters for simulating the mechanical system.

```

Dreimassenschwinger.m x +
4
5 %Controller parameter
6 PR = 100 ; % P-gain
7 DR = 1000 ; % D-gain
8 IR = 0 ; % I-gain
9
10 %Damping matrix D = alpha.*M + beta.*C;
11 alpha =10; % damping factor ;
12 beta = 0.0003; % damping factor ;
13
14
15 fq = 5; % excitation frequency [Hz]
16 pd = 0.1; % phase delay for simulation start [s]
17
18 d = 0.01; % diameter of the roller [m]
19 a = 0.612; % length of the roller (length between bearings) [m]
20
21 Nel= 4; % number of the roller elements
22 a1 = 0.076; % element 1: Distance from bearing 1 to profile ring 1 [m]
23 a2 = 0.23; % element 2: Distance from profile ring 1 to steel-mass [m]
24 a3 = 0.23; % element 3: Distance from steel-mass to profile ring 2[m]
25 a4 = 0.076; % element 4: Distance from profile ring 2 to bearing 2[m]
26
27 % Steel and POM masses
28 m_st = 1.832; % Steel mass (incl. ring & bolts) [kg]
29 m_po = 0.236; % POM mass (incl. ring & bolts) [kg]
30
31 %Bearing stiffness
32 cL1 = 10e16; % stiffness bearing 1
33 cL2 = 5e16; % stiffness bearing 2
34
35 aw = (d/2)^2*pi; %Kreisfläche der Walze [m²]
36 rho = 7800; %Dichte Stahl [kg/m³]
37 rho_p = 1420; %Dichte POM [kg/m³]
38 J = (pi*d^4)/64; %Flächenträgheitsmoment
39 E = 2.1e11; %E-Modul Stahl
40
41 N = 2*Nel+2; %DOF
42 NN =2*N;
43 mic=rho*aw*a;
44 fa = 1/fq;
45 cw = (48*E*J)/(a^3); %Roller stiffness
46
47 %Carriage parameters
48 m_sch = 1.303 %Mass in kg
49 c_sch = 0.02 %Spring stiffness in N/m

```

Figure 8.9 Simulation parameters of the test setup

Basically, the test setup can be modelled as a beam with three masses as depicted in Figure 8.10. The mathematical model is realized as described in Chapter 5.1 for 4 discretizations and 8 DOF, and then simulated with Matlab/Simulink [102].

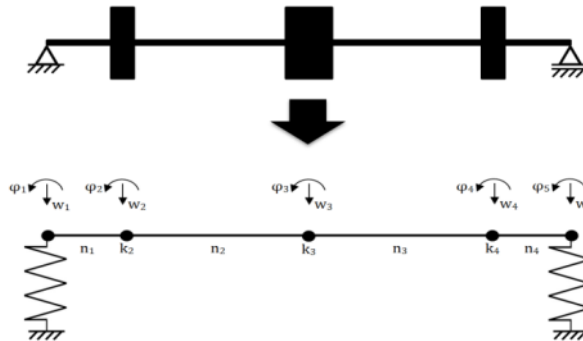


Figure 8.10 Mathematical model of the test setup

The 3 masses have to be added to the mass matrix M for the roller in the positions where are applied, consequently to the elements (3,3), (5,5) and (7,7). The stiffness of the bearings $cL1$ and $cL2$ are added to the elements (1,1) and (7,7) of the stiffness matrix C of the roller. Figure 8.11 shows how these additions are realized in the simulation program:

```

% Adding bearing stiffness
C(1,1) = C(1,1) + cL1;
C(9,9) = C(9,9) + cL2;

% Adding the 3 masses
M(3,3) = M(3,3) + m_po;
M(5,5) = M(5,5) + m_st;
M(7,7) = M(7,7) + m_po;

```

Figure 8.11 Adding the 3 masses and the bearing stiffness to the mass and the stiffness matrices

The factors α and β for the damping matrix are experimentally determined, that the model shows similar behavior as the measurements as shown in Figure 8.16. The dynamic equation of the system is transformed in state space form. The simulation system is reduced for the first 4 mode shapes using modified modal analysis and the eigen vectors $EV1$ (complex number) are separated in real and imaginary part as shown in Figure 8.12 and saved in the matrix $evmod$.

```

% modified modal form
evanz=Nred; %first 4 modshapes, Nred = 4
for iev=1:evanz
for j=1:NN %here j=1:20 NN=20
evmod(j,2*ie-1)=real(EV1(j,k+1-2*ie));
evmod(j,2*ie)=imag(EV1(j,k+1-2*ie));
end
end

```

Figure 8.12 Adding the 3 masses and the bearing stiffness to the mass and the stiffness matrices

For simulation, the modal matrices are calculated as described in Section 5.3. The state space matrix A is transformed in λ . The control matrix $B_{20 \times 3}$ defines the positions for applying the disturbance force (in DOF 5 with $B(5,2)=1$) and for applying the compensating forces (in DOF 3 and 7 with $B(3,1)=1$ and $B(7,3)=1$). The matrix is transformed now in Bred. The output matrix $C_{3 \times 20}$ has elements 1 and 0 (similar to matrix B) and gives the measured displacements (for the 3 masses: $C(1,3)=1$, $C(2,5)=1$, $C(3,7)=1$). The matrix C is transformed now to $Cred$, by multiplication of C with $evmod$.

The model is implemented in Simulink as depicted in Figure 8.13. For comparing the simulation results with the measurements, the controllers are deactivated.

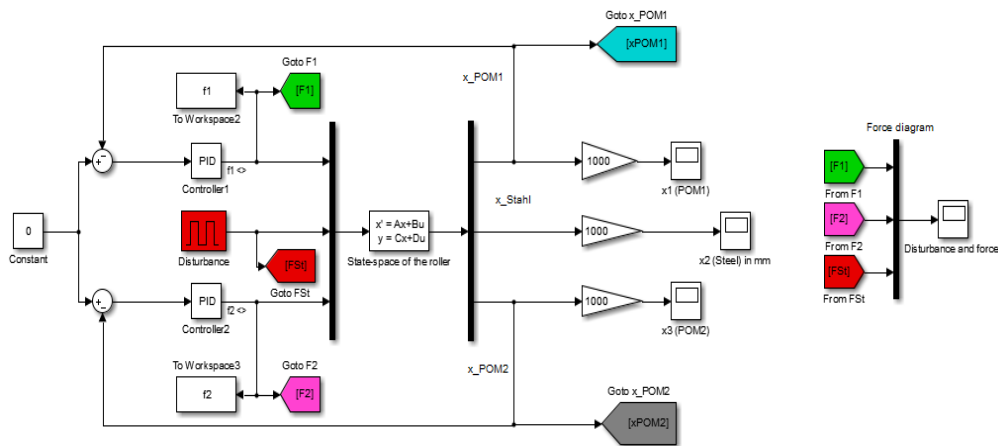


Figure 8.13 Closed-loop model of the roller in Simulink

The parameters for the plant are given in Figure 8.14.

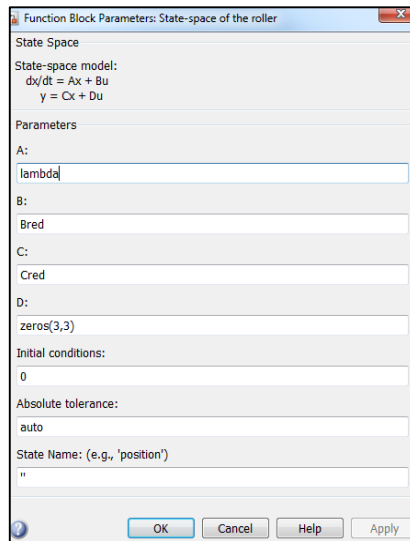


Figure 8.14 State-Space parameters

Figure 8.16 shows that the measurement data (red) and the open-loop simulation data (black) coincide very well. After model matching and verification, a PID controller has been designed in order to reduce the vibration of mass 2. The parameters of the PID controller are defined in Matlab and introduced in Simulink as depicted in Figure 8.15 a.

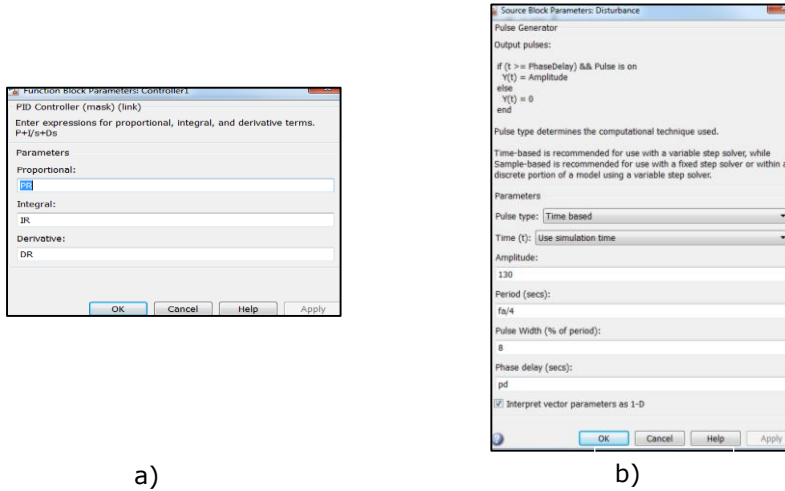


Figure 8.15 a) Parameters for PID controller, b) Parameter for the disturbance

The closed-loop simulation for a square-wave excitation with the parameters shown in Figure 8.15 b is depicted in blue. The displacements are measured with laser distance sensors Wenglor YP06MGVL80 with technical data presented in Table 8.2. The output from controllers defines the necessary forces for damping vibrations, which have to be generated with the help of profile rings on the test setup, by pressing onto the elastic carriages.

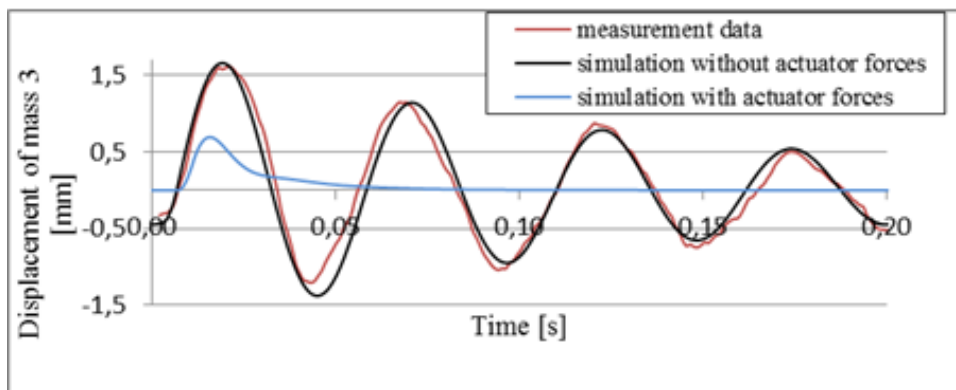


Figure 8.16 Experimental and simulation results for the displacement of mass 3


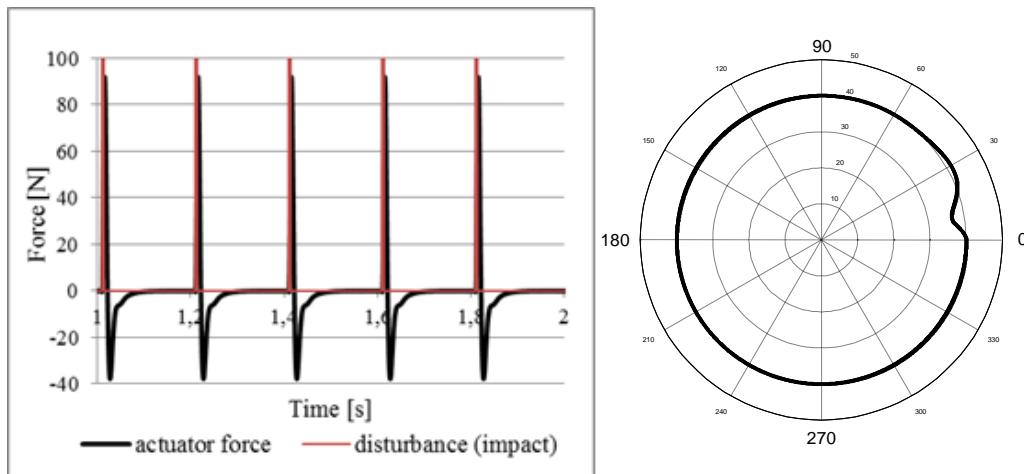
Sensor type	Wenglor YP06MGVL80		
Range	mm	40...60	
Measuring distance	mm	50	
Measuring range	mm	20	
Resolution	µm	< 10	
Linearity	%	0,5	
Supply voltage (DC)	V	18...30	
Analog Output	V	0...10	
Wave length	nm	655	

Table 8.2 Technical data of the laser distance sensors

Knowing the stiffness of the elastic elements (20 N/mm), the profile of the damping rings can be plotted in polar coordinates, as shown in Figure 8.17 and sent to a CAD-Program (e.g. Catia V5) to generate a 3D model (Figure 8.18).



a)

b)

Figure 8.17 a) Actuator forces from simulation; b) Profile ring generated from the compensating forces in a)

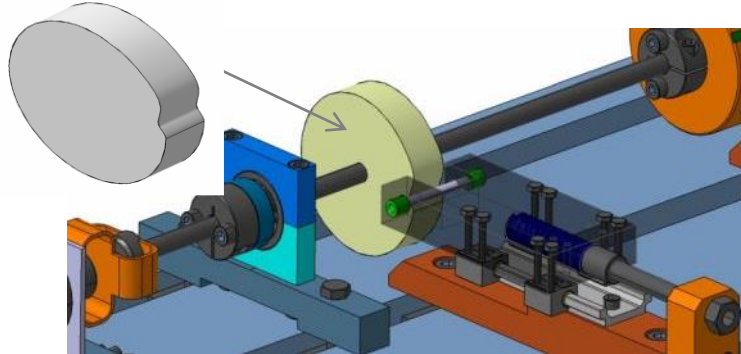


Figure 8.18 Profile ring

Comparing the measurements in the resonance case, the rotational frequency of the steel mass gives the reference for presented results, which is approximately $4,5 \text{ s}^{-1}$. The results presented in Figure 8.19 show that the amplitudes can be minimized by a targeted application of forces. The depicted forces are calculated from the measured displacements of the damping rings and the known stiffness of the elastic elements (see Figure 8.7 - number 4). The values of the disturbance forces are reduced from 4 N to 0,6 N, it means a reduction of 85%.

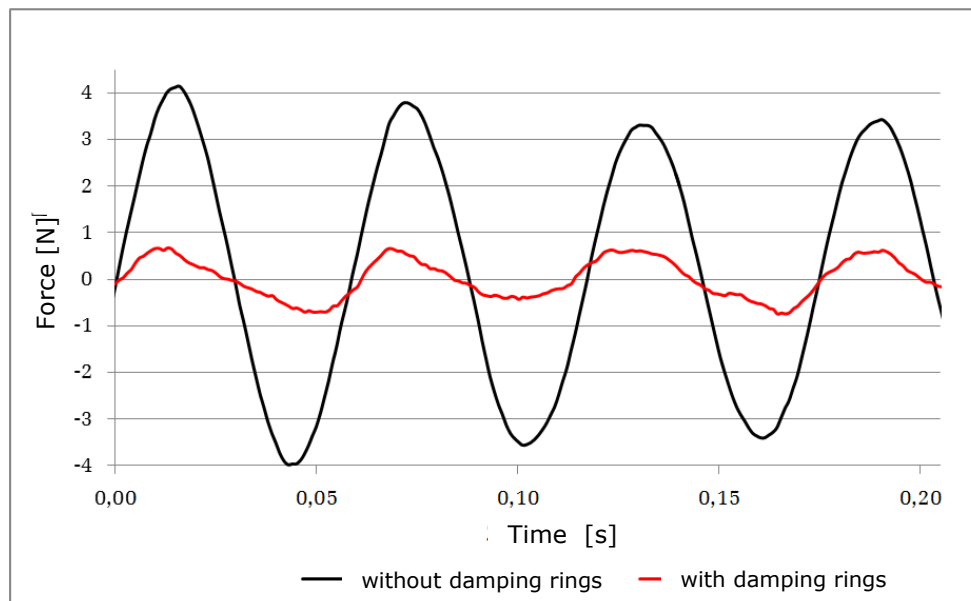


Figure 8.19 Vibration reducing effect of the profile rings

8.3. Advantages of damping vibration with profile rings

In this chapter, a new method for semi-active solution of rotating roller is presented. It is used to damp the periodical forces with the roller rotation. It uses profile rings as passive elements mounted on/in the plate cylinder and the rotating energy from the roller. The profile of the passive elements has to be determined and optimized specially for a disturbance periodically repeated with roller rotation (e.g. a printing plate in flexographic printing machines).

Vibration damping ring can be mounted on the outer side of the plate cylinder. In contrast to e.g. patent [36], it can be mounted on different machines or roller systems with small or completely without modification and therefore is also suitable for existing plants.

This solution requires no additional active elements. Nevertheless, vibration damping forces adapted to an excitation are introduced selectively in the roller. The profile is designed specifically for each printing plate (in the flexography). The height and width of the ring can have different dimensions.

The profile form can be calculated by simulation calculations (e.g. with software Matlab/ Simulink) or by testing on a test ring as described above. The production of the profile ring can be made simultaneously with the manufacture of the printing plate for flexographic printing machines. This way, the costs of expensive active control systems can be saved.

8.4. Chapter Summary in Romanian

Pornind de la ideea reducerii vibratiilor valturilor din masinile de tiparit cu ajutorul unor elemente active, ca de exemplu cu actuatori piezoelectrice, idee prezentata in capitolul 6 si figura 8.2, s-a observat ca anumite vibratii apar periodic datorita matritei de tiparit. Prin ridicaturile in materialul elastic care transmit vopseaua pe suportul de imprimat, acestea provoaca la fiecare rotire a valtului aceleasi vibratii. Aceste vibratii pot fi reduse cu ajutorul unor inele din material elastic, care sa genereze forte compensatoare. Ideea amortizarii vibratiilor cu inele pasive profilate (figura 8.1) folosind energia de rotatie a unui valt a fost propusa spre patentare [71] (denumita amortizare semiactiva). Inelele pot fi asezate pe valt in apropierea lagarelor (figura 8.4) sau in alta pozitie, in functie de necesitate si spatiu. O alta idee de a introduce forte compensatoare este prezentata in figura 8.5 unde o rola se roteste pe inelul compensator plasat in interiorul valtului. Necesitatea, locul si forma inelului compensator se pot determina cu ajutorul unui model matematic ce poate fi simulat cu diferite programe, de exemplu Matlab/Simulink.

Pentru testarea ideii amortizarii semiactive cu inele profilate, a fost construit un stand de incercare prezentat in figura 8.4. Pe un valt cu diametru mic (1) sunt asezate 3 greutati (2,3) pentru a reduce prima frecventa proprie a standului de incercare la o valoare de aproximativ 18 Hz. Greutatea din mijloc este construita din otel, iar celelate doua greutati sunt mai mici, fiind construite dintr-un material denumit POM (Polioximetilena) cu densitate redusa in comparatie cu otelul. Pe greutatea (2) sunt amplasate la distante egale pe circumferinta 4 proeminente dintr-un material elastic, care in contact cu o rola, creeaza patru forte perturbatoare. In acest fel, se poate reduce frecventa de rotatie a rolei la 4,5 Hz ca sistemul sa se afle in rezonanta. Masurand amplitudinile vibratiilor cu ajutorul unor senzori de proximitate optici de la firma Wenglor, sunt observate momentele cand trebuie aplicate forte compensatoare. Standul de incercare este modelat matematic, dupa

descrierea din capitoul 5 și simulat cu Matlab/Simulink. După asimilarea rezultatelor simulării sistemului cu bucla deschisă (fără reglare) cu măsurătorile efectuate (figura 8.10), a fost parametrizat un regulator proporțional-derivativ pentru compensarea vibrațiilor. Simularea sistemului cu bucla închisă, folosind un asemenea regulator, a demonstrat că în cazul prezentat în figura 8.7, vibrațiile provocate pot fi cel mai bine reduse în urma aplicării de forțe elastice compensatoare în pozițiile în care se află greutatea (3). Aceste greutăți cu forma inelară (denumite și inele compensatoare) se rotesc pe role fără profil, ce se află amplasate pe sinele elastice (4). Aceste sine se pot mișca, fiind fixate cu ajutorul unor arcuri elastice, ce poate permite crearea unor forțe elastice definite ($F=k*x$) prin atingerea inelelor. Această soluție a fost aleasă pentru a evita prelucrarea permanentă a inelelor (3) ceea ce ar duce la consum de material foarte mare, precum și la timpuri de prelucrare foarte lungi. Cu ajutorul regulatorului proporțional-derivativ, au fost calculate forțele compensatoare necesare. Cunoscând rigiditatea arcurilor, au fost calculate abaterile necesare de la dimensiunile inițiale ale inelelor (3), în funcție de unghiul de rotație a rolei, pentru a reduce vibrațiile. Rezultatele de la simularea cu Matlab/Simulink sunt exportate în software-ul de desen Catia V5 unde este generat profilul inelului compensator. Acest inel compensator este prezentat în figura 8.12. În figura 8.13 sunt prezentate forțele perturbatoare cu și fără inele profilate pentru compensare. Aceste forțe au fost generate cunoscând amplitudinile vibrațiilor care au fost măsurate, pentru a ajunge la concluzia de la care a pornit ideea anunțată spre patentare, aceea că vibrațiile ce apar periodic pot fi compensate folosind elemente pasive în locul unor actuatori foarte scumpi. Se observă o reducere de 85% a amplitudinii vibrațiilor în acest caz.

Un dezavantaj al acestei idei de amortizare a vibrațiilor este spațiul necesar aplicării inelelor profilate, care de cele mai multe ori poate fi foarte mic, precum și eventualele schimbări constructive care pot apărea în acest caz. De aceea, la mașinilor flexografice există ideea de a include inelele perturbatoare în cadrul matritei de tipărit sau prelucrate împreună cu aceasta, idee care nu a fost verificată până în momentul încheierii acestei teze.

9. CONTRIBUTIONS, CONCLUSIONS AND FUTURE WORKS

9.1. Conclusions

This thesis deals with improving the dynamic behaviour of rollers in a printing unit from a flexographic printing machine in respect of two goals:

- active vibration damping of the roller systems of a flexographic printing machine.
- development of new sensors for dynamic measurement of nip forces in printing roller systems as basis for an optimal adjustment of the printing unit and for a controller design

This work is structured in 9 chapters. After a short introduction in Chapter 1 to the evolution of the printing machines, the process of flexographic printing and a description of the motivation and goals of the presented research work, in Chapter 2 the state of the art for measuring of nip pressure and forces, of roller vibration as well as the existing solutions for vibration damping of roller systems are presented.

Chapter 4 deals with the first goal of this thesis, the development of new sensors for dynamic measurement of the nip forces in printing roller systems. The new sensors are piezoelectric sensors based on acrylic paint with a high concentration of piezoelectric particles. The manufacturing process of the piezopaint sensors is improved to semi-automatized manufacturing with the help of a robot KUKA R3 to obtain sensors with constant thickness of piezopaint, which is very important for the quality, functionality and reproducibility of the sensors. The piezopaint sensors are tested and the measurements results are compared with those of a calibrated piezoelectric force sensor with good results. The sensors show the required properties for measuring the nip forces in roller systems, by applying them onto the roller underneath the printing plate in a flexographic printing unit.

A downscaled model of the flexographic printing unit is developed and constructed in the Laboratory of the University of Applied Sciences Osnabrück. For this test setup as well as for the printing unit of an industrial printing machine, active bearings with piezoelectric stack actuators for damping vibrations of the plate cylinder are designed. Vibrations are generated by discontinuous contact between rollers, realized with a printing plate. The design of the active bearings for the printing unit is a successful solved challenge. Problematic are the space limitation for mounting the bearings, the demands on installation conditions to avoid damage to the actuators (e.g. tensile forces, bending moments) and limitation of the piezoelectric actuators the small displacements which only can be generated. The test setups are described in Chapter 7.

First the test setups (model and printing unit) are simulated using FEM methods with Matlab/Simulink, as presented in chapter 5. The reduction of the degrees of freedom is made using the modal analysis with modified form, taking into account just the first 6 natural modes, which can appear in the test runs. With this method the differential equations for each DOF are decoupled and the complex eigenvalues are separated in real numbers as described in Chapter 5. So the number of DOFs could be diminished, which reduces simulation time. The simulation program is validated by comparing the simulation results to the measurements on the printing unit.

In Chapter 6 concepts for active vibration damping are presented. The active vibration damping is tested on the downscaled test setup, using two algorithms:

- a simulation-based proportional-derivative controller
- an experimental-based feed-forward and a feedback control. The feed-forward control is realized using the Least Mean Squares algorithm (LMS), based on identification of the periodical disturbances with the rotational angle (identification period is 2 seconds) and generating counter-vibrations for optimization the dynamic behaviour of the roller. The feedback control is realized with a proportional-derivative controller for damping vibration which can appear occasionally. This active vibration damping algorithm was evaluated on the downscaled roller system gaining a reduction of the vibrations of 85%.

Based on the concept of determining the periodical forces with a LMS algorithm and generating these forces with piezoelectric actuators, idea of generating counteract forces for vibration reduction using profile rings came up. The profile rings are described in Chapter 8. This method is applied with success on a bending roller in another test rig in the laboratory of the University of Applied Sciences Osnabrück. On the roller are mounted 3 discs with relatively great masses, 2 of them are equipped with profile rings and one mass with applied disturbances placed in the middle of the roller. A mathematical model of the test rig is built and in simulations a PD-controller generates the needed forces for vibration reduction. With that the shape of the profile rings is determined and designed with Catia V5 by importing the shape parameters from Matlab. Measurements show an improvement of the dynamic behaviour of the roller by means of a 85% reduction of the vibration amplitude.

The mentioned issues led to the subject of this thesis, to optimize the dynamic behaviour of printing roller systems. According to this goal, it was defined a working plan, concretized in the 9 chapters of this thesis, the appendices and the used bibliography.

Some student works (projects, master thesis, bachelor theses) contributes to this thesis as follows: [7, 43, 44, 72, 73, 101, 102, 109, 117, 131, 132].

9.2. Contributions to the Fundamental and Experimental Research

In pursuit of the main goal of this work, it was developed a theoretical content and an experimental part with following original contributions:

- The development, manufacturing and tests of piezoelectric sensors based on piezoelectric paint for dynamic measurement of the nip forces. This piezoelectric paint, developed by Professor Hale from the University of New Castle upon Tyne and is not available on the market, thus the developed sensors are absolutely new as manufacturing concept and application as force sensors, particularly for measuring the dynamic forces in the nip and their application onto the roller underneath the printing plate. Thus, the developed sensors open new possibilities for monitoring the roller behaviour during the printing process. Also a contribution is the concept of the test setups and the measurements with piezoelectric paint sensors.

- The concept of the construction of a downscaled test setup of a printing unit for testing active vibration damping.
- The development of active bearings with piezoelectric stack actuators is well-known. However, the constructive way to transmit vibrations (forces and displacements) to the roller for damping vibrations for two test setups is an innovative concept.
- In the simulation of the roller systems with Matlab/Simulink, a contribution is the application of mass, stiffness and damping matrix for a flexographic printing unit, as well as the created applications for simulation of roller systems.
- Modal reduction of DOFs for the finite element model of the printing unit as basis for fast simulations and for control algorithms is a contribution.
- The use of the Least Mean Squares Algorithm in designing a feed-forward control for compensation of the periodical disturbances generated by the printing plate in a flexographic printing unit, which is a contribution to the optimization of the behaviour of printing rollers.
- The method of damping periodic oscillations with a rotation of the printing roller by generating counter-vibrations with piezoelectric actuators introduces the idea of a semi-active vibration damping using passive profile rings and the rotating energy of the roller system. This idea is new and was announced to be patented and it can be found in internet under the identification ID "Offenlegungsschrift DE10 2010 026 204 A1"
- The method to generate the damping rings profile by exporting the simulated parameters from Matlab/Simulink to the CAD design program Catia V5 and the experimental results of vibration reduction obtained with the test setup in the laboratory presented in Chapter 8 is an original contribution. The results of vibration with profile rings open a new possibility to optimize of the dynamic behaviour of printing rollers.

A feasibility study [104] and a master thesis [135] were developed from these research works. The subject is to improve the application of piezoelectric paint sensors:

- on the spherical surfaces for measuring forces e.g. in the ball joint of a trailer
- in the rubber bearings of a wind turbine for measuring forces.

9.3. Dissemination of the Research Results

The conducted research in order to elaborate the thesis was used in the development and co-development of 8 papers, presented to national and international conferences and published in different journals and proceedings of the conferences. Two papers are ISI indexed.

Together with other colleagues, I applied for the German patent No. 10 2010 026 204.8 from July 2nd 2010 [71], which has published in Internet on the site of the German Patent Institution dpma.de on January 5th 2012 with the number DE10 2010 026 204 A1:

„Verfahren sowie Vorrichtung zur Kompensation von über den Umfang eines rotierenden, insbesondere zylindrischen, Bauteils, insbesondere einer Walze, periodisch wiederkehrenden Störanregungen sowie Verfahren zur Bestimmung der

Oberflächenstruktur eines ringförmigen Profils zur Kompensation von Störanregungen“

- The ISI indexed papers are:
 1. *Analysis of sensors for vibration and nip forces monitoring of rubber coated roller* – M.C. Voicu, R. Schmidt, B. Lammen, H.H. Hillbrand, I. Maniu, Applied Mechanics and Materials Vols. 24-25, S. 83-88, Trans Tech Publications, 2010 und BSSM 7th International Conference on Advances in Experimental Mechanics, Liverpool 2010
 2. *Simulation of Bending Vibrations of a Roller System*, M.C. Voicu, B. Lammen, R. Schmidt, I. Maniu, Applied Mechanics and Materials Vol. 162 pp. 47-56, Trans Tech Publications, 2012 and The XI International Conference on Mechanisms and Mechanical Transmissions and the International Conference on Robotics, Clermont-Ferrand 2012
- Other contributions are:
 3. *Measuring the nip forces in roller systems using piezoelectric paint* – M.C. Voicu, R. Schmidt, B. Lammen, I. Maniu, Annals of DAAAM for 2010 & Proceedings of the 21st International DAAAM Symposium Zadar 2010, Volume 21, No. 1, 2010
 4. *Messung der Anpressdrücke im Nip von Walzensystemen mit neuentwickelten piezoelektrischen Sensoren* – M.-C. Voicu, B. Lammen, R. Schmidt, H.H. Hillbrand, I. Maniu, Fachtagung Mechatronik 2011, S. 19-22, 2011
 5. *Aktive Schwingungstilgung in Walzensystemen mit piezoelektrischen Aktoren* – M.-C. Voicu, B. Lammen, R. Schmidt, F. Weigt – VDI 7. Fachtagung Schwingungen in Antrieben, Leonberg 2011 and VDI-Berichte 2155, S. 103-114, 2011
 6. *Active bearing for vibration damping of roller systems with piezoelectric actuators* - M.-C. Voicu, R. Schmidt, B. Lammen, M. Mersch, I. Maniu – Mechanisms, transmissions and applications, Springer 2011, S. 247-256 und 1st Workshop on Mechanisms, Transmissions and Applications, Timisoara 2011
 7. *Design of an active vibration control for a roller system* – M.-C. Voicu, H.-H. Hillbrand, R. Schmidt, B. Lammen, 12th International Workshop on Research and Education in Mechatronics, Kocaeli 2011
 8. *Active vibrations damping of bending for printing rollers* - M.-C. Voicu, B. Lammen, R. Schmidt, Annals & Proceedings of 22th DAAAM World Symposium, Wien 2011
- Another publications containing the results from another research project are:
 9. *Simulation-based Design of an Energy-efficient Vacuum Control of a Milking Machine* - M.-C. Voicu, R.-G. Schmidt, B. Lammen, Annals of DAAAM for 2010 & Proceedings of the 21st International DAAAM Symposium Zadar 2010, Vol. 21, No. 1, 2010

10. *Simulation of the Vacuum Control of a Milking Machine* - M.-C. Voicu, R.-G. Schmidt, M. Jänecke, B. Lammen, 11th International Workshop on Research and Education in Mechatronics, Ostrava 2010

9.4. Future Work

The results obtained during this work open new directions for research and development to optimize the dynamic behaviour of printing roller system, but also for other applications.

The developed piezoelectric paint sensors have to be applied for measuring the nip forces in the printing unit, with the help of the sensors glued on the plate cylinder underneath the printing plate.

The mathematical model for the actuators and their amplifiers can be included in the model of the roller system in a master thesis. The influence of different types of printing plates, with respect to the material properties, the thickness and the form can be studied in a student advanced project.

The developed concept for vibration reduction of the plate cylinder from the downscaled test setup has to be applied and tested on the printing unit. Also other control algorithm especially model based algorithms can be validated for vibration reduction as subject for master or bachelor thesis.

The patent application [71] developed during this thesis can be improved and its application on other rotating shafts, e.g. turbines, motors can be proven. In the case of successful patenting of this method, it can be generate new ideas for applications in the industry and new research projects.

A project proposal for the German program FHprofUnt was developed from the research work, but this proposal couldn't be financed although the peer reviews were positive. It deals with development and improvement of piezoelectric sensors based on acrylic paint with piezoelectric powder and also based on rubber with piezoelectric powder.

BIBLIOGRAPHY

- 1 Aenis M., Knopf E., Nordmann R.: "Active Magnetic Bearings for the Identification and Fault Diagnosis in Turbomachinery", *Mechatronics*, Vol. 12, Issue 8, pp. 1011-1021, Elsevier, 2002
- 2 Alizadeh A.: Robust control for active vibration damping of elastic rotors with piezo-stapel-actuators, PhD Thesis, Technical University Darmstadt, Darmstadt, 2005
- 3 Al-Wahab M.A.: „Neue Aktorsysteme auf Basis strukturierter Piezokeramik“, PhD Thesis, 2004
- 4 Angermann A., Beuschel M., Rau M., Wohlfahrt U: "Matlab-Simulink-Stateflow", 7th Edition, Oldenbourg, 2011
- 5 Bayer H. R.: "Modeling and Optimization of a Circular Bimorph Piezoelectric Actuator", Faculty of Rensselaer at Hartford, Hartford, 2003
- 6 Bill B.: „Messen mit Kristallen: Grundlagen und Anwendungen der piezoelektrischen Messtechnik“, *Moderne Industrie*, 2002, Bd. 227
- 7 Bohlmann S., Kunzer J., Roßmann S., Werning S.: „Anwendung piezoelektrischer Lacke zur Druck- und Kraftmessung“, Student Project, University of Applied Sciences Osnabrück, 2013
- 8 Bruel & Kjaer: Documentation about sensor's properties
- 9 Burdisso R.A., Heilmann J.D.: "A New Dual-Reaction Mass Dynamic Vibration Absorber Actuator for Active Vibration Control", *Journal of Sound and Vibration*, Vol. 214, No. 5, 1998
- 10 Cedrat Recherche Sarl: "Actionneur Piezoactif amplifié à raideur élevée", Patent Application, FR2740276A1, 1995
- 11 Ceramtec: Information on <http://www.ceramtec.de>, last check on 16.03.2012
- 12 Christel R.: „Bearing unit for a printing cylinder and a method for reducing of oscillations of printing cylinders“, *Offenlegungsschrift DE 102007024767A1*, 2008
- 13 Christel R.: Active Vibration Control of Coupled-Cylinders in Web Offset Presses Using Piezoceramic Actuators in the Bearings, PZH, 2010
- 14 Daraji A.H., Hale J.M., Bicker R.: "Active Vibration Control of a Smart Structure", <http://www.ncl.ac.uk/mech/students/conference/documents/Daraji.pdf>, accessed on 14.08.2014

- 15 Druce C. Moore: "Principal Component Analysis in Linear Systems: Controllability, Observability, and Model reduction", IEEE Transactions on Automatic Control, Vol. AC-26, No.1., 1981
- 16 Deutsch V., Platte M.: "Film Thickness Measuring", Castell Publisher, 2005
- 17 DFTA: Information on <http://www.dfta.de/de/flexodruck/flexodruck-technik/technik-des-flexodruck/#prettyPhoto>, accessed on 01.09.2013
- 18 Dresig H., Holzweißig F.: „Maschinendynamik“, Springer, 10th Edition, 2010
- 19 Ehmann C., Schönhoff U., Nordmann R.: Active Vibration Damping of Portal Milling Machines by Using Piezoactuators, VDI – Vibration in Industrial Plants and Machines, Veitshöchheim, 2001
- 20 Ehmann C.: "Vibration Damping of Rotors with Active Bearing with Robust Control", Darmstadt, 2003
- 21 Ehmann. C, Nordmann R.: Comparison of Control Strategies for Active Vibration Control of Flexible Structures, Archives of Control Sciences, Vol. 13, 2003, No 3, pp 303-312
- 22 Fehren H. et al: "Method and Devices for Reducing Vibrations on Rotating Parts, and vibration-damped rotating part", Patent Application WO2004016431 A1, 2004
- 23 Fleischer E.: "Integration von kapazitiven Abstandssensoren in ein vollständig magnetisch gelagertes Turbogebläse sowie Implementierung von Regelungsstrategien basierend auf stochastischer Zustandsschätzung", Diploma Thesis; Technical University Chemnitz, 2007
- 24 Flint Group Flexographic Products: "Sleeves in offset printing offer new freedom", Press Release, June 2010, on <http://www.flintgrp.com/> and information on http://flintgrp.com/en/documents/Printing-Plates/nyloflex/nyloflex_techn_data_EN.pdf, accessed on 10.09.2013
- 25 Fraunhofer Institut: "Adaptronische Aktor-Sensor Einheit", Press Release, Information on www.iwu.fraunhofer.de, accessed on 14.02.2013
- 26 Fuji Film: Information on www.fujifilm.com/products/prescale, last check 02.05.2012
- 27 Gasch R., Nordmann R., Pfützner H.: „Rotordynamik“, Springer, 2nd Edition, 2002
- 28 Gautschi G.: "Piezoelectric Sensorics: Force, Strain, Pressure, Acceleration and Acoustic Emission Sensors, Materials and Amplifiers", Springer, 2002
- 29 Gawehn, W.: "Finit Elements Methods, FEM-Basics for Statik and Dynamic", Books on Demand GmbH, 2008
- 30 Glöckner E.H., Keller B., Ulrich H.: „Verfahren und Vorrichtung zur Tilgung der Drehschwingungen einer Druckmaschine“, Patent WO 01/50035 A1, 2000
- 31 Glöckner E.H., Keller B.: „Verfahren und Anordnung zur Kompensation von Schwingungen rotierender Bauteile“, Patent DE 199 63 945 C1

- 32 Gnad G.: "Ansteuerkonzept für piezoelektrische Aktoren", PhD Thesis, University Otto-von-Guericke, 2005
- 33 Goldfarb M., Celanovic N.: "Modeling Piezoelectric Stack Actuators for Control of Micromanipulation", IEEE Control Systems 0272-1708/97, pp. 69-79, 1997
- 34 Groß D., Hauger W., Schröder J., Wall W.A.: "Technische Mechanik 2", 11th Edition, 2012
- 35 Hader P., Meitner R.: "Active Vibration-Damping Method", Patent EP 1333122B2, 2007
- 36 Hader P.: "Roll with vibration damper and method for damping vibrations of a roll", European Patent EP 1 936 214 A2, 2007
- 37 Hale J.M., Tuck J.: "A Novel Thick-Film Strain Transducer Using Piezoelectric Paint", ImechE, 1999, pp. 613-622
- 38 Hale J.M., White J. R., Stephenson R., Liu F.: "Development of piezoelectric paint thick-film vibration sensors," Proc. ImechE Vol. 219 Part C, Mechanical Engineering Science, 2005
- 39 Hoffmann J.: „Taschenbuch der Messtechnik“, 5. Edition, Fachbuchverlag Leipzig im Carl-Hanser-Verlag, 2007
- 40 Hoffmann, Liebau: „Beitrag zur Untersuchung des dynamischen Verhaltens von Druckwerke in Rollenoffset-Rotationsdruckmaschinen“, PhD Thesis, TH Karl-Marx-Stadt, Chemnitz, 1969
- 41 Holzweißig F.: „Dynamische Untersuchung an der Zylindergruppe einer Offsetmaschine“, PhD Thesis, TH Dresden, Dresden, 1959
- 42 Horst H.-G. : „Aktive Schwingungsminderung an elastischen Rotoren mittels piezokeramischer Aktoren“, PhD Thesis, TU Darmstadt, Aachen, Shaker Verlag, 2005
- 43 Hufendiek H., Sellmann F.: „Robotergestützte Herstellung von Kraftsensoren auf Basis von Piezofarbe“, Hausarbeit, WS10/11, Hochschule Osnabrück, 2011
- 44 Huffendiek H., Sellmann F: „Verbesserung der Schwingungsverhalten von Walzensystemen durch aktive Schwingungstilgung mit Piezoaktoren“, Student Project, University of Applied Sciences Osnabrück, 2010
- 45 Information on <http://commons.wikimedia.org/wiki/File:Flexodruckmaschine.jpg>, accessed on 01.09.2013
- 46 Information on http://www.meas-spec.com/product/t_product.aspx?id=2488, last check on 30.08.2014
- 47 Information on <http://www.vdd-net.de/index.php/vorstand?id=68:direktgravur-ausblick-in-die-zukunft-des-flexodrucks&catid=1:hauptkategorie>, accessed on 02.09.2013
- 48 Information on http://www.wuh-group.com/de/products/vistaflex_pics.html, accessed on 10.09.2013

- 49 Inometa Press Release: „Du Pont Packaging Graphics bringt kompressible Adapter von Inometa auf den Markt“, 07.09.2011
- 50 Jalili N.: „Piezoelectric-Based Vibration Control, From Macro to Micro/Nano Scale Systems“, Springer, 2010
- 51 Juhász L., Maas J., Borovac B.: Parameter identification and hysteresis compensation of embedded piezoelectric stack actuators
- 52 Kipphan H. (Hrsg.): „Handbook of Print Media“, Springer, 2000
- 53 Kistler: „Guide to the Measurement of Force“, Institut of Measurement and Control, 1998
- 54 Klein B.: „Grundlagen und Anwendungen der Finite-Elemente-Methode“, 3rd Edition, Vieweg, 1999
- 55 Knopf E. : Aktive Reduktion von Drehschwingungen in Bogenoffsetdruckmaschinen, Heidelberger Druckmaschinen AG, VDD Jahrestagung 2006
- 56 Kressmann R.: „Linear and non-Linear Piezoelectric Response of Charged Cellular Polypropylene“, J. Appl. Phys., Vol. 90, pp. 3489 – 3496, 2001
- 57 Kressmann R.: „New Piezoelectric Polymer for Air-borne and Water-borne Sound Transducers“, J. Acoust. Soc. Am., Vol. 109, S. 1412 – 1416, 2001
- 58 Kreßmann R.: „Kapazitive Schallwandler mit interner Polarisation auf Polymerbasis sowie in Siliziummikromechanik“, PhD Thesis, Shaker, 2001
- 59 Kumme E., Mack O., Bill B., Gossweiler Ch., Haab H.R.: „Dynamic Properties and Investigations of Piezoelectric Force Measuring Devices“, Kistler special print 920-233e-12.03
- 60 Kuratle H. R., Signer A.: „The Basic of Piezoelectric Measurement Technology“, Kistler Reprint 20.188e 7.99
- 61 Lakers J., Koch T., Kütemann A.: „Modellbildung und Simulation eines Piezoaktors“, Hausarbeit, WS10/11, University of Applied Sciences Osnabrück, 2011
- 62 Lammen B., Reike M.: „Steuerungs- und Regelungstechnik Vorlesungsskript“, University of Applied Sciences Osnabrück, 2010
- 63 Lammen B., Schmidt R., Voicu M.C. : Research proposal „Entwurf von profilirten zur Schwingungsdämpfung von rotierenden Wellen“, University of Applied Sciences Osnabrück, 2010
- 64 Li W.: „Aktive Dämpfung und Kompensation von Rotorschwingungen über active Piezo-Stapel-Aktuator-Lager“, PhD Thesis, Technical University Chemnitz, Shaker, 2005
- 65 Li X., Zhang Y.: „Analytical Study of Piezoelectric Paint Sensor for Acoustic-Emission-based Fracture Monitoring“, Fatigue & Fracture of Engineering Materials & Structures, Vol. 31 Issue 8, 2008

- 66 Mahinzaeim M., Hale J.M., Swailes D.C., Schmidt R., Johanning B.: Development of an active vibration regulation system to improve driving comfort in convertibles, to be published in ATZ 2007, 2007
- 67 Mahinzaeim M., Hale J.M., Swailes D.C., Schmidt R.: "Dynamic modelling and optimal vibration regulation of a flexible half-car model subjected to random road inputs and harmonic engine excitations", to be published in Journal of Sound and Vibration 2007
- 68 Mahinzaeim M., Schmidt R.: "An approach towards the development of an active torsion control (ATC) system for convertibles", Adaptive Structures 2006, Bristol, UK, 10th-12th July 2006
- 69 Maness W., Golden R., Benjamin M., Podoloff R.: Improved Pressure and Contact Sensor System for Measuring Dental Occlusion, European Patent EP0379524B1, 2004
- 70 Meißner U., Menzel A.: „Die Methode der finiten Elemente“, Springer, 1989
- 71 Mersch M., Voicu M.C., Hillbrand H.H., Lammen B., Schmidt R.: German Patent Application No. 10 2010 026 204 A1 from 02.07.2010: „Verfahren sowie Vorrichtung zur Kompensation von über den Umfang eines rotierenden, insbesondere zylindrischen, Bauteils, insbesondere einer Walze, periodisch wiederkehrenden Störanregungen sowie Verfahren zur Bestimmung der Oberflächenstruktur eines ringförmigen Profils zur Kompensation von Störanregungen“
- 72 Mersch M.: „Gestaltung und Konstruktion aktiver Lagerungen zur Schwingungsdämpfung“, Engineering Practical Training, University of Applied Sciences Osnabrück, 2010
- 73 Mersch M.: Konstruktion / Auslegung aktiver Lagerungen, Bachelor Thesis, University of Applied Sciences Osnabrück, 2010
- 74 Messer M., Wölfel H.P., Friedmann H., Pankoke S., Wölfel M. R.: „Methoden und Werkzeuge zur aktiven Beherrschung von Biegeschwingungen rotierender Zylinder in Druckmaschinen“, Research Report, TU Darmstadt, 2006
- 75 Messer M.: " Active Damping of Coupled-Rotor Vibrations in a Sheet-Fed Offset Printing Machine from Excitation Due to Channel Impact ", VDI, 2007
- 76 Metso Paper Inc.: "Presse mit langem Walzenspalt einer Papier-/Pappmaschine", Patent Application DE10392407T5, 2005
- 77 Metso Paper Inc.: "iRoll Runnability Analysis", Press Release, [http://www.metso.com/MP/marketing/Vault2MP.nsf/BYWID/WID-080418-2256E-6C732/\\$File/42109_V2_EN.pdf?OpenElement](http://www.metso.com/MP/marketing/Vault2MP.nsf/BYWID/WID-080418-2256E-6C732/$File/42109_V2_EN.pdf?OpenElement), accessed on 13.05.2013
- 78 Meyer K.H., DFTA: "Technic of Flexoprint", 5th Edition, Rek & Thomas Medien AG, 2006
- 79 Micro-Epsilon: „Mess- und Prüfsysteme für die Gummi- und Reifen-Industrie, Documentation on www.micro-epsilon.de, last check on 03.03.2014
- 80 Mirow: Information on www.mirow.de, last check on 01.11.2012

- 81 Montagne G.T., Kascak A.F., Palazzolo A., Manchala D., Thomas E.: "Feed-forward Control of Gear Mesh Vibration Using Piezoelectric Actuators", NASA Technical Memorandum 106366, U.S. Army Research Laboratory, 1994
- 82 Mücke G., Neuschütz E.: "Messrolle zum Feststellen von Planheitsabweichungen", BFI Betriebsforschungsinstitut VDEj- Institut für Angewandte Forschung GmbH, Patent Application DE 19918699 A1,1999
- 83 Muhs D., Wittel H., Jannasch D., Voßik J.: „Roloff/Matek Maschinenelemente, Normung, Berechnung, Gestaltung“, 18th Edition, Vieweg, 2007
- 84 Neuschütz E., Mücke G.: "Umlenkmesrolle", Patent Application DE19616980A1, 1997
- 85 Nöll M.: "Kompensation diskreter Drehschwingungen bei Bogenoffsetdruckmaschinen", PhD Thesis, TU Darmstadt, 2004
- 86 Nordmann R.: Use of mechatronic components in rotating machinery, Vibration Problems ICOVP 2005, Springer Editor, 2007
- 87 Paschedag J., Hatzl S.: "Anwendung adaptiver Störgrößenaufschaltungen zur Dämpfung von Kfz-Motorvibrationen im Mehrkanalfall", Proceedings of „Methoden und Anwendungen der Regelungstechnik“, Hirschberg 2005/2006
- 88 Paschedag, J.: "Aktive Schwingungsisolation in Kfz-Motoraufhängungen – Systemkonfiguration und Methoden", PhD Thesis, 2007
- 89 Payo I., Hale J.M.: "A piezoelectric paint thick-film strain sensor for vibration monitoring purposes", Proceeding of ISMA 2010, Leuven 2010, pp. 1045-1052
- 90 Peschel D.: „Neuentwicklungen im Bereich Flexodruckmaschinen“, Windmüller & Hölscher, Flexo Swiss Forum, 2007
- 91 Physik Instrumente:Information on www.physikinstrumente.de, last check on 15.08.2014
- 92 Pickelmann L.: "Low Voltage Highly Dynamic Piezo Actuators", Documentation on www.piezomechanik.com on 11.09.2011
- 93 Pickelmann L.: "Piezo-Mecanical and Electrostrictive Stack and Ring Actuators", Documentation on www.piezomechanik.com on 11.09.2011
- 94 Pickelmann L.: "Electronic Supplies for Piezomechanics: Technical Data", Documentation on www.piezomechanik.com, accessed on 11.09.2011
- 95 Pickelmann L.: "First steps towards piezoaction", 2012
- 96 Pictures from [www.wikipedia .de](http://www.wikipedia.de), last check on 19.08.2014
- 97 Pietruszka W.D.: „Matlab und Simulink in der Ingenieurpraxis, Modellbildung, Berechnung und Simulation“, 2nd Edition, Teubner, 2006
- 98 Ram Y.M., Inman D.J.: "Optimal Control for Vibrating Systems", Mechanical Systems and Signal Processing, Vol. 13, No. 6, 1999

- 99 Raptis P.N., Stephenson R., Hale J.M., White J.R.: "Effect of Exposure of Piezoelectric Paint to Water and Salt Solution", *Journal of Materials Science* 39, 2004, pp. 6079-6081
- 100 Roshdi A.: Robuste Regelung zur aktiven Schwingungsdämpfung elastischer Rotoren mit Piezo-Stapelaktoren, PhD Thesis, TU Darmstadt, 2005
- 101 Sander S.: „Dimensionierung, Konstruktion und Inbetriebnahme eines Versuchsstandes zur aktiven Dämpfung von Walzenschwingungen“, Bachelor Thesis, University of Applied Sciences Osnabrück, 2010
- 102 Schauer M.: "Simulation, Aufbau und Inbetriebnahme eines Prüfstandes zur Schwingungstilgung rotierender Wellen mit periodischen Störanregungen", Bachelor Thesis, University of Applied Sciences Osnabrück, 2011
- 103 Shawn L.: "Active Vibration Control of a Flexible Beam", Master Theses, San Jose State University, 2009
- 104 Schmidt R., Lammen B., Kreßmann R., Voicu M.C.: Feasibility Study „Test exemplarischer Anwendungen von piezoelektrischen Druck- und Kraftsensoren auf Basis von Akryllack“, University of Applied Sciences Osnabrück, 2012
- 105 Schmidt R., Lammen B.: Research proposal "Active vibration systems", University of Applied Sciences Osnabrück, 2008
- 106 Schmidt R., Mahinzaeim M.: "A method for simplifying complicated multibody models for use in experimental control", IOMAC11 – 4th International Modal Analysis Conference, Istanbul, 2011
- 107 Schmidt R., Waller H.: „Schwingungslehre für Ingenieure, Theorie, Simulation, Anwendungen“, Wissenschaftsverlag, 1989
- 108 Schmidt R., Wöhrmann H.: Grundlagenuntersuchung zum Vergleich von CFK- und Stahlwalzen in Druckmaschinen, Hochschule Osnabrück, 2002
- 109 Simon S.: "Simulation of an Active Vibration Damping System for a Printing Roller", Master Thesis, Politehnica University of Timișoara and University of Applied Sciences Osnabrück, 2011
- 110 Smart Material: www.smartmaterial.de, last check on 04.05.2014
- 111 Sparkler Ceramics: Sparkler Ceramics, General Information, Information on www.sparklceramics.com accessed on 01.08.2014
- 112 Spies P.: "Piezotex: Piezoelectric Textile Fibers and Fabrics for Sensors and Energy Harvesting", Fraunhofer IIS, 2011
- 113 Strohschein D.: „Experimentelle Modalanalyse und active Schwingungsdämpfung eines biegeelastischen Rotors“, PhD Thesis, Universität Kassel, 2011
- 114 Tehrani M. G., Elliott R.N.R., Mottershead J. E.: "Partial Pole Placement in Structures by the Method of Receptances: Theory and Experiments", *Journal of Sound and Vibration* 329, pp. 5017-5035, 2010
- 115 Tekscan: Information on www.tekscan.com, last check 02.05.2012

152 Bibliography

- 116 Tichi J., Gautschi G.: "Piezoelectric Measurement Technology", Springer, 1980
- 117 Topmann S.: „Entwicklung einer dezentralen, webbasierten Prozessvisualisierung“, Bachelor Thesis, University of Applied Sciences Münster, 2010
- 118 Tränkler H.-R., Obermeier E. (Hrsg.): „Sensortechnik, Handbuch für Praxis und Wissenschaft“, 1. Auflage, Springer Verlag, 1998
- 119 VDEh Press Release, Information on www.bfi.de accessed on 10.03.2013
- 120 Voicu M.-C., Hillbrand H.-H., Schmidt R., Lammen B.: "Design of an active vibration control for a roller system", 12th International Workshop on Research and Education in Mechatronics, Kocaeli, 2011
- 121 Voicu M.-C., Lammen B., Schmidt R., Hillbrand H.H., Maniu I.: „Messung der Anpressdrücke im Nip von Walzensystemen mit neuentwickelten piezoelektrischen Sensoren“, Fachtagung Mechatronik 2011, S. 19-22, 2011
- 122 Voicu M.C., Lammen B., Schmidt R., Maniu I. : "Simulation of Bending Vibrations of a Roller System", Applied Mechanics and Materials, Vol. 162, pp. 47-36, Trans Tech Publications, 2012
- 123 Voicu M.-C., Lammen B., Schmidt R., Weigt F.: „Aktive Schwingungstilgung in Walzensystemen mit piezoelektrischen Aktoren“, VDI 7. Fachtagung Schwingungen in Antrieben, Leonberg 2011 und VDI-Berichte 2155, S. 103-114, 2011
- 124 Voicu M.-C., Lammen B., Schmidt R.: "Active vibrations damping of bending for printing rollers", Annals & Proceedings of 22th DAAAM World Symposium, Wien, 2011
- 125 Voicu M.C., Schmidt R. , Lammen B., Hillbrand H.H., Maniu I.: "Analysis of Sensors for Vibration and Nip Forces Monitoring of Rubber Coated Roller", Applied Mechanics and Materials Vols. 24-25, S. 83-88, Trans Tech Publications, 2010 und BSSM 7th International Conference on Advances in Experimental Mechanics, Liverpool, 2010
- 126 Voicu M.C., Schmidt R., Lammen B., Maniu I.: "Measuring the nip forces in roller systems using piezoelectric paint", Annals of DAAAM for 2010 & Proceedings of the 21st International DAAAM Symposium Zadar 2010, Volume 21, No. 1, 2010
- 127 Voicu M.-C., Schmidt R., Lammen B., Mersch M., Maniu I.: "Active bearing for vibration damping of roller systems with piezoelectric actuators", Mechanisms, transmissions and applications, Springer 2011, S. 247-256 and 1st Workshop on Mechanisms, Transmissions and Applications, Timisoara, 2011
- 128 Voicu M.C., Schmidt R., Lammen B.: Research Report „Active Roller System“, University of Applied Sciences Osnabrück, 2011
- 129 Völklein F., Zetterer T.: "Practical knowledge of microsystems technology", 2nd edition, Vieweg, 2006
- 130 Wang Q.: „Piezoaktoren für Anwendungen im Kraftfahrzeug, Messtechnik und Modellierung“, PhD Thesis, 2006

- 131 Weigt F., Korte S.: „Experimentelle Untersuchung von piezoelektrischen Kraftsensoren“, Student Project, University of Applied Sciences Osnabrück, 2011
- 132 Weigt F.: "Aktive Schwingungsdämpfung bei einem Walzensystem", Student Project, University of Applied Sciences Osnabrück, 2011
- 133 Weiß J.: „Modellbildung und Simulation radial gekoppelter Rotoren“, Report 1/2008, Technical University Chemnitz, 2008
- 134 Wendt L.: „Taschenbuch der Regelungstechnik“, Harri Deutsch, 2012
- 135 Werning S.: „Charakterisierung neuartiger piezoelektrischer lacke, Konstruktion und Inbetriebnahme eines Demonstrators zur Druck- und Kraftmessung in den Getriebeisolationselementen einer Windenergieanlage“, Master Thesis, University of Applied Sciences Osnabrück, 2013
- 136 White J. R., De Poumeyrol B., Hale J.M., Stephenson R.: "Piezoelectric paint: Ceramic-polymer composites for vibration sensors", Journal of Material Science, 2004
- 137 Wimmel R. : „Strukturkonformes Aktives Interface – Einsatzerfahrung, Weiterentwicklung und Transfer in rotierende Systeme“, Adaptronic Congress 2004
- 138 Windmüller & Hölscher: Internal Documentation
- 139 Winter J., Golden R.: "Flexible, Tactile Sensor for Measuring Foot Pressure Distribution and for Gaskets, European Patent EP0457900B1, 1994
- 140 Yeh T.-J., Lu S.-W., Wu T.-Y.: "Modeling and Identification of Hysteresis in Piezoelectric Actuators", Journal of Dynamic Systems, Measurement and Control, Vol. 128, pp. 189-196, 2006
- 141 Yoo B., Purekar A.S., Zhang Y., Pines D.J.: "Piezoelectric Paint-based Two-dimensional Phased Sensor Arrays for Structural Health Monitoring of Thin Panels", Smart Materials and Structures 19, 2010
- 142 Zheng Sh.: "Lernende Regelung für Rotorsysteme", PhD Thesis, TU München, Advanced Reports VDI, Series 11, Nr. 187, VDI, 1993
- 143 Zienkiewicz O. C., Taylor R. L. : "The Finite Element Method", Vol. 1 "Basic Formulation and Linear Problems", 4th Edition, McGraw-Hill, 1989

I thank to the authors of the following works: [7, 43, 44, 72, 73, 101, 102, 109, 117, 131, 132] for their contributions to this thesis.

APPENDICES

Appendix A

Linearity of Piezoelectric Paint Sensors (similar to Figure 4.17 and Figure 4.18)

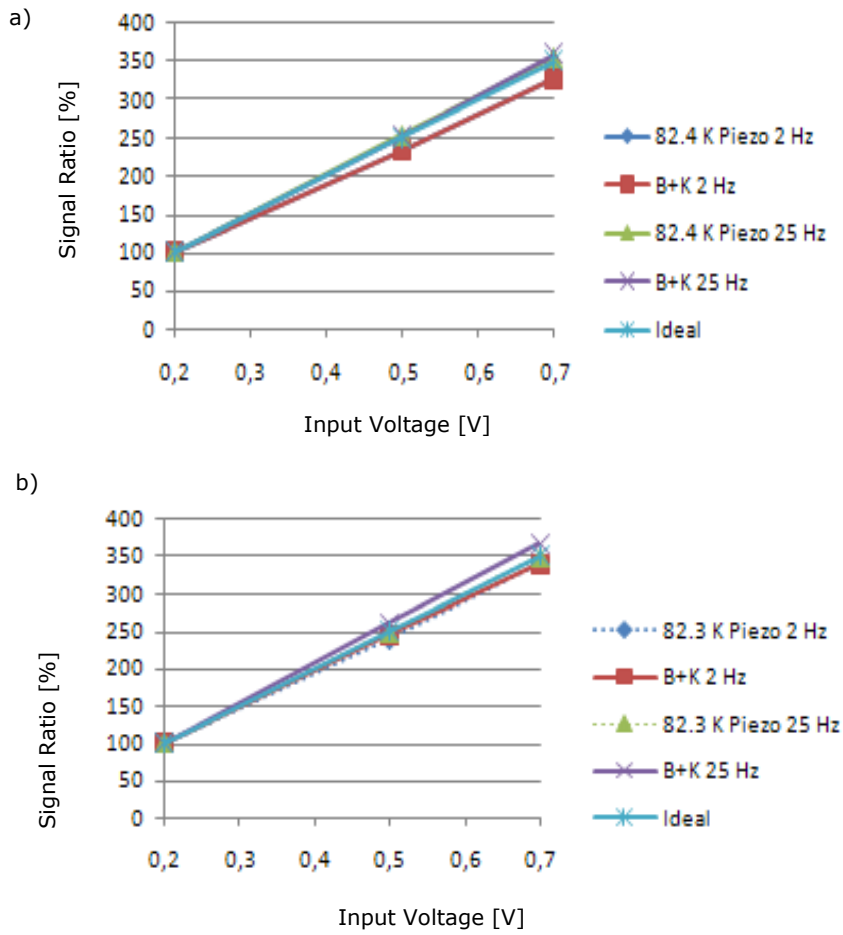


Figure A1. 1 Linearity measurement of the two sensors: a) 82.4K and b) 82.3K) with a thickness of the piezo paint layer of 82 μm

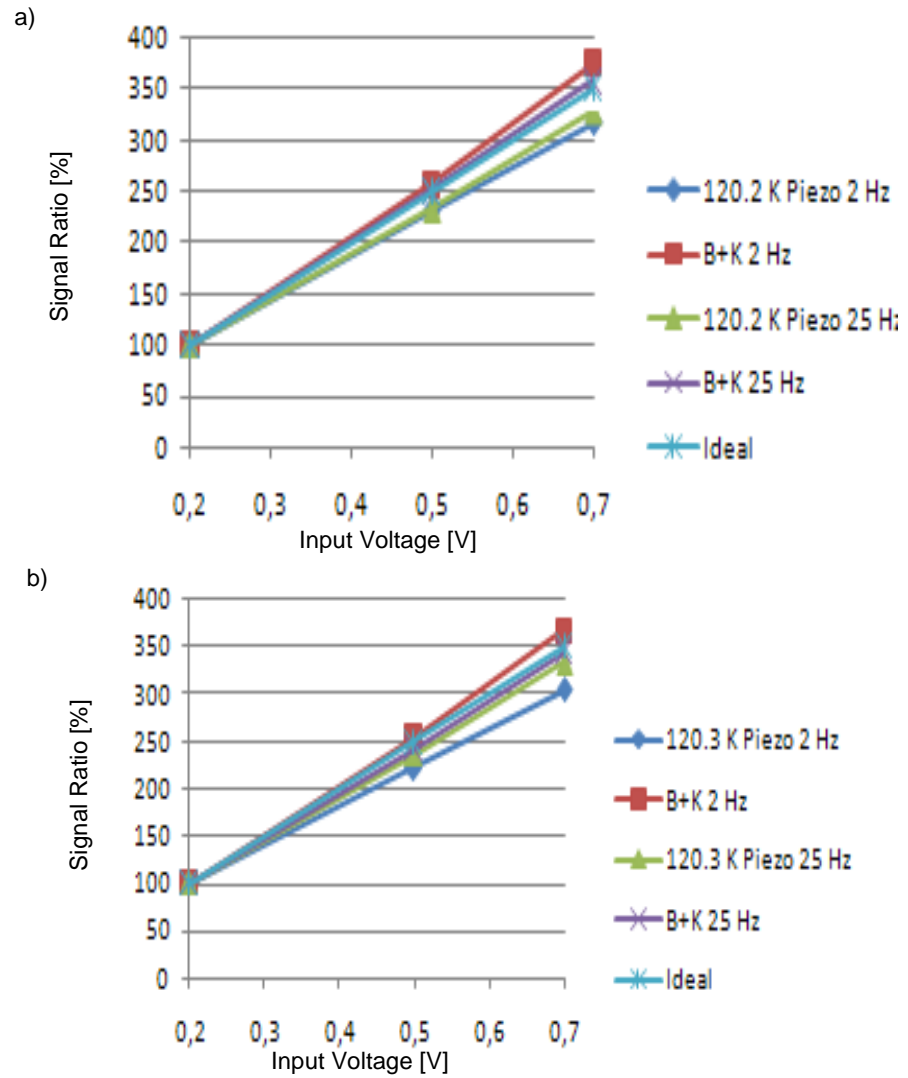


Figure A1. 2 Linearity measurement of the two sensors (named a) 120.3K and b)120.3K with a thickness of the piezo paint layer of 120 μ m

Appendix B

Patent Application

(19)  Deutsches Patent- und Markenamt



(10) DE 10 2010 026 204 A1 2012.01.05

(12) **Offenlegungsschrift**

(21) Aktenzeichen: **10 2010 026 204.8**
 (22) Anmeldetag: **02.07.2010**
 (43) Offenlegungstag: **05.01.2012**

(51) Int. Cl.: **F16C 13/00 (2006.01)**
B41F 13/08 (2006.01)

(71) Anmelder:
**Fakultät Ingenieurwissenschaften und Informatik
 Fachhochschule Osnabrück, 49076, Osnabrück,
 DE**

(56) Für die Beurteilung der Patentfähigkeit in Betracht
 gezogene Druckschriften:

DE	199 63 945	C1
DE	199 14 613	A1
DE	10 2007 024 767	A1
DE	10 2008 053 931	A1
DE	10 2008 060 740	A1
EP	1 936 214	A2
WO	01/ 50 035	A1
WO	2004/ 016 431	A1

(74) Vertreter:
BOEHMERT & BOEHMERT, 28209, Bremen, DE

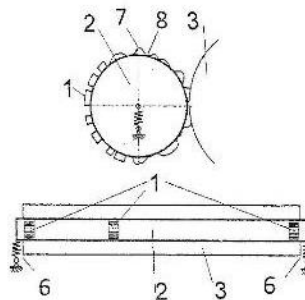
(72) Erfinder:
**Mersch, Michael, 49545, Tecklenburg, DE; Voicu,
 Mariana-Claudia, 33775, Versmold, DE; Schmidt,
 Rainhard, 49080, Osnabrück, DE; Lammen,
 Benno, 49477, Ibbenbüren, DE; Hillbrand, Heinz-
 Hermann, 49076, Osnabrück, DE**

Prüfungsantrag gemäß § 44 PatG ist gestellt.

Die folgenden Angaben sind den vom Anmelder eingereichten Unterlagen entnommen

(54) Bezeichnung: **Verfahren sowie Vorrichtung zur Kompensation von über den Umfang eines rotierenden insbesondere zylindrischen, Bauteils, insbesondere einer Walze, periodisch wiederkehrenden Störansregungen sowie Verfahren zur Bestimmung der Oberflächenstruktur eines ringförmigen Profils zur Kompensation der Störansregungen**

(57) Zusammenfassung: Verfahren zur Kompensation von über den Umfang eines rotierenden, insbesondere zylindrischen, Bauteils, insbesondere einer Walze, periodisch wiederkehrenden Störansregungen, dadurch gekennzeichnet, dass mittels mindestens eines ringförmigen Profils, das auf der Außenseite oder der Innenseite des Bauteils angebracht oder darin integriert ist oder das auf oder in einer separaten Einrichtung angebracht oder darin integriert ist, die mit dem Bauteil in Kontakt ist, gezielt Kräfte zur Kompensation der Störansregungen erzeugt werden und Vorrichtung zur Durchführung desselben und Verfahren zur Bestimmung der Oberflächenstruktur eines solchen Profils.



DE 10 2010 026 204 A1 2012.01.05

Beschreibung

[0001] Die vorliegende Erfindung betrifft ein Verfahren sowie eine Vorrichtung zur Kompensation von über den Umfang eines rotierenden, insbesondere zylindrischen, Bauteils, insbesondere einer Walze, periodisch wiederkehrenden Störanregungen sowie ein Verfahren zur Bestimmung der Oberflächenstruktur eines ringförmigen Profils zur Kompensation von über den Umfang eines rotierenden, insbesondere zylindrischen, Bauteils, insbesondere einer Walze, periodisch wiederkehrenden Störanregungen. Insbesondere betrifft die vorliegende Erfindung die Schwingungsreduktion in Walzensystemen von Druck- und Beschichtungsmaschinen.

[0002] Bei dem rotierenden Bauteil kann es sich u. a. um eine einzelne Walze, zum Beispiel einer Beschichtungsmaschine, aber auch um Walzensysteme, zum Beispiel in Druckmaschinen, und auch Wellen, zum Beispiel in Turbinen, handeln.

[0003] Um die Produktionsgeschwindigkeit von Druck- und Beschichtungsmaschinen zu erhöhen, können entweder die Walzen bzw. Walzensysteme verbreitert werden oder kann die Bahngeschwindigkeit vergrößert werden. Beide Maßnahmen erfordern eine Prozessoptimierung und führen zu einer stärkeren Schwingungsanfälligkeit der Walzen bzw. Walzensysteme. Durch Störanregungen verursachte Schwingungen beeinträchtigen die Druck- oder Beschichtungsqualität, unter anderem durch Streifenbildung, und führen zu einer unerwünschten Wärmeentwicklung in der Walzenbeschichtung.

[0004] Schwingungen in Walzen bzw. Walzensystemen werden nach dem aktuellen Stand der Technik dadurch reduziert, dass

- die einzelnen Walzen gut ausgewuchtet werden,
- die Eigenfrequenzen der Walzen möglichst hoch gelegt werden, indem die Walzen möglichst steif und leicht gebaut werden, zum Beispiel durch Einsatz von Kohlefaserwerkstoffen,
- die Anpresskräfte der Walzen untereinander optimiert, d. h. möglichst klein gehalten werden,
- passive Dämpfer eingebaut werden, und
- aktive Systeme, wie zum Beispiel Piezoaktoren, in Lagern verwendet werden, bei denen ein großer Aufwand bezüglich Investitionen und Energie für die Aktoren und deren Regelung betrieben werden muss und die noch nicht serienmäßig eingesetzt werden.

[0005] Die EP 1 936 214 A2 beschreibt die passive Schwingungsdämpfung einer Hohlwalze mit einer in der Walze befindlichen passiven Einrichtung, die mindestens eine bewegliche Masse als Schwingungstücker oder ein Dämpfermaterial, wie Granulat, zur Umsetzung von Schwingungsenergie in Wärme beinhaltet.

[0006] In der WO2004/016431 A1 wird ein Verfahren zur aktiven Schwingungsdämpfung beschrieben. Die durch den Kanalschlag einer Formatwalze erzeugte Schwingung wird mit Hilfe einer Überhöhung reduziert, die eine phasenversetzte Schwingung erzeugt und im Idealfall die Schwingung des Kanalschlags teilweise auslöscht. Das Verfahren erzielt eine Reduktion von impulsförmig angeregten Eigenschwingungen. Die Überhöhung befindet sich auf einer zweiten Walze und ist in Höhe und Lage auf dem Umfang veränderlich.

[0007] Aus der DE 10 2007 024 767 A1 ist ein aktive Lagereinheit mit piezoelektrischen Stellementen zum Reduzieren von Schwingungsamplituden der Biegeformen bei Druckwerkszylindern bekannt.

[0008] Die WO 01/50035 A1 offenbart ein Verfahren zur Verminderung von Biegeschwingungen durch eine axiale Anordnung von Aktuatoren in Zylindern von Rotationsdruckmaschinen.

[0009] Desweiteren ergibt sich aus der DE 10 2008 060 740 A1 eine Druckmaschine mit einem Kurvengetriebe, welchem unstetige Sprünge aufgeprägt sind, die Schwingungen erzeugen, welche zur Auslöschung ungewollter Walzenschwingungen führen.

[0010] Darüber hinaus sind aus der Literatur folgende Verfahren zur aktiven und passiven Reduktion von Schwingungen in Walzensystemen bekannt: Die Druckform im Flexodruck steht im Gegensatz zum Offset- oder Tiefdruck nicht im kontinuierlichen Kontakt mit Gegendruckzylinder bzw. Rasterwalze. Dadurch können Kanten des Druckreliefs aufgrund der Druckzylinderrotation beim Auftreffen auf die jeweilige Walze Stöße auslösen. Diese Stöße können wiederum Resonanzen im Druck- und Farbwerk erzeugen. Sichtbare Folgen davon sind oft Streifen im Druckbild bis hin zu Druckaussetzern. Diese meist als Schwingungsstreifen bezeichneten Erscheinungen sind in ihrer Ausprägung hauptsächlich abhängig von der Druckgeschwindigkeit und dem Druckmotiv, d. h. der Position der Bildelemente auf der Flexodruckform. Wenn die druckenden Bildteile ungünstig verteilt sind, ist das Auftreten von Schwingungsstreifen sogar bei niedrigen Druckgeschwindigkeiten möglich (siehe Flint Group: Press Release, Februar 2009).

[0011] Die erste bekannte Forschungsarbeit über Schwingungen an Offsetdruckmaschinen stammt von Holzweißig (Holzweißig, F.: „Dynamische Untersuchung an der Zylindergruppe einer Offsetmaschine“, Dissertation, TH Dresden, Dresden, 1959). Hoffmann und Liebau beschäftigen sich in „Hoffmann, Liebau: „Beitrag zur Untersuchung des dynamischen Verhaltens von Druckwerken in Rollenoffset-Rotationsdruckmaschinen“, Dissertation, TH Karl-Marx-

Stadt, Chemnitz, 1969) mit Biegeschwingungen in Rollenoffsetdruckmaschinen. In „Schmidt, Wöhrmann: „Grundlagenuntersuchung zum Vergleich von CFK- und Stahlwalzen in Druckmaschinen“, Fachhochschule Osnabrück“ wurden die Schwingungen an Stahl- und CFK-Walzen mit Hilfe von Dehnungsmessstreifen untersucht. Messer untersucht in „Markus Messer, Bad Neuheim – „Aktive Schwingungsminderung an gekoppelten Zylindern in Bogenoffsetdruckmaschinen bei Erregung infolge von Kanalschlag“, VDI-Verlag, 2007“ die Schwingungen in Bogenoffsetdruckmaschinen bei Erregung infolge von Kanalschlag.

[0012] In „Eric Knopf: „Aktive Reduktion von Drehschwingungen in Bogenoffsetdruckmaschinen“, Heidelberger Druckmaschinen AG, VDD Jahrestagung 2006“ präsentiert Knopf ein Verfahren zur aktiven Schwingungsminderung an Bogenoffsetdruckmaschinen, das die Schwingungen in der Maschine misst, die Schwingungsamplituden bestimmt und daraus Momente berechnet, die auf den Hauptantrieb aufgeschaltet werden, wodurch die Schwingungen der Maschine reduziert werden. In „Dresig, Holzweißig: „Maschinendynamik“, Springer Verlag, 8. Auflage, 2007“ stellen Dresig und Holzweißig ein Modell zur Berechnung der Torsionschwingungen des Druckwerkes einer Offsetdruckmaschine vor.

[0013] Horst beschäftigt sich in „Horst, H.-G.: „Aktive Schwingungsminderung an elastischen Rotoren mittels piezokeramischer Aktoren“, Dissertation, TU Darmstadt, Aachen, Shaker Verlag, 2005“ mit der aktiven Schwingungsminderung an elastischen Rotoren mittels piezokeramischen Stapelaktoren. Er untersucht theoretisch und experimentell drei Prinzipien: die aktive Schwingungsminderung mit einer aktiven Lagerung mit piezokeramischen Stapelaktoren, die Verwendung der aktiven Lagerung zur elektromechanischen Tilgung und die aktive Schwingungsminderung mit rotorgebundenen piezokeramischen Elementen. Für den geregelten Fall vergleicht er eine lineär-quadratische Regelung mit der μ -Synthese.

[0014] Mit der aktiven Schwingungsminderung an Zylindern von Rollenoffsetdruckmaschinen beschäftigt sich Wimmel in der Veröffentlichung „Wimmel: „Strukturkonformes Aktives Interface – Einsatzerfahrung, Weiterentwicklung und Transfer in rotierende Systeme“, Adaptronic Congress 2004“. Er integriert Piezoelemente in einen Druckzylinder, um kanalerregte Biegeschwingungen zu mindern. Wie in der DE 199 63 945 C1 sind 32 Piezoelemente über den Umfang der Walze verteilt und wirken in axialer Zylinderrichtung. Wimmel entwickelt einen Regler, der aus einem Trigger- und einem Wegsignal Phase und Amplitude für eine impulsartige Ansteuerung der Aktorik erzeugt.

[0015] In der Literatur sind verschiedene Regelungsstrategien zu finden. Verbesserte Regelgüte und Robustheit erhält man mit Störgrößenaufschaltungen, die auch als Feedforward – Algorithmen bezeichnet werden (siehe Burdisso, Heilmann: „A New Dual-Reaction Mass Dynamic Vibration Absorber Actuator for Aktive Vibration Control“, Journal of Sound and Vibration, Vol. 214, No. 5, 1998“), linear-quadratischen Optimalreglern (siehe Ram, Inman: „Optimal Control for Vibrating Systems“, Mechanical Systems and Signal Processing, Vol. 13, No. 6, 1999“) oder robusten Reglern nach der μ -Synthese (siehe Horst, H.-G.: „Aktive Schwingungsminderung an elastischen Rotoren mittels piezokeramischer Aktoren“, Dissertation, TU Darmstadt, Aachen, Shaker Verlag, 2005“). Zheng stellt in „Zheng: „Lernende Regelung für Rotorsysteme“, Dissertation, TU München, Fortschritt-Berichte VDI, Reihe 11, Nr. 187, VDI-Verlag, 1993“) eine lernende Regelung für Rotorsysteme vor.

[0016] Die passiven Verfahren zeichnen sich durch die Vorteile Robustheit, Einfachheit und Verlässlichkeit aus. Hingegen sind die aktiven Regelungen viel wirkungsvoller auf die Schwingungsminderung.

[0017] In „Gasch, Nordmann, Pfützner: „Rotordynamik“, Springer Verlag, 2. Auflage, 2002“ sind Konzepte zur passiven und aktiven Magnetlagerung von rotierenden Wellen dargestellt.

[0018] Eine aktive Regelung nach der μ -Synthese mit Hilfe von Piezoaktoren wird bei einer Portalfräsmaschine in „Ehmann, Schönhoff, Nordmann: „Aktive Schwingungsdämpfung bei Portalfräsmaschinen, Verbesserung der Spanleistung beim Fräsen am Beispiel eines Portalfräsen-Labormodells mit integrierten Piezoaktoren zur aktiven Dämpfungserhöhung“, VDI-Tagung eingesetzt.

[0019] Sowohl die aus oben genannten Patenten als auch die aus der aufgeführten Literatur bekannten Verfahren und Vorrichtungen weisen verschiedene Nachteile auf:

- Generell verursachen aktive Lösungen hohe Kosten, zum Beispiel für Aktoren, Sensoren, Regler, Steuerungshardware, Software, und großen Konstruktions- und Entwicklungsaufwand für die Integration der Komponenten und zur Entwicklung der Steuerungs- und Regleralgorithmen.
- Die bekannten Verfahren erfordern größere Veränderungen und Umbauarbeiten an der Maschine.
- Alle bekannten Verfahren sind auf eine spezielle Maschine abgestimmt, wobei die Adaption an verschiedene Waizen und/oder Klischees einen großen Aufwand erfordert.
- Die bekannten passiven Verfahren sind nicht ausreichend effektiv, da sie nicht auf eine spezielle Störangabe abgestimmt sind.

DE 10 2010 026 204 A1 2012.01.05

[0020] Der Erfindung liegt somit die Aufgabe zugrunde, Schwingungen, wie zum Beispiel Biegeschwingungen, von rotierenden Bauteilen, insbesondere Walzen, deutlich zu reduzieren.

[0021] Diese Aufgabe wird bei dem Verfahren zur Kompensation der eingangsgenannten Art dadurch gelöst, dass mittels mindestens eines ringförmigen Profils, das auf der Außenseite oder der Innenseite des Bauteils angebracht oder darin integriert ist oder das auf oder in einer separaten Einrichtung angebracht oder darin integriert ist, die mit dem Bauteil in Kontakt ist, gezielt Kräfte zur Kompensation der Stör- anregungen erzeugt werden.

[0022] Weiterhin wird diese Aufgabe bei dem Verfahren zur Bestimmung der Oberflächenstruktur gemäß der eingangsgenannten Art dadurch gelöst, dass die periodisch wiederkehrenden Stör- anregungen mittels einer Simulationsrechnung simuliert werden, die Aufbringung von Kräften zur Erzeugung von Gegenschwingungen in einem Bereich, in dem das Profil angebracht oder angeordnet werden soll, oder in der Nähe desselben mittels Simulationsrechnungen simuliert und zur Minimierung der Schwingungen des Bauteils optimiert wird und die berechneten optimierten aufgebrauchten Kräfte in Erhöhungen und Vertiefungen der Oberflächenstruktur des Profils umgesetzt werden.

[0023] Darüber hinaus wird diese Aufgabe bei dem gattungsgemäßen Verfahren zur Bestimmung der Oberflächenstruktur alternativ dadurch gelöst, dass das Bauteil zum Erzeugen der periodisch wiederkehrenden Stör- anregungen gedreht wird, Kräfte mittels Aktoren in einem Bereich, in dem das Profil angebracht oder angeordnet werden soll, oder in der Nähe desselben zur Erzeugung von Gegenschwingungen aufgebracht werden, die Schwingungen des Bauteils mittels Sensoren gemessen, die Kräfte zur Minimierung der Schwingungen des Bauteils optimiert werden und die optimierten Kräfte in Erhöhungen und Vertiefungen der Oberflächenstruktur des Profils umgesetzt werden.

[0024] Darüber hinaus wird diese Aufgabe bei der Vorrichtung gemäß der eingangsgenannten Art dadurch gelöst, dass auf der Außenseite und/oder der Innenseite des Bauteils mindestens ein ringförmiges Profil angebracht oder darin integriert ist oder in einer separaten Einrichtung, die mit dem Bauteil schwingungstechnisch gekoppelt ist, mindestens ein ringförmiges Profil angebracht oder darin integriert ist, wobei das Profil eine Oberflächenstruktur zur gezielten Erzeugung von Kräften zur Kompensation der Stör- anregungen aufweist.

[0025] Günstigerweise wird/werden bei dem Verfahren zur Kompensation das ringförmige Profil bzw. die

ringförmigen Profile individuell für ein jeweiliges Bauteil erzeugt.

[0026] Insbesondere kann dabei vorgesehen sein, dass die Oberflächenstruktur des Profils bzw. jedes Profils durch eine Simulationsrechnung und/oder experimentell ermittelt wird.

[0027] Zweckmäßigerweise wird/werden das Profil bzw. die Profile gleichzeitig mit der Herstellung des Bauteils oder eines Mantels des Bauteils erzeugt.

[0028] Gemäß einer besonderen Ausführungsform der erfindungsgemäßen Vorrichtung ist mindestens eine fest gelagerte Rolle zum Abrollen des mindestens einen Profils vorgesehen.

[0029] Alternativ ist auch denkbar, dass mindestens ein weiteres rotierendes, insbesondere zylindrisches, Bauteil, insbesondere eine Walze, vorgesehen ist, wobei das Bauteil und das weitere Bauteil aufeinander abrollend rotieren.

[0030] Günstigerweise ist die separate Einrichtung ein an ein Längsende des Bauteils angesetzter Adapterring.

[0031] Gemäß einer weiteren besonderen Ausführungsform der Erfindung ist das Bauteil ein Druckwerkszylinder.

[0032] Vorteilhafterweise weist der Druckwerkszylinder einen Mantel auf, der als austauschbares Klichschee ausgeführt ist.

[0033] Schließlich kann vorgesehen sein, dass das Bauteil eine Walze mit austauschbarer Ummantelung ist und das Profil in der Ummantelung integriert ist.

[0034] Der Erfindung liegt die überraschende Erkenntnis zugrunde, dass sich die Schwingungen einer langen schlanken Welle dadurch reduzieren lassen, dass Kräfte oder Weganregungen vorzugsweise im Lager oder in der Nähe desselben derart aufgebracht werden, dass Gegenschwingungen zu den zu dämpfenden Schwingungen der Welle entstehen, die diese dann tilgen. Im Gegensatz zu anderen Systemen handelt es sich bei der vorliegenden Erfindung weder um einen passiven Dämpfer, noch sollen die Kraft- und Weganregungen durch teure aktive Systeme erfolgen. Mit der vorliegenden Erfindung lassen sich Walzenschwingungen durch Aufbau von „Gegenschwingungen“ deutlich reduzieren. Damit werden Voraussetzungen geschaffen, um bei gleichbleibender oder besserer Qualität der Produkte die Produktionsgeschwindigkeit von Druck- und Beschichtungsprozessen deutlich über den aktuellen Stand der Technik hinaus zu erhöhen.

[0035] Zumindest mittels besonderer Ausführungsformen der Erfindung lassen sich folgende Vorteile erzielen:

- Schwingungsdämpfung erfolgt passiv mit Hilfe eines auf einem Formatzylinder befindlichen ringförmigen Profils, das für eine bestimmte, periodisch mit der Formatzylinderumdrehung wiederkehrende Störانregung (zum Beispiel ein bestimmtes Klischee) optimiert wurde.
- Das ringförmige Profil zur Schwingungsdämpfung befindet sich auf der äußeren Seite des Formatzylinders. Es kann im Gegensatz zum Beispiel zur in der EP 1 936 214 A2 beschriebenen Schwingungsdämpfung ohne Umbauarbeiten an jeder Maschine bzw. jedem Walzensystem angebracht werden und eignet sich daher auch für bestehende Anlagen.
- Es werden keine zusätzlichen aktiven Stellelemente benötigt. Trotzdem werden gezielt auf die Störانregung abgestimmte Kräfte zur Schwingungstilgung in die Walze eingeleitet. Das Profil wird für jedes Klischee individuell angefertigt, wobei die Höhe und Breite des Profils variabel sind.
- Die Form des Profils wird mit Simulationsrechnungen und/oder durch Versuche an einem Versuchsstand optimiert. Das Profil wird berechnet, über den Umfang verteilt, um die Schwingungsmoden zu kompensieren.
- Die Fertigung des ringförmigen Profils kann gleichzeitig mit der Herstellung eines Klischees erfolgen. Dadurch werden Kosten für teure aktive Steuerungs- oder Regelungssysteme gespart.

[0036] Weitere Merkmale und Vorteile der Erfindung ergeben sich aus den Ansprüchen und der nachfolgenden Beschreibung, in der mehrere Ausführungsbeispiele anhand der schematischen Zeichnungen im einzelnen erläutert werden. Dabei zeigt:

[0037] **Fig. 1** eine Längsseitenansicht (unten) und eine Stirnseitenansicht (oben) von einer Vorrichtung zur Kompensation von über den Umfang einer Walze periodisch wiederkehrenden Störانregungen gemäß einer besonderen Ausführungsform der Erfindung;

[0038] **Fig. 2** eine Längsseitenansicht (unten) und eine Stirnseitenansicht (oben) von einer Vorrichtung zur Kompensation von über den Umfang einer Walze periodisch wiederkehrenden Störانregungen gemäß einer weiteren besonderen Ausführungsform der Erfindung;

[0039] **Fig. 3** eine Längsseitenansicht (unten), eine Stirnseitenansicht (rechts oben) und eine Detailansicht (links oben) teilweise im Schnitt von einer Vorrichtung zur Kompensation von über den Umfang einer Walze periodisch wiederkehrenden Störانregungen gemäß einer weiteren besonderen Ausführungsform der Erfindung;

[0040] **Fig. 4** eine Längsschnittansicht (unten), eine Stirnseitenansicht (links oben) und eine Detailansicht (rechts oben) teilweise im Schnitt von einer Vorrichtung zur Kompensation von über den Umfang einer Walze periodisch wiederkehrenden Störانregungen gemäß einer weiteren besonderen Ausführungsform der Erfindung;

[0041] **Fig. 5** eine perspektivische Ansicht einer Versuchsanordnung zur Durchführung eines experimentellen Verfahrens zur Bestimmung der Oberflächenstruktur eines ringförmigen Profils zur Kompensation von über den Umfang einer rotierenden Walze periodisch wiederkehrenden Störانregungen gemäß einer besonderen Ausführungsform der Erfindung;

[0042] **Fig. 6** ein Regelschema zur Durchführung des Verfahrens; und

[0043] **Fig. 7** den periodischen Kraftverlauf eines Piezoaktors über den Umfang an einem Ende einer Walze.

[0044] Bei der in **Fig. 1** gezeigten Vorrichtung ist eine längliche zylinderförmige Walze 2 mittels zweier Lager 6 horizontal drehbar gelagert. Auf der Außenseite der Welle 2 sind im Bereich der beiden Lager 6 sowie in einem Bereich in der Nähe der Mitte jeweils ein ringförmiges Profil 1 aus Erhebungen und Vertiefungen, von denen lediglich jeweils eine mit der Bezugszahl 7 (Erhöhung) bzw. 8 (Vertiefung) gekennzeichnet ist, angebracht, mit Hilfe dessen sich periodisch mit der Drehzahl auftretende Störانregungen wirkungsvoll dämpfen lassen. Besagte Profile 1 sind entsprechend einer bestimmten Störانregung bzw. eines bestimmten Störانregungsmusters derart entworfen, dass durch den ungleichmäßigen Andruck an wenigstens eine weitere Walze 3 Gegenschwingungen in der Walze 2 erzeugt werden, um die durch die Störانregung bzw. Störانregungsmuster verursachten Schwingungen (Biegeschwingungen) der Walze 2 zu dämpfen. Es handelt sich einerseits um ein passives System, da keine zusätzlichen Aktoren eingesetzt werden müssen, andererseits werden aber über die Profile 1 Aktivkräfte in die Walze 2 eingeleitet, um die obengenannten Gegenschwingungen zu erzeugen, wobei die notwendige Energie dem Antrieb des aus den beiden Walzen 2 und 3 bestehenden Walzensystems entnommen wird.

[0045] **Fig. 2** zeigt eine Ausführungsform der Vorrichtung, bei der über die Profile 1 ebenfalls Gegenschwingungen in der Walze 2, aber durch Andruck an fest gelagerten Rollen 4 anstelle einer weiteren Walze erzeugt werden. In dem gezeigten Beispiel weist die Vorrichtung nur zwei statt drei Profile 1 auf und folgt ein Andruck bei dem Profil 1 auf der linken Seite der **Fig. 2** durch eine obere fest gelagerte Rolle 4 und eine untere, d. h. um 180 Grad versetzt angeordnete gelagerte Rolle 4, während auf der rechten Seite

DE 10 2010 026 204 A1 2012.01.05

ein Andruck an lediglich einer oberen fest gelagerten Rolle 4 erfolgt. In anderen Ausführungen könnte auch eine einzige fest gelagerte Rolle 4 ausreichen.

[0046] Alternativ zur in Fig. 1 gezeigten Ausführungsform können die Profile 1 anstelle auf der Außenseite der Walze 2 auch an der Innenseite derselben angeordnet sein (siehe Fig. 3). Dementsprechend sind die fest gelagerten Rollen 4 ebenfalls auf der Innenseite der Walze 2 angeordnet, so dass Kräfte zur Schwingungsdämpfung durch Abrollen der Profile 1 auf den fest an einem Gestell gelagerten Rollen 4 erzeugt werden.

[0047] Fig. 4 zeigt eine Ausführungsform der Vorrichtung, bei der an den Längsenden der Walze 2 jeweils ein Adapterring 5 angesetzt ist. Im Inneren der Adapterringe 5 befindet sich jeweils ein Profil 1. Die Profile 1 rollen wiederum auf jeweiligen fest gelagerten Rollen 4 ab. Mit besagtem Profil in Verbindung mit einer Anpresswalze lassen sich prinzipbedingt nur Druckkräfte erzeugen. Sind auch Kräfte in Gegenrichtung (mit umgekehrten Vorzeichen) erforderlich, muss mit mehreren Anpresswalzen gearbeitet werden. In Fig. 4 nicht dargestellt ist die Lösung mit mindestens einem schwingungsdämpfenden Profil auf der Innen- und Außenseite des Adapterrings 5 oder alternativ mit zwei um 180 Grad versetzten Andruckwalzen, um Kräfte mit unterschiedlichen Vorzeichen zu erzeugen.

[0048] Die optimale Form eines auf beispielsweise der Außenseite einer Walze aufzubringenden Profils lässt sich mit Hilfe von Simulationsrechnungen oder experimentell mit einer beispielhaft in Fig. 5 gezeigten Versuchsanordnung ermitteln.

[0049] Fig. 6 illustriert exemplarisch die prinzipielle Vorgehensweise zur Bestimmung des optimalen Kraftverlaufs. Zunächst werden mittels Aktoren in Form von Piezoaktoren 11 Gegenschwingungen erzeugt. Der optimale Kraftverlauf, der von den Piezoaktoren 11 auf die Walze 2 bzw. auf ein Walzensystem aufgebracht wird, kann mit Hilfe eines in Fig. 6 gezeigten Regelschemas ermittelt werden, in dem die Walze 2 mit einem Lagewinkelsensor 13 und Sensoren 15, zum Beispiel Dehnungsmessstreifen, versehen wird, die die auftretenden Schwingungen messen, die gemessenen Schwingungen mit der Walze 2 als Eingang in einen Regler 14 gegeben werden, der die Stellsignale $u_1(t)$ und $u_2(t)$ und damit die Stellkräfte der Piezoaktoren 11 dann dahingehend optimiert, dass die gemessenen Schwingungen minimal werden. Die Kraftverläufe der Piezoaktoren 11 werden so für jeweils eine Umdrehung der Walze 2 entweder durch schnelle Regler oder mit Hilfe von Optimierungsstrategien dahingehend optimiert, dass die Biegeschwingungen der Walze 2 minimal werden. Die periodisch über den Umfang der Walze 2 wiederkehrenden Stellkräfte F und der Lagewinkel φ

(siehe Fig. 7) werden aufgezeichnet. Wie in Fig. 7 dargestellt ist, können die Stellkräfte F als Funktion des Lagewinkels φ aufgetragen werden. Die Stellkräfte können nachfolgend in eine entsprechende Anordnung der Erhöhungen 7 und Vertiefungen 8 des Profils 1 umgesetzt werden. Das Profil 1 kann beispielsweise dadurch realisiert werden, dass ein Band oder ein Ring auf der Walze 2 aufgebracht wird. Die Walze 2 kann anschließend in eine Maschine eingebaut und dann ohne aktive Elemente schwingungsoptimiert betrieben werden.

[0050] Die Vorgehensweise der Ermittlung der optimalen Form, d. h. der Oberflächenstruktur der Profile 1 mittels Simulationsrechnungen ist ähnlich der experimentellen Vorgehensweise, nur dass die Schwingungen der Walze nicht gemessen, sondern simuliert werden. Dafür wird ein Finite-Element-Modell der Walze bzw. des Walzensystems erstellt, mit dem das Schwingungsverhalten der Walze bzw. der einzelnen Walzen sowie die Störanregung durch ein Klischee simuliert wird. Der Verlauf der Störanregung über den Umfang der Walze hängt ab vom Profil eines speziellen Klischees und muss für jedes Klischee speziell ermittelt werden. Die Kräfte zur aktiven Schwingungsdämpfung werden im Rechenmodell an den Querschnitten eingeleitet, an denen das ringförmige Profil befestigt werden soll. Anschließend kann die Optimierung der Kräfte mittels Simulationsrechnungen erfolgen. Die Kraftverläufe werden für jeweils eine Umdrehung der Walze entweder durch schnelle Regler oder mit Hilfe von Optimierungsstrategien oder dahingehend optimiert, dass die Biegeschwingungen der Walze minimal werden. Die notwendigen Kräfte werden aufgezeichnet und dann in entsprechender Anordnung der Erhöhungen 7 und Vertiefungen 8 des Profils 1 umgesetzt werden.

[0051] Die in der vorstehenden Beschreibung, in den Zeichnungen sowie in den Ansprüchen offenbarten Merkmale der Erfindung können sowohl einzeln als auch in beliebigen Kombinationen für die Verwirklichung der Erfindung in ihren verschiedenen Ausführungsformen wesentlich sein.

Bezugszeichenliste

1	Profil
2	Walze
3	weitere Walze
4	feste gelagerte Rollen
5	Adapterringe
6	Lager
7	Erhöhung
8	Vertiefung
11	Piezoaktoren
13	Lagewinkelsensor
14	Regler
15	Sensoren

DE 10 2010 026 204 A1 2012.01.05

ZITATE ENTHALTEN IN DER BESCHREIBUNG

Diese Liste der vom Anmelder aufgeführten Dokumente wurde automatisiert erzeugt und ist ausschließlich zur besseren Information des Lesers aufgenommen. Die Liste ist nicht Bestandteil der deutschen Patent- bzw. Gebrauchsmusteranmeldung. Das DPMA übernimmt keinerlei Haftung für etwaige Fehler oder Auslassungen.

Zitierte Patentliteratur

- EP 1936214 A2 [0005, 0035]
- WO 2004/016431 A1 [0006]
- DE 102007024767 A1 [0007]
- WO 01/50035 A1 [0008]
- DE 102008060740 A1 [0009]
- DE 19963945 C1 [0014]

Zitierte Nicht-Patentliteratur

- Flint Group: Press Release, Februar 2009 [0010]
- Holzweißig, F.: „Dynamische Untersuchung an der Zylindergruppe einer Offsetmaschine“, Dissertation, TH Dresden, Dresden, 1959 [0011]
- Hoffmann, Liebau: „Beitrag zur Untersuchung des dynamischen Verhaltens von Druckwerken in Rollenoffset-Rotationsdruckmaschinen“, Dissertation, TH Karl-Marx-Stadt, Chemnitz, 1969 [0011]
- Schmidt, Wöhrmann: „Grundlagenuntersuchung zum Vergleich von CFK- und Stahlwalzen in Druckmaschinen“, Fachhochschule Osnabrück [0011]
- Markus Messer, Bad Neuheim – „Aktive Schwingungsminderung an gekoppelten Zylindern in Bogenoffsetdruckmaschinen bei Erregung infolge von Kanalschlag“, VDI-Verlag, 2007 [0011]
- Eric Knopf: „Aktive Reduktion von Drehschwingungen in Bogenoffsetdruckmaschinen“, Heidelberger Druckmaschinen AG, VDD Jahrestagung 2006 [0012]
- Dresig, Holzweißig: „Maschinendynamik“, Springer Verlag, 8. Auflage, 2007 [0012]
- Horst, H.-G.: „Aktive Schwingungsminderung an elastischen Rotoren mittels piezokeramischer Aktoren“, Dissertation, TU Darmstadt, Aachen, Shaker Verlag, 2005 [0013]
- Wimmel: „Strukturkonformes Aktives Interface – Einsatzverfahren, Weiterentwicklung und Transfer in rotierende Systeme“, Adaptronic Congress 2004 [0014]
- Burdisso, Heilmann: „A New Dual-Reaction Mass Dynamic Vibration Absorber Actuator for Active Vibration Control“, Journal of Sound and Vibration, Vol. 214, No. 5, 1998 [0015]
- Ram, Inman: „Optimal Control for Vibrating Systems“, Mechanical Systems and Signal Processing, Vol. 13, No. 6, 1999 [0015]
- Horst, H.-G.: „Aktive Schwingungsminderung an elastischen Rotoren mittels piezokeramischer Aktoren“, Dissertation, TU Darmstadt, Aachen, Shaker Verlag, 2005 [0015]
- Zheng: „Lernende Regelung für Rotorsysteme“, Dissertation, TU München, Fortschritt-Berichte VDI, Reihe 11, Nr. 187, VDI-Verlag, 1993 [0015]
- Gasch, Nordmann, Pfützner: „Rotordynamik“, Springer Verlag, 2. Auflage, 2002 [0017]
- Ehmann, Schönhöf, Nordmann: „Aktive Schwingungsdämpfung bei Portalfräsmaschinen, Verbesserung der Spanleistung beim Fräsen am Beispiel eines Portalfräsen-Labormodells mit integrierten Piezoaktoren zur aktiven Dämpfungserhöhung“, VDI-Tagung [0018]

DE 10 2010 026 204 A1 2012.01.05

Patentansprüche

1. Verfahren zur Kompensation von über den Umfang eines rotierenden, insbesondere zylindrischen, Bauteils, insbesondere einer Walze (2), periodisch wiederkehrenden Störanregungen, **dadurch gekennzeichnet**, dass mittels mindestens eines ringförmigen Profils (1), das auf der Außenseite oder der Innenseite des Bauteils angebracht oder darin integriert ist oder das auf oder in einer separaten Einrichtung angebracht oder darin integriert ist, die mit dem Bauteil in Kontakt ist, gezielt Kräfte zur Kompensation der Störanregungen erzeugt werden.

2. Verfahren nach Anspruch 1, **dadurch gekennzeichnet**, dass das ringförmige Profil (1) bzw. die ringförmigen Profile individuell für ein jeweiliges Bauteil erzeugt wird/werden.

3. Verfahren nach Anspruch 2, **dadurch gekennzeichnet**, dass die Oberflächenstruktur des Profils (1) bzw. jedes Profils durch eine Simulationsrechnung und/oder experimentell ermittelt wird.

4. Verfahren nach einem der Ansprüche 1 bis 3, **dadurch gekennzeichnet**, dass das Profil (1) bzw. die Profile gleichzeitig mit der Herstellung des Bauteils oder eines Mantels des Bauteils erzeugt wird/werden.

5. Verfahren zur Bestimmung der Oberflächenstruktur eines ringförmigen Profils (1) zur Kompensation von über den Umfang eines rotierenden, insbesondere zylindrischen, Bauteils, insbesondere einer Walze (2), periodisch wiederkehrenden Störanregungen, **dadurch gekennzeichnet**, dass die periodisch wiederkehrenden Störanregungen mittels einer Simulationsrechnung simuliert werden, die Aufbringung von Kräften zur Erzeugung von Genschwingungen in einem Bereich, in dem das Profil (1) angebracht oder angeordnet werden soll, oder in der Nähe desselben mittels Simulationsrechnungen simuliert und zur Minimierung der Schwingungen des Bauteils optimiert wird und die berechneten optimierten aufgebrauchten Kräfte in Erhöhungen (7) und Vertiefungen (8) der Oberflächenstruktur des Profils (1) umgesetzt werden.

6. Verfahren zur Bestimmung der Oberflächenstruktur eines ringförmigen Profils (1) zur Kompensation von über den Umfang eines rotierenden, insbesondere zylindrischen, Bauteils, insbesondere einer Walze (2), periodisch wiederkehrenden Störanregungen, **dadurch gekennzeichnet**, dass das Bauteil zum Erzeugen der periodisch wiederkehrenden Störanregungen gedreht wird, Kräfte mittels Aktoren in einem Bereich, in dem das Profil (1) angebracht oder angeordnet werden soll,

oder in der Nähe desselben zur Erzeugung von Genschwingungen aufgebracht werden, die Schwingungen des Bauteils mittels Sensoren (15) gemessen, die Kräfte zur Minimierung der Schwingungen des Bauteils optimiert werden und die optimierten Kräfte in Erhöhungen (7) und Vertiefungen (8) der Oberflächenstruktur des Profils (1) umgesetzt werden.

7. Vorrichtung zur Kompensation von über den Umfang eines rotierenden, insbesondere zylindrischen, Bauteils, insbesondere einer Walze (2), periodisch wiederkehrenden Störanregungen, **dadurch gekennzeichnet**, dass auf der Außenseite und/oder der Innenseite des Bauteils mindestens ein ringförmiges Profil (1) angebracht oder darin integriert ist oder in einer separaten Einrichtung, die mit dem Bauteil schwingungstechnisch gekoppelt ist, mindestens ein ringförmiges Profil (1) angebracht oder darin integriert ist, wobei das Profil (1) eine Oberflächenstruktur zur gezielten Erzeugung von Kräften zur Kompensation der Störanregungen aufweist.

8. Vorrichtung nach Anspruch 7, **dadurch gekennzeichnet**, dass mindestens eine fest gelagerte Rolle (4) zum Abrollen des mindestens einen Profils (1) vorgesehen ist.

9. Vorrichtung nach Anspruch 7, **dadurch gekennzeichnet**, dass mindestens ein weiteres rotierendes, insbesondere zylindrisches, Bauteil, insbesondere eine Walze (3), vorgesehen ist, wobei das Bauteil und das weitere Bauteil aufeinander abrollend rotieren.

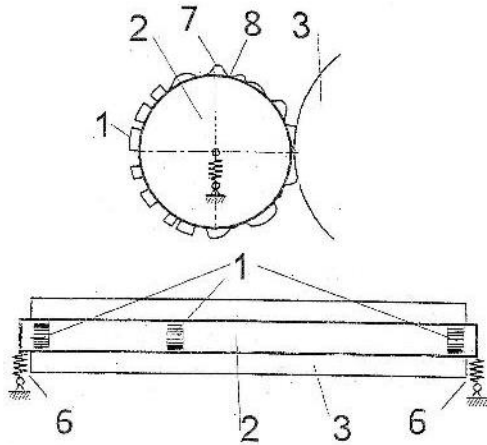
10. Vorrichtung nach einem Ansprüche 7 bis 9, **dadurch gekennzeichnet**, dass die separate Einrichtung ein an ein Längsende des Bauteils angesetzter Adapterring (5) ist.

11. Vorrichtung nach einem der Ansprüche 7 bis 10, **dadurch gekennzeichnet**, dass das Bauteil ein Druckwerkszylinder ist.

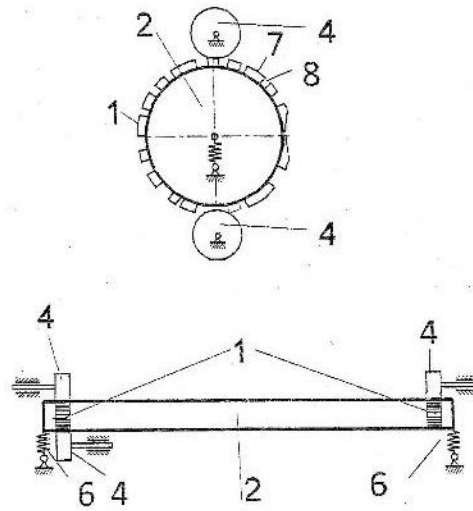
12. Vorrichtung nach Anspruch 11, **dadurch gekennzeichnet**, dass der Druckwerkszylinder einen Mantel aufweist, der als austauschbares Klischee ausgeführt ist.

13. Vorrichtung nach einem der Ansprüche 7 bis 10, **dadurch gekennzeichnet**, dass das Bauteil eine Walze mit austauschbarer Ummantelung ist und das Profil (1) in der Ummantelung integriert ist.

Es folgen 7 Blatt Zeichnungen



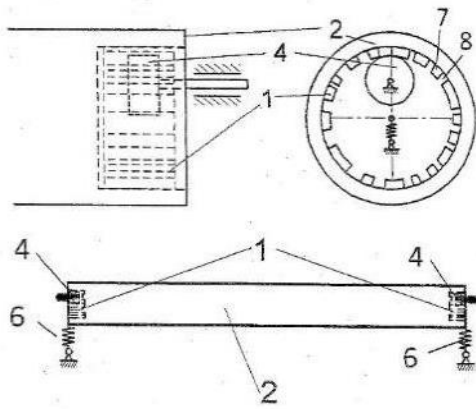
Figur 1



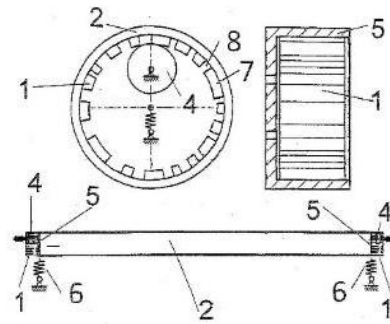
Figur 2

DE 10 2010 026 204 A1 2012.01.05

DE 10 2010 026 204 A1 2012.01.05



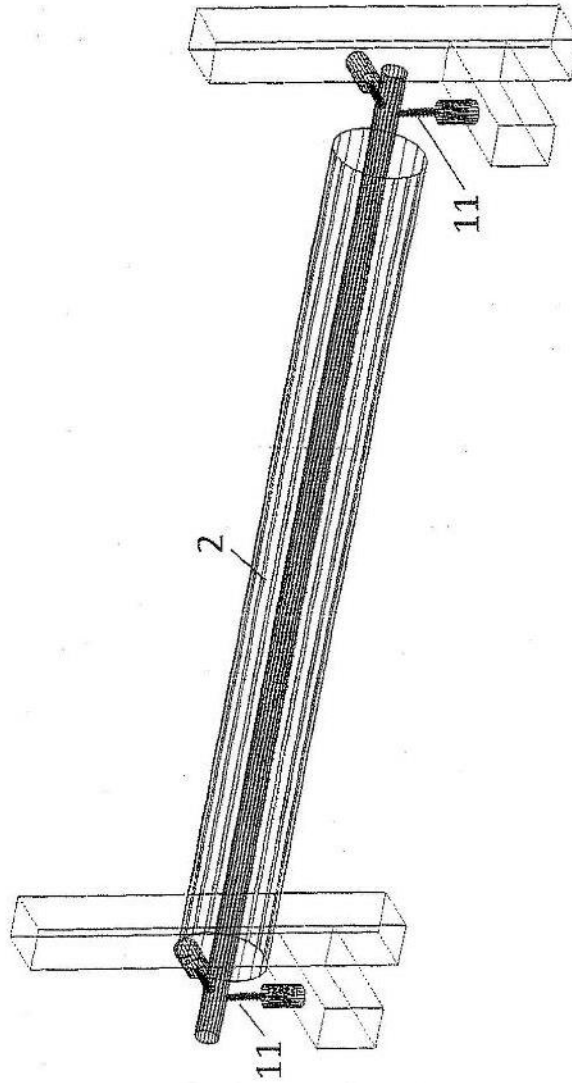
Figur 3



Figur 4

11 / 15

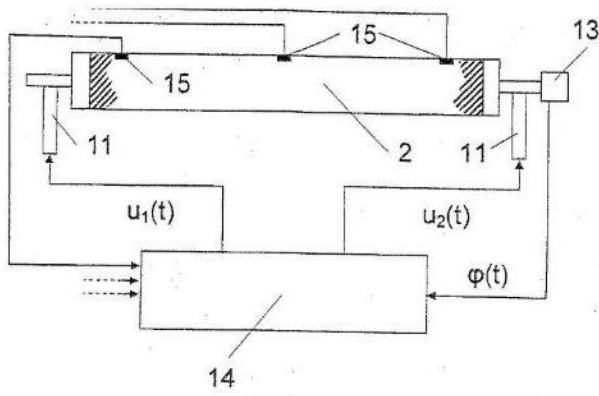
12 / 15



Figur 5

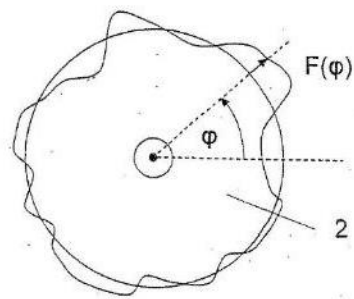
DE 10 2010 026 204 A1 2012.01.05

DE 10 2010 026 204 A1 2012.01.05



Figur 6

14 / 15



Figur 7

15 / 15